Bioaccumulation and Toxicokinetics of Polycyclic Aromatic Compounds and Metals in Giant Floater Mussels (*Pyganodon grandis*) Exposed to a Simulated Diluted Bitumen Spill

Jonathan Y. Séguin

Thesis submitted to the University of Ottawa
in partial fulfillment of the requirements for the
M.Sc. degree in Biology, Specialization in Chemical and Environmental Toxicology

Department of Biology
Faculty of Science
University of Ottawa

Abstract

Canadian bitumen is mainly transported in a diluted form via pipeline and train, all posing a risk as they can lead to the release of diluted bitumen (dilbit) in the environment. In the summer of 2018, a collaborative large-scale field experiment was conducted at the International Institute for Sustainable Development - Experimental Lakes Area (IISD-ELA), a world-renowned aquatic research facility. The research objectives of the Boreal lake Oil Release Experiment by Additions to Limnocorrals (BOREAL) project were to understand the fate, behaviour, and potential toxic effects of dilbit in a freshwater Boreal lake to inform evidence-based management strategies for the transport of dilbit. A range of controlled dilbit spills was performed in seven 10 m diameter limnocorrals (~100,000 L of water) resulting in environmentally realistic dilbit:water dilutions ranging from 1:69,200 to 1:504, representing the upper half of the distribution of oil spill sizes in North America in the last decade. Additionally, two limnocorrals not treated with dilbit were studied as controls.

This thesis identifies the bioaccumulating compounds derived from naturally weathered dilbit in adult giant floater mussels (*Pyganodon grandis*), to determine the rates at which they were accumulated and excreted. More specifically, the bioaccumulation potential and toxicokinetic parameters of polycyclic aromatic compounds (PACs) and various metals were assessed in mussels exposed *ex situ* for 41 days (25 days of exposure and 16 days of depuration) to water from the limnocorrals. These compounds have shown to be toxic, carcinogenic, and mutagenic to aquatic organisms. Mussels exposed to dilbit-contaminated water experienced significantly greater TPACs concentrations (0.40 – 0.90 $\mu g\ L^{-1}$, n=12) compared to mussels from the Control (0.017 $\mu g\ L^{-1}$, n=4). Furthermore, dilbit-contaminated water had a higher proportion of alkylated PACs compared to their parent counterpart, demonstrating petrogenic PAC profiles.

We detected significantly greater TPACs concentrations in mussels exposed to dilbit-contaminated water (25.92 – 27.79 µg g^{-1}, ww Lipid, n=9, at day 25 of the uptake phase) compared to mussels from the Control (average of 2.62 ± 1.95 µg g^{-1}, ww Lipid; ±SD, n=17). Alkylated PACs represented 96.4 ± 1.8%, ±SD, n=12 of TPACs in mussels from dilbit-contaminated treatments at day 25 of the uptake phase, indicating the importance of conducting a more inclusive assessment of petrochemical mixtures as most studies only focus on parent PACs. From first-order one-compartment models derived from nonlinear curve fitting of the accumulation phase or sequential modelling method, uptake (0.66 – 24.65 L g^{-1} day^{-1}, n=87) and depuration (0.012 – 0.37 day^{-1}, n=87) kinetic rate constants, as well as bioconcentration factors (log values from 3.85 – 6.12 L kg^{-1}, n=87) for the 29 PACs that bioaccumulated in mussels suggested that alkylated PACs have greater bioaccumulation potential compared to their parent PAC counterpart. Results from this study also demonstrated that giant floater mussels could be used to biomonitor PAC contamination following oil spills as PACs accumulated in mussel tissue and were still present following the 16 day depuration phase. The results of this study are the largest, most comprehensive set of toxicokinetic and bioaccumulation information of PACs (44 analytes) in freshwater mussels obtained to date.

Metal contamination following the controlled dilbit spill was minimal, but mussels exposed to water contaminated with naturally weathered dilbit experienced elevated concentrations of dissolved zinc (30.26 – 38.26 µg L^{-1}, n=12) compared to the mussels in the uncontaminated water (6.75 ± 3.31 µg L^{-1}, n=4), surpassing the Canadian water quality guidelines for the protection of aquatic life. However, it is not clear if dilbit contamination caused elevated zinc concentrations in the water as other factors, such as limnocorral building materials and/or galvanized minnow traps

used in the limnocorrals, could have contributed to zinc contamination. Nonetheless, giant floater mussels did not accumulate zinc in their tissues.

Acknowledgements

I would like to thank my supervisor, Dr. Jules Blais, for all the great opportunities and experiences I have received throughout this M.Sc.. Your continued support has made me a more confident scientist. I would also like to thank my committee members and thesis evaluators, Dr. Craig Hebert, Dr. Vance Trudeau, Dr. Paul White, and Dr. Ian Clark for your advice, knowledge, and feedback. A very special thank you to Dave Eickmeyer, Linda Kimpe, and Keval Shah. You guys always made me feel welcomed in the lab and you were always there to answer my questions (I have lost count… maybe a million?). Dave, thank you very much for being available all the time, especially during those late nights in the lab. You always answered my crazy long texts and reassured me that everything will be fine, I truly appreciate everything you have done for me.

To Papa Pepe, thank you, thank you, thank you,… and thank you. Your guidance throughout this process was greatly appreciated and I honestly would not have been able to do this without you. I was a crazy wildling running around in the bush trying to keep fish, tadpoles, and mussels alive without really knowing what I was doing. You were always there for me, during the highs and the lows… and there were many lows. I already miss those F&S breakfasts, music festivals, and long road trips to the IISD-ELA.

I would like to thank Sawyer Stoyanovich for his continuous support and friendship. You have been a true friend going all the way back to our undergrad. I would also like to thank the rest of the Blais lab members (current and previous), Lauren Gallant, Kirsten Smythe, M.C. Roy, Cynthia Cheney, Brian Moeun, Jennifer[2] (Keir & Kissinger), Madison Bell, Julie Bilodeau, Leslie Saunders, Mija Ažđajić, Alexandre Salat, Braden Gregory, Phil Thomas, and Claudia Tanamal, for your support, advice, and friendships. I will never forget you guys!

I would like to thank my field partner Johanna Mason. This experiment would not have been successful without your significant input and help collecting our samples. We were both going through a really tough time during the field season but we came out on top! Thank you to all of the BOREAL members including Jeff Cederwall, Sam Patterson, Tyler Black, Lauren Timlick, Hannah Kosichek, Leah Cundall, and Daniel Denton as well as all of the great people I got to meet at IISD-ELA. I had a heck of a summer with you guys, thanks for the memories!

Many thanks to my friends, especially my cousins JJ and Greg Loncaric, and the boys at 387 ½ Chapel street (Tommy Detlor and Cyrus Hiranandani) for all of those NFL Sundays, Monday wing nights, Boko bakery cookies, Catan nights, and those late-night drop-ins after long days in the lab. I would like to especially thank my parents, Caroline Bériault and Jacques Séguin, for supporting me and pushing me to reach my potential. I am the man that I am today because of you and I greatly appreciate everything you have done for me. Finally, I would like to thank mon amour Lauren Hayhurst. You have always been there for me and supported my tough decisions. I am really glad to have you on my team and my success is your success… We did it!!

Sarnia, October 2020

Table of Contents

List of Abbreviations

AIC	Akaike's Information Criteria
Alkyl	Alkylated
ANOVA	Analysis of variance
AOS	Athabasca Oil Sands
ASE	Accelerated solvent extraction
BAF	Bioaccumulation factor
BDL	Below detection limit
BCF	Bioconcentration factor
BCF_C	BCF calculated from the ratio of concentration in tissue and water
BCF_K	BCF calculated from the ratio of uptake and depuration rate constants
BIC	Bayesian Information Criteria
BNT	Benzonaphthothiophene
BOREAL	Boreal lake Oil Release Experiment by Additions to Limnocorrals
BT	Benzothiophene
BTEX	Benzene, toluene, ethylbenzene, and xylene
BSAF	Biota-sediment accumulation factor
C1-*parent*	Specified parent PAC with 1 alkyl substitution
C2-*parent*	Specified parent PAC with 2 alkyl substitutions
C3-*parent*	Specified parent PAC with 3 alkyl substitutions
C4-*parent*	Specified parent PAC with 4 alkyl substitutions
CAPP	Canadian Association of Petroleum Producers
C_B	Chemical concentration in the organism
CCME	Canadian Council of Ministers of the Environment
CLB	Cold Lake blend
C_S	Chemical concentration in the exposure medium
CYP	Cytochrome-P450
DBT	Dibenzothiophene
DCM	Dichloromethane
DNA	Deoxyribonucleic acid
dw	Dry weight
DWH	Deepwater Horizon
ECCC	Environment and Climate Change Canada
ECHA	European Chemicals Agency
FaBS	Fate and behaviour' subtheme
GC-MS	Gas chromatography coupled with mass spectrometry
GPx	Glutathione peroxidase
GSH	Glutathione
GST	Glutathione-S-transferase
H_2S	Hydrogen sulfide
HMW	High molecular weight
HNO_3	Nitric acid
HSD	Honestly significant difference
ICP-ES	Inductively coupled plasma emission spectroscopy
ICP-MS	Inductively coupled plasma mass spectrometry

IDL	Instrument detection limit
IISD-ELA	International Institute for Sustainable Development – Experimental Lakes Area
k_1	Uptake rate constant
k_2	Depuration rate constant
k_E	Elimination by fecal egestion rate constant
k_G	Growth dilution rate constant
k_M	Metabolic transfer rate constant
K_{ow}	Octanol-water partition coefficient
LMW	Low molecular weight
MDL	Method detection limit
MFO	Mixed function oxygenase
MT	Metallothionein
MW	Molecular Weight
Na_2SO_4	Sodium Sulfate
NADPH	Nicotinamide adenine dinucleotide phosphate
OC	Organic compound
OECD	Organization for Economic Co-operation and Development
OM	Organic matter
PAC	Polycyclic aromatic compound
PAH	Polycyclic aromatic hydrocarbon
PFA	Perfluoroalkoxy
PTFE	Polytetrafluoroethylene
PVC	Polyvinyl chloride
RC	Rate Coefficient
ROS	Reactive oxygenated species
RSC	Royal Society of Canada
S^o	Elemental sulfur
SE	Standard error
SD	Standard deviation
Sigma	Model metrics standard error
SOD	Superoxide dismutase
SULT	Sulfotransferase
t_{95}	Time required to reach 95 % of steady state
t	Days
TMP	2,2,4-Trimethylpentane
TPACs	Total polycyclic aromatic compounds
TSS	Total suspended solids
WO_3	Tungstic oxide
UGT	Uridine diphosphate glucuronosyltransferase
U.S. EPA	United States Environmental Protection Agency
WAF	Water accommodated fraction
WC	Water content
Ww	Wet weight

List of Figures

List of Tables

1. General Introduction

1.1. Introduction

Bitumen is a highly viscous, unconventional crude oil that constitutes most of Canada's petroleum resources in the Athabasca Oil Sands (AOS) in northeastern Alberta. Its transport to refineries and markets via pipelines and trains requires dilution with natural gas condensates. The resulting compound, dilbit, is the product of mixing diluent with oil sands bitumen. Dilbit production volume is projected to increase due to expansion in the production and transportation of unconventional oils, (CAPP, 2019; Environment Canada et al., 2013; K. Lee et al., 2015), increasing the frequency of spills. Previous dilbit spills have caused a number of negative ecological impacts to aquatic and terrestrial environments but there are still a number of critical knowledge gaps associated with how dilbit will behave following a spill in a freshwater environment.

A recent report commissioned by the Royal Society of Canada (RSC) identified a number of research needs regarding oil spills (K. Lee et al., 2015). One of their recommendations was to conduct controlled field experiments to better understand how oil behaves in a freshwater environment. They also identified knowledge gaps associated with the uptake and depuration of a wide array of individual and alkylated PAHs (polycyclic aromatic hydrocarbons) for a variety of aquatic species. Another research need the K. Lee et al. (2015) report recognised was to better understand the magnitude of metal contamination following oil spills and potential effects on aquatic organisms.

1.2. Diluted Bitumen

Canada has the third largest oil reserve in the world, spanning from western Saskatchewan to British Columbia. Most oil extraction occurs in the AOS region, where 170 billion barrels of oil is recoverable with current technology (CAPP, 2019). In the oil sands region, bitumen is naturally infused in sandstone containing a mixture of sand, clay, and water. Bitumen derives from former conventional crude oils that extensively biodegraded and chemically transformed *in situ* over geological time (Alsaadi et al., 2018; K. Lee et al., 2015). It is the heaviest class of crude oil, composed of a complex mixture of hydrocarbons and nonhydrocarbon impurities such as N-, O-, S-heteroatoms, and metal-containing constituents (K. Lee et al., 2015; National Academies of Sciences, Engineering, and Medicine, 2016; Z. Wang et al., 1998, 2003). Once recovered, bitumen has high density and viscosity, thus does not flow well through pipelines unless it is heated and/or diluted by diluents (light petroleum products; CAPP, 2019; K. Lee et al., 2015). The mixture of bitumen and diluents is called diluted bitumen, or dilbit. Industries typically use a ratio of 30% diluents to 70% bitumen for its transportation via pipelines, with higher diluent proportions added at lower temperatures (K. Lee et al., 2015; Oil Sands Magazine, 2018, 2020). The diluent in most frequent use is a condensate composed of ultra-light oils partitioned from natural gas wells. In general, dilbit is a complex mixture of roughly 50% hydrocarbons (saturates and aromatic compounds), with the remainder as resins, asphaltenes, naphthenic acids and metals.

1.2.1. Hydrocarbons: Aromatics

The aromatic fraction of dilbit includes cyclic, planar, unsaturated hydrocarbon compounds composed of single or multiple fused benzene rings (Alegbeleye et al., 2017; K. Lee et al., 2015). PAHs are a subclass of aromatic hydrocarbons with two or more fused benzene rings and may contain one or more alkylated side chain. PAHs have gained scientific interest because they can persist in the environment and can be toxic and carcinogenic to organisms. Some PAHs (listed in Figure 1.1) have been classified as 'priority pollutants' (Abdel-Shafy & Mansour, 2016; Canadian Council of Ministers of the Environment, 1999). In general, PAHs are ubiquitous in the environment, where they are mainly formed through pyrogenesis or petrogenesis (K. Lee et al., 2015; Manzetti, 2013; Neff, 2002b). Pyrogenic PAHs derive from the incomplete combustion of organic matter such as petroleum, coal, and wood, while petrogenic PAHs form at lower temperatures from diagenesis and the formation of petroleum. The degree of alkylation of the parent PAH (i.e. PAH compound with no alkylated side chain) is inversely proportional to the formation temperature (Manzetti, 2013). Thus, petrogenic PAHs will contain more alkylated side chains compared to pyrogenic PAHs.

The majority of PAHs (80 to 95%) in diluted bitumen contain alkylated side chains that can alter the compound's physical and chemical properties (Environment Canada et al., 2013; King et al., 2017; K. Lee et al., 2015). In fact, alkylated PAHs have a higher modeled hydrophobicity compared to their parent homologue; thus, they tend to have greater bioaccumulation potential and may be more toxic than their corresponding parent counterpart (Bilodeau et al., 2019; Kang et al., 2016; Lin et al., 2015; Rhodes et al., 2005; Sørensen et al., 2019; Wayland et al., 2007). However, most of the research has overlooked the alkylated homologues and focused on the 16 parent PAHs selected by the United States Environmental Protection Agency (U.S. EPA; Figure 1.1) as priority

pollutants since some were shown to be genotoxic and/or carcinogenic (Andersson & Achten, 2015; Stout et al., 2015). In addition to PAHs, sulfur-containing heterocycles, such as benzothiophenes (BTs), dibenzothiophenes (DBTs), and benzonaphthothiophenes (BNTs) have also shown evidence of bioaccumulation in aquatic organisms (Wayland et al., 2007; Bilodeau et al., 2019). Since BT, BNTs, and DBT are sulfur-containing analogs of PAHs, they are grouped with PAHs as polycyclic aromatic compounds (PACs). Petrochemical mixtures contain many PACs that are not included in the U.S. EPA 16 priority PAHs list, particularly alkylated PACs, leading K. Lee et al. (2015) to recommend a more inclusive assessment to assess the bioaccumulation potential and toxicity of petrogenic compounds.

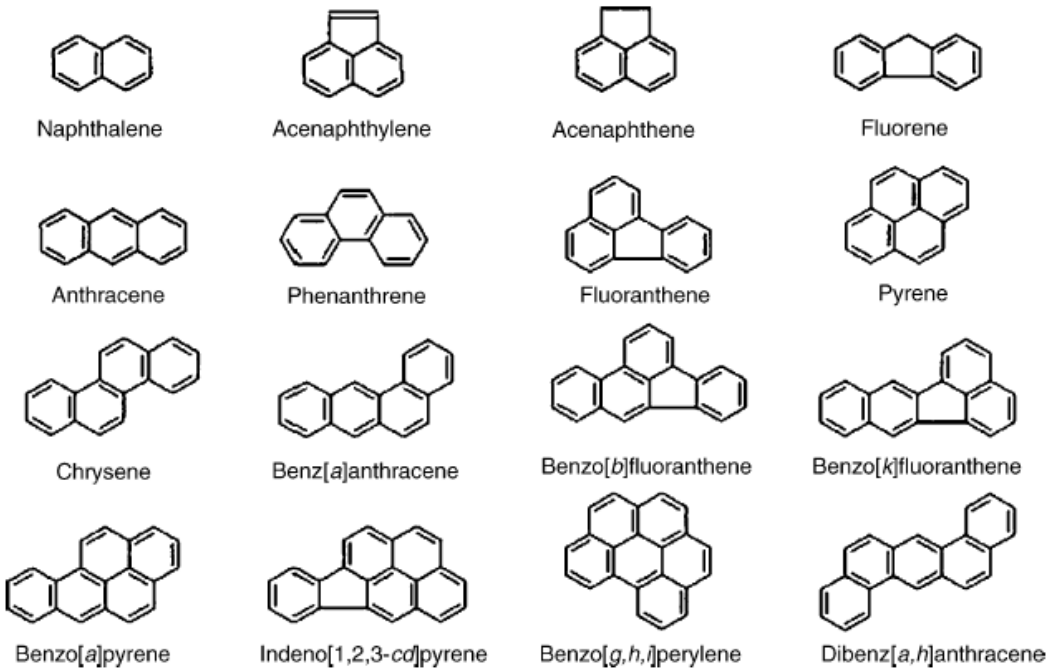

Figure 1.1: The chemical structure of the 16 U.S. EPA Priority PAHs (Anyakora et al. 2011).

1.2.2. Metals and Sulfur

Metals are only a minor component in dilbit, but they can be responsible for significant environmental contamination from oil spills and in areas near oil extraction and refining activities (e.g. AOS region in Alberta; Brooks et al., 2011; K. Lee et al., 2015; Pilote et al., 2018). However, metals in crude oils, especially dilbit, have not received much scientific interest although some metals may reach 1,000 mg kg^{-1} in some oils (Filby, 1994; K. Lee et al., 2015; Mirnaghi et al., 2019; Vale et al., 2008). Generally, vanadium and nickel are the most abundant trace elements in petroleum products and are referred to as 'oil-soluble metals' (Filby, 1994; Mirnaghi et al., 2019). They originate from organic sources (plants and animals) and are present as either non-polar porphyrin or polar non-porphyrin complexes, where their concentrations increase from lighter to heavier crude oils (K. Lee et al., 2015; Mirnaghi et al., 2019; Vale et al., 2008). Other metals, such as zinc, titanium, and calcium can be complexed with naphthenic acid, forming organometallic compounds (K. Lee et al., 2015; Mirnaghi et al., 2019).

The effects of metals associated with dilbit on aquatic species have only been assessed by two controlled laboratory experiments (Krohn et al., 2020; Robidoux et al., 2018), and all other dilbit and bitumen research reported PAH concentrations without data on metals (Alderman et al., 2017; Alsaadi et al., 2018; Barron et al., 2018; Charbonneau, 2016; Chow, 2016; Dew et al., 2015; Everitt, 2020; Madison et al., 2015, 2017, 2020; McDonnell et al., 2019; Philibert et al., 2016; Sereneo, 2016). The study conducted by Krohn et al. (2020) revealed elevated vanadium, molybdenum, and cadmium in wood frog tadpoles (*Lithobates sylvaticus*) exposed to naturally weathered dilbit, but not at levels expected to harm development. Furthermore, assessments of previous oil spills (of various petroleum products) as well as near oil production facilities (e.g. AOS), showed evidence of metals contamination in the water column and sediment (Carmichael

et al., 2012; Kelly et al., 2010; K. Lee, 1983; Pilote et al., 2018; Prego, 2003, 2003; Santos-Echeandía et al., 2008; Wise et al., 2014). Once in the organism, some metals generate reactive oxygen species (ROS) in the mitochondria, leading to oxidative stress causing DNA damage and lipid peroxidation in tissues (Berntssen et al., 2000; Martínez-Álvarez et al., 2005; Rowe et al., 2009; Schiffer, 2016; Soares et al., 2008; Stohs & Bagchi, 1995). The lack of research on metals from dilbit emphasizes the need for a practical assessment of their bioaccumulation potential and toxicokinetics in aquatic organisms.

Sulfur is also a minor constituent in dilbit and is mostly bonded to carbon atoms (organic sulfur), with a small amount (usually > 1%) occurring as elemental sulfur (S^o) or as hydrogen sulfide gas (H_2S; K. Lee et al., 2015). Organic sulfur is generally not an environmental concern, however H_2S is a major concern for toxicity at low concentrations, corrosion to infrastructure (e.g., pipelines and surface handling facilities), and explosion potential in confined spaces (e.g., rail cars). Depending on the water content of the oil and its pH, H_2S may exist as a gas or may dissolve in the water phase. Roughly 35% of the bitumens from the AOS region are diluted for transport and then upgraded into a light synthetic crude before being sold to refineries (K. Lee et al., 2015; Oil Sands Magazine, 2020). Upgrading bitumen removes the sulfur and heavier components as well as to reduce its viscosity. However, high-conversion refineries have integrated "upgrading" equipment and can accept better quality dilbits if they meet pipeline regulations for long-distance travel. Bitumen from the Cold Lake area in the AOS region contain relatively more alkanes and less asphaltenes; are less viscous and sulfurous than other bitumens and can therefore be sent directly to high-conversion refineries once diluted for transport (Keesom & Gieseman, 2018). Therefore, Cold Lake blend (CLB) dilbit will tend to have a higher sulfur content than other dilbits and other products being transported via pipeline.

1.3. Giant Floater Mussels

Giant floater mussels (*Pyganodon grandis*) are freshwater unionid bivalves with a wide distribution in North American lakes and river systems (Grabarkiewicz & Davis, 2008). This species has shown tolerance to a large range of habitats compared to many other freshwater mussels. They are found in shallow streams, lakes, and pools with fine sediment, along with areas dominated by sand and gravel with little to no flowing water. They are relatively large bivalves that can grow as much as 25 cm in length (Grabarkiewicz & Davis, 2008), providing enough biomass for chemical analysis. They are also important ecologically as prey for fish, birds, and mammals.

Mussels are benthic filter feeders, consequently being exposed to contaminants found in both the water column and the sediment. They also have limited mobility, making them more likely to be exposed to pollutants, rather than avoiding them like other mobile species. Many studies have demonstrated that mussels can tolerate a wide range of environmental conditions as well as contaminants, both organic and metallic compounds (Azizi et al., 2018; Farris & Van Hassel, 2007; Grabarkiewicz & Davis, 2008). In particular, mussels are able to accumulate high concentrations of PACs since they have low ability to metabolize organic contaminants compared to other vertebrates (e.g. fish; Azizi et al., 2018; Ko et al., 2018; Livingstone, 1998; Neff, 2002b; Rust et al., 2004; Sreedevi et al., 1992; Stegeman & Lecht, 1991; van Haelst et al., 1996). Monitoring programs around the world (e.g., Mussel Watch Program in North America and the Mediterranean Mussel Watch program in Europe) use different species of bivalves to monitor water and sediment pollution. In fact, a number of studies used bivalve species to assess contamination near offshore oil and gas production areas, or following an oil spill in marine environments (André Lourenço et al., 2015; Breitwieser et al., 2018; Carmichael et al., 2012; Hwang et al., 2014; Soriano et al., 2006;

Sureda et al., 2013; Thomas et al., 2007; Thompson et al., 2017). Giant floater mussels themselves were useful bioindicators for metal contamination in mining areas of northern Québec (Bonneris et al., 2005; Campbell et al., 2005; Cooper et al., 2010, 2013; Couillard et al., 1995; Perceval et al., 2002, 2006; D. Wang et al., 1999) as well as the AOS region (Pilote et al., 2018). Giant floater mussels are useful for bioaccumulation and toxicokinetics studies of PACs and metals from dilbit because they are important ecologically, they are exposed directly to contaminants in both the water and sediment, and they can accumulate high concentrations of PACs in their tissues without detrimental effects, allowing them to integrate environmental conditions over time.

1.4. Bioaccumulation

Bioaccumulation is the net chemical uptake of a substance through all possible routes of exposure (e.g. respiratory surface, dermal absorption, ingestion) taking into account biotransformation and elimination processes (Gobas & Morrison, 2000; Neff, 2002a; Newman & Unger, 2003). In an aquatic environment, sources of PACs and metals to giant floater mussels can include food (plankton), suspended particulates, the water column for dissolved contaminants, and sediment. Once in contact with the organism, both PACs and metals can penetrate through lipid-rich membranes and accumulate in their tissues. These compounds may be transformed and/or incorporated into tissues, or eliminated through metabolism and/or excretion (Livingstone, 1998; Newman & Unger, 2003; Soto et al., 2003). Metabolism is the most important elimination route and is mainly regulated by the hepatopancreas and the kidney, therefore PACs and metals tend to distribute and accumulate in these organs (Fernández et al., 2012; Soto et al., 2003). Studies have also assessed the toxic effects and bioaccumulation potential of petrogenic contaminants on different species of bivalves (André Lourenço et al., 2015; Carmichael et al., 2012; Hwang et al.,

2014; Soriano et al., 2006; Sureda et al., 2011, 2013; Thomas et al., 2007). For example, Hwang et al. (2014) reported lysosomal membrane destabilization in mussels (*Mytilus spp.*) with elevated PAC concentrations collected from oil-impacted sites following the Dubai Star bunker fuel spill in San Francisco Bay, reaching total PAH concentrations of 86,000 ng g^{-1}, dry weight. Assessments of dilbit-derived bioaccumulating compounds in freshwater mussels has not yet been observed in the literature. Since there is a lack of information on the bioaccumulation potential of a wide array of parent and alkylated PACs and metals from dilbit, more studies are required to determine which compounds should be monitored in the event of a dilbit spill, a knowledge gap that was highlighted by the RSC report on the transportation of dilbit in Canada (K. Lee et al., 2015).

1.4.1. Bioaccumulation – PACs

Due to their hydrophobic properties, PACs have low solubility in water and tend to have a strong affinity for the organic phase of suspended particulates and sediment, making both the water column and sediment important exposure routes for bottom dwelling, filter feeding organisms (Alsaadi et al., 2018; Bilodeau et al., 2019; Dong et al., 2016; Iannuzzi et al., 2011; K. Lee et al., 2015; Manzetti, 2013; Rabodonirina et al., 2015). PACs can accumulate in aquatic organisms via passive diffusion through the gills and dermal absorption, respiration (gills), and ingestion of particulate matter or sediment. The hydrophobicity of a compound indicates its affinity for the organic phase (e.g. lipid-rich membranes or organics in sediment) vs. water and can be defined by the octanol-water partition coefficient (K_{OW}; European Chemicals Agency, 2017; Gobas & Morrison, 2000). A compound's K_{OW} value has been used to predict the distribution of a substance in various environmental compartments and typically, PACs with more rings and alkylated groups have higher K_{OW}, making them less soluble in water (European Chemicals Agency, 2017; Gobas

& Morrison, 2000). Generally, gill uptake efficiency of organic contaminants increases in kind with log K_{OW} values between 0.5 and 3. This relationship then plateaus until compounds become very hydrophobic (log K_{OW} greater than 6.0), beyond which uptake efficiency declines due to reduced membrane permeability and/or low aqueous bioavailability (Gobas & Morrison, 2000).

Bioaccumulated PACs in mussels may be metabolized by phase I enzymes from the mixed function oxygenase (MFO) system and phase II enzymes (Brown et al., 1998; Livingstone, 1998; Zanette et al., 2010). The largest class of the MFO system utilizes the heme-thiolate monoxygenase enzyme super family, cytochrome-P450 (CYP) enzymes, also referred to as phase I enzymes (Gauthier et al., 2014). A lack of mechanistic understanding exists regarding CYPs regulation in bivalves (Rebelo et al., 2003; Zanette et al., 2010), but biochemical changes involving CYPs are useful as sensitive biomarkers of exposure to organic contaminants (Bowen et al., 2018; Brown et al., 1998; Fernández et al., 2012; Lopes et al., 2012; Rewitz et al., 2006; Trisciani et al., 2012; Zanette et al., 2010). These studies demonstrated elevated activity of several CYP phase I enzymes (nicotinamide adenine dinucleotide phosphate (NADPH) cytochrome c reductase, CYP2L1, CYP4Y1, and CYP30) in bivalves exposed to organic contaminants in laboratory and field experiments. CYP enzymes oxidize PACs into reactive intermediates such as quinones, epoxides, dihydrodiols, and phenols (Livingstone, 1998; Michel & Beasse, 1995; van der Oost et al., 2003). These reactive metabolites can cause DNA adducts, ROS, lipid peroxidation, membrane disruption, and/or endocrine disruption, resulting in DNA damage and/or genotoxic effects that can lead to development of diseases (i.e. cancer) (Hodson, 2017; Hwang et al., 2014; Manzetti, 2013; Stowers & Anderson, 1985; Xue & Warshawsky, 2005; Zhang et al., 2016). With that being said, PACs themselves are not necessarily carcinogenic until they are activated by phase I enzymes, a process commonly referred to as bioactivation (van der Oost et al., 2003; Xue &

Warshawsky, 2005). Conjugation of the metabolized compounds by phase II enzymes, such as uridine diphosphate glucuronosyltransferases (UGTs), sulfotransferases (SULTs), and glutathione-S-transferases (GSTs), attaches a large polar moiety (e.g. glutathione, sulfate, glucuronide, etc.) to the metabolized compound, rendering them more water soluble and amenable for transport outside the cell, facilitating excretion (Bebianno et al., 2007; Fernández et al., 2012; Guo et al., 2017; Trisciani et al., 2012). Given that PACs are a significant component of dilbit, can be persistent in the aquatic environment, and have bioaccumulation potential in some aquatic organisms that can lead to chronic toxicity (Alsaadi et al., 2018; Dew et al., 2015; Hodson, 2017; K. Lee et al., 2015; Livingstone, 1998, 2003; Shanese Crosby et al., 2013), this thesis will examine the largest, most comprehensive set of toxicokinetic and bioaccumulation information of PACs in freshwater mussels obtained to date. More specifically, 44 analytes, including both parent and alkylated PACs as well as sulfur-containing heterocycles, were analysed in water, sediment, and mussel tissue samples.

1.4.2. Bioaccumulation – Metals

Once in the environment, metals can partition into many different fractions, such as dissolved, organic, carbonate, and iron-manganese oxides. Partitioning, and therefore mobility and solubility of the metal, are all influenced by the metal's oxidative state, which in turn is affected by variations in pH and environmental factors such as temperature, redox potential, organic content, and salinity, all influencing a metal's bioavailability (Azizi et al., 2018; John & Leventhal, 1995). Similar to PACs, metals can also accumulate in sediment, making it an important exposure route for filter feeding benthic organisms (Chon et al., 2012; González-Macías et al., 2006; John & Leventhal, 1995). Trace metals are usually found in the environment at low concentrations and can be

essential to living organisms if they stay within a certain range of concentration. For example, at low concentrations, calcium and zinc are essential elements to organisms as they are important for cell functions, such as membrane stability, metabolism, and enzymatic activities (Laity & Andrews, 2007; Miller, 2004; Soto et al., 2003). However, if their concentrations fall outside the range of sufficiency, either too low or above a certain threshold, they can alter metabolic processes. In contrast, certain trace metals in the environment have no biological functions (e.g., cadmium, lead, and mercury). These non-essential metals can mimic other essential elements and bind with various ligands, altering a variety of biological functions. Metal induced toxicity includes the disruption of vital enzymatic functions, disruption of ion regulation, and catalysing the production of ROS leading to lipid peroxidation and the formation of DNA and protein adducts (Gauthier et al., 2014; Schiffer, 2016; Soto et al., 2003). In order to regulate the accumulation of these trace metals, organisms use physiological and biochemical detoxification processes including excretion, binding to cellular ligands, and sequestration in mineralized granules (Deb & Fukushima, 1999; Soto et al., 2003).

Similar to PACs, dissolved metals can also be taken up by mussels through their gills but metals only enter cells through ion-channels (e.g. calcium and zinc) or pinocytosis (e.g. iron; Bonneris et al., 2005; Deb & Fukushima, 1999; Neff, 2002a; Soto et al., 2003). Furthermore, since mussels are benthic filter feeding organisms, they may ingest any metals bound to particles in the water column or in the sediment. Ingested metals will generally accumulate in the hepatopancreas via the digestive tract where they are metabolized and subsequently excreted (Soto et al., 2003). Kidneys also play an important role in metabolic regulation and excrete the accumulated metals through urine (Deb & Fukushima, 1999; Soto et al., 2003). Organisms have sequestering and detoxifying systems in place to counteract the influx of metals. For example, a variety of metal-

specific P-type ATPases are responsible for maintaining metal-homeostasis within the cell (Gauthier et al., 2014). Furthermore, free metal ions can bind to metallothioneins (MTs), cysteine-rich metal-binding proteins, rendering them unavailable to exert toxicity. Free metals can also be incorporated by lysosomes as intracellular metal rich granules or transported with circulating haemolymph cells (Hogstrand & Haux, 1991; Soto et al., 2003; Thirumoorthy et al., 2007).

If the cells' capacity to regulate metal concentrations is surpassed, metals are capable of catalyzing the production of ROS (e.g. hydroxyl radicals, hydroxyl ions, hydrogen peroxide, etc.), causing oxidative stress leading to DNA damage and lipid peroxidation (Berntssen et al., 2000; Fernández et al., 2012; Schiffer, 2016; Stohs & Bagchi, 1995; Vlahogianni et al., 2007). In addition to regulating metal bioaccumulation, MTs are also capable of scavenging ROS derived from both metals and PAC metabolites (Thirumoorthy et al., 2007). The upregulation of glutathione (GSH) and related antioxidant proteins, such as GSTs, superoxide dismutase (SOD), and glutathione peroxidase (GPx), are other cellular responses used by organisms to regulate the production of ROS in the cell (Gauthier et al., 2014; Newton & Gregory Cope, 2006; Soares et al., 2008). As very little work has been done to determine the bioaccumulating metals derived from crude oil, especially dilbit, I will conduct a more comprehensive accumulation-elimination experiment in this thesis to evaluate the toxicokinetics and bioaccumulation potential of metals derived from dilbit, as recommended by K. Lee et al. (2015).

1.5. Uptake-Depuration Experiment and Toxicokinetics

One of the noted knowledge gaps in the K. Lee et al. (2015) report was the dearth of uptake and depuration rate constants for a wide array of unsubstituted parent and alkylated PACs for a variety of species. Toxicokinetic parameters for compounds can be determined by conducting an uptake-depuration experiment where Figure 1.2 demonstrates ideal first-order rate curves for the uptake and depuration phases. Initially, a short, gradual increase of the contaminant's concentration occurs in an organism until tissue concentrations are at steady state with respect to the exposure medium (Gobas & Morrison, 2000). Following termination of the exposure period, the organism is placed in an uncontaminated exposure medium where the concentration of the contaminant in their tissue decreases, in this case, exponentially (Figure 1.2).

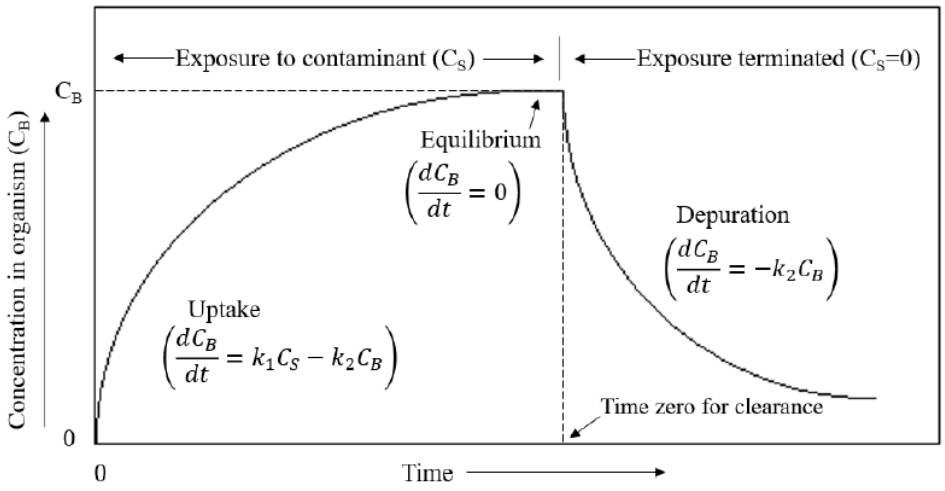

Figure 1.2: Ideal uptake and depuration curve of accumulation-elimination experiments through time (Gobas & Morrison, 2000).

1.5.1. First-Order Toxicokinetic Compartment-Based Modeling

First-order rate coefficient (RC) models can relate the amount or concentration of a compound in one compartment with that in another. When used in an environmental context, RC models describe the organism and environment containing the contaminant as two separate homogeneous compartments and involve first-order uptake from the source (environment) into one compartment (organism) (Gobas & Morrison, 2000; Landrum et al., 1992; Thorsen et al., 2007):

$$\frac{dC_B}{dt} = k_1 C_S - k_2 C_B \quad (1)$$

where C_s (mg L^{-1} for water and mg kg^{-1} for sediment) and C_B (mg kg^{-1}) are the concentration of the contaminant in the exposure medium and in the organisms, respectively, k_1 (L g^{-1} day^{-1}) and k_2 (day^{-1}) are the uptake and depuration rate constants, respectively. From this toxicokinetic model, the depuration phase can be described as:

$$\frac{dC_B}{dt} = -k_2 C_B \quad (2)$$

If the elimination of PACs follows a first-order rate reaction, k_2 can be determined from the natural logarithmic-transformed tissue concentration through time where the slope represents the depuration rate constant (Gobas & Morrison, 2000; OECD, 2012).

If chemical concentrations in the exposure medium remain constant throughout the uptake phase, equation 1 can be integrated to give (DiMauro, 2012; OECD, 2012; Thorsen et al., 2007):

$$C_B = \frac{k_1}{k_2} \times C_S \times (1 - e^{-k_2 t}) \quad (3)$$

Equation 3 can be rearranged to solve for k_1 if k_2 is already determined:

$$k_1 = \frac{C_B \times k_2}{C_S(1 - e^{-k_2 t})} \quad (4)$$

If enough time points exist to capture the accumulation of compounds, and the exposure is sufficiently long so that the uptake curve begins to plateau, uptake and depuration rate constants can also be determined through nonlinear curve fits to an uptake curve using equation 3 (Landrum et al., 1992).

Depuration kinetic rates can also be used to calculate the time required to reach 95 % of steady state (Gewurtz et al., 2002; Meador, 2003; Schmidt et al., 2013; Thorsen et al., 2004):

$$t_{95} = -\ln 0.05 \times k_2 \quad (5)$$

1.5.2. Bioaccumulation Potential

The bioaccumulation potential of different contaminants in aquatic organisms have often been described using bioconcentration factors (BCFs; Gobas & Morrison, 2000; Thomann & Komlos, 1999). BCFs are described as the accumulation of waterborne chemicals in the organism while considering elimination processes such as elimination via respiratory surfaces, fecal matter, metabolic transformation, and growth dilution (Gobas & Morrison, 2000; Landrum et al., 1992). Uptake and elimination processes involved in the accumulation of waterborne chemicals can be represented by the following differential equation (Arnot & Gobas, 2006; Gobas & Morrison, 2000; OECD, 2012; W.A. Thorsen et al., 2007):

$$\frac{dC_B}{dt} = k_1 C_S - (k_2 + k_E + k_M + k_G) C_B \quad (6)$$

where C_B (mg kg^{-1}) and C_S (mg L^{-1}) are the chemical concentration in the organism and the exposure medium (e.g., water column, sediment), respectively, while k_E (day^{-1}), k_M (day^{-1}), and k_G (day^{-1}) represent the first-order rate constants for chemical elimination by fecal egestion, metabolic transfer and growth dilution, respectively. BCFs (L kg^{-1}) in mussels can be calculated either as the

ratio of the concentration of chemicals in mussels and water at steady state, or as the ratio of the uptake and depuration rate constants (Arnot & Gobas, 2006; DiMauro, 2012; OECD, 2012; Thorsen et al., 2007):

$$BCF = \frac{C_B}{C_W} = \frac{k_1}{k_2} \quad (7)$$

The Organization for Economic Co-operation and Development (OECD) guidelines, which describes a procedure for characterizing the bioconcentration potential of organic contaminants in aquatic organisms, recommends expressing BCF values on a 5% lipid content (OECD, 2012). A compound is considered to be bioaccumulative when BCF values are greater or equal to 5,000 (log value of 3.7; Arnot & Gobas, 2006; Government of Canada, 2000). Note that BCFs can vary from one individual to another depending on its life stage (e.g., juveniles and adults) as well as the species of the organism (e.g., fish and bivalves). Thus, using BCFs in cross-species or ecosystem comparisons may not be the best representation for a compound's impacts on that specific environment and must be done with a degree of caution.

1.6. Study Objectives

This thesis will look to address some of the research needs identified in the RSC report on the transportation of dilbit in Canada (K. Lee et al., 2015) by examining the accumulation and toxicokinetics of PACs and metals from naturally weathered dilbit in giant floater mussels. Bivalves are particularly susceptible to petroleum contamination as they are in contact with both sediment and the water column. They are also considered sessile organisms and filter feeders; therefore, they cannot displace themselves by great distances to avoid an oil spill if such an event should occur. For these reasons, they can integrate environmental conditions over time, making

them good bioindicators for water quality in both marine and freshwater environments (Azizi et al., 2018; Schøyen et al., 2017; Soriano et al., 2006; Sureda et al., 2013; Ujević et al., 2015). This thesis represents the first study assessing the bioaccumulation of compounds derived from naturally weathered dilbit in freshwater mussels and will examine, for the first time, the bioaccumulation potential of: (1) polycyclic aromatic compounds (PACs), and (2) metals derived from naturally weathered dilbit in freshwater mussels.

The first objective of this thesis is to determine the bioaccumulation potential of parent and alkylated PACs in giant floater mussels exposed to naturally weathered dilbit. It is well established in the literature that bivalves exposed to oil spills accumulate PACs in their tissues (Breitwieser et al., 2018; Brooks et al., 2011; Hwang et al., 2014; Soriano et al., 2006; Sureda et al., 2013; Thompson et al., 2017). However, no studies have assessed the bioaccumulation potential of PACs from naturally weathered dilbit in freshwater bivalves. I hypothesize that giant floater mussels exposed to dilbit-contaminated water will bioaccumulate PACs. Furthermore, given that recent studies showed greater bioaccumulation potential of alkylated PACs compared to parent (unsubstituted) PACs (Bilodeau et al., 2019; Wayland et al., 2007), I predict that bioconcentration factors (BCFs) for alkylated PACs will be greater than those determined for their unsubstituted parent counterpart. Subsequently, uptake and depurating toxicokinetic parameters will be determined for each PAC.

The second objective of my thesis is to determine the bioaccumulation potential of metals from naturally weathered dilbit in giant floater mussels. As previously mentioned, the concentration of metals in crude oil increases from lighter to heavier crude oils, therefore it is important to consider this fraction when looking at the bioaccumulation potential of dilbit constituents. I hypothesize that giant floater mussels exposed to dilbit-contaminated water will

bioaccumulate metals. I predict that the BCF values for vanadium and nickel will surpass the Canadian persistence and bioaccumulation regulations (BCF values larger than 5,000) as there will be significant contamination of these metals in the water, surpassing the mussel's ability to regulate them. Subsequently, uptake and depuration toxicokinetic parameters will be determined for each metal.

Finally, the third objective of this thesis is to identify compounds that could be potential markers of petroleum exposures. Bivalves have been used a number of times as biomonitoring species to assess the level of contamination in marine and freshwater environments (Azizi et al., 2018; Cooper et al., 2013; Couillard et al., 1995; Pilote et al., 2018; Schøyen et al., 2017; Thompson et al., 2017). I expect that some parent and alkylated PACs will still be detected in tissue following the depuration phase because bivalves in general have lower ability to metabolize organic contaminants compared to vertebrates (Azizi et al., 2018; Livingstone, 2003; Neff, 2002a). If this prediction is confirmed, bivalves may serve as good bioindicators of petroleum contamination in natural environments.

2. In-Lake Limnocorral Study

2.1. General Study Design

We simulated a dilbit spill to a freshwater ecosystem using a series of limnocorrals at the International Institute for Sustainable Development – Experimental Lakes Area (IISD-ELA) in northwestern Ontario during the summer of 2018. This large-scale, collaborative field experiment involved researchers and students from three academic institutes (University of Ottawa, University of Manitoba, and Queen's University) with the in-kind support of Environment and Climate Change Canada (ECCC), Fisheries and Oceans Canada, the Ontario Ministry of Environment and Climate Change, and the National Energy Board. Nine 10 m diameter limnocorrals (Figure 2.1) were installed in May 2018 into Lake 260, a small (34 ha, max depth 15 m) oligotrophic boreal shield lake (Figure 2.2). These limnocorrals were composed of a decagonal floating ring constructed by connecting vinyl-wrapped foam pieces with a metal bracket at each apex. We attached a large reinforced open-ended cylindrical clear polyethylene bag to the floating collar that extended to the bottom sediment. The natural underlying sediment was sealed from the rest of the lake with sandbags, encompassing a natural community of planktonic and benthic organisms. Each enclosure had an approximate average depth of 1.5 m, encompassing roughly 100,000 L of lake water (Table 2.1).

Volume estimates of each enclosure were made using a radioactive tracer (tritium) and monitored over time as described by Rodriguez-Gil et al. (in preparation). A small, partitioned area was created by enclosing a corner of the limnocorral with a piece of floating vinyl-wrapped foam (similar to the floating collar) with a 30 cm deep reinforced plastic material attached to it. This was done to prevent floating oil from crossing over and covering sampling equipment. Outside of each enclosure, adjacent to the partitioned area, a floating dock was attached to the

floating collar, facilitating sample collection through the partitioned area. In the center of each enclosure, a sampling port constructed of 3" polyvinyl chloride (PVC) tube and wye fittings allowed water samples to be collected at three different depths (~ 0.1 m above the sediment, ~ 0.5 m below the water surface, and center depth). We placed three long pieces of plastic tube (one for each depth) inside the sampling port that extended to the floating dock. We labeled these tubes with their appropriate depth and collected water samples from the desired depth with a peristaltic pump.

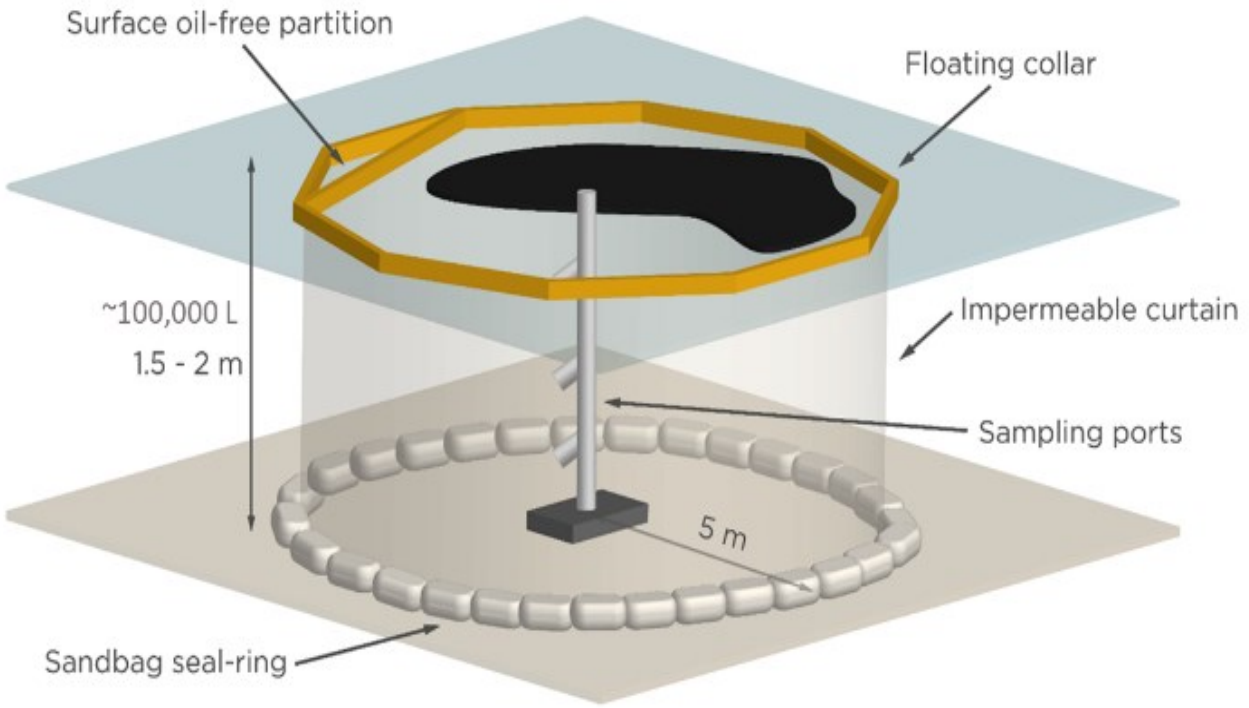

Figure 2.1: A semi-schematic diagram of one of the limnocorrals constructed for the 2018 large scale, in-lake dilbit study.

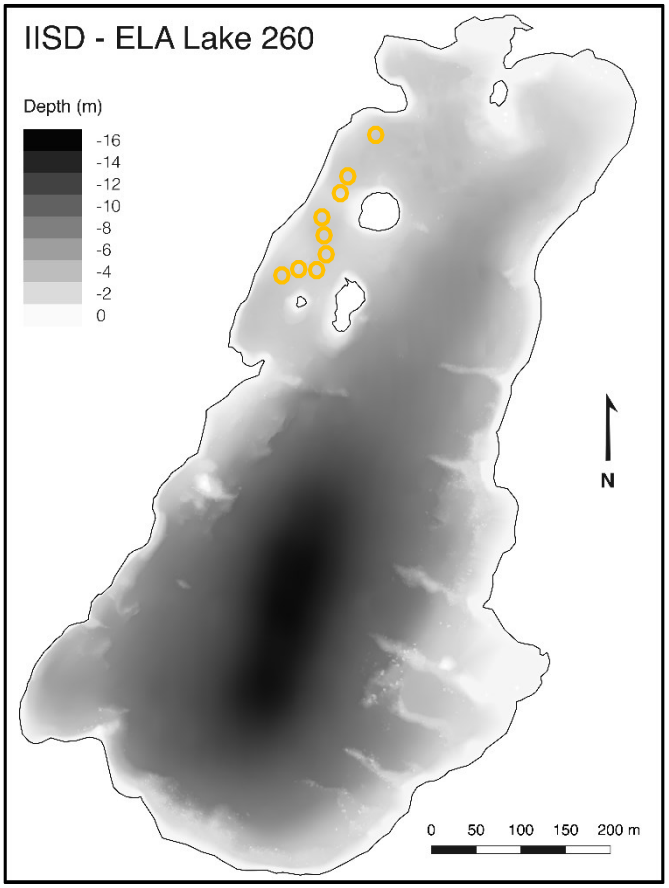

Figure 2.2: Bathymetric map and general information of Lake 260 demonstrating where the dilbit experiment was conducted (yellow decagons). Sources: BOREAL project and IISD-ELA.

Figure 2.3: Overview of the nine limnocorrals used for the simulated dilbit spill conducted at Lake 260.

Table 2.1: The size of each limnocorral and the amount of dilbit added on June 20th, 2018.

Limnocorral	Center Depth (m)	Limnocorral Volume (m^3)	Dilbit (L)	Dilution (Dilbit:Water, v/v)
L4 - Control (Near Field Control)	1.7	103.0	0	N/A
L9 (Far Field Control)	1.5	93.2	0	N/A
L6	1.6	103.8	1.5	1 : 69,200
L5	1.6	97.8	2.9	1 : 33,724
L2	1.5	93.4	5.5	1 : 16,982
L7	1.9	106.8	18.1	1 : 5,901
L3 - Low	1.7	106.5	42.3	1 : 2,518
L8 - Medium	1.7	97.3	81.8	1 : 1,189
L1 - High	1.4	90.7	179.8	1 : 504

Following a brief pre-addition monitoring period (two weeks), different treatments consisting of specific amounts of CLB dilbit (winter blend; Table 2.1) were randomly assigned and added to seven of the nine enclosures and monitored for a total of 80 days (June 20th to September 8th). The oil treatments followed a regression design to simulate a dilbit spill over a range of intensities, resulting in dilbit:water dilutions from 1:69,200 to 1:504, consistent with the upper 50% of the distribution of spill sizes over the last decade in North America (Canada Energy Regulator, 2017; USDOT, 2017), assuming these spills had occurred in a generic boreal lake (volume ~ 2 million m^3). These quantities of oil also fall within the ecologically relevant range for dilbit exposures in a variety of freshwater organisms (Alderman et al., 2017; Alsaadi et al., 2018; Barron et al., 2018; Dew et al., 2015; Madison et al., 2015, 2017; McDonnell et al., 2019; Philibert et al., 2016). This experimental design responded to one of the key research needs identified by K. Lee et al. (2015), that experimental designs for oil spill studies require a wide range of exposure scenarios. The

remaining two limnocorrals were designated as controls for this experiment, in which no dilbit was added. The near-field control (L4) was in proximity to the other limnocorrals treated with various amounts of dilbit, while the other (far-field) control (L9) was located far from the other limnocorrals (Figure 2.3). This design was intended to account for any potential atmospheric re-deposition between the limnocorrals that could transpire throughout the 80 day simulated dilbit spill.

2.2. Bioaccumulation Study Design

In a shed adjacent to Lake 260, we used four 10-gallon aquaria (37.8 L, washed with bleach and uncontaminated Lake 260 water, Figure 2.4) to house giant floater mussels that we collected from a nearby, non-oiled, lake. We filled each aquarium with roughly 8 cm of sand collected from a nearby sand pit at the IISD-ELA. We used a sieve with 1.18 mm opening to remove any twigs and larger particles from the sand. Each aquarium contained 36 mussels with similar size and age (~ 9.0 cm shell length; 7-10 years old) to provide sufficient biomass for both PAC and metals analysis of whole body tissue. Three of these aquaria exposed mussels to contaminated water from the limnocorrals to which the three highest amounts of oil had been added (179.8 L, 81.8 L, and 42.3 L of dilbit designated as the Low, Medium, and High treatments). The last aquarium contained water collected from L4, the near-field control limnocorral and will be referred to as the Control for the remainder of this thesis. The average water temperature and percent saturation of dissolved oxygen during the experiment were 20.4 ± 1.4 °C and 87.2 ± 12.9

Figure 2.4: Aquaria used to house the giant floater mussels. The amount of dilbit added to the respective limnocorral and resulting dilbit:water dilutions of each aquarium are labelled on top.

% (± SD, n=20), respectively. Average pH for the Control, Low, Medium, and High treatments during the exposure phase were 7.2 ± 0.3, 7.4 ± 0.3, 7.4 ± 0.4, and 7.3 ± 0.4, respectively (± SD, n=5 for each treatments).

Following an acclimation period of three days, the experiment consisted of two phases: an initial exposure phase (25 days), allowing the bioaccumulation of oil-derived compounds in mussel tissues, and a subsequent depuration phase (16 days), allowing the accumulated compounds to be excreted. During the exposure phase, we collected water from the limnocorrals (at the lowest depth) with a peristaltic pump in 26.5 L water containers. We conducted roughly eighty percent water renewals every 12 hours for the 25 day uptake period. At six different time points (1 d, 2 d, 5 d, 11 d, 20 d, and 25 d after the start of the exposure period), three mussels, water and sediment samples were collected and stored appropriately (refer to sections 2.3 to 2.5 for more information on how samples were collected and stored). We collected an additional water sample from the High treatment at day zero, resulting in 7 water samples for the High treatment and 6 water samples for the Control, Low, and Medium treatments. Following the exposure period, the remaining mussels were transferred to new aquaria containing clean lake water collected from the dilbit experiment lake, but outside of the treated limnocorrals. Roughly eighty percent water renewals using clean lake water were conducted every 24 hours. Three mussels, water and sediment samples (top 1 cm layer) were collected from these depurating tanks at five different time points (1 d, 2 d, 4 d, 8 d, and 16 d after the start of the depuration period).

2.3. Analysis of Mussel Tissue and Sediment Samples

Once collected, I placed each mussel and sediment sample in individual 120 mL Nasco Whirl-Pak™ bags and stored them at -20 ºC. The age of each mussel was determined by counting the number of well-defined external rings on the shell, each line constituting a rest period during cold weather (Grabarkiewicz & Davis, 2008). Prior to subsampling, samples were thawed overnight. Mussel samples were homogenized by flash freezing using liquid nitrogen and ground into a fine powder using a Magic Bullet 3-piece blender. Sediment samples were simply mixed in the Whirl-Pak™ bags.

2.3.1. Parent and Alkylated PACs

All quantified parent and alkyl PACs and their abbreviations are in Appendix A. The method limits of quantification for target analytes, based on a signal to noise ratio of 3:1, are in Appendix B. Instrument detection limits (IDLs) and method detection limits (MDLs) were calculated based on the equations presented in Loconto (2006). For quality assurance, reference material consisting of 100 mg of 2974a Organics Standard Reference Material® (Freeze-dried *Mytilus edulis* mussel tissue, National Institute of Standards and Technology, USA) was extracted with each set of samples. All samples were blank corrected to remove background PAC contamination. Average recovery rates (average ± SD) were 72 ± 25% for mussel samples (n = 93) and 80 and ± 17% for sediment samples (n= 13).

For parent and alkylated PAC analysis, ~8 g of wet tissue and 14 g of sediment were subsampled and placed in a 50 mL centrifuge tube. Hydromatrix™ (Varian Inc., Palo Alto, CA, USA) was mixed with the tissue or sediment to remove excess water. Each sample was spiked with deuterated surrogate mixture containing naphthalene (D_8, 99.5%), acenaphthene (D_{10}, 99%),

phenanthrene (D_{10}, 98%), benz[a]anthracene (D_{12}, 98%), and perylene (D_{12}, 98%) (Cambridge Isotope Laboratories Inc. Tewksbury, MA, USA). These samples were extracted using accelerated solvent extraction (ASE-200, Dionex Corporation, Sunnyvale, CA, USA) and settings optimized to: dichloromethane (DCM), a pressure of 1500 psi, a heating time of 7 min at 150 ^{o}C, two static cycles of 5 min, and a 50% flush. Samples were then evaporated down to roughly 7 mL under a gentle stream of nitrogen (TurboVap, Biotage, Charlotte, NC, USA) and centrifuged at 6,000 rpm for 10 minutes to remove any remaining particles and water. The supernatants were subsequently evaporated to 1 mL under a gentle stream of nitrogen on the N-Evap (Reacti-Vap™ Model 18780, Pierce, Rockford, IL, USA). Samples were then fractionated using silica gel column chromatography (6 g - Grade 644; Fisher S7441) where 22 mL of *n*-hexane and 40 mL of 1:1 dichloromethane (DCM):*n*-hexane mixture were used to separate the F1 (alkanes and petrogenic biomarkers) and F2 (PACs) fractions, respectively. Samples were once again evaporated to 1 mL in 2,2,4-Trimethylpentane (TMP) under a gentle stream of nitrogen at 23 ^{o}C and 0.4 bar (TurboVap®, Biotage, Charlotte, NC, USA). Finally, samples were spiked with 10 µL *p*-terphenyl-D_{14} as an internal standard before being quantified by gas chromatography coupled with mass spectrometry (GC-MS). All solvents used for this analysis were high-grade Optima® from Fisher Chemical, except TMP (Sigma-Aldrich, Oakville, ON, Canada). Tissue and sediment samples were corrected for percent recovery and tissue samples were normalized by lipid content (see section 2.3.3 for lipid content determination).

2.3.2. Metals

For metals analysis, roughly 15 g of wet mussel tissue and 1.5 g of wet sediment were subsampled and placed in scintillation vials. These samples were freeze dried for a period of 2 days, homogenized and sent to the Geochemistry Laboratory at the University of Ottawa for analysis using inductively coupled plasma mass spectrometry (ICP-MS). In brief, 50 mg of dry tissue or sediment was weighed into a 7 mL perfluoroalkoxy (PFA) vial (Savillex Corporation) and 1.5 mL of high purity concentrated nitric acid (HNO_3) was added. Samples were then placed on a temperature-controlled hot plate and heated at 100 ^{o}C overnight. Digested samples were quantitatively transferred to 15 mL polypropylene vials and diluted to 10 mL gravimetrically with deionized water. A 1 mL portion of the above solution was further gravimetrically diluted by ten-fold (resulting in an approximately 2,000-fold dilution factor) and used for ICP-emission and ICP-mass spectrometric measurements. ICP-ES measurements were performed with an Agilent 5110 Asynchronous Dual View Inductively Coupled Plasma Spectrometer, while ICP-MS measurements were made using an Agilent 8800 Triple Quadrupole Inductively Coupled Plasma Mass Spectrometer. For quality assurance, measurements were done at different dilutions by ICP-ES and ICP-MS, with and without the addition of He as the cell reaction gas and compared to verify potential interferences from polyatomic ions and/or verification purposes. Furthermore, in-house multi-element Check standards were measured for quality control efforts. All samples were blank corrected to remove background metal contamination.

2.3.3. Lipid Content in Mussel Tissue

In addition to PAC and metals analysis, 100 mg of tissue was subsamples for total lipid content determination. Following the Smedes Method (Smedes, 1999), an Ultra-Turrax® homogenizer

(IKA® T10 basic) was used to blend and mix the sample with 800 µL 2-propanol, 1 mL cyclohexane, and 1.1 mL of distilled water. Samples were then centrifuged for 10 minutes at 1500 rpm, where the supernatant was pipetted to a pre-weighed metal weighing dish. The previous steps were repeated once again, this time without mixing in 1.1 mL of distilled water. The resulting supernatant was added to the weighing dish and then air-dried for approximately 24 hours. The lipid content percentage was calculated based on the difference of weight following this equation:

$$\%\ Lipid = \frac{(Dried\ Sample\ with\ Dish - Empty\ Dish)}{Sample\ Wet\ Weight} \times 100\% \quad (9)$$

Giant floater mussels used in this experiment had a mean lipid content of 0.90 ± 0.10 % (± SD n=123).

2.3.4. Percent Organic Carbon in Sediment

Roughly 500 mg of wet sediment was subsampled for percent organic carbon determination. Samples were acid fumigated for 48 hours using hydrochloric acid and then neutralized by distilled water, allowing the samples to settle for a period of 24 hours. The overlying distilled water was then removed using a Pasteur pipette and the previous steps were then repeated two more times. Finally, excess water was removed by freeze drying. Samples were submitted to the Ján Veizer lab at the University of Ottawa, where ~70 mg was weighed into tin capsules and mixed with tungstic oxide (WO_3). Prepared capsules are flash combusted in a Micro Cube elemental analyser (Elementar, Germany) at a temperature of 1800 ºC with the addition of oxygen. Gas products were carried by ultra-pure helium through reducing/oxidizing columns before being trapped within a single "trap and purge" adsorption column. Detection was accomplished by a thermal conductivity detector, with a routine analytical precision (2 sigma) of +/-0.1%.

2.4. Analysis of Water Samples

2.4.1. Parent and Alkylated PACs

Water samples for hydrocarbon analysis were collected in 1 L amber glass jars and stored at 4 ºC. Within 7 days of sample collection, 50 mL of DCM as well as 1 mL of surrogate standard mixture (containing 20 ppm *o*-terphenyl, 20 ppm $C_{24}D_{50}$ and 1 ppm deuterated PAHs - manufactured by SPEX CertiPrep Labs, NJ, USA) were added to the sample. The bottle was then sealed and shaken vigorously, venting periodically, until there was no visible/audible gas coming out of the bottle (roughly 45 seconds). Water samples were then placed onto a roller apparatus (DWK Life Sciences Wheaton™ Bottom-Drive R2P 2.0 Roller Apparatus, Product # WWRBPR 5050), allowing samples to mix for a period of at least 16 hours at 8 rpm. The DCM phase was then collected with a glass pipette and stored in 125 mL amber jars at 4 ºC for further sample processing in Ottawa.

Any water remaining in the sample was removed using Na_2SO_4 and then evaporated to roughly 2 mL through roto-evaporation (Rotavapor® R-210 / R-215, BÜCHI Labortechnik, 9230 Flawil, Switzerland) at 40 ºC and 125 rpm. Similar to the analysis of PACs in mussel tissue, water samples were fractionated using silica gel column chromatography (3 g - Grade 644; Fisher S7441) but this time, 12 mL of n-hexane and 15 mL of 1:1 dichloromethane (DCM):n-hexane mixture were used to separate the F1 (alkanes and petrogenic biomarkers) and F2 (PACs) fractions, respectively. Samples were evaporated to 1 mL and solvent exchanged to TMP under a gentle stream of nitrogen at 23 ºC and 0.4 bar (TurboVap®, Biotage, Charlotte, NC, USA). Finally, samples were spiked with 10 µL *p*-terphenyl-D_{14} as an internal standard before being quantified by GC-MS. All solvents used in this study were high-grade Optima® from Fisher Chemicals, except for TMP (Sigma-Aldrich, Oakville, ON, Canada).

All quantified parent and alkyl PACs and their abbreviations are listed in Appendix A. The method limits of quantification for target analytes, which were based on a signal to noise ratio of 3:1, are detailed in Appendix B. IDLs and MDLs were calculated based on the equations presented in Loconto (2006). All samples were blank corrected to remove background PAC contamination and corrected for percent recovery. Average recovery rates (average ± SD, n=32) were 53 ± 10% for water samples.

2.4.2. Metals

Water samples for metals analysis were collected in 50 mL digiTUBEs® (PerkinElmer®) at each time point. 15 mL of the 50 mL was filtered using a 0.45 µm digiFILTER™ for dissolved metal analysis while the remaining water sample (35 mL) was designated for total metals. Samples were preserved using 70% HNO_3 (1% of total volume) after filtering and stored at 4 °C. Samples were submitted to the Geochemistry Laboratory at the University of Ottawa for analysis using ICP-MS. For quality insurance, measurements were done by ICP-ES and ICP-MS, with and without the addition of He as the cell reaction gas, and compared to verify potential interferences from polyatomic ions, or verification purposes. All samples were blank corrected to remove background metal contamination. Total metals for DB-1342 (Low treatment at day 2 of the uptake phase) could not be analysed because the sample was accidently spilled during processing.

2.5. Statistical Analysis

One-way ANOVAs (parametric test), Welch one-way and t-tests (parametric tests), Tukey's honest significant differences (HSD) tests (parametric test), Kruskal-Wallis rank sum test (non-parametric test), pairwise comparisons using Wilcoxon rank sum tests (non-parametric test), or unpaired two sample t-test (parametric test) were performed when assumptions were met (where applicable) to test for differences in PAC and metal concentrations present in the water column and sediment across treatments and within treatments over time (p-value of 0.05). These tests were also used to determine if there were any differences between PAC toxicokinetic parameters and bioconcentration factors. Shapiro-Wilk and Levene's tests were used to verify the normality of distribution and the homogeneity of variance (p-values of 0.05). When required, the data were transformed prior to statistical analysis to meet parametric assumptions. If the transformed data did not meet parametric assumptions, non-parametric statistical tests were performed. Uptake and depuration rate constants and their 95% confidence intervals were compared to determine if there were any significant differences in toxicokinetic parameters between treatments. Simple linear regressions were used to analyse the relationship between concentrations (in mussel tissue and water), toxicokinetic parameters, log K_{OW} and molecular weight. All statistical analyses were conducted using R studio (version 3.5.2).

3. Accumulation of PACs in Giant Floater Mussels

3.1. PAC Concentrations in the Exposure Water and Sediment

A one-way ANOVA analysis revealed significant differences in TPAC concentrations between dilbit-contaminated treatments and the Control as well as Lake 260 water (p-value < 0.001). Dilbit-contaminated water had significantly greater TPAC concentrations compared to water from the Control and Lake 260 (Table E.2) where the Low, Medium, and High treatments had average TPAC concentrations of 0.40 ± 0.09 µg L^{-1} (±SD, n=5), 0.51 ± 0.15 µg L^{-1} (±SD, n=6), and 0.90 ± 0.24 µg L^{-1} (±SD, n=7), respectively, while the Control and Lake 260 water had TPAC concentrations of 0.017 ± 0.012 µg L^{-1} (±SD, n=5), and 0.0092 ± 0.0008 µg L^{-1} (±SD, n=3), respectively (Figure 3.1). Pairwise comparisons using Tukey's honestly significant difference (HSD) test revealed significantly higher TPAC concentrations in the water from the High treatment compared to the Medium and Low treatments (p-values < 0.001 and 0.001, respectively). However, I observed no significant differences in TPAC concentrations between the Low and Medium treatments (p-value 0.79). I also observed no significant differences in TPAC concentrations between the Control and Lake 260 water (p-value > 0.99).

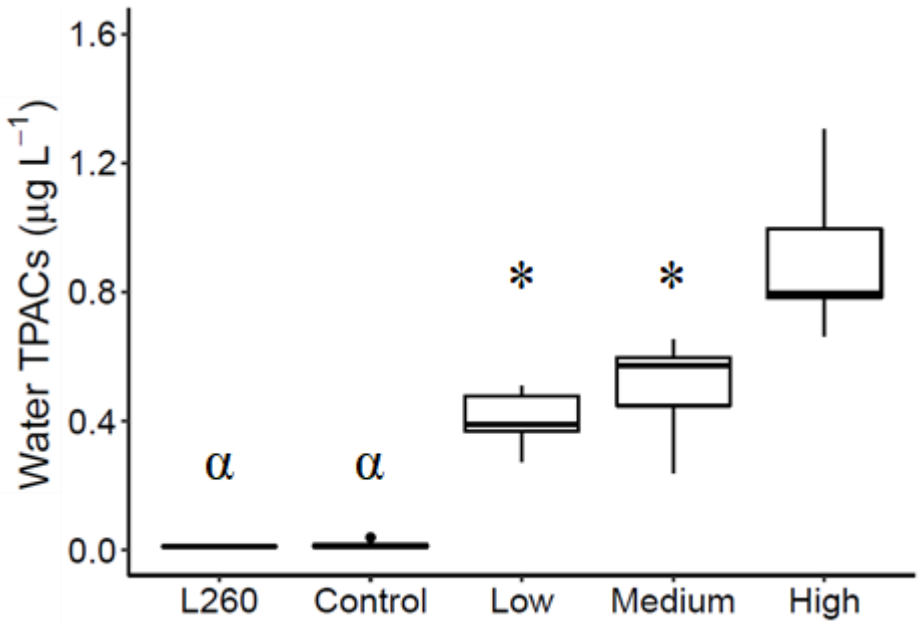

*Figure 3.1: Box plot illustrating TPAC concentrations in aquaria water during the uptake phase of the bioaccumulation study (n=5, 5, 6, 7, and 3 for the Control, Low, Medium, and High treatments, as well as Lake 260, respectively). One-way ANOVA analysis (Table E.1) and pairwise comparisons using Tukey's HSD test (Table E.2) conducted in R Studio revealed no significant differences between the Low and Medium treatments (p-value 0.79, denoted by *) as well as the Control and Lake 260 (p-value 1.00, denoted by α) while all other comparisons were significantly different (p-value < 0.05).*

One of the water samples collected from the Low treatment on day 20 of the uptake phase (DB-1561) had relatively high PAC concentrations; especially pyrene concentrations where they were 78 times higher than the average (n=5; excluding DB-1561) from the Low treatment. We found elevated concentrations of petroleum biomarkers, such as a number of terpanes, hopanes, and steranes, in this sample as a result of small dilbit particles in the water. Furthermore, filtering contaminated water through 0.45 µm filter for other analyses (dissolved metals analysis) revealed very small, trapped particles of dilbit for a small number of samples. Two water samples (DB-1761 and DB-1794) collected from the Control on day 25 of the uptake phase and Lake 260 during the depuration phase had relatively high PAC concentrations, mainly C3-fluorenes, which was 31

times and 27 times higher than the average from the control (n=5; excluding DB-1761) and Lake 260 (n=3; excluding DB-1794), respectively. We compared their chromatograms to a dilbit sample and it revealed that contamination was not related to dilbit. No other water sample had any apparent contamination unrelated to dilbit. Therefore, DB-1561, DB-1761, and DB-1794 water samples were all removed from any analyses conducted in this thesis (including the analyses previously conducted in this chapter).

Statistical analyses revealed that TPAC concentrations in the dilbit-contaminated water from the aquaria used for the bioaccumulation study were significantly lower than the TPAC water concentrations in the enclosures, as measured in the 'fate and behaviour' subtheme (FaBS) of the BOREAL project (Table E.3, Figure 3.2). Water samples for FaBS were collected directly from the limnocorrals and stored in 1 L amber bottles for PACs analysis while water samples for this bioaccumulation study were collected in 26.5 L plastic jugs, transported to the shed onshore, and then stored in 1 L amber bottles, which took approximately 1 hour. Differences in sample collection could have resulted in lower PACs concentrations compared to the FaBS study. Nonetheless, the general trends between the two studies are similar. For example, TPAC concentrations in the High treatments from both studies were higher than the Low and Medium treatments (Figure 3.2). Furthermore, TPAC concentrations from the Low and Medium treatments for both studies were very similar. I also found no significant differences when I compared the Control treatments from the two studies (p-value 0.11).

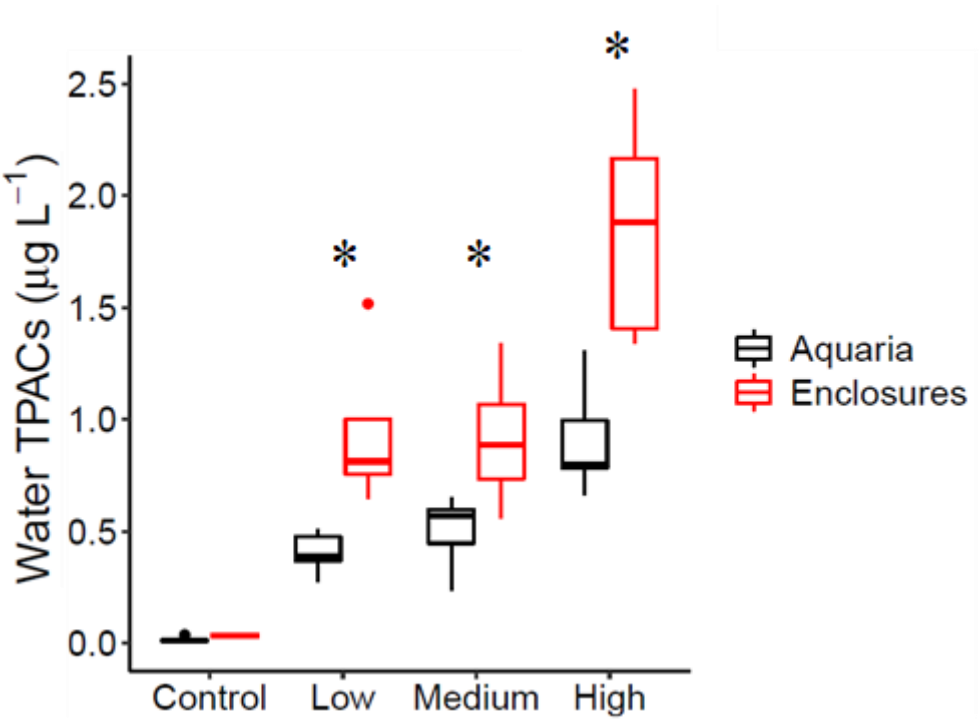

*Figure 3.2: Box plot demonstrating TPAC concentrations in aquaria water during the uptake phase of the bioaccumulation study (aquaria, n=5, 5, 6, and 7 for the Control, Low, Medium, and High treatments, respectively), as well as TPAC concentrations in the water collected within the same time frame from the limnocorrals for the FaBS (limnocorrals, n=6 per treatment). Student's t-tests and unpaired Wilcoxon rank sum tests (Table E.3) conducted in R Studio revealed significant differences (p-value < 0.05, denoted by *) between the two studies when comparing the same dilbit-contaminated treatments.*

PAC concentration profiles of the dilbit-contaminated water (Figure 3.3), and statistical comparisons between the Low, Medium, and High treatments revealed significantly higher concentrations of alkylated PACs (especially with 1, 2, or 3 alkyl substitution [C1-, C2-, and C3-]) compared to their parent counterparts (p-value < 0.05; Table E.4). Alkylated PACs typically indicate a petrogenic source (K. Lee et al., 2015; Manzetti, 2013; Wang et al., 2003), and follows the general chemical profiles of the CLB bitumen used for the BOREAL project (Figure 3.4). We observed increasing Σalkyl PACs concentrations in the Low, Medium, and High treatments (0.38 ± 0.09 µg L^{-1} (±SD, n=5), 0.48 ± 0.15 µg L^{-1} (±SD, n=6), and 0.87 ± 0.22 µg L^{-1} (±SD, n=7),

respectively) while Σparent PACs were 0.024 ± 0.008 µg L^{-1} (±SD, n=5), 0.024 ± 0.012 µg L^{-1} (±SD, n=6), and 0.030 ± 0.020 µg L^{-1} (±SD, n=7), respectively (Figure 3.5). On average, Σalkyl PACs accounted for 94%, 95%, and 97% of the TPACs in the Low, Medium, and High treatments, respectively. We observed a higher proportion of parent PACs (25%) in water samples from the Control indicating that dilbit spills in freshwater environments result in the enrichment of alkylated PACs in the water; compounds that studies have shown to bioaccumulate in aquatic organisms (Bilodeau et al., 2019; Enwere et al., 2009; Sørensen et al., 2019; Thorsen et al., 2004; Wayland et al., 2007)

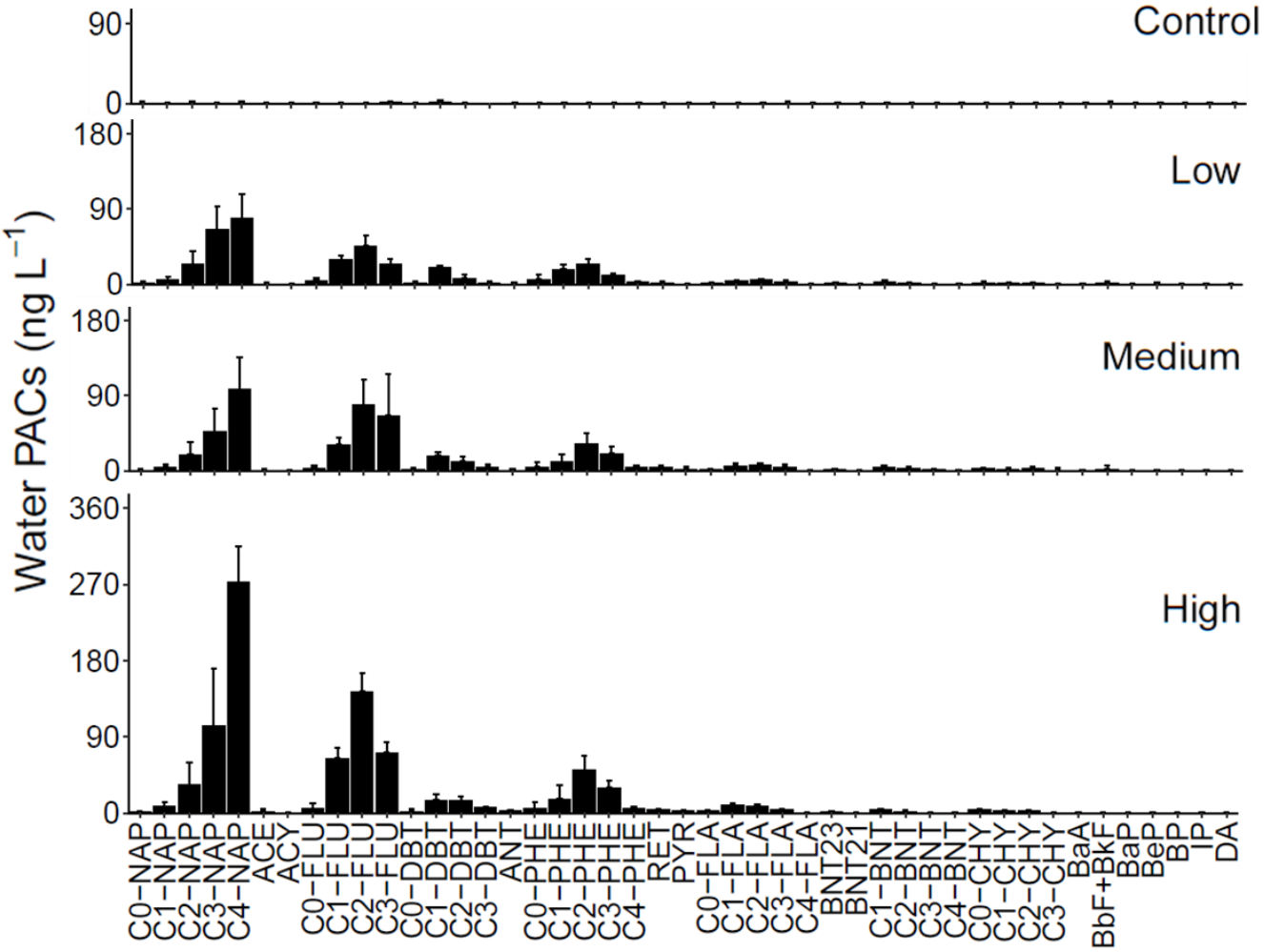

Figure 3.3: Mean (±SD) PAC concentrations (n=5, 5, 6, and 7 for the Control, Low, Medium, and High treatments, respectively; ng L^{-1}) in the aquaria water for all four treatments during the accumulation phase. Abbreviations are found in Appendix A.

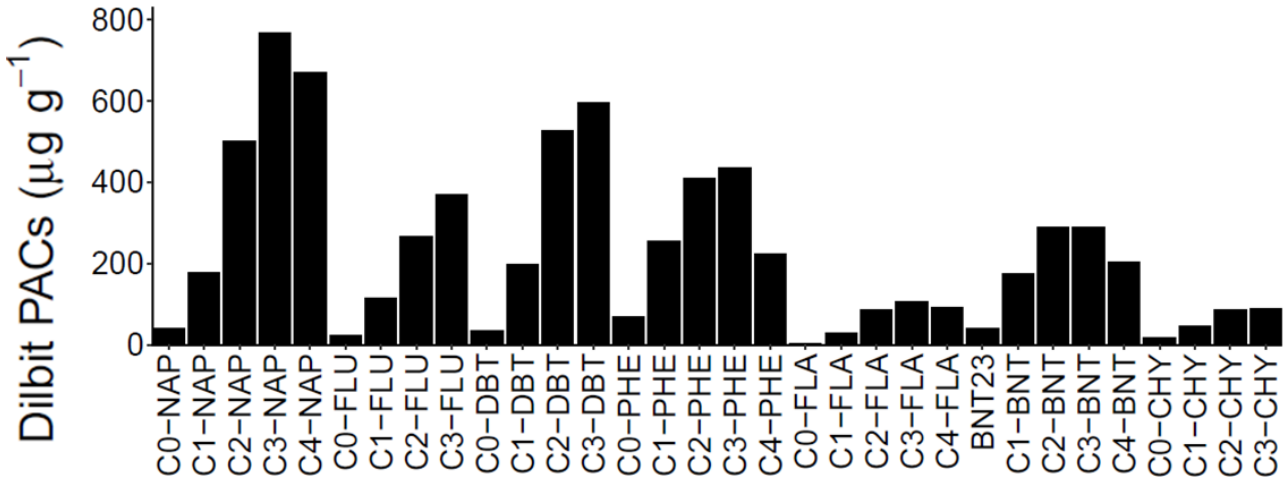

Figure 3.4: PAC concentrations of the Cold Lake diluted bitumen used in the BOREAL project. Abbreviations are found in Appendix A.

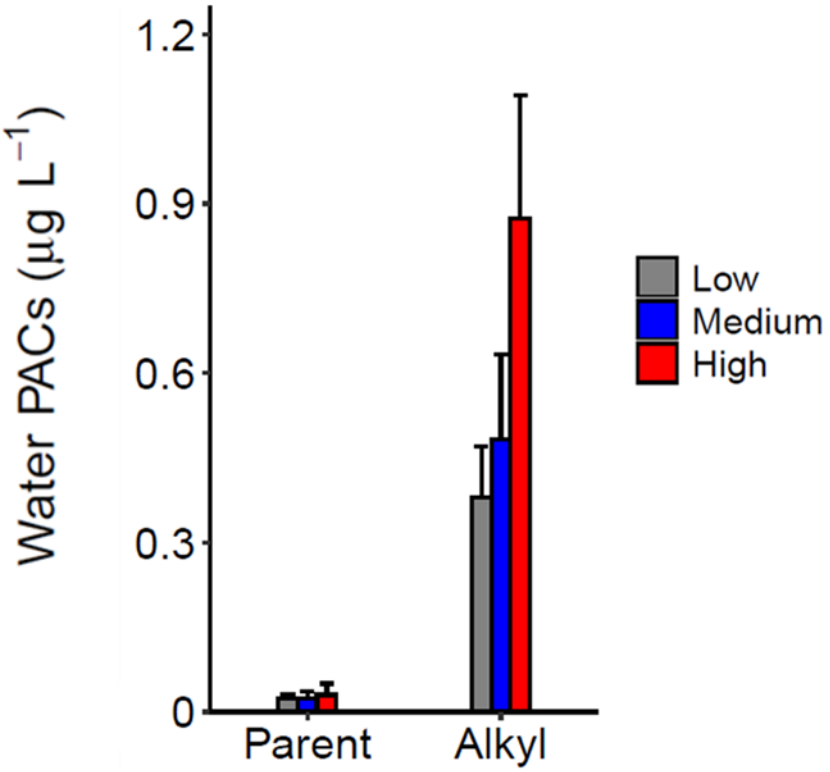

Figure 3.5: Mean (±SD) parent and alkyl PAC concentrations (n= 5, 6, and 7 for the Low, Medium, and High treatments, respectively; µg L^{-1}) in the water collected from all three treatments during the uptake phase. Student's t-tests and unpaired Wilcoxon rank sum tests (Table E.4) conducted in R Studio revealed significant differences (p-value < 0.05) when comparing Σparent and Σalkyl PACs concentrations for every dilbit-contaminated treatment.

The most abundant parent PACs in all three contaminated treatments were (in descending order): phenanthrene, fluorene, and chrysene. The alkylated PAC groups that accounted for the most of the TPAC concentrations in the Low, Medium, and High treatments were alkyl naphthalenes (C1-, C2-, C3-, C4-; 42%, 33%, and 46% in the Low, Medium, and High treatments, respectively), alkyl fluorenes (C1-, C2-, C3-; 25%, 35%, and 32% in the Low, Medium, and High treatments, respectively), and alkyl phenanthrenes (C1-, C2-, C3-, C4-, retene; 14%, 14%, and 12% in the Low, Medium, and High treatments, respectively). Similar to TPAC concentrations, significantly greater concentrations of individual PACs were detected in the High treatment compared to the Low and Medium treatments while few significant differences were found between the Low and Medium treatments (Tables E.2). Overall, the concentration of 36 PACs were significantly greater in dilbit-contaminated treatments compared to the Control. Notably, none of the PACs from any of the treatments surpassed the Canadian Water Quality Guidelines for the Protection of Aquatic Life (Canadian Council of Ministers of the Environment, 1999). This outcome was similar to the Kalamazoo spill in Michigan where the large majority of PAC concentrations in the water samples (list of PACs or concentrations not reported) did not surpass U.S. EPA nor the Mississippi Department of Environmental Quality water quality criteria (U.S. Fish and Wildlife Service et al., 2015). However, none of these guidelines include alkyl PACs; potentially underestimating the impact of these compounds as they are much more prevalent in dilbit-contaminated waters compared to parent PACs.

Linear regression analyses of log-transformed PAC concentrations in the water against log K_{OW} revealed no significant relationships for all three dilbit-contaminated treatments (Figure 3.6). This is surprising as hydrophobicity is often related to the compound's affinity for the aqueous phase and we might expect a negative correlation. However, since alkyl PAC concentrations in

dilbit are an order of magnitude higher than their parent counterparts, higher concentrations of the more hydrophobic alkyl PACs were detected in water samples, resulting in no significant relationship. In fact, regression analyses of log-transformed PAC concentrations in water and dilbit revealed significant positive relationship for all three dilbit-contaminated treatments where alkyl PACs were elevated in dilbit and in water (Figure 3.7). Interestingly, linear regression analyses of log-transformed PAC concentrations in the water and their associated molecular weight revealed a significant negative relationship for the High and Low treatments (p-values 0.048 and 0.049, respectively), where lighter PACs occurred at higher concentrations compared to heavier PACs (Figure 3.8). There is also a negative relationship for the Medium treatment, but this was not significant (p-value 0.30).

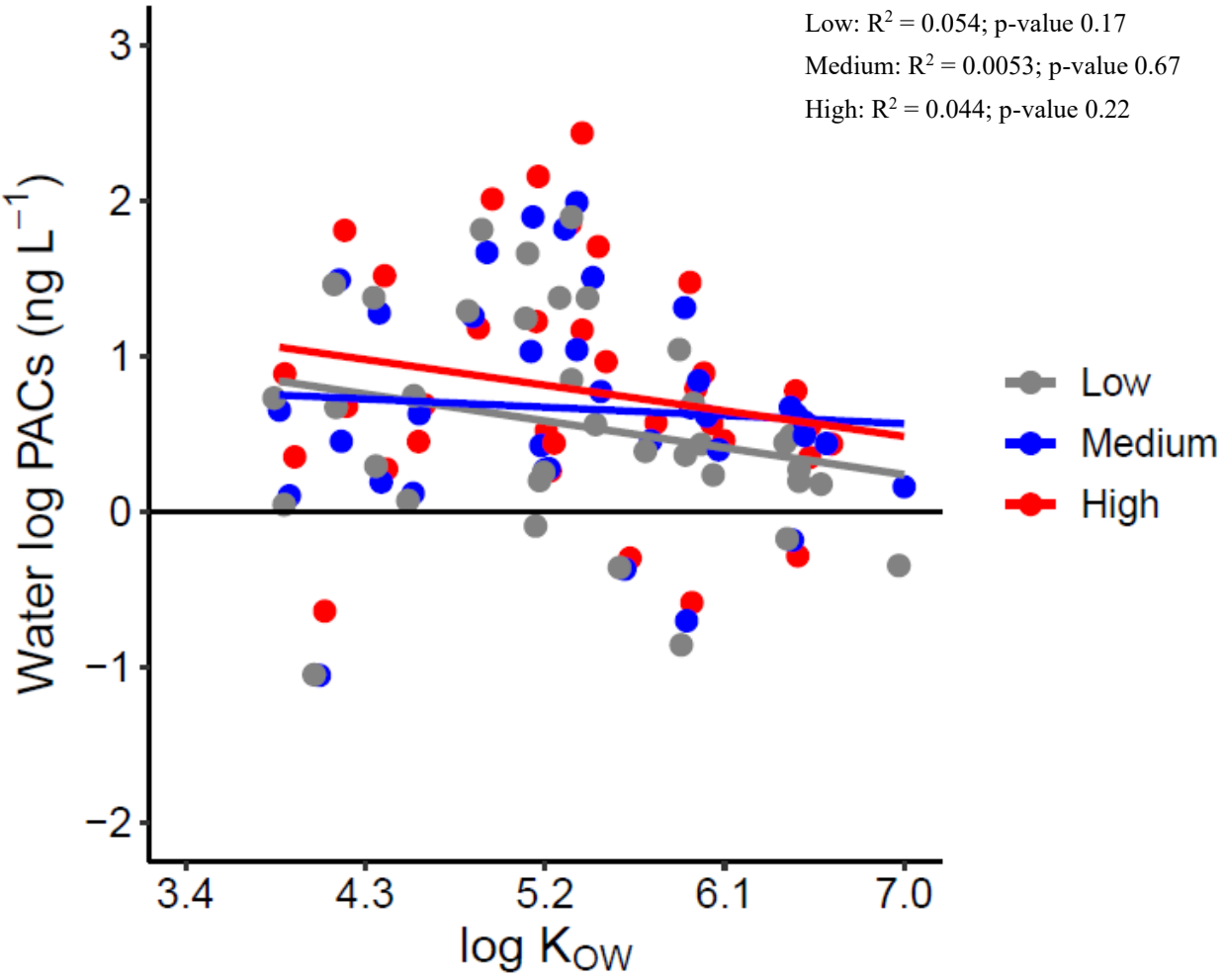

Figure 3.6: Log concentrations of individual PACs (n=36 per treatment) in dilbit-contaminated water in comparison to the compound's log-transformed hydrophobicity (K_{OW}). Only PACs that were significantly greater in water-contaminated with dilbit compared to the Control were selected. Water concentrations are the average log-transformed concentrations of all uptake time points (n=5, 6, and 7 for the Low, Medium, and High treatment, respectively) for each treatment contaminated with dilbit. Data were analysed by linear regression using R Studio and revealed no significant relationships (p>0.05).

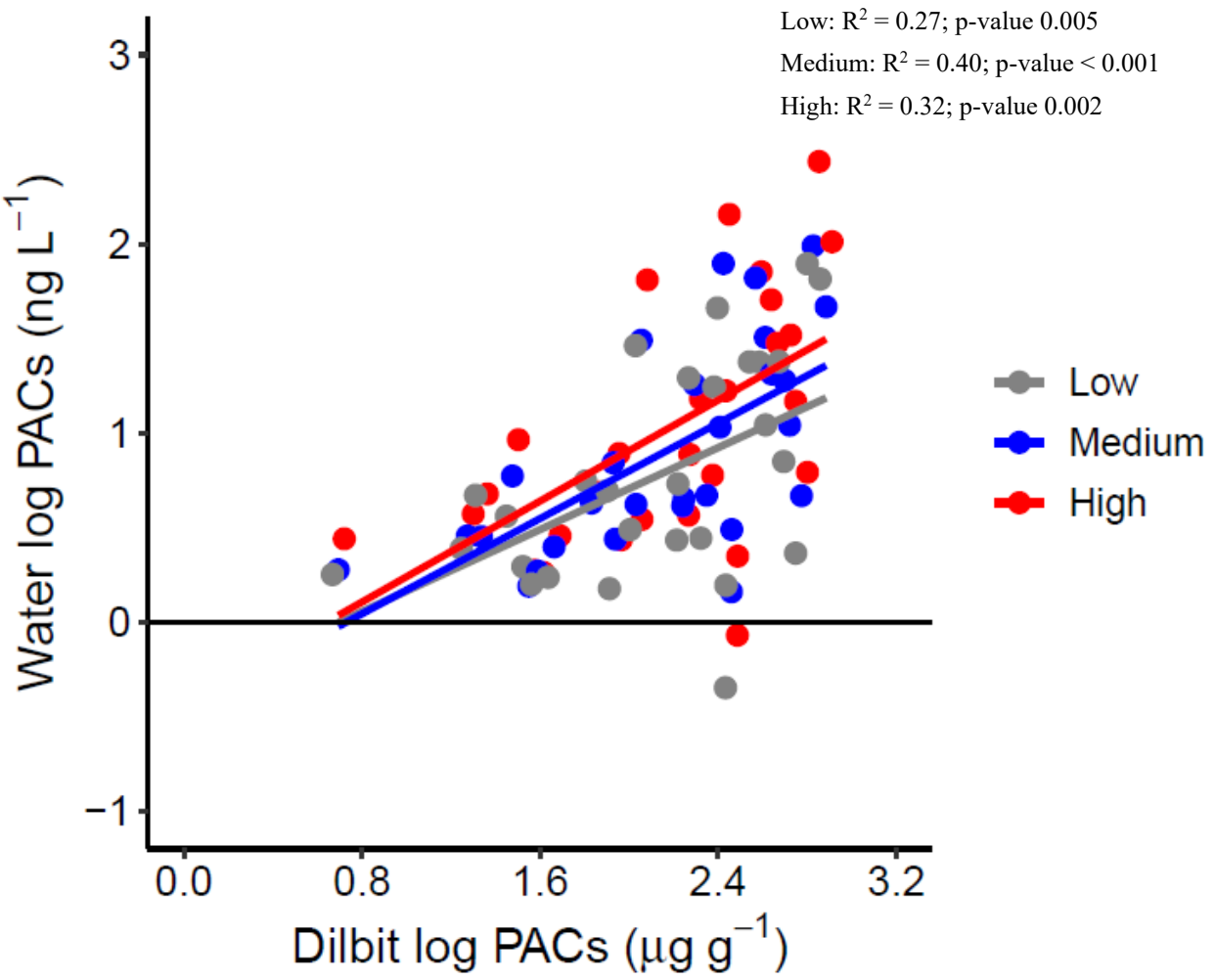

Figure 3.7: Log concentrations of individual PACs (n=28 per treatment) in contaminated water versus log concentrations of individual PACs in CLB dilbit. PACs were only included if they were significantly higher in dilbit treatments compared to the Control and if they are listed in Table C.4. Water concentrations are the average log-transformed concentrations of all uptake time points (n=5, 6, and 7 for the Low, Medium, and High treatment, respectively) for each treatment contaminated with dilbit. Data were analysed by linear regression using R Studio and revealed significant relationships for all three dilbit-contaminated treatments (p<0.05).

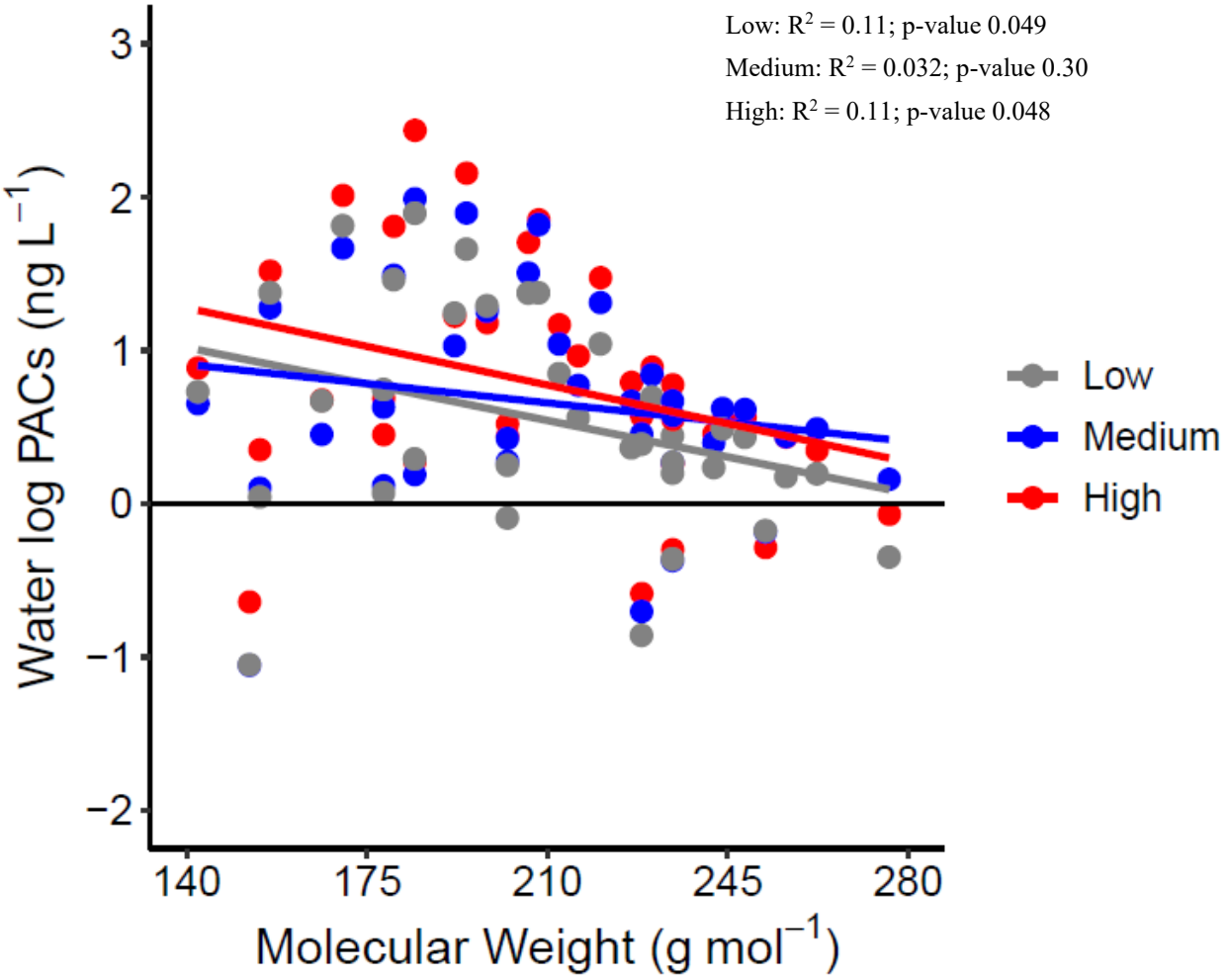

Figure 3.8: Log concentrations of individual PACs (n=36 per treatment) in the dilbit-contaminated water in comparison to the compound's molecular weight. Only PACs that were significantly greater in water-contaminated with dilbit compared to the Control were selected. Water concentrations are the average log-transformed concentrations of all uptake time points (n=5, 6, and 7 for the Low, Medium, and High treatment, respectively) for each treatment contaminated with dilbit. Data were analysed by linear regression and significant relationships for the High and Low treatments were found ($p<0.05$) but not for the Medium treatment ($p>0.05$).

One-way ANOVA analysis revealed no significant differences in sediment TPAC concentrations when comparing all four treatments (p-value 0.55, Appendix E.8), indicating no PAC contamination in the bottom sand as a result of the dilbit-contaminated water, likely due to its very low organic content (average of 0.034 ± 0.005%, n=3 ±SD). Tukey's HSD tests showed that C1-naphthalenes from the High treatment were significantly greater than the Medium treatment (p-value 0.02, Appendix E.9), but concentrations in both treatments were very low and I found no significant differences between the Control and High treatment (p-value 0.46, Appendix E.9). If both the water and sediment were significant contributors of PAC exposure, it would be difficult to differentiate which exposure medium contributed to the accumulation of PACs in the organism and would add complexity when modelling the accumulation of PACs. Since PAC contamination in the sediment was not a factor in this experiment, any PAC accumulation in mussel tissue was a result of exposure to contaminated water only. However, dilbit can sink in freshwater, as seen in the Kalamazoo River spill (U.S. Fish and Wildlife Service et al., 2015), as well as in a study involving outdoor microcosms containing natural lake water (Stoyanovich et al., 2019), making dilbit-contaminated sediment a potential source of PACs for freshwater mussels. Studies have demonstrated the relevance of PAC contaminants in the sediment for bivalves (Baumard et al., 1999; C.-H. Lee et al., 2014; Thorsen et al., 2004). Therefore, further research to determine the potential source of PACs from sediment contaminated with dilbit to freshwater mussels is required.

3.2. PAC Bioaccumulation in Giant Floater Mussels (*Pyganodon grandis*)

Giant floater mussels used in the bioaccumulation study had a mean wet weight (ww) of 24.60 ± 9.27 g (± SD n=117, excluding shells), average shell length of 8.87 ± 0.71 cm long (± SD n=123) and between 7 to 10 years old, making them all adults. We determined the age of mussels by counting the number of lines found on their external shells, which is an indication of a rest period during cold weather (Grabarkiewicz & Davis, 2008). These mussels had a mean lipid content of 0.90 ± 0.10 % (±SD n=123) and a mean percent water content of 94.80 ± 2.89 % (± SD n=123).

Five mussels (t2-M4-1, t2-M3-2, t11-M8-3, t20-M3-3, t1-M3-1-D), collected from different treatments at different time points, could not be analysed for PACs due to insufficient amount of tissue available. These mussels were smaller than the average and more tissue was required for PACs analyses than originally anticipated. Additionally, two mussels (t5-M8-2 and t8-M8-2-D), both collected from the Medium treatment but at different time points (days 5 and 33 of the experiment), had relatively high TPAC (total PACs) concentrations compared to any other mussels from the medium treatment at the same time points (5 and 3 times higher, respectively). We found no petroleum biomarkers suggesting that these spikes in TPACs is not due to attached dilbit particles to the mussel. Furthermore, we compared the chromatograms from tissue samples and a bitumen sample and the PAC peaks were very different, implying that the contamination was not associated with dilbit. Therefore, t5-M8-2 and t8-M8-2-D mussel samples were omitted from any analyses conducted in this thesis.

A large number of mussels from all four treatments at various time points, including a mussel collected for background PAC concentrations, had relatively high concentrations of C2-chrysenes (representing as much as 69% of TPACs). When we compared chromatograms from tissue samples and a bitumen sample, the C2-chrysenes peaks for both samples were very different. This suggests

that elevated concentrations are most likely related to sample matrix interferences with the GC-MS as lipids were not removed from tissue samples. C2-chrysenes concentration were thus removed from any analyses conducted in this thesis.

Three giant floater mussels were analysed to assess background TPAC concentrations (at time 0). The average background TPAC concentrations (1.37 ± 1.09 μg g^{-1}, ww Lipid, ±SD, n=3) detected in mussels from this study were lower or very close to what has been previously reported in bivalves (both freshwater and marine) collected from reference sites in a number of biomonitoring studies (André Lourenço et al., 2015; Breitwieser et al., 2018, 2018; Brooks et al., 2011; Sureda et al., 2013; Thompson et al., 2017; Uno et al., 2010). Background PAC concentrations were also low enough to observe clear uptake and accumulation of PACs once exposed to dilbit-contaminated water. Throughout both phases of this bioaccumulation experiment, I observed no mortalities. However, one mussel collected at day 11 from the Low treatment had very low TPAC concentrations (~2.3 times lower) compared to the two other mussels from the same time point. A possible explanation for this low TPAC value was undetected mortality by the assistant who helped collect mussels. I observed no evidence that any other mussels died during this bioaccumulation experiment, and I personally collected the large majority of the mussels.

We detected peak TPAC concentrations in mussels at day 25 of the uptake phase (last time point) suggesting that PACs may have not reached steady state (discussed later in the chapter). All dilbit-contaminated treatments at day 25 had similar TPAC concentrations in mussels, reaching concentrations of 27.48 ± 4.17 μg/g, ww Lipid (±SD, n=3), 25.92 ± 11.08 μg g^{-1}, ww Lipid (±SD, n=3), and 27.79 ± 6.91 μg/g, ww Lipid (±SD, n=3) in the Low, Medium, and High treatments, respectively (Figure 3.9). The mean TPAC concentrations in mussels from the Control aquarium

during the uptake phase were 2.62 ± 1.95 µg/g, ww Lipid (±SD, n=17; Figure 3.9). TPAC concentrations reported in mussels from this study were higher than those reported in freshwater mussels following the Kalamazoo dilbit spill (U.S. Fish and Wildlife Service et al., 2015). Most of the PACs (list of PACs not reported) in mussel tissue were below detection limits. TPAC concentration from this study were also higher than those in mussel tissue following the Deepwater Horizon Spill (Carmichael et al., 2012). However, mussel tissues collected for TPAC analysis from a large number of oil spills (Prestige oil spill in 2002, Solar I oil spill in 2006, Kinder Morgan spill in 2007, and Dubai Star oil spill in 2009, to name a few examples) as well as near oil and gas production sites were similar or higher than those reported in this study (André Lourenço et al., 2015; Baumard et al., 1999; Boehm et al., 2005; Hwang et al., 2014; Soriano et al., 2006; Stantec, 2012; Thomas et al., 2007; Thompson et al., 2017; Uno et al., 2010).

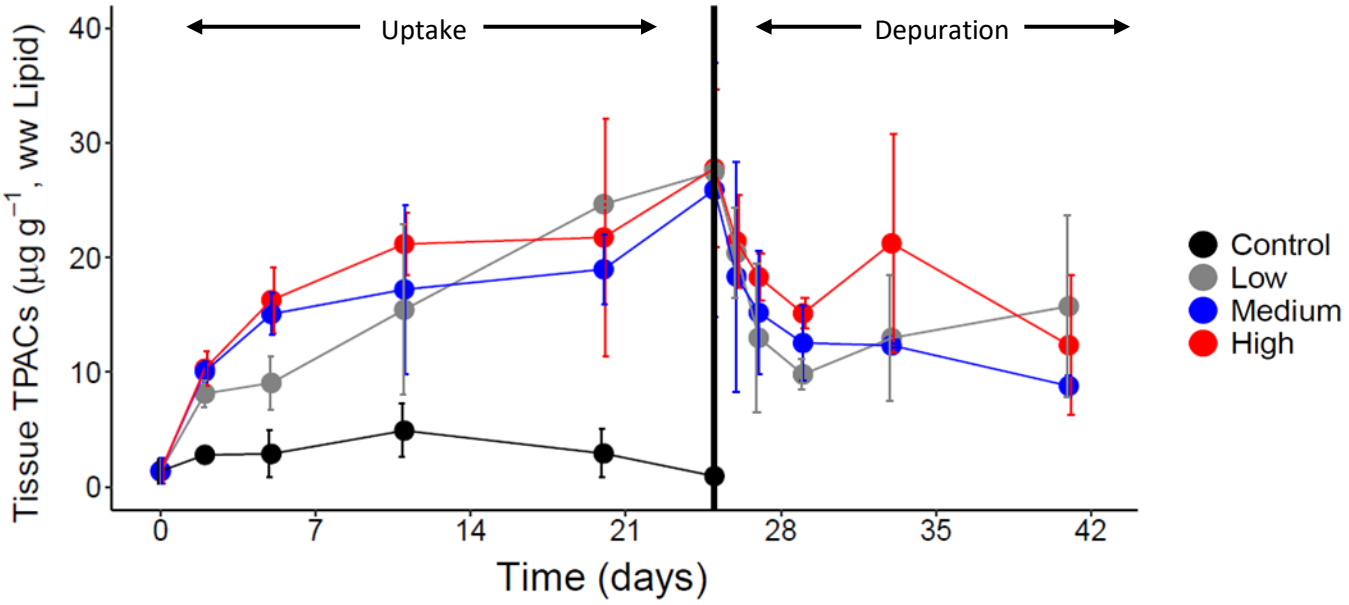

Figure 3.9: Mean (±SD) concentration (µg g^{-1}, ww Lipid) of TPACs in giant floater mussels throughout the 25-day uptake phase and the 16-day depuration phase. Samples in triplicate. Black line at day 25 denotes the end of the uptake phase and the start of the depuration phase.

As soon as the mussels were placed in aquaria containing uncontaminated Lake 260 water for the depuration phase, TPAC concentrations in mussels from the three contaminated treatments decreased (Figure 3.9). TPAC concentrations decreased rapidly for the first four days and then leveled off for the last 12 days of the depuration phase (from day four to day sixteen of the depuration phase), demonstrating apparent second order elimination. Thorsen et al. (2004) also reported second order kinetics for the elimination of the majority of individual PACs in mussel tissue (*Elliptio complanata*) but they attributed this to the unidentified fungal or bacterial growth beginning four days after the start of the depuration phase. Another study conducted by Rantamäki et al. (1997) reported a two-phase elimination for the release of PACs from *Mytilus edilus* soft tissues and attributed the two-phase process to low metabolic activity. However, the large majority of studies involving freshwater and marine bivalves have reported first-order kinetic elimination of PACs (Enwere et al., 2009; Gewurtz et al., 2002; Gobas & Morrison, 2000; Schøyen et al., 2017; H. Wang et al., 2017; Yakan et al., 2011). Therefore, I used first-order kinetics to describe the depuration of individual PACs from giant floater mussels.

The large majority of PACs showed evidence of first-order elimination despite TPACs demonstrating apparent second order elimination (Figure C.1). Only the depuration of fluorene compounds (parent and alkylated homologues) showed apparent second order kinetics where we observed a rapid decline of PACs in the first four days, followed by a slower steady decline for the remainder of the depuration phase, never reaching background concentrations (Figure 3.10). Uptake of fluorenes in mussels from the depuration water is not the cause of the two-phase elimination as PAC concentrations in Lake 260 were similar to the Control and water renewals were conducted every day. Apparent second order kinetics could be caused by lower metabolic activity, as described by Rantamäki et al. (1997). We observed a similar pattern with TPAC

concentrations, likely because the fluorene compounds, especially the alkyl fluorenes (C1-, C2-, C3-), represented roughly 50% of TPACs in mussels exposed to dilbit-contaminated water (Tables C.6 and C.7). Nonetheless, the majority of the PACs (both parent and alkyl PACs) were still present in giant floater mussel tissues by the end of the 16-day depuration phase, which is consistent with the literature (Enwere et al., 2009; Gewurtz et al., 2002; Hwang et al., 2008; Schøyen et al., 2017; Thorsen et al., 2004; Yakan et al., 2011). In fact, only eight of the 29 PACs that accumulated in mussel tissues (acenaphthylene, C3-C4-phenanthrenes, C2-C3-dibenzothiophenes, Benzo[b]naphtho[2,3-/1,2-d]thiophene, Benzo[b]naphtho[2,1-d]thiophene, and C1-benzonaphthothiophenes) returned to background concentrations by the end of the depuration phase for all three contaminated treatments. These results confirm our prediction that PACs will still be detected in tissue following the depuration phase making giant floater mussels valuable for biomonitoring of petroleum contamination in freshwater environments.

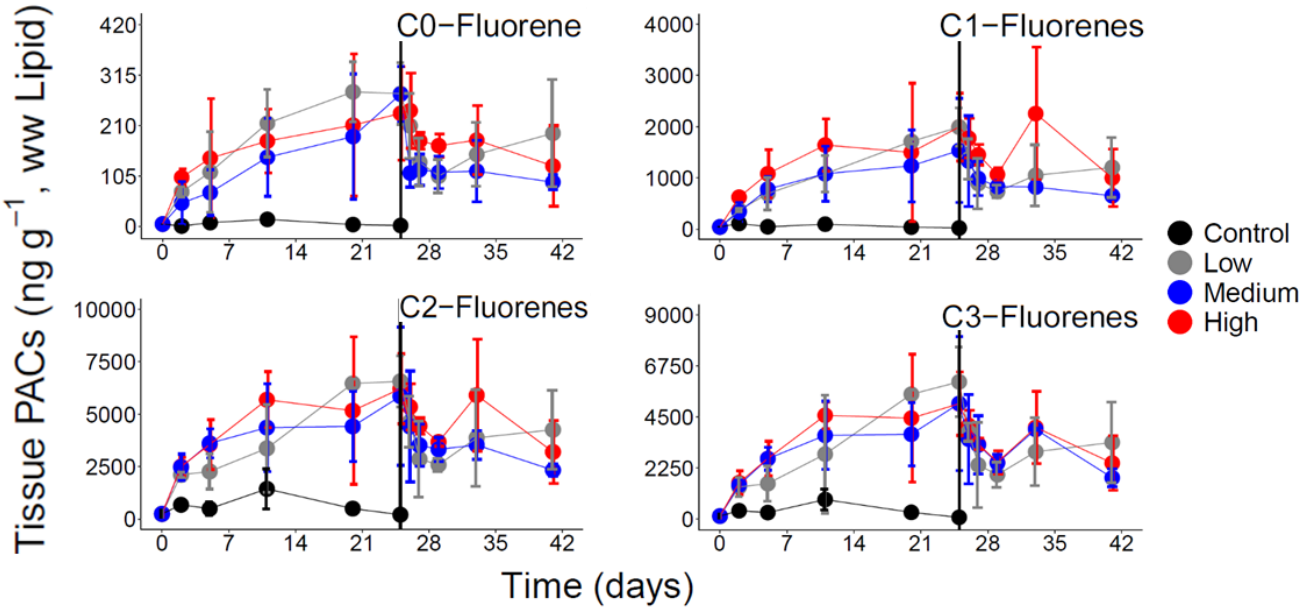

Figure 3.10: Mean (±SD) concentration (µg g^{-1}, ww Lipid) of C0-C1-C2-C3-fluorenes in giant floater mussels throughout the 25-day uptake phase and the 16-day depuration phase. Samples in triplicate. Black line at day 25 denotes the end of the uptake phase and the start of the depuration phase.

The accumulation of individual PACs (both parent and alkylated) demonstrated two general trends (Figure C.1.). Some of the PACs increased rapidly during the first few time points of the uptake phase and then slowed down as their concentrations approached steady state while most PACs increased in mussel tissue steadily through time, never approaching steady state. This makes sense as several bivalve exposure studies have reported that it takes longer than 25 days for most PACs to reach steady state (Baussant et al., 2001; Enwere et al., 2009; Hwang et al., 2008; Noh et al., 2018; Richardson et al., 2005; Thorsen et al., 2004; H. Wang et al., 2017; Yakan et al., 2011). A 25 day uptake phase was the longest possible given the circumstances. The limnocorrals from the in-lake BOREAL study had to be removed before water temperatures became too cold thus forcing us to conclude the bioaccumulation study after 41 days. However, an uptake phase of 25 days or shorter is not uncommon for a PAC bioaccumulation study involving bivalves (Baussant et al., 2001; Enwere et al., 2009; Hwang et al., 2008; Richardson et al., 2005; Thorsen et al., 2004). Furthermore, with modern modeling programs, toxicokinetic parameters can be calculated without obtaining steady state conditions through nonlinear curve fits to an uptake curve using equation 3 (Landrum et al., 1992).

The proportion of parent to alkyl PACs was higher in mussels at time zero (9.1 ± 5.3% ±SD, n=3) and mussels from the Control (5.6 ± 3.8%, ±SD, n=14) compared to mussels from the dilbit-contaminated treatments at day 25 (3.3 ± 0.1% for the Low treatment, 4.4 ± 3.3% for the Medium treatment, and 3.0 ± 0.2% for the High treatment, ±SD, n=3). In fact, Σalkyl PACs in mussel tissue averaged an order of magnitude higher than Σparent PACs throughout the experiment for all three dilbit-contaminated treatments (Figure 3.11). Not only did mussels exposed to dilbit-contaminated water have greater concentrations of alkyl PACs in their tissues compared to parent PACs, most of the individual groups of alkyl PACs (e.g., C1-, C2-, C3-, and C4-phenanthrenes) were much

higher than their unsubstituted parent counterpart (e.g., C0-phenanthrene) throughout both phases of this bioaccumulation experiment (Figure 3.12). Overall, fluorenes, naphthalenes, and phenanthrenes were the most abundant alkyl PAC groups, and fluorene, chrysene, and phenanthrene were the most abundant parent PACs in mussel tissue. Interestingly, even with significant differences in water PAC concentrations between treatments, I observed little differences in tissue PAC concentrations between dilbit-contaminated treatments (Figure 3.12).

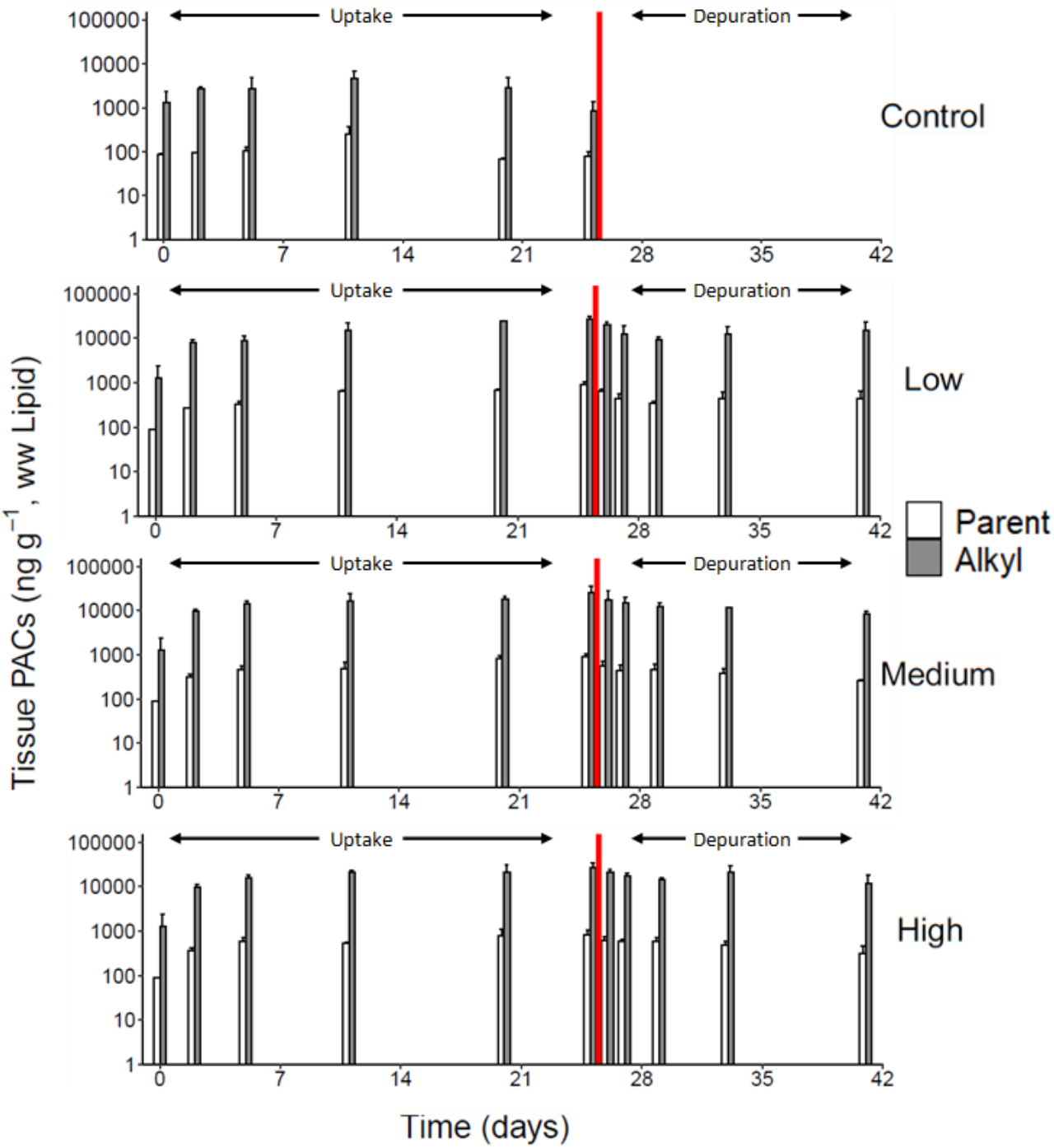

Figure 3.11: Semi-log plot demonstrating mean Σparent and Σalkyl PACs (ng g^{-1}, ww lipid; ±SD) in giant floater mussels exposed to dilbit-contaminated water at various time points (days) during the uptake and depuration phase. Tissue concentrations are represented on a logarithmic scale, with samples in triplicate. Red line at day 25 denotes the end of the uptake phase and the start of the depuration phase.

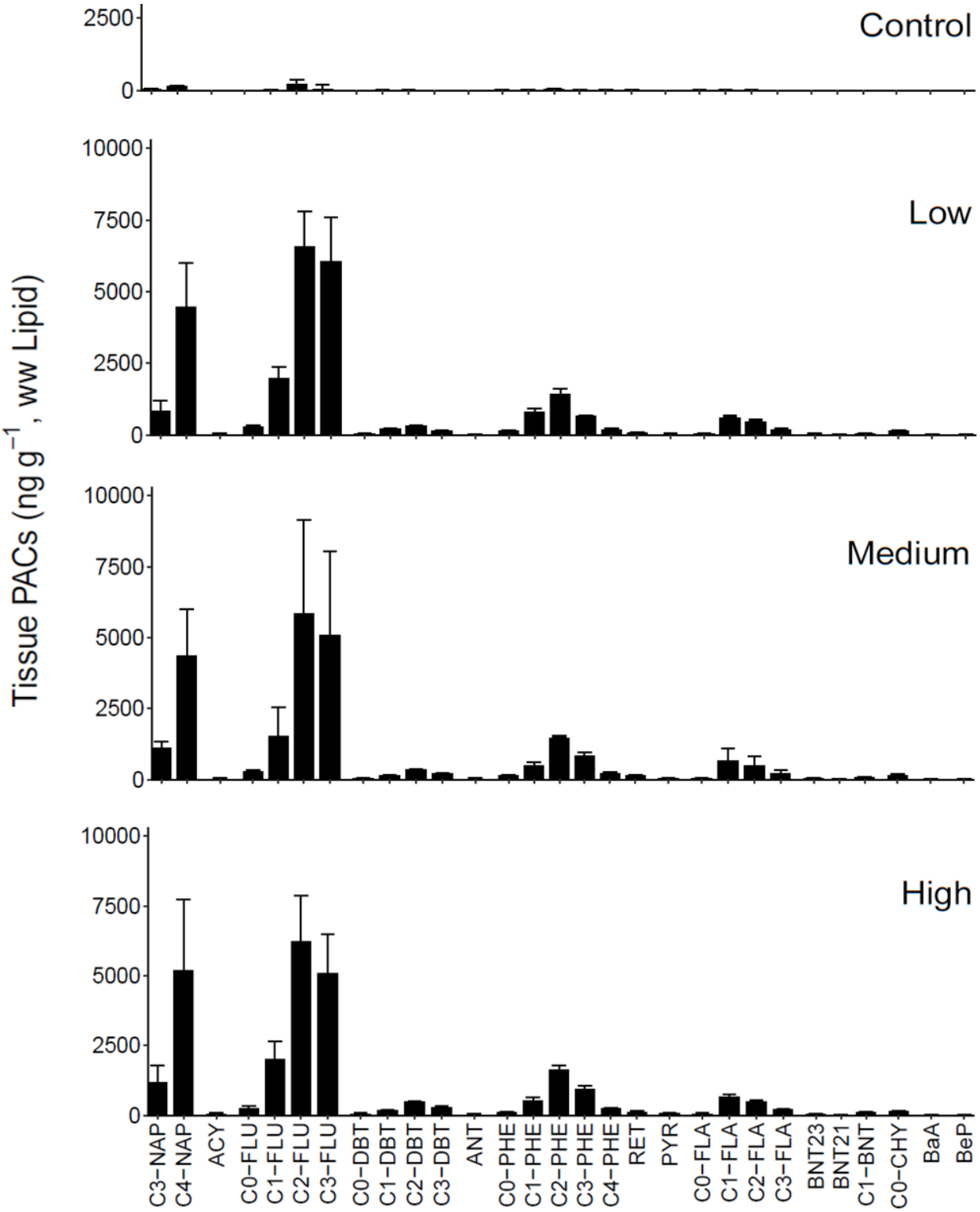

Figure 3.12: Mean PAC concentration profiles (ng g^{-1}, ww Lipid; ±SD) of giant floater mussels on day 25 of the uptake phase. Samples are in triplicate. Only the 29 PACs that demonstrated apparent accumulation in mussels exposed to dilbit-contaminated water were included. Abbreviations are found in Appendix A.

One of the original aspects of this study was that freshwater mussels were exposed to naturally weathered dilbit for the first time. Generally, I did not find many differences when comparing results from this study to other experiments exposing bivalves to various types of crude oil. Both freshwater and marine bivalves exposed to elevated concentrations of hydrocarbons accumulated a greater proportion of lighter, alkylated PACs. Furthermore, the mortality rates of mussels exposed to oil are commonly very low, similar to this study. However, dilbit is diluted with lower molecular weight diluents (benzene, toluene, ethylbenzene and xylene isomers (BTEX) are commonly used), which have shown to be more water-soluble than other hydrocarbons and could be acutely toxic to aquatic organisms (K. Lee et al., 2015; National Research Council, 2005). These diluents are extremely volatile and Sawyer et al. (in preparation) showed that they evaporated out of the water within 24 hours in the BOREAL enclosures. Since this bioaccumulation study began 35 days after the addition of dilbit to the limnocorrals, giant floater mussels were never exposed to the potentially toxic diluents in dilbit. Some laboratory studies have found that high treatments of dilbit is acutely toxic to early life stages of fish (Alderman et al., 2017; Barron et al., 2018; Charbonneau, 2016; Philibert et al., 2016), while other studies have found no such evidence (Alsaadi et al., 2018; Madison et al., 2015; McDonnell et al., 2019). These laboratory experiments used the water accommodated fractions (WAFs) of dilbit that undergoes vigorous mixing to release hydrocarbons from the source oil into the water, thus influencing hydrocarbon concentrations, including BTEX compounds, in the exposure water (Hodson et al., 2019). Furthermore, most of these studies do not assess BTEX concentrations in their WAFs. More research is needed to determine if naturally weathered dilbit is acutely toxic to different life stages of aquatic organisms.

3.3. PAC Toxicokinetics

Following first-order toxicokinetics, I determined the uptake and elimination rate constants for the 29 PACs that accumulated in giant floater mussels for the three dilbit-contaminated treatments (Figure 3.13, Appendix D). I calculated k_1 and k_2 by nonlinear curve fitting of the accumulation phase using equation 3, and by sequential estimation where k_2 was determined from the natural log-transformed depuration phase and then sequentially used to calculate k_1 by nonlinear curve fitting of the accumulation phase using equation 3. I compared the two models using ANOVA, as well as looking at model accuracy metrics, such as residual standard error (Sigma), Bayesian Information Criteria (BIC), and Akaike's Information Criteria (AIC) to determine which model best fit the accumulation phase (Tables D.7-9). In general, sequential estimation was the best method for defining uptake and elimination rate coefficients for individual PACs because it generated lower standard error for k_1 values (average of 0.44 ± 0.37; ±SD, n=84) and for k_2 values (average of 0.036 ± 0.029; ±SD, n=84), compared to estimating k_1 and k_2 by nonlinear curve fitting of the accumulation phase (average of 2.33 ± 3.01; ±SD, n=78 for k_1 values and 0.066 ± 0.084; ±SD, n=78 for k_2 values). However, I could not determine the toxicokinetic parameters of acenaphthylene through sequential estimation and the toxicokinetic parameters of retene, C0-fluoranthene, and benzo[e]pyrene through nonlinear curve fitting of the accumulation phase. Mussels excreted acenaphthylene and accumulated retene, C0-fluoranthene, and BeP too quickly and earlier depuration and uptake time points (< 24 hours) would have been required. Nonetheless, the lower standard error associated with sequential estimation of toxicokinetic parameters stresses the importance of adding a depuration phase to bioaccumulation experiments instead of solely relying on the accumulation phase to generate bioaccumulation models.

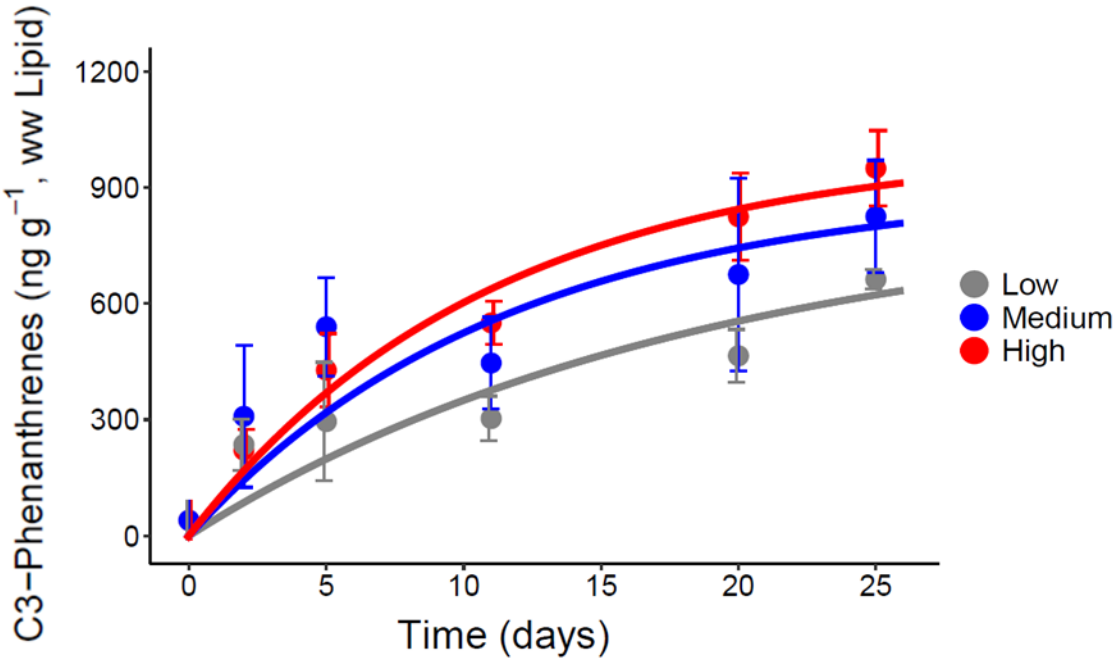

Figure 3.13: Mean (±SD) concentration (ng g^{-1}, ww Lipid) of C3-phenanthrenes (one of the 29 modelled PACs) in giant floater mussels during the uptake phase. Samples in triplicate. Toxicokinetic parameters were calculated by sequential estimation and then used to model the accumulation of PACs using equation 3.

It was apparent that steady state of C0-fluoranthene in mussels from the Low and Medium treatments was attained at day 11 and 20, respectively, while retene steady state was reached at day 11 for both treatments. However, for the High treatment, steady state for C0-fluoranthene and retene were never attained in mussels. I was therefore able to use equation 4 to calculate the uptake rate constants for C0-fluoranthene (5.53 L g^{-1} d^{-1} and 4.29 L g^{-1} d^{-1} for the Low and Medium treatments, respectively) and retene (9.41 L g^{-1} d^{-1} and 5.63 L g^{-1} d^{-1} for the Low and Medium treatments, respectively; Figure 3.14). The resulting models visually fit the data relatively well while the models generated from nonlinear curve fitting of the accumulation phase had a lot of uncertainty (e.g., k_1 for C0-fluoranthene from the Low treatment was 105 ± 19,000 L g^{-1} d^{-1}) due to the very rapid increase of these compounds in giant floater mussels.

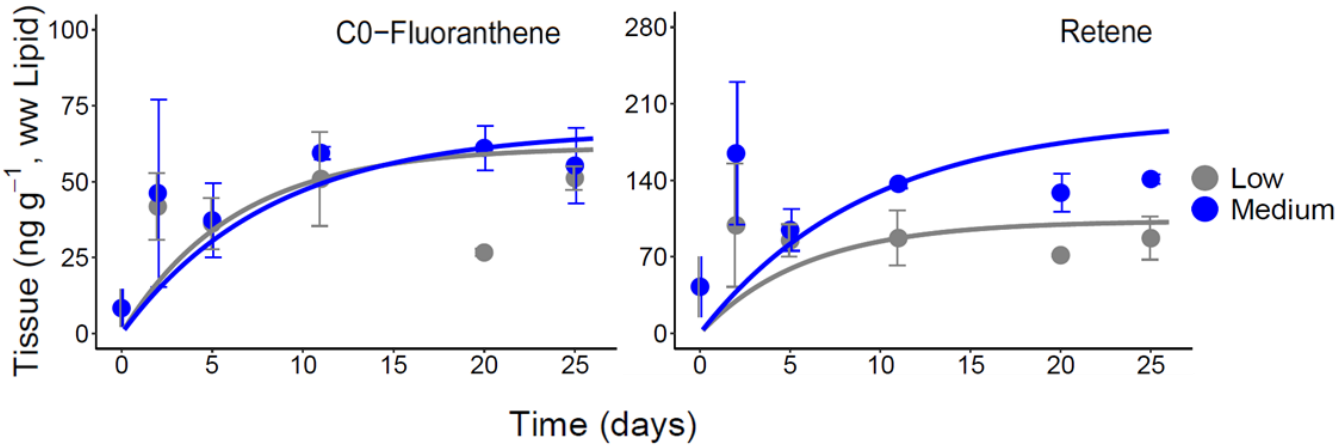

Figure 3.14: Mean (±SD) concentration (ng g^{-1}, ww Lipid) of C0-fluoranthene (left) and retene (right) (two of the 29 modelled PACs) in giant floater mussels during the uptake phase. Samples in triplicate. Depuration rate constants used for these accumulation models were calculated from the log-transformed depuration phase while uptake rate constants were determined using equation 4. Toxicokinetic parameters were then used to model the accumulation of PACs using equation 3.

For the fluorene compounds that demonstrated second order elimination, k_2 values were optimized by only selecting the first four time points of the depuration phase (describing the rapid phase) generating significant linear relationships between natural log-transformed tissue concentrations and time (first-order elimination), ultimately producing more accurate bioaccumulation models. For example, looking at C1-fluorenes, if all of the time points from the depuration phase were kept, the simple linear regressions analysis between natural log-transformed tissue concentrations and time (to generate k_2) would be insignificant (p-value > 0.05) and the resulting k_2 values would be 0.015 day^{-1}, 0.035 day^{-1}, and 0.03371 day^{-1} for the Low, Medium, and High treatments, respectively. This would ultimately generate a model that does not fit the accumulation phase well (Table 3.1). However, if only the first four days of the depuration phase were used (describing the rapid phase), the k_2 values would be 0.079 day^{-1}, 0.095 day^{-1}, and 0.15 day^{-1} for the Low, Medium, and High treatments, respectively, which would generate a much more accurate bioaccumulation model. For the other PACs that demonstrated apparent first-order

elimination, the whole depuration phase was used to determine k_2 values unless background concentrations were reached before the end of the 16-day depuration phase.

Table 3.1: Depuration rate constants (k_2; day^{-1}) for C1-fluorenes as well as accuracy metrics for the bioaccumulation models generated by k_2 if all six time points, or only the first four time points, of the depuration phase were selected. Accuracy metrics include standard error (Sigma), Bayesian Information Criteria (BIC), and Akaike's Information Criteria (AIC).

	Low		Medium		High	
Depuration Phase	**16 days (6 time points)**	**4 days (4 time points)**	**16 days (6 time points)**	**4 days (4 time points)**	**16 days (6 time points)**	**4 days (4 time points)**
k_2	0.015	0.079	0.035	0.095	0.034	0.151
SE	0.025	0.052	0.020	0.109	0.019	0.042
Sigma	246	229	511	490	676	590
AIC	211	209	248	247	289	284
BIC	212	210	249	248	290	286

Uptake rate constants (k_1) for all three dilbit-contaminated treatments ranged from 0.66 L g^{-1} day^{-1} to 19.42 L g^{-1} day^{-1} (n=87; Table 3.2). The average uptake rate constant was 5.70 ± 3.63 L g^{-1} day^{-1} (±SD, n=29) for the Low treatment, 5.52 ± 3.55 L g^{-1} day^{-1} (±SD, n=29) for the Medium treatment, and 4.13 ± 3.87 L g^{-1} day^{-1} (±SD, n=29) for the High treatment (Figure 3.15). The PACs with highest k_1 value in the Low, Medium, and High treatments were: acenaphthylene (15.69 L g^{-1} day^{-1}, 19.42 L g^{-1} day^{-1}, and 19.22 L g^{-1} day^{-1}, respectively), C3-fluorenes (14.40 L g^{-1} day^{-1}, 9.42 L g^{-1} day^{-1}, and 12.17 L g^{-1} day^{-1}, respectively), and benzo[e]pyrene (6.13 L g^{-1} day^{-1}, 9.98 L g^{-1} day^{-1}, and 10.88 L g^{-1} day^{-1}, respectively). Uptake rate constants for individual PACs were in range with the literature for marine and freshwater bivalves exposed to PACs (Baussant et al., 2001;

Bruner et al., 1994; S. W. Fisher et al., 1993; Gossiaux et al., 1996; Yakan et al., 2011). It is difficult to compare k_1 between studies involving bivalves due to variations in exposure media (water, sediment, suspended particles, and food), length of the uptake phase, experimental design (flow-through versus stock renewals), type of sediment (different organic content affecting bioavailability), and biological variations between species and life-stages. Some toxicokinetic studies calculated rate constants differently (Richardson et al., 2005; Yakan et al., 2017), while others did not report the units of k_1 (Bender et al., 1988; Hwang et al., 2008). Caution must therefore be taken when comparing uptake and depuration rate constants between studies. Furthermore, a number of toxicokinetic studies have focused on the parent PACs and have overlooked the alkylated homologues, a knowledge gap highlighted in the RSC report (K. Lee et al., 2015). This is the first study, to our knowledge, to assess the uptake and elimination rate constants as well as the bioaccumulation of parent and alkyl PACs derived from naturally weathered oil in a freshwater bivalve. Results of this study are also the largest, most comprehensive set of toxicokinetic and bioaccumulation information of PACs (44 analytes) in freshwater mussels obtained to date.

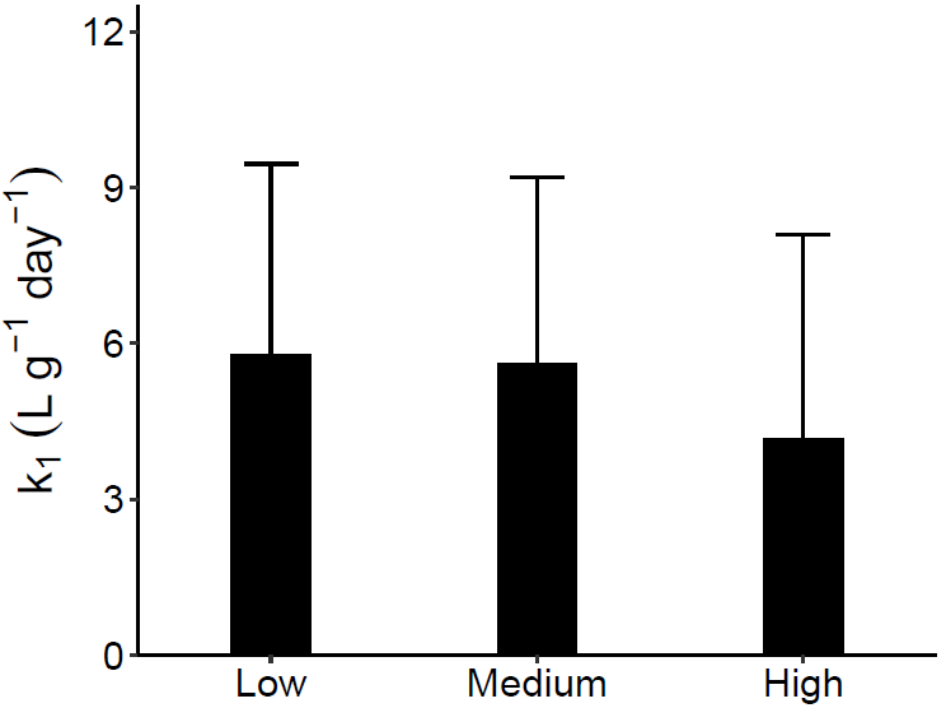

Figure 3.15: Mean (±SD, n=29 per treatment) uptake rate constants of parent and alkyl PACs from all three dilbit-contaminated treatments.

Depuration rate constants (k_2) ranged between 0.012 to 0.37 day^{-1} (n=87; Table 3.3) and were in range with the literature regarding bivalves (Bruner et al., 1994; Enwere et al., 2009; Gewurtz et al., 2002; Hwang et al., 2008; Richardson et al., 2005; Schøyen et al., 2017; Thorsen et al., 2004; H. Wang et al., 2017; Yakan et al., 2011, 2017). The average elimination rate constants from this study were 0.10 ± 0.08 day^{-1} (± SD, n=29) for the Low treatment, 0.12 ± 0.07 day^{-1} (± SD, n=27) for the Medium treatment, and 0.097 ± 0.065 day^{-1} (± SD, n=29) for the High treatment, demonstrating little variation between treatments (Figure 3.16). The PACs with the lowest k_2 value from the Low, Medium, and High treatments were (in ascending order): acenaphthylene (0.01171 day^{-1}, 0.01882 day^{-1}, and 0.04500 day^{-1}, respectively), C2-fluoranthenes (0.022 day^{-1}, 0.037 day^{-1}, and 0.036 day^{-1}, respectively), and C1-fluoranthenes (0.025 day^{-1}, 0.041 day^{-1}, and 0.037 day^{-1}, respectively).

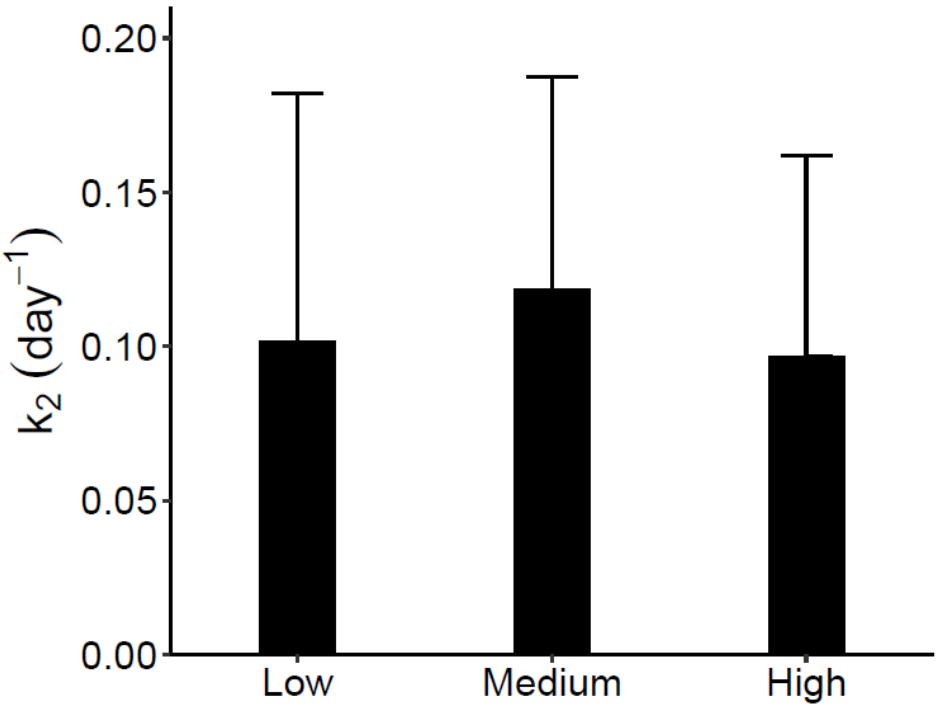

Figure 3.16: Mean (±SD, n=29 per treatment) depuration rate constants of PACs (both parent and alkylated) from all three treatments contaminated by dilbit.

To determine any significant differences in uptake and depuration rate constants between treatments for individual PACs, I compared k_1 and k_2 values and their 95% confidence intervals (Table 3.2). I determined the uptake rates for C0-fluoranthene and retene from the Low and Medium treatments using equation 4, however I could not determine their k_1 confidence intervals. In general, k_1 values for more than half of the PACs (15 of 27 PACs) from the High treatment were significantly lower than k_1 values from the Low and/or Medium treatments. Notably, the accumulation of every PAC in mussels from the three dilbit-contaminated treatments followed apparent first-order kinetics. When comparing k_1 values from the Low and Medium treatments, we observed no significant differences between the two treatments for more than half of the PACs (16 of 27 PACs). As previously mentioned, PAC concentrations in mussel tissue during the

accumulation phase were relatively similar across the three dilbit-contaminated treatments even when there were significant differences in PAC concentrations in the contaminated water. For example, water concentrations of C3-phenanthrenes from the High treatment (29.80 ± 8.53 ng L^{-1}, ±SD, n=7) were higher than the Medium (20.49 ± 8.36 ng L^{-1}, ±SD, n=6) and Low (11.02 ± 8.53 ng L^{-1}, ±SD, n=5) treatments but mussel tissue concentrations are relatively similar across the three dilbit-contaminated treatments (Figure 3.13). The resulting uptake rate constant of C3-phenanthrenes from the High treatment (3.09 L g^{-1} day^{-1}) was significantly lower than the uptake rate constants from the Low (4.11 L g^{-1} day^{-1}) and Medium (3.83 L g^{-1} day^{-1}) treatments. If I were to use the average k_1 value from the Low and Medium treatments (3.97 L g^{-1} day^{-1}) for the High treatment, the resulting first-order bioaccumulation model overpredicts the accumulation of C3-phenanthrenes in mussels from the High treatment (Figure 3.17).

Significant differences of k_1 values between the treatments may be a result of differences in filtration rates for mussels in the High treatment compared to the Low and Medium treatments. Research by Mouabad et al. (2001) and Andrade et al. (2016) revealed changes in valve closure patterns for mussels exposed to contaminants. Both studies reported significant negative relationships between trace metal concentrations in the water and mussel filtration rates. Visual observations of the mussels from this study revealed that the shells of the mussels from the High treatment were mainly closed while the shells of the mussels from the Low and Medium treatments were mostly open. Lower filtration rates for mussels in the High treatment could have reduced PAC accumulation in their tissues, resulting in concentration-dependent uptake rates in mussels. Another possible reason for the similar tissue concentrations between the three treatments could be higher metabolizing rates in the mussels from the High treatment compared to the Medium and Low treatments. A number of studies (Cheung et al., 2001; Livingstone, 1998; Livingstone et al.,

1985; Lopes et al., 2012) revealed that PAC biotransformation rates and metabolizing enzyme activity (phase I and phase II enzymes) in bivalves were dependent on tissue concentrations. Mussels from the High treatment could have been metabolizing and excreting PACs faster as a result of higher tissue concentrations, resulting in similar PAC tissue concentrations between the three treatments. From what is available in the literature, it is not clear if there is concentration-dependence associated with PAC uptake rates in bivalves. For example, a study conducted by Wang et al. (2017) revealed that benzo[a]pyrene k_1 value for *Pinctada martensii* was dependent on water concentration while benzo[a]pyrene k_1 value for *Perna viridis* was not. Furthermore, a study conducted by Yakan et al. (2011) exposing *Mytilus galloprovincialis* to benzo(a)anthracene-contaminated sediment revealed substantial differences in k_1 values between different treatments while a study conducted by C.-H. Lee et al. (2014) exposing the manila clam (*Ruditapes philippinarum*) to crude oil-contaminated sediments did not. Future studies to understand how filtration rate and metabolism affect PACs uptake rates are necessary since it is not clear from the literature how much these factors can influence the uptake of PACs in bivalves. Interestingly, even if uptake rate constants were significantly different between treatments, the depuration rate constants for all PACs were not (Table D.10).

Table 3.2: Uptake rate constants (k_1; L g^{-1} day^{-1}) and their 95% confidence intervals. Bolded compounds represent significantly lower k_1 values for mussels collected from the High treatment compared to the Low and/or Medium treatments. Abbreviations are found in Appendix A. Confidence intervals and k_1 values were calculated in R Studio.

	Low			**Medium**			**High**		
PAC	**k_1**	**2.5%**	**97.5%**	**k_1**	**2.5%**	**97.5%**	**k_1**	**2.5%**	**97.5%**
C3-NAP	**1.89**	**1.57**	**2.20**	**3.33**	**2.69**	**3.97**	**1.67**	**1.28**	**2.06**
C4-NAP	**3.15**	**2.65**	**3.64**	**8.84**	**7.09**	**10.59**	**2.58**	**2.00**	**3.17**
ACY	15.69	10.22	50.11	19.42	3.28	62.89	19.22	14.12	24.32
C0-FLU	5.59	4.77	6.41	7.84	6.09	9.59	4.90	3.62	6.18
C1-FLU	5.97	5.34	6.59	4.99	3.66	6.32	4.45	3.46	5.45
C2-FLU	**11.57**	**10.05**	**13.08**	**7.75**	**5.89**	**9.62**	**5.81**	**4.72**	**6.89**
C3-FLU	14.40	6.60	27.03	9.42	7.31	11.52	12.17	10.17	14.16
C0-DBT	1.48	1.24	1.72	2.60	2.23	2.97	1.87	1.45	2.29
C1-DBT	0.66	0.58	0.74	0.86	0.74	0.98	0.82	0.71	0.92
C2-DBT	6.24	5.51	6.98	4.69	3.96	5.41	5.33	3.75	7.65
C3-DBT	4.85	4.20	5.50	4.86	4.17	5.56	4.43	4.07	4.80
ANT	**2.36**	**1.96**	**2.77**	**3.82**	**3.22**	**4.43**	**0.94**	**0.69**	**1.19**
C0-PHE	**1.89**	**1.53**	**2.25**	**2.74**	**2.46**	**3.02**	**1.56**	**1.27**	**1.84**
C1-PHE	**3.33**	**2.80**	**3.85**	**6.39**	**5.76**	**7.02**	**2.13**	**1.76**	**2.50**
C2-PHE	**8.41**	**7.37**	**9.46**	**8.51**	**7.37**	**9.65**	**3.83**	**3.45**	**4.22**
C3-PHE	**4.11**	**3.45**	**4.78**	**3.83**	**3.13**	**4.53**	**3.09**	**2.86**	**3.32**
C4-PHE	**7.50**	**5.96**	**9.03**	**6.81**	**5.59**	**8.02**	**4.18**	**3.33**	**5.02**
PYR	**6.31**	**5.07**	**7.54**	**3.06**	**2.57**	**3.55**	**2.22**	**1.86**	**2.57**
C1-FLA	**8.80**	**7.80**	**9.79**	**5.97**	**4.20**	**7.74**	**4.17**	**3.53**	**4.81**
C2-FLA	**4.85**	**4.27**	**5.44**	**3.66**	**2.60**	**4.71**	**3.55**	**3.01**	**4.09**
C3-FLA	3.17	2.78	3.56	2.75	2.06	3.43	3.56	2.95	4.17
BNT23	1.91	1.57	2.25	3.26	2.45	4.06	1.86	1.01	3.17
BNT21	3.99	3.14	4.83	3.28	2.36	4.20	2.00	0.99	3.73
C1-BNT	**5.27**	**4.16**	**6.39**	**2.14**	**1.58**	**2.69**	**3.20**	**2.69**	**3.71**
C0-CHY	**5.92**	**4.82**	**7.03**	**5.40**	**4.18**	**6.61**	**2.04**	**1.09**	**3.50**
BaA	**5.04**	**3.70**	**6.37**	**3.99**	**3.34**	**4.63**	**3.00**	**2.34**	**3.66**
BeP	6.13	4.61	7.64	9.98	7.26	12.70	10.88	9.62	12.13

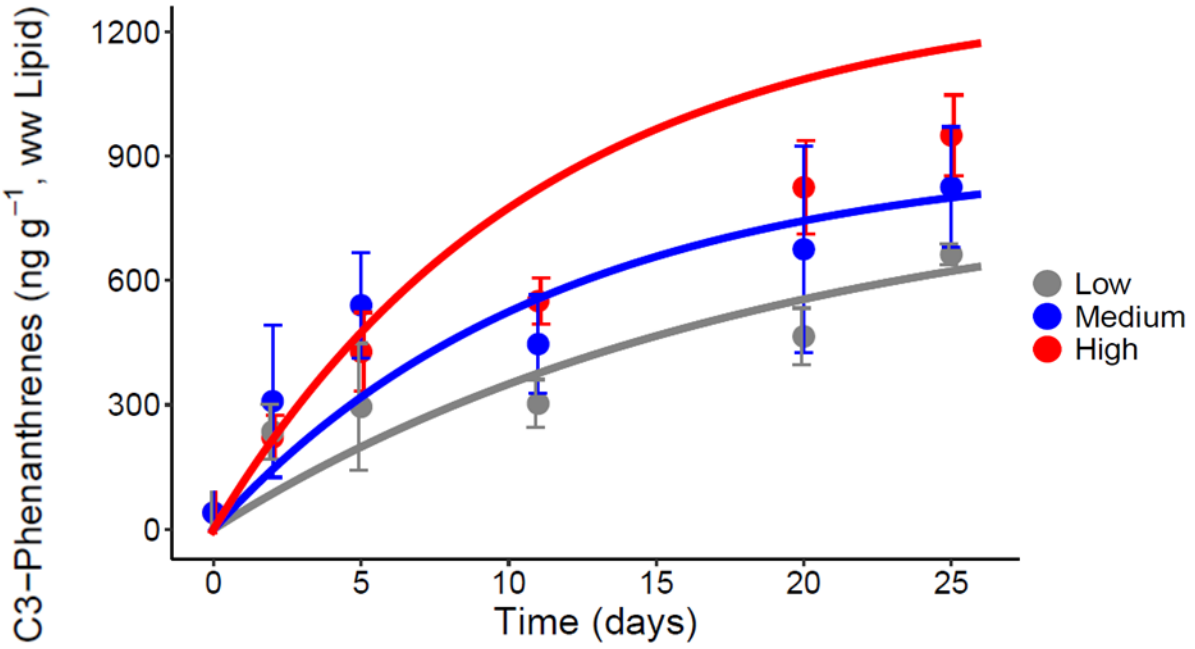

Figure 3.17: Mean (±SD) concentration (ng g^{-1}, ww Lipid) of C3-phenanthrenes in giant floater mussels during the uptake phase. Samples in triplicate. The uptake rate constant used to develop the bioaccumulation model for the High treatment (4.05 L g^{-1} day^{-1}) is the average k_1 value of the Low and Medium treatments. Toxicokinetic parameters for the Low and Medium treatments were calculated by sequential estimation and then used to model the accumulation of PACs.

The time required for a PAC to reach 95% of steady state was calculated from k_2 values using equation 5. For most PACs, the 25-day uptake phase was insufficiently long for compounds to reach steady state. In fact, from these values, only three PACs reached steady state for all three contaminated treatments (benzo[e]pyrene, C2-dibenzothiophenes, and C2-phenanthrenes; Table 3.3). It is also apparent from looking at tissue accumulation over time that most PACs have not reached steady state after 25 days of accumulation (Figure C.1.). On average (±SD, n=87), it would have taken 46 ± 40 days for PACs to reach steady state which would have resulted in a 62 day bioaccumulation experiment (46 day accumulation phase plus 16 day depuration phase). Furthermore, some PACs took much longer to reach steady state including acenaphthylene (160 ± 95 days; ±SD, n=3), C2-fluoranthenes (106 ± 27 days; ±SD, n=3), and C1-fluoranthenes (91.32 ±

26 days; ±SD, n=3). Given that the limnocorrals had to be removed from Lake 260 before fall turnover, the bioaccumulation experiment had to be concluded after 41 days, preventing PACs to reach steady state conditions. The 95% steady state values obtained from this study were a little higher than what was reported by Gewurtz et al. (2002) and Thorsen et al. (2004). These studies used a flow-through design, which could explain the differences in 95% steady state values. Regardless, consistent with results from this experiment, a number of mussel studies have reported that it would take longer than 25 days for most PACs to reach steady state (Baussant et al., 2001; Enwere et al., 2009; Hwang et al., 2008; Noh et al., 2018; Richardson et al., 2005; Thorsen et al., 2004; H. Wang et al., 2017; Yakan et al., 2011).

Table 3.3: The time required for PACs to reach 95% steady state conditions (t_{95}) in giant floater mussels collected from all three dilbit-contaminated treatments. t_{95} values were calculated in R Studio using equation 5. Abbreviations are found in Appendix A.

	Low		Medium		High	
PAC	**k_2 (days^{-1})**	**t_{95} (days)**	**k_2 (days^{-1})**	**t_{95} (days)**	**k_2 (days^{-1})**	**t_{95} (days)**
C3-NAP	0.12	24	0.18	17	0.18	17
C4-NAP	0.026	117	0.23	13	0.14	21
ACY	0.012	256	0.019	159	0.045	67
C0-FLU	0.075	40	0.082	37	0.081	37
C1-FLU	0.079	38	0.095	31	0.15	20
C2-FLU	0.060	50	0.098	31	0.13	24
C3-FLU	0.028	105	0.13	23	0.17	17
C0-DBT	0.045	67	0.067	45	0.065	46
C1-DBT	0.053	56	0.12	26	0.065	46
C2-DBT	0.16	18	0.14	21	0.18	17
C3-DBT	0.068	44	0.11	27	0.081	37
ANT	0.13	24	0.16	19	0.081	37
C0-PHE	0.062	49	0.077	39	0.062	48
C1-PHE	0.067	45	0.14	22	0.075	40
C2-PHE	0.16	18	0.20	15	0.13	24
C3-PHE	0.054	56	0.087	34	0.092	33
C4-PHE	0.092	33	0.16	19	0.12	25
RET	0.17	18	0.11	28	0.067	45
PYR	0.13	24	0.14	22	0.086	35
C0-FLA	0.16	19	0.12	25	0.074	41
C1-FLA	0.025	121	0.041	73	0.037	80
C2-FLA	0.022	137	0.033	90	0.033	90
C3-FLA	0.022	134	0.043	70	0.043	70
BNT23	0.065	46	0.11	27	0.023	128
BNT21	0.23	13	0.13	23	0.041	73
C1-BNT	0.32	9	0.11	27	0.11	28
C0-CHY	0.13	24	0.089	34	0.026	116
BaA	0.071	42	0.052	58	0.088	34
BeP	0.31	10	0.37	8	0.34	9

One of the main objectives of this study was to identify any differences in accumulation between parent and alkylated PACs. Although we observed higher concentrations of alkyl PACs in mussels than parent PACs, I observed no significant differences in k_1 and k_2 values when comparing parent and alkylated compounds (p-values 0.15 and 0.69, respectively). The similarity between parent and alkyl PACs could be due to the large variations of k_1 values for parent PACs. For example, k_1 for C0-phenanthrene in the medium treatment is 2.74 L g^{-1} day^{-1} while k_1 for acenaphthylene in the same treatment is 19.42 L g^{-1} day^{-1}. To reduce the variation, only parent PACs with alkylated homologues analysed were included (n=7; Figure 3.18). For this subset of PACs, k_1 values for alkyl PACs were significantly greater than their parent PAC counterparts (p-value 0.009; Figure 3.19). Conversely, I observed no significant differences in k_2 values between alkylated homologues and their parent PACs counterparts (p-value 0.37), suggesting that both parent and alkyl PACs were metabolized through similar pathways, as previously demonstrated by a number of reviews (Manzetti, 2013; Neff, 2002b; van der Oost et al., 2003).

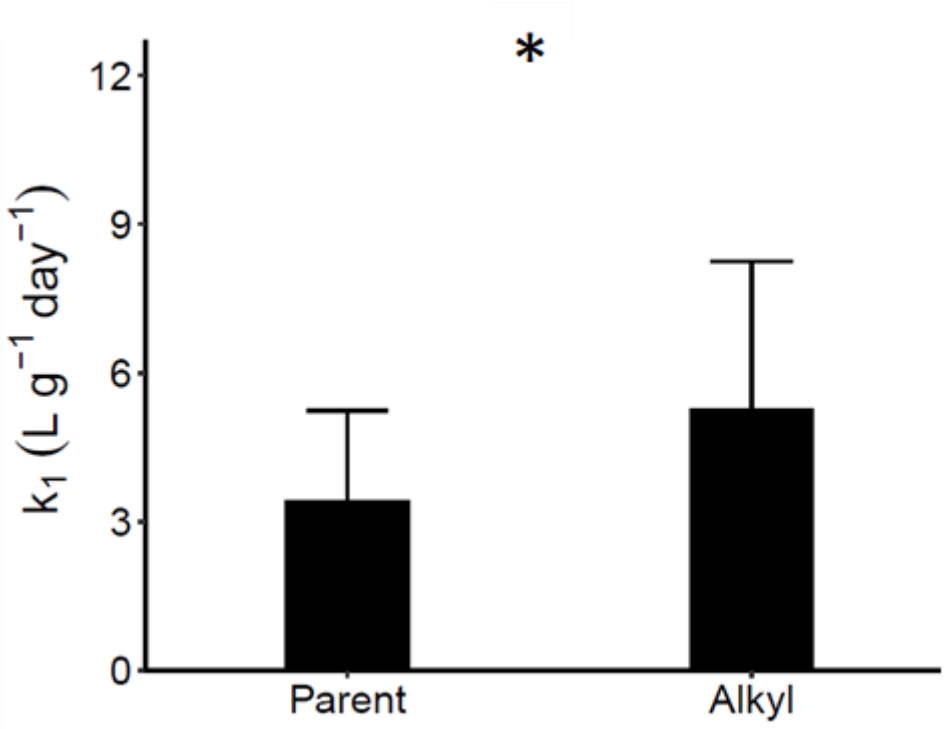

*Figure 3.18: Mean (±SD) uptake rate constants of parent (n=7) and alkylated (n=17) PACs (k_1 - L g^{-1} day^{-1}). Only parent PACs with analysed alkylated PACs are shown in this figure. All three treatments contaminated with dilbit were grouped (n=70). Unpaired Wilcoxon rank sum test (Table E.10) performed in R Studio on log-transformed data (p-value 0.009) revealed significant differences (indicated by *) in uptake rate constants between parent and alkylated PACs. Data were back-transformed.*

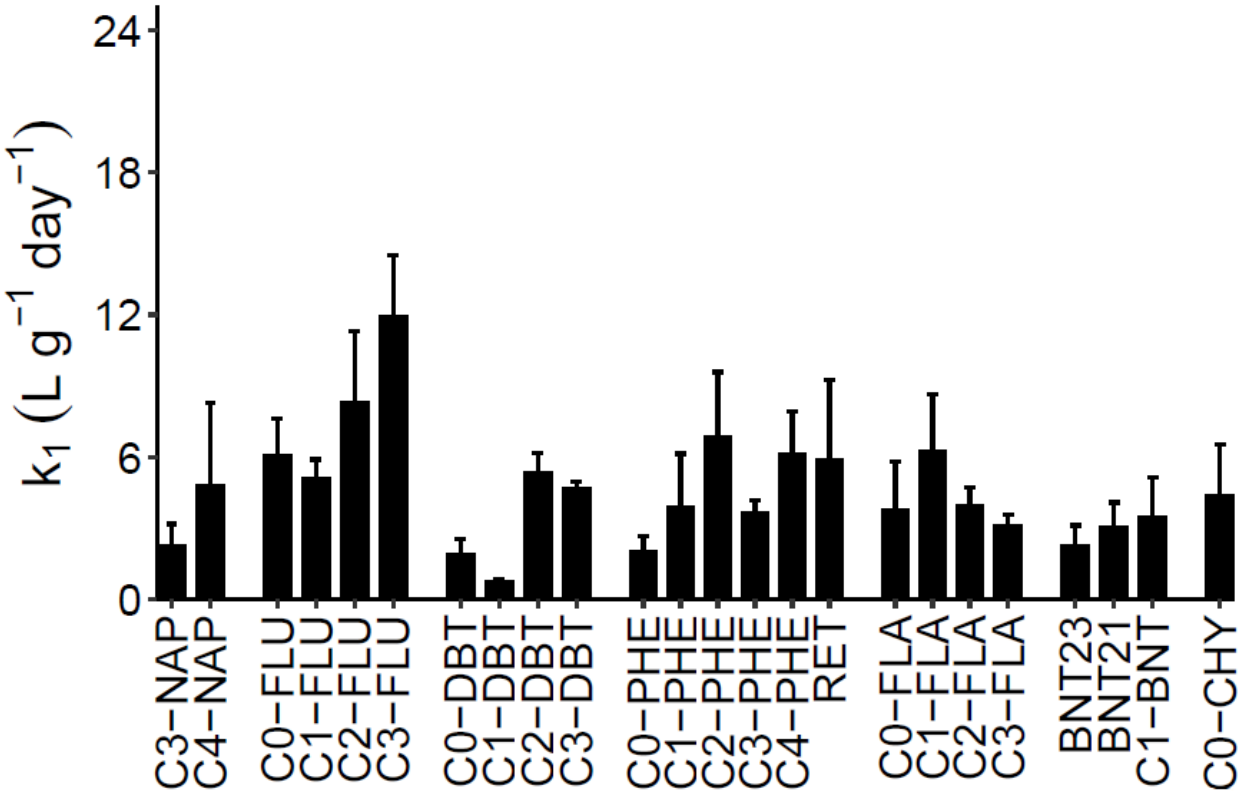

Figure 3.19: Mean (±SD, n=3) PAC uptake rate profiles (k_1 - L g^{-1} day^{-1}) of unsubstituted parent PACs and their alkylated counterparts. Uptake rate constants from all three dilbit-contaminated treatments were grouped. Abbreviations are found in Appendix A.

To determine whether significant differences in uptake and depuration rate constants exist between PACs, I divided the PACs by their number of rings (2-3 rings and 4-5 rings). I observed no significant differences in k_1 and k_2 values between 2-3 and 4-5 ring PACs (p-values 0.59 and 0.27, respectively) when combining all three treatments and when I compared individual dilbit-contaminated treatments. The lack of significant differences is a result of large variations within the two groups. For example, the average k_1 value for acenaphthylene is 18.11 ± 2.10 L g^{-1} day^{-1} (±SD, n=3) while the k_1 value for C1-dibenzothiophene is 0.78 ± 0.10 L g^{-1} day^{-1} (±SD, n=3), both of which have 3 rings.

A number of toxicokinetic studies exposing bivalves to PACs have reported a significant negative relationship between depuration rate constants and hydrophobicity (log $K_{OW;}$ Bender et al., 1988; Enwere et al., 2009; Gewurtz et al., 2002; Hwang et al., 2008; Schøyen et al., 2017). However, in this study, I observed no such relationship in any of the three treatments (Figure 3.20). A slight positive trend was mainly driven by benzo[e]pyrene, which recorded relatively high k_2 values. Once removed, the k_2 and log K_{OW} relationship flattened and was similar to what Hwang et al. (2008) found when they exposed eastern oysters (*Crassostrea virginica*) to a larger mixture of PACs (parent and alkylated). Furthermore, when comparing PAC's k_1 values and their respective log-transformed K_{OW} values from the three dilbit-contaminated treatments, no significant relationships were found (Figure 3.20). Finally, regression analyses were also conducted between the molecular weight of PACs and their respective uptake and depuration rate constant for all three treatments but they revealed no significant differences except for a significant relationship between k_2 and molecular weight for the Low treatment (p value 0.019; Figure 3.21). However, this significant relationship is driven by the high k_2 values of C1-benzonaphthothiophenes and benzo[e]pyrene from the Low treatment and removing these two compounds from analysis flattens the relationship, making it non-significant (p-value 0.34).

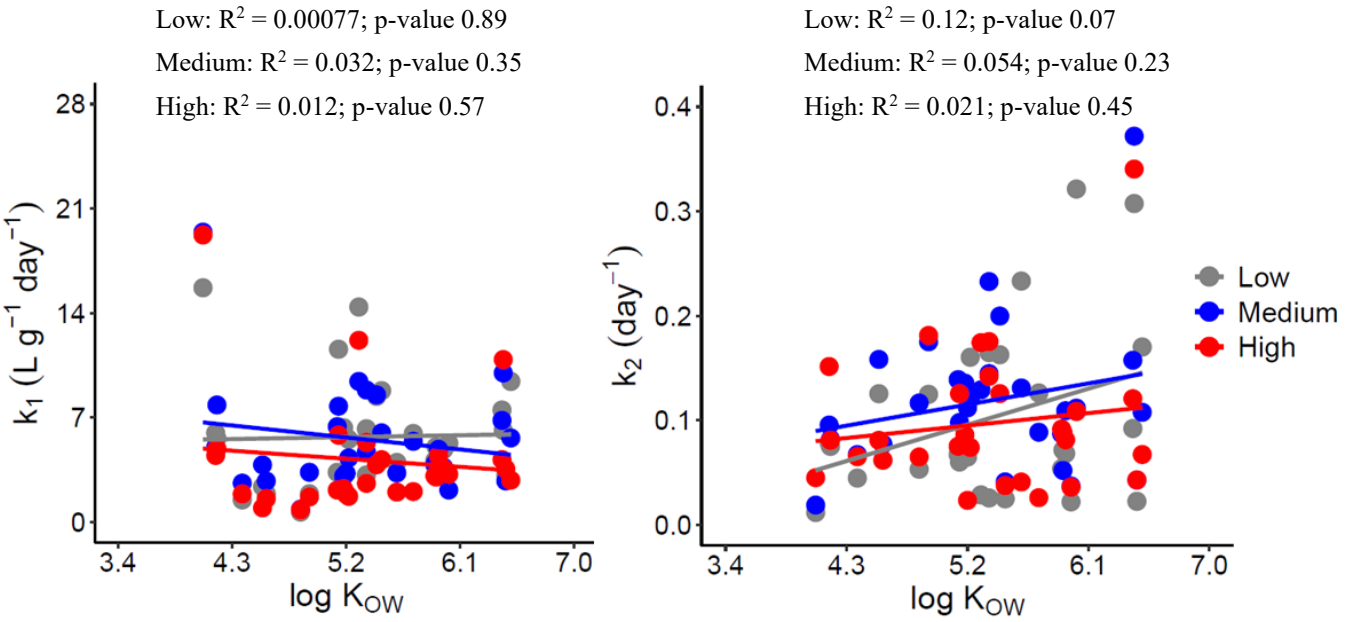

Figure 3.20: Linear regression analyses between uptake (L $g^{-1}day^{-1}$ - left) and depuration (day^{-1} - right) rate constants of PACs (n=29 per treatment) and their associated log K_{OW} values. Regression analyses revealed no significant relationships (p-value >0.05) between the toxicokinetic parameters of PACs and their associated hydrophobicity for all three treatments.

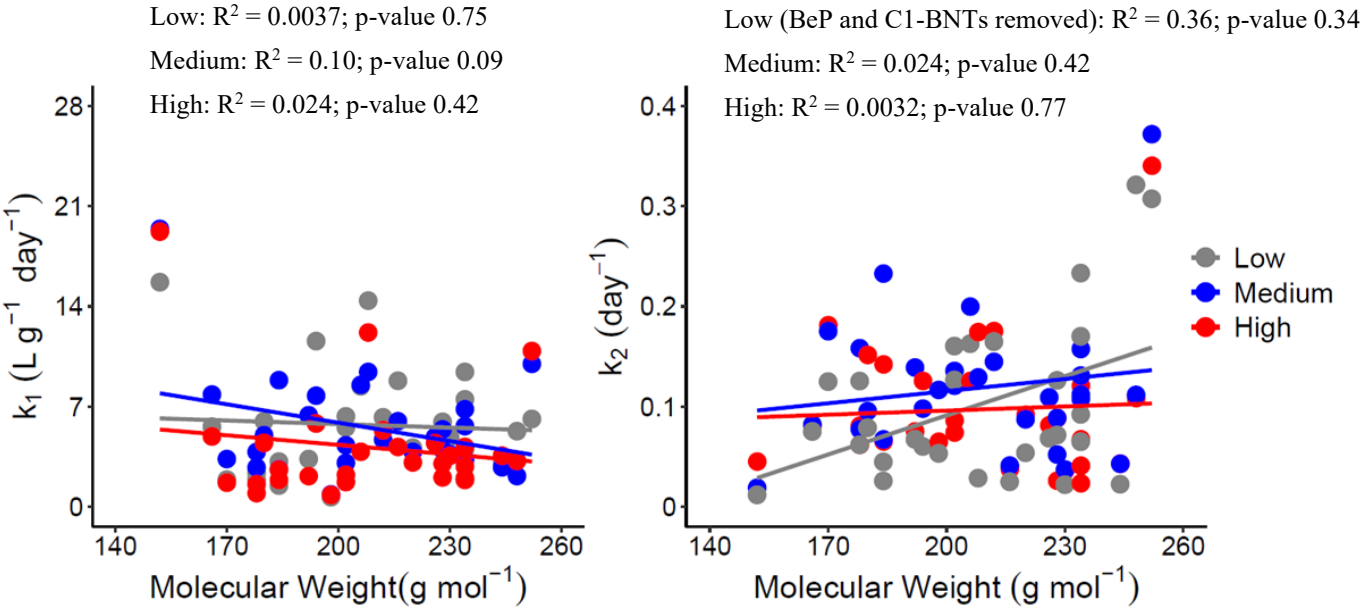

Figure 3.21: Linear regression analyses between uptake (L g^{-1} day^{-1} - left) and depuration (day^{-1} - right) rate constants of PACs (n=29 per treatment) and their associated molecular weight (g mol^{-1}). Regression analyses performed in R Studio revealed no significant relationships (p-value >0.05) for the Medium and High treatment. Removing k_2 of C1-benzonaphthothiophenes and benzo[e]pyrene from the Low treatment (outliers) revealed no significant differences between the PACs k_2 values and their associated molecular weight (p-value 0.34).

Uptake rate constants from this study were higher than the uptake rate constants reported by studies involving other aquatic organisms (e.g. fish and tadpoles) exposed to PACs (Baussant et al., 2001; Bilodeau et al., 2019; Mathew et al., 2008; Neff, 2002b; Willis & Oris, 2014). The faster uptake rates in mussels compared to fish and tadpoles can be explained by PAC metabolism, which was higher in aquatic vertebrates, as well as tadpoles, compared to invertebrates (Bilodeau et al., 2019; Ko et al., 2018; Livingstone, 1998; Neff, 2002b; Rust et al., 2004). During the accumulation phase of the studies involving fish and tadpoles, PACs in tissue declined due to metabolism, despite continuous exposure, resulting in lower uptake rate constants. However, when bivalves were exposed to PACs, tissue concentrations continuously increased until steady state conditions, never really fluctuating due to metabolism, resulting in higher uptake rate constants. Furthermore, once placed in clean water, results from this study and other experiments involving bivalves revealed a slower release of accumulated PACs than fish and tadpoles, resulting in lower depuration rate constants for mussels (Bilodeau et al., 2019; Enwere et al., 2009; Mathew et al., 2008; Neff, 2002b; Rust et al., 2004; Willis & Oris, 2014).

Bioconcentration factors (BCFs) were used as a measure of the bioaccumulation potential of PACs to giant floater mussels and were calculated as either the ratio of k_1 and k_2 (BCF_K) or the ratio of PAC concentrations in mussels and water (BCF_C) at day 25 of the accumulation phase (generally the highest concentration in mussel tissue; Table 3.4). BCF_K values were generally higher than BCF_C (69% of the compounds from all three treatments; n=87) also indicating that PACs did not reach steady state in giant floater mussels. Therefore, BCF_K values were used for all analyses in this thesis. Log BCFs ranged from 3.87 to 6.13 L kg^{-1} (n=87) and the PACs with the highest log BCF values were acenaphthylene (mean of 5.92 ± 0.26 L kg^{-1}; ±SD, n=3), C3-fluorenes (mean of 5.14 ± 0.19 L kg^{-1}, ±SD; n=3), and C2-fluorenes (mean of 4.94 ± 0.30 L kg^{-1}; ±SD, n=3).

BCF values reported in this thesis are conservative as they do not take into account the accumulation of PACs from dilbit particles in the water. The exposure associated with dilbit particles could not be quantified therefore, bioaccumulation factors (BAFs) could not be determined. BAFs take into account accumulation from every exposure route (e.g., water and consumption of particles). However, BCFs from this study were similar to what has been previously reported in experiments involving bivalves (Arnot & Gobas, 2006; Baussant et al., 2001; S. W. Fisher et al., 1993; Gossiaux et al., 1996; Hwang et al., 2008; Yakan et al., 2011).

Table 3.4: Bioconcentration factors calculated from the ratio of uptake and depuration rate constants (BCF_K; L kg^{-1}) and the ratio of PAC concentrations in mussels and water at day 25 (day 11 and 20 for C0-fluoranthene from the Low and Medium treatments, respectively, and day 11 retene from the Low and Medium treatments) of the uptake phase (BCF_C; L kg^{-1}) for the 29 PACs that accumulated in giant floater mussels. BCF values are expressed on a ~1% lipid content.

	Low (L kg^{-1})		**Medium (L kg^{-1})**		**High (L kg^{-1})**	
PAC	**log BCF_K**	**log BCF_C**	**log BCF_K**	**log BCF_C**	**log BCF_K**	**log BCF_C**
C3-NAP	4.18	4.11	4.28	4.38	3.96	4.06
C4-NAP	5.09	4.76	4.58	4.65	4.26	4.28
ACY	6.13	5.59	6.01	5.63	5.63	5.41
C0-FLU	4.87	4.77	4.98	4.99	4.78	4.69
C1-FLU	4.88	4.84	4.72	4.70	4.47	4.49
C2-FLU	5.26	5.16	4.90	4.87	4.67	4.64
C3-FLU	5.70	5.41	4.86	4.89	4.84	4.85
C0-DBT	4.52	4.42	4.59	4.51	4.46	4.46
C1-DBT	4.10	4.01	3.87	3.87	4.10	4.06
C2-DBT	4.58	4.63	4.51	4.50	4.48	4.51
C3-DBT	4.85	4.82	4.65	4.64	4.74	4.68
ANT	4.28	4.32	4.38	4.41	4.07	4.05
C0-PHE	4.49	4.44	4.55	4.47	4.40	4.38
C1-PHE	4.69	4.67	4.66	4.65	4.45	4.50
C2-PHE	4.71	4.78	4.63	4.66	4.49	4.51
C3-PHE	4.88	4.78	4.64	4.60	4.53	4.50
C4-PHE	4.91	4.83	4.64	4.67	4.54	4.59
RET	4.74	4.67	4.72	4.56	4.62	4.46
PYR	4.70	4.73	4.35	4.34	4.41	4.35
C0-FLA	4.54	4.46	4.55	4.51	4.37	4.08
C1-FLA	5.55	5.22	5.16	5.05	5.05	4.85
C2-FLA	5.35	4.97	4.99	4.85	5.00	4.79
C3-FLA	5.15	4.80	4.81	4.69	4.92	4.76
BNT23	4.47	4.42	4.46	4.45	4.90	4.56
BNT21	4.23	4.35	4.40	4.39	4.69	4.52
C1-BNT	4.22	4.34	4.28	4.27	4.47	4.50
C0-CHY	4.67	4.72	4.79	4.73	4.90	4.57
BaA	4.85	4.71	4.88	4.76	4.53	4.53
BeP	4.30	4.26	4.43	4.44	4.50	4.50

Based on the Canadian Persistence and Bioaccumulation regulation (a substance is bioaccumulative when its BCF value surpasses 5,000 L kg^{-1}), all 29 PACs that accumulated in mussel tissue were considered to be bioaccumulative (Government of Canada, 2000). However, OECD guidelines for testing of chemicals recommends expressing BCF values on a 5% lipid content (OECD, 2012). Mussels from this experiment had a mean lipid content of roughly 1% and bivalves, in general, have lower lipid content than 5% (Baussant et al., 2001; Hwang et al., 2008; Thorsen et al., 2004; H. Wang et al., 2017). Nonetheless, if BCF values from this study were expressed on a 5% lipid content, most PACs (20 of the 29 PACs) would still be considered bioaccumulative for all three dilbit-contaminated treatments. Furthermore, four PACs would still be considered bioaccumulative for two of the treatments and two PACs would still be considered bioaccumulative for one of the treatments. Only three of the 29 PACs that accumulated in mussel tissue (C3-naphthalenes, anthracene, and C1-dibenzothiophenes) would not be considered bioaccumulative under the Canadian regulations. However, these three compounds would still be considered bioaccumulative based on European Chemicals Agency (ECHA) guidelines which state that compounds with BCF values of 2,000 L kg^{-1} or greater are bioaccumulative while compounds with BCF values surpassing 5,000 L kg^{-1} are 'very bioaccumulative'. Finally, since the sediment in the aquaria was not a source of PACs to the giant floater mussels, biota-sediment accumulation factors (BSAFs) could not be calculated. Future research is therefore needed to assess the bioaccumulation potential of PACs derived from dilbit-contaminated sediments to freshwater mussels and how varying degrees of organic content in the sediment affects accumulation.

I found no significant differences in BCF values between the three treatments (p-value 0.24, Figure 3.22). However, I did observe a lot of variation in BCFs within a treatment (BCF values ranged from 12 to 1340 L day^{-1} for the Low treatment, 7 to 1032 L day^{-1} for the Medium treatment, and 9.2 to 427 L day^{-1} for the High treatment) which may explain why I observed no statistically significant differences among treatments. In Figure 3.22, BCFs for PACs in the three dilbit-contaminated treatments demonstrated a decreasing trend where BCF in the Low (132 ± 256 L day^{-1}, ±SD, n=29) and Medium (83 ± 185 L day^{-1}, ±SD, n=29) treatments were higher than the High treatment (56 ± 76 L day^{-1}, ±SD, n=29), similar to k_1 values. Furthermore, no significant differences were found when comparing BCFs of parent PACs and their alkylated homologues (p-value 0.18, Figure 3.23). However, this may also be the result of high variations of BCF values within the alkylated group (ranged from 7 to 505 L day^{-1}). Looking at BCFs for individual PACs (Figure 3.24), similar to k_1 values, BCFs for alkyl PACs were generally higher than their parent counterparts. This observation supports our prediction that alkyl PACs were more bioaccumulative than their parent counterpart, which Baussant et al. (2001) also reported when they exposed *Mytilus edulis* to water contaminated with dispersed crude oils. Higher BCF values for alkyl PACs further emphasizes the need to include these compounds when analyzing for PACs and not just focus on the 16 U.S. EPA priority parent PACs (Andersson & Achten, 2015; Stout et al., 2015).

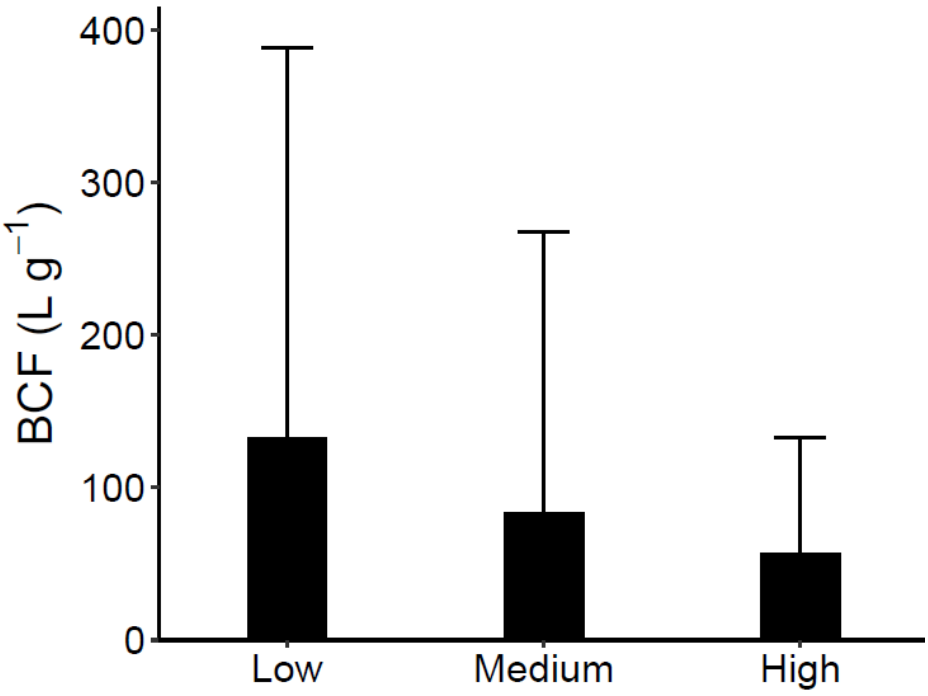

Figure 3.22: Mean (±SD, n=29 per treatment) bioconcentration factors (BCF - L g^{-1}) of PACs for all three dilbit-contaminated treatments. Non-parametric statistical analysis (Kruskal-Wallis rank sum test; Table E.18) performed in R Studio on log-transformed data revealed no significant differences (p-value 0.24) between the three treatments. Data were back-transformed.

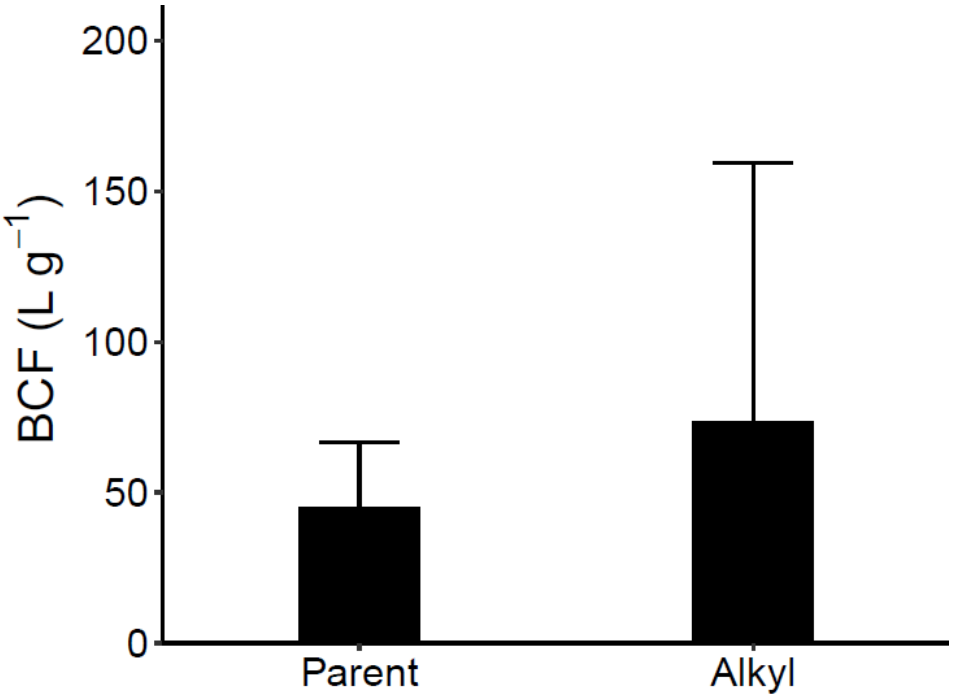

Figure 3.23: Mean (±SD) bioconcentration factors (L g^{-1}) of parent (n=21) and alkyl (n=51) PACs. All three dilbit-contaminated treatments were grouped. Only the analyses of parent PACs with alkylated homologues are included. Student's t-test (with no assumption of equal variance; Table E.19) performed in R Studio on log-transformed data revealed no significant differences (p-value 0.18) between parent and alkyl PACs. Data were back-transformed.

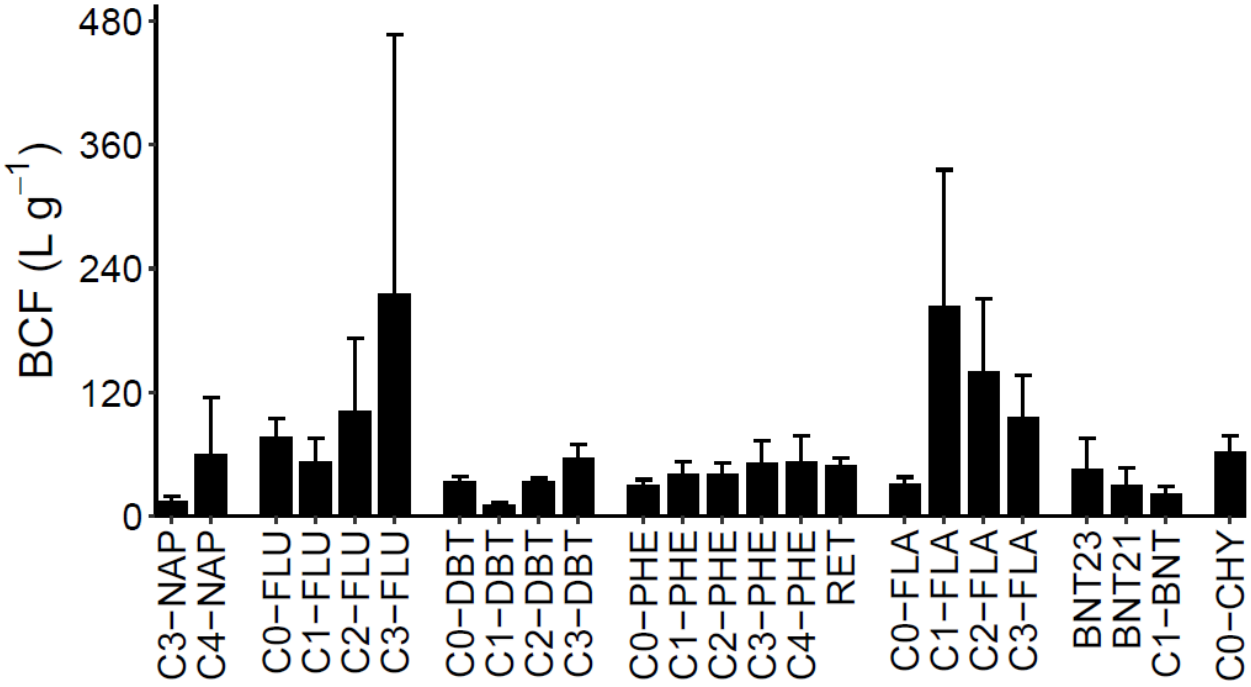

Figure 3.24: Mean (±SD, n=3) PAC bioconcentration factor profiles (BCF - L g^{-1}) of unsubstituted parent PACs and their alkylated counterparts. Bioconcentration factors from all three treatments contaminated with dilbit were grouped. Abbreviations are found in Appendix A.

Many studies involving fish have reported a parabolic relationships between log BCF and log K_{OW} (Baussant et al., 2001; Gobas & Morrison, 2000), while studies involving mussels have reported no such pattern (Baussant et al., 2001; Hwang et al., 2008; Meador, 2003). I likewise observed no significant relationship between log BCF and log K_{OW} (Figure 3.25). Caution must therefore be taken when comparing toxicokinetic parameters (k_1, k_2, BCF) between different types of aquatic species as differences in metabolism between species may lead to significant differences in toxicokinetic parameter values and trends.

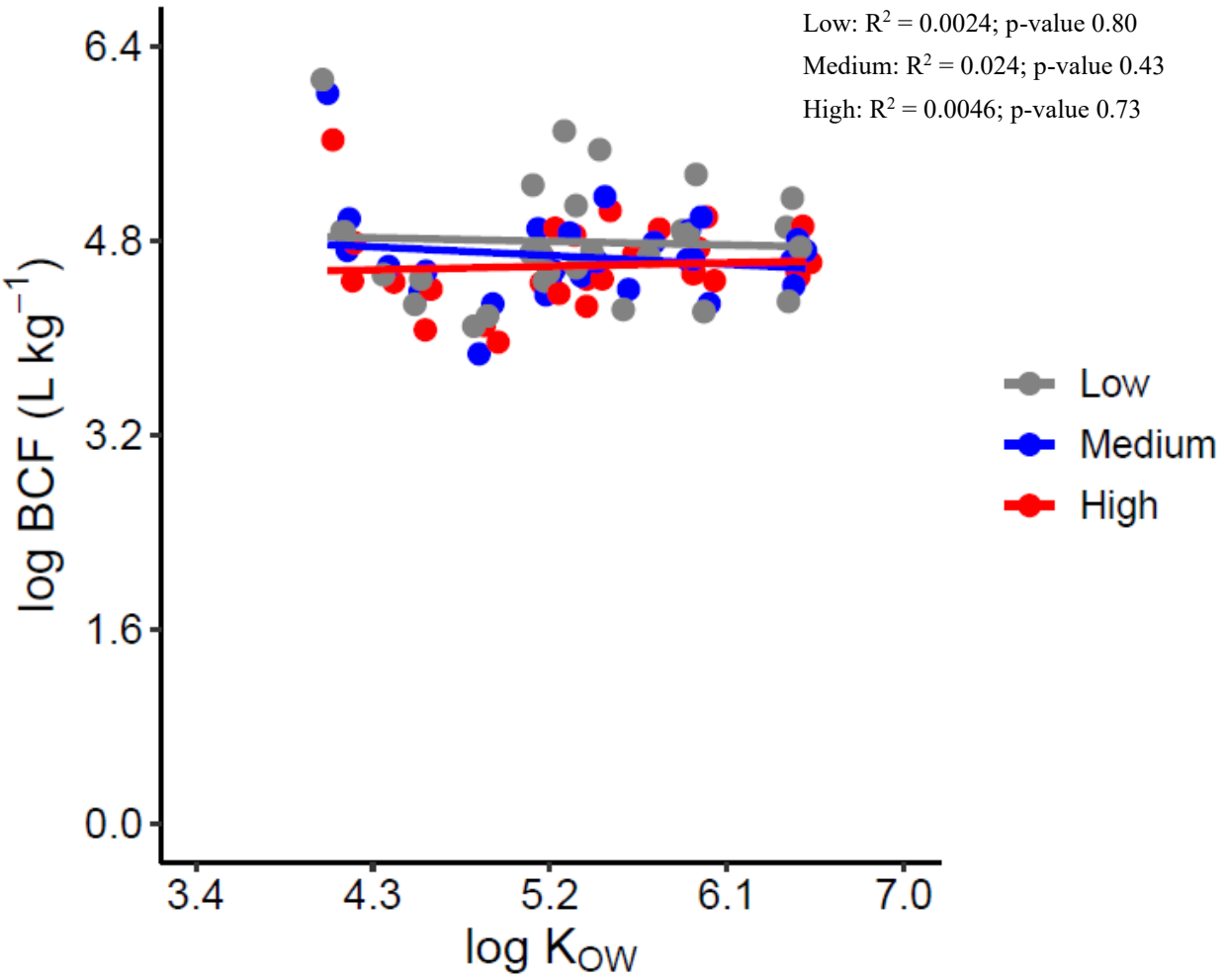

Figure 3.25: Linear regressions between log-transformed bioconcentration factors of the 29 PACs that accumulated in mussel tissues and their associated log K_{OW} value. Linear regression analysis performed using R Studio revealed no significant relationship for all three treatments (p-value > 0.05).

3.4. PACs Chapter Conclusion

This *ex-situ* field experiment revealed the uptake and elimination rate constants of parent and alkyl PACs in the freshwater mussel *Pyganodon grandis* exposed to water contaminated with naturally weathered Cold Lake diluted bitumen blend for 25 days. I observed no mortalities during this experiment where 29 of the 46 analysed PACs bioaccumulated in mussel tissue. Alkyl PACs accounted for roughly 95% of the TPACs detected in mussel tissue at the end of the uptake phase,

generally following petrogenic PAC profiles of dilbit. Statistical analysis revealed no significant differences in uptake rates between parent and alkyl PACs k_1 and BCF values increased as the number of alkylated groups increased, especially for C2 and C3 alkyl PACs. This study confirmed that alkyl PACs have greater bioaccumulation potential than their unsubstituted parent PACs.

This bioaccumulation study also revealed the possibility of concentration-dependence associated with PAC accumulation where uptake rate constants from the Low and Medium treatments were significantly greater than the uptake rate constants from the High treatment. We believe that this could be a result of differences in filtration rates and/or differences in metabolizing rates between the treatments, resulting in lower PAC uptake rates for the High treatment. Nonetheless, 29 PACs bioaccumulated in giant floater mussels exposed to dilbit-contaminated water, demonstrating the lower metabolic capability of bivalves to excrete PACs compared to other aquatic species. Most of the PACs were still detected in mussel tissue following the 16-day depuration phase, suggesting that giant floater mussels could be used as bioindicators for petroleum contamination in a freshwater ecosystem following a dilbit spill. This field experiment also highlights the importance of including alkyl PACs in toxicological studies and environmental monitoring of petroleum products. Improved PACs accumulation models for a wide variety of aquatic organisms is useful for the risk assessment of chemicals and will inform stakeholders on best practices when addressing future oil spills.

4. Dilbit-Derived Metals and Sulfur in Giant Floater Mussels

4.1. Metal and Sulfur Concentrations in the Exposure Water and Sediment

Concentrations of total and dissolved metals were measured in the exposure water, directly from the aquaria, to quantify the exposure of giant floater mussels to metal contamination. In addition to the data presented in this thesis, a separate in-depth assessment of the temporal trends of metals in the water column of the in-lake enclosures is presented in Rodriguez-Gil et al. (in preparation).

Total and dissolved metal concentrations in the aquaria water were similar except for significantly greater concentrations of scandium, vanadium, strontium, zinc, magnesium, and calcium (ordered by increasing concentration and discussed later in the chapter) in the dilbit-contaminated treatments compared to the Control (Appendix G). Total and dissolved concentrations for most of the previously mentioned metals were however significantly slightly greater in the Control compared to Lake 260 water and were most likely affected by the limnocorrals themselves. The enclosures were separated from the rest of the lake from early July to the end of August and many factors such as primary production, lake stratification, uptake by biofilm, and binding to the curtain could have contributed to differences in metal concentrations between the Control and Lake 260. Furthermore, materials used for the construction of the limnocorrals (e.g., metal brackets, zinc plated bolts, components of the sampling port, etc.) and galvanised minnow traps (Gee's minnow traps) used to fish and house minnows in the limnocorrals could have contributed to metal enrichment in these systems.

One-way ANOVA analyses showed significant differences in total and dissolved vanadium concentrations when comparing between treatments (p-values < 0.001 and < 0.001, respectively). As predicted, multiple pairwise comparisons using Tukey's honestly HSD test revealed that total

and dissolved vanadium concentrations in the water from all three dilbit-contaminated treatments were significantly greater than the Control and Lake 260 water samples (Figure 4.1). I observed no significant differences in vanadium concentrations between the dilbit-affected treatments. Furthermore, total and dissolved vanadium concentrations from the dilbit-contaminated treatments (0.160 ± 0.019 µg L^{-1}; ± SD, n=12, and 0.096 ± 0.017 µg L^{-1}; ± SD, n=13, respectively) were only slightly higher than in the Control (0.084 ± 0.016 µg L^{-1}; ± SD, n=4, and 0.027 ± 0.004 µg L^{-1}; ± SD, n=4, respectively). This, coupled with no significant differences between dilbit-contaminated treatments suggests that vanadium in the dilbit was not readily soluble in the water and was instead strongly associated with the organic ligands present in the dilbit.

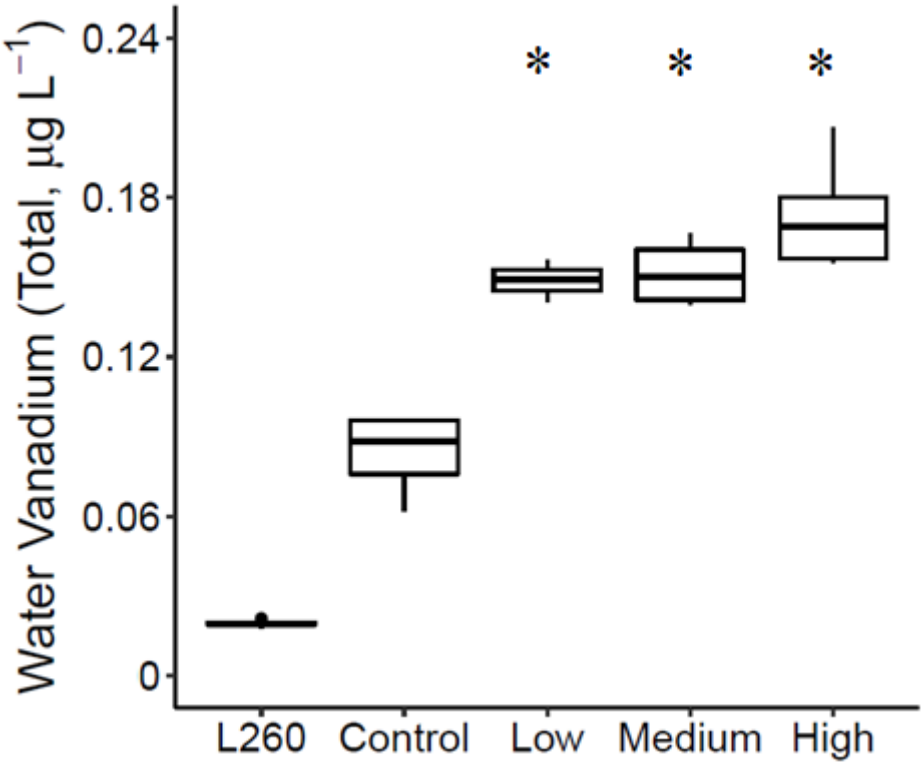

*Figure 4.1: Box plot of total vanadium concentrations in dilbit-contaminated aquaria water (n=3, 4, and 5 for the Low, Medium, and High treatments) and the Control (n=4) during the uptake phase, as well as water collected from Lake 260 (n=4). Pairwise comparisons using Tukey's HSD test (Table G.2) conducted in R Studio revealed no significant differences (p-value > 0.05, denoted by *) when comparing dilbit-contaminated treatments while all other comparisons between treatments and Lake 260 were significant (p-value < 0.05).*

Notably, total vanadium concentrations recorded for day 25 were much higher than any other time point from the same treatments. For example, total vanadium concentrations in water from the Control and Medium treatment on day 25 were roughly 2 times greater than the average (excluding day 25). On day 25, we observed no notable differences in temperature, precipitation, wind, sediment suspension, etc., relative to the days before or after, to account for such an increase in vanadium. Therefore, the markedly high total vanadium concentrations on day 25 may be a result of sampling and/or analytical errors. In addition, 8 other metals (total concentrations) were

roughly twice as concentrated on day 25 relative to the respective averages. All water samples (total and dissolved) collected on day 25 were thus excluded from analysis in this thesis (including the analyses previously conducted in this chapter).

Total and dissolved nickel concentrations in the dilbit-contaminated water were below detection limit (> 0.0288 μg L^{-1}). This was unexpected since nickel is one of the most prevalent metals in dilbit (Emergencies Science and Technology Division, 2006; K. Lee et al., 2015). This suggests that nickel likely acts in a similar manner to vanadium where, despite the presence of nickel in the source oil, it is not readily soluble in the water but is instead strongly associated to the ligands in dilbit. Another possible reason for low nickel concentrations in the aquaria water is a result of dilbit processing that requires roughly 3 barrels of freshwater for every barrel of bitumen produced (Oil Sands Magazine, 2020). Water washing of bitumen once extracted from the oil sands removes many of the polar and water-soluble components, resulting in elevated concentrations of these compounds in bitumen process water (Allen, 2008; K. Lee et al., 2015). Nickel may be removed during the initial processing of bitumen because of its association with porphyrin compounds (polar compounds), reducing its concentration in dilbit. It would therefore be useful to characterise metal concentrations in dilbit and not just bitumen.

Our low vanadium and nickel concentrations (total and dissolved) in water were similar to those previously reported in two laboratory studies conducted by Krohn et al. (2020) and Robideaux et al. (2018). Furthermore, environmental monitoring of surface waters following the Deepwater Horizon spill also revealed no elevated concentrations of vanadium and nickel (Joung & Shiller, 2013). Contrarily, Santos-Echeandía et al. (2008) found elevated concentrations of vanadium and nickel in the Atlantic Ocean following the sinking of the Prestige oil tanker (carrying roughly 77,000 tonnes of heavy fuel oil), off the coast of Spain. It is important to note that results

presented in this thesis are from water samples collected 35 days after we added dilbit to the limnocorrals. It is thus possible that dilbit- derived metals in solution partitioned into the sediment and that metals bound to particulate had settled prior to our sampling. However, Rodriguez-Gil et al. (in preparation) collected water samples from the limnocorrals closer to the date of dilbit addition and total vanadium concentrations in the enclosure water did not reach a plateau during the observed period (70 days after the addition of dilbit). Furthermore, nickel concentrations in the limnocorrals were similar to aquaria water from this study. Nonetheless, there is not much available in the literature regarding dilbit-associated metals and how they partition in water. In order to understand the environmental impacts of metal contamination resulting from a dilbit spill, it would be beneficial to conduct a laboratory study investigating the stability of metals in a slick once it comes in contact with water (both salt and freshwater).

Using one-way ANOVA tests, I found significant differences when I compared total and dissolved zinc concentrations between treatments (p-values < 0.001 and < 0.001, respectively; Figure 4.2). Zinc concentrations (total and dissolved) in water from the dilbit-contaminated treatments were significantly greater than in the Control. For most of the uptake phase, zinc was the only metal that surpassed water quality guidelines set by the Canadian Council of Ministers of the Environment (CCME). In the Low treatment, dissolved zinc concentrations (average of 38.26 ± 7.05 µg L^{-1}, ±SD, n=3) surpassed CCME guidelines for short-term exposures (37 µg L^{-1}, dissolved), except for samples collected on day 20. Conversely, in the High treatment, dissolved zinc concentrations (average of 30.48 ± 8.84 µg L^{-1}, ±SD, n=5) only surpassed the guidelines on day 20. Pairwise comparisons using Tukey's HSD test revealed no significant differences between the High and Low treatments (p-value 0.37) and between the High and Medium treatments (p-value 0.40). Dissolved zinc concentrations in the Medium treatment (average of 22.95 ± 6.73 µg

L^{-1}, ±SD, n=4) were significantly lower than the Low treatment (p-value 0.02) and did not surpass CCME guidelines for short-term exposure. Nevertheless, for the entirety of the uptake phase, the guideline for long-term exposures (7 µg L^{-1}, dissolved) was surpassed in all three dilbit-contaminated treatments.

It is unclear if elevated zinc concentrations in the water column was caused by dilbit contamination. Dissolved zinc concentrations in the Far Field Control limnocorral (100 ± 32 µg L^{-1}, ±SD, n=6; samples collected by Rodriguez-Gil et al. (in preparation)) were higher than dissolved zinc concentrations in the dilbit-contaminated treatments (ranging from 30.26 – 38.26 µg L^{-1}, n=12) and Control (6.75 ± 3.31 µg L^{-1}, n=4) from this thesis. Water samples from the Far Field Control were collected differently but we still expected higher zinc concentrations in the water contaminated with dilbit. Further investigation by Rodriguez-Gil et al. (in preparation) should determine if dilbit-contamination contributed to elevated zinc concentration in the water. Nonetheless, one of the environmental assessments conducted following the Deepwater Horizon blowout by Carmichael et al. (2012) reported elevated zinc concentrations (concentrations not reported) in the water column. Furthermore, Prego (2003) reported elevated zinc concentration in the water column following the Prestige oil spill (~60,000 tonnes of heavy crude oil spilled from a sunken tanker in the Northeast Atlantic). These results show the importance of monitoring metal contamination, especially zinc, following an oil spills as long-term exposures of these elevated concentrations could be detrimental to aquatic organisms.

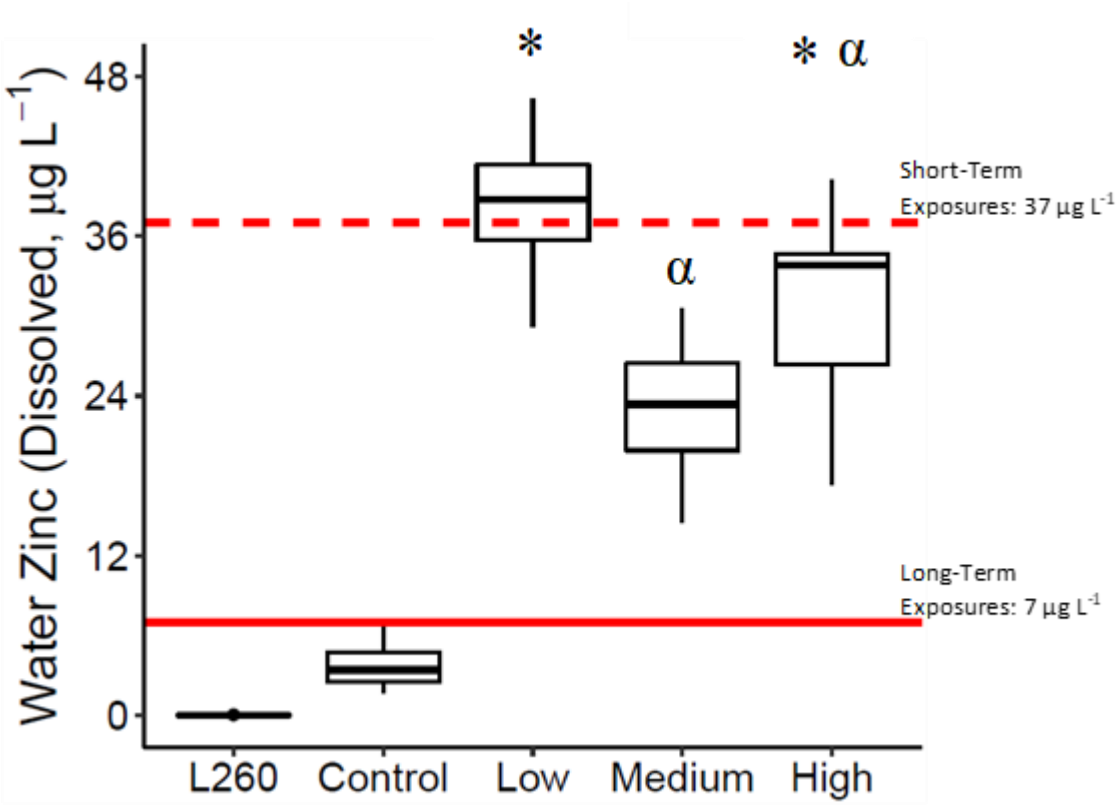

*Figure 4.2: Box plot of dissolved zinc concentrations in dilbit-contaminated aquaria water (n=3, 4, and 5 for the Low, Medium, and High treatment and the Control (n=4) during the uptake phase, as well as water collected from Lake 260 (n=4). Pairwise comparisons using Tukey's HSD test (Table G.4) in R Studio revealed no significant differences (p-value > 0.05, denoted by * and α) when comparing the Low and High treatments and the High and Medium treatments. All other comparisons between treatments and Lake 260 were significant (p-value < 0.05). The solid red line indicates the CCME guidelines for long-term exposure limits to zinc (7 µg L^{-1}, dissolved) for the protection of aquatic life while the red dotted line indicates CCME guidelines for short-term exposures to zinc (37 µg L^{-1}, dissolved).*

Major elemental analysis of the aquaria water revealed significantly greater total and dissolved concentrations of calcium (average of 2.98 ± 0.08 mg L^{-1} and 3.16 ± 0.04 mg L^{-1}, ±SD, n=5, respectively) and magnesium (0.68 ± 0.01 mg L^{-1} and 0.70 ± 0.03 mg L^{-1}, ±SD, n=5, respectively) in the High treatment compared to total and dissolved concentrations of calcium (average of 2.51 ± 0.06 mg L^{-1}, n=11 and 2.76 ± 0.04 mg L^{-1}, n=12, ±SD, respectively) and magnesium (0.59 ± 0.01 mg L^{-1}, n=11 and 0.63 ± 0.06 mg L^{-1}, n=12, ±SD, respectively) in the Control, Low, and

Medium treatments (Figures 4.3 and 4.4). The elevated calcium concentrations (total and dissolved) were not detrimental to mussels as mussels require relatively high calcium concentrations for the production of their shells (over 12 mg L^{-1}; Cohen, 2005; Thomsen et al., 2018). Total and dissolved magnesium concentrations were lower than calcium concentrations in the High treatment and were not considered to be a concern as magnesium is an essential metal and there are no guidelines in place for the protection of aquatic organisms. Furthermore, a number of studies have shown that elevated concentrations of calcium and magnesium have decreased the toxicity of metals due to competition for uptake sites of the organism (Gillis et al., 2008; Liu et al., 2016; Rathore & Khangarot, 2003; Yim et al., 2006). Elemental analysis of CLB dilbit (Emergencies Science and Technology Division, 2006) revealed elevated calcium and magnesium concentrations compared to other metals, which coincides with the elevated concentrations in the High treatment. However, it is surprising that total and dissolved calcium and magnesium concentrations were not higher in the Medium and Low treatments. Environmental monitoring following the Deepwater Horizon spill demonstrated elevated magnesium concentrations in the water column (Carmichael et al., 2012). Calcium and magnesium are not often included in elemental analysis following the release of petroleum products in the environment. We suggest that future research include calcium and magnesium in the analysis of petroleum-affected water as elevated concentrations have shown to protect aquatic organisms from metal toxicity.

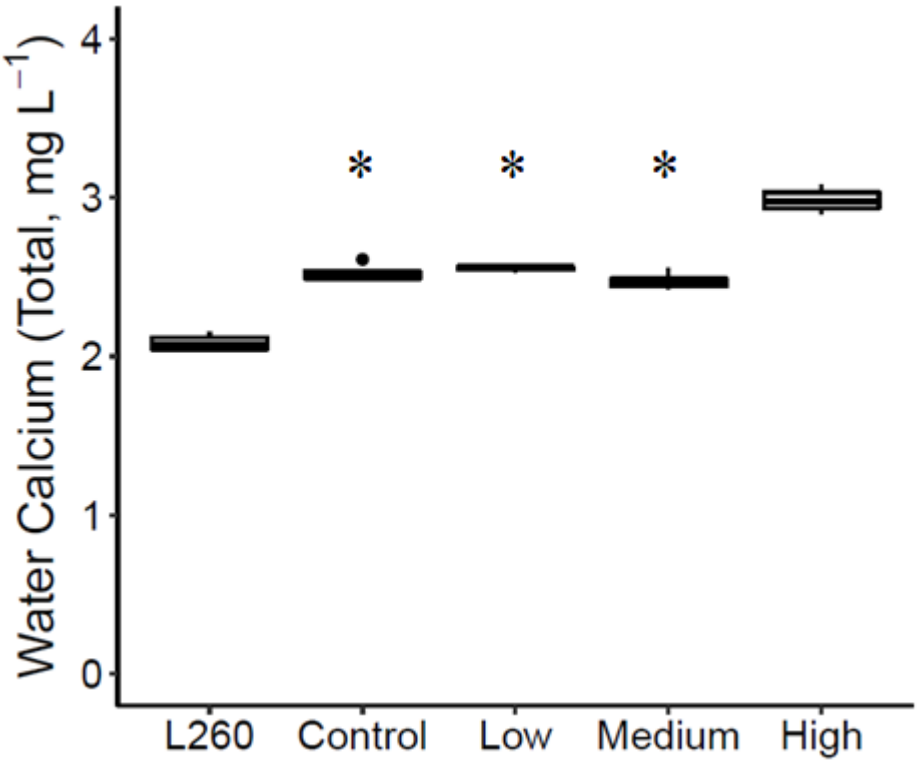

*Figure 4.3: Box plot of total calcium concentrations in dilbit-contaminated aquaria water (n=3, 4, and 5 for the Low, Medium, and High treatments) and the Control (n=4) during the uptake phase, as well as water collected from Lake 260 (n=4). Pairwise comparisons using Tukey's HSD test (Table G.2) conducted in R Studio revealed no significant differences between the Low, Medium treatments and the Control (p-value > 0.05, denoted by *) while all other comparisons were significant.*

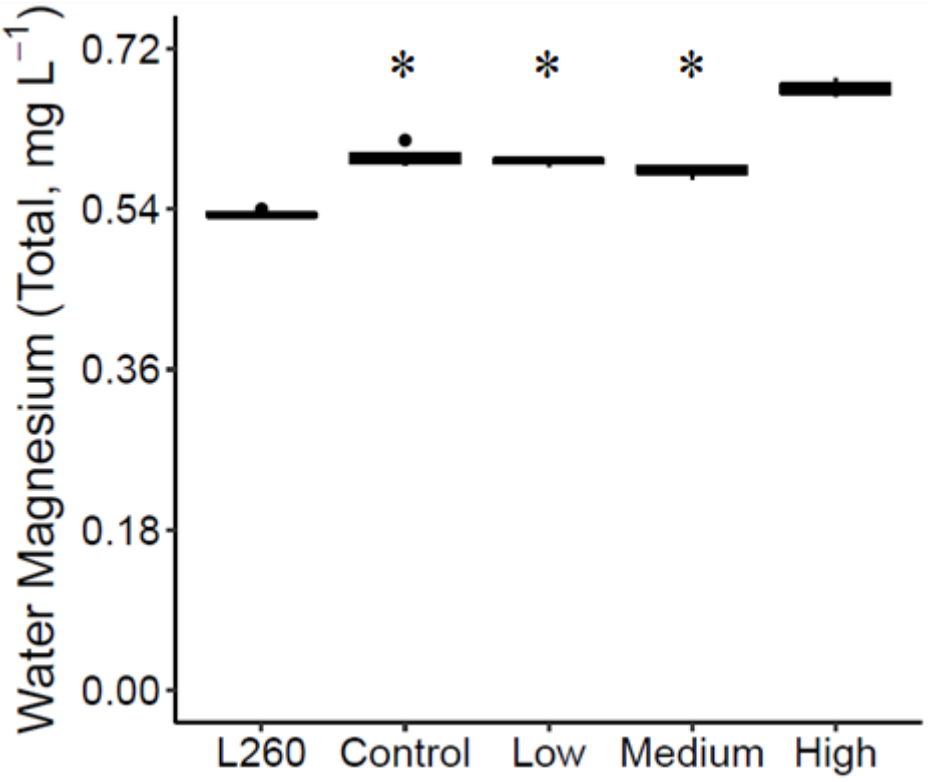

*Figure 4.4: Box plot of total magnesium concentrations in dilbit-contaminated aquaria water (n=3, 4, and 5 for the Low, Medium, and High treatments) and the Control (n=4) during the uptake phase, as well as water collected from Lake 260 (n=4). Pairwise comparisons using Tukey's HSD test (Table G.2) conducted in R Studio revealed no significant differences between the Low, Medium treatments and the Control (p-value > 0.05, denoted by *) while all other comparisons were significant.*

In the Control and Low, Medium, and High treatments, total and dissolved water sulfur concentrations exhibited a clear significant dose-relationship (p-values < 0.001 and 0.001, respectively; Appendix G). Total and dissolved concentrations in the High treatment (average of 0.94 ± 0.03 mg L^{-1} and 0.94 ± 0.04 mg L^{-1}, ±SD, n=5, respectively) were significantly greater than those in the Medium (average of 0.63 ± 0.01 mg L^{-1} and 0.62 ± 0.01 mg L^{-1}, ±SD, n=4, respectively) and Low (average of 0.57 ± 0.01 mg L^{-1}, n=3, and 0.56 ± 0.01 mg L^{-1}, n=4, ±SD,

respectively) treatments, as well as in water samples from the Control (average of 0.44 ± 0.01 mg L^{-1} and 0.45 ± 0.03 mg L^{-1}, ±SD, n=4) and Lake 260 (average of 0.45 ± 0.01 mg L^{-1} and 0.44 ± 0.00 mg L^{-1}, ±SD, n=4; Figure 4.5). I also found significant differences in total and dissolved sulfur concentrations between the Medium and Low treatments (p-values 0.001 and 0.03, respectively) and between the Low treatment and the Control (p-values < 0.001 and 0.03, respectively). CLB dilbit has a relatively high sulfur content, as much as 5% (Emergencies Science and Technology Division, 2006; K. Lee et al., 2015), explaining why sulfur concentrations increased with the concentration of dilbit. Furthermore, I observed no significant difference in water total and dissolved sulfur concentrations from the Control and Lake 260 (p-values > 0.99 and 0.69, respectively), further suggesting that dilbit was the source of sulfur contamination. Most of the sulfur found in crude oils (> 99%) is organic, which generally poses no environmental concern (K. Lee et al., 2015). Nonetheless, it is still important to monitor sulfur following a dilbit spill as hydrogen sulfide (H_2S) can be toxic to humans and aquatic species.

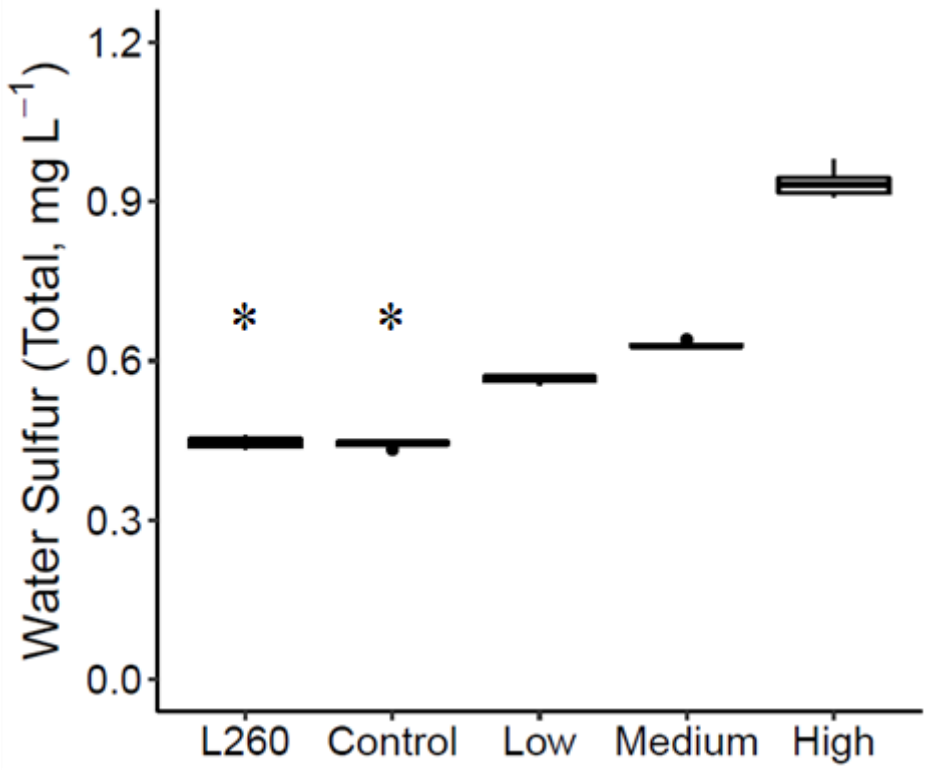

*Figure 4.5: Box plot of total sulfur concentrations in dilbit-contaminated aquaria water (n=3, 4, and 5 for the Low, Medium, and High treatments) and the Control (n=4) during the uptake phase, as well as water collected from Lake 260 (n=4). Pairwise comparisons using Tukey's HSD test (Table G.2) conducted in R Studio revealed no significant differences (p-value > 0.05, denoted by * and α) between the Control and Lake 260 while all other comparisons were significant.*

Total arsenic, barium, iron, potassium, and sodium concentrations (ordered by increasing concentration) were significantly greater in the Control compared to the dilbit-contaminated treatments (Appendix G). However, only dissolved potassium and sodium were significantly greater in the Control compared to dilbit-contaminated treatments. Notably, there were three adult white suckers (*Catostomus commersonii*) trapped in the Control limnocorral which are demersal fish that stir up sediments as they feed, thus resuspending sediments in the limnocorral. We therefore suspect that in the process of feeding, the white suckers enriched the overlying water

column with metals that were previously settled in the sediment. In fact, total suspended solids (TSS) in the Control limnocorral (average of 1.52 ± 1.29 mg L^{-1}; ± SD, n=10) were generally greater than in the Low, Medium, and High limnocorrals (average of 0.76 ± 0.58 mg L^{-1}, 0.52 ± 0.50 mg L^{-1}, 0.56 ± 0.47 mg L^{-1}, respectively; ± SD, n=10), but the differences were not significant (p-value 0.17; Figure 4.6).

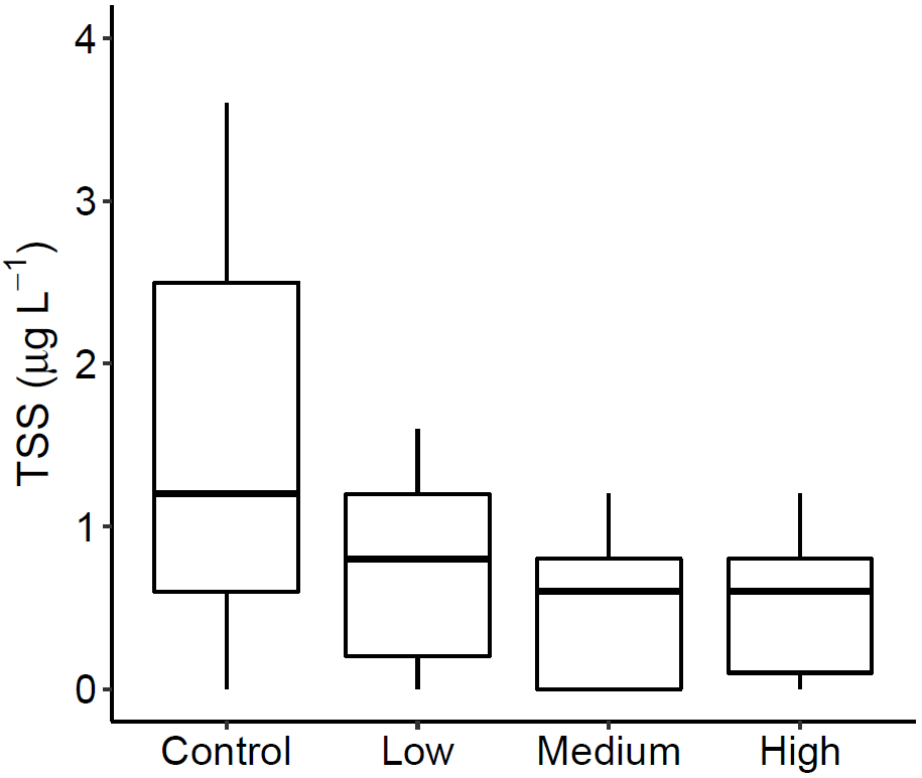

Figure 4.6: Box plot of total suspended solids (TSS) in the Control, Low, Medium, and High treatment limnocorrals. TSS data were collected from the limnocorrals between June 6th to August 28th, 2018 (n=20 per treatment). Welch's one-way test (Table G.5) conducted in R Studio revealed no significant differences (p-value 0.17) between dilbit-contaminated treatments and the Control.

Most metals in the water did not increase in concentration following dilbit addition and accordingly, metal concentrations in the sand were consistently low during the uptake phase. Furthermore, metal concentrations in the aquaria sand were not significantly different between treatments (Table G.6) and never surpassed the CCME sediment quality guidelines. The relatively constant metal concentrations in the sand throughout the uptake phase suggest that the metals in the sand prior to the experiment were not incorporated by mussels. Furthermore, throughout the experiment, the sand was never in contact with the dilbit slick itself, reducing the potential of metal transfer from the slick to the sand. Notably, dilbit has shown to sink in freshwater environments (Stoyanovich et al., 2019; U.S. Fish and Wildlife Service et al., 2015), potentially contaminating sediments in a natural setting. Further research is therefore required to determine if sunken weathered dilbit is a source of metal contamination to sediments.

4.2. Metal Accumulation in Giant Floater Mussels (*Pyganodon grandis*)

In most cases, water metal concentrations were not significantly different between dilbit-contaminated treatments and the Control. Therefore, we opted to restrict our metals analysis to mussel tissues collected from the Control and High treatment only. Mussels in dilbit-contaminated aquaria did not accumulate any metals including elevated water concentrations of scandium, vanadium, strontium, magnesium, calcium, and sulfur. Only zinc showed slight accumulation in mussel tissue (discussed later in the chapter). The lack of metal accumulation is similar to findings by Roubideaux et al. (2018) that dilbit-treated water resulted in no significant metal accumulation by rainbow trout (*Oncorhynchus mykiss*), nor in two invertebrate species, daphnia (*Daphnia magna*) and ceriodaphnia (*Ceriodaphnia dubia*), when exposed to WAF of dilbit. However, the study by Krohn et al. (2020) revealed that wood frog (*Lithobates sylvaticus*) tadpoles raised in a

dilbit-contaminated environment had higher vanadium, molybdenum, and cadmium than tadpoles raised in their control treatment, but not at levels known to negatively impact development. Contrary to our prediction, the giant floater mussels in this study were able to regulate metal uptake, despite the slightly elevated concentrations of some metals in the dilbit-contaminated water.

Zinc concentrations in mussels from both the High and Control treatments were similar during the accumulation phase, except for days 20 and 25, where zinc concentrations in the High treatment exceeded those in the Control (Figure 4.7). In both treatments, zinc concentrations increased slightly during the first few time points of the uptake phase (until day 2 in the Control and until day 5 in the High treatment). Concentrations then plateaued at roughly 160 μg g^{-1}, dw for both treatments, possibly reaching steady state conditions. Once the mussels were placed in clean aquaria containing Lake 260 water for the depuration phase, tissue concentrations increased for a day and then rapidly decreased, returning to initial concentrations after 34 days (day 8 of the depuration phase; Figure 4.7).

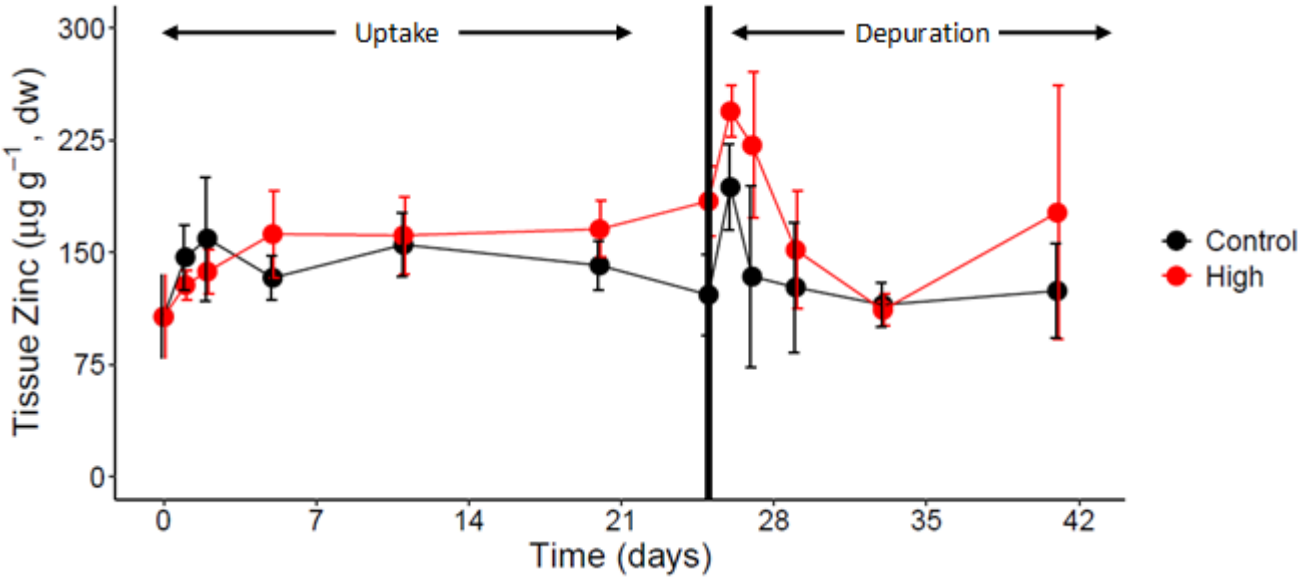

Figure 4.7: Mean (±SD) concentration (µg g^{-1}, dw) of zinc in giant floater mussels throughout the 25-day uptake phase and the 16-day depuration phase. Samples in triplicate. Black line at day 25 denotes the end of the uptake phase and the start of the depuration phase.

During the accumulation phase, I observed a slight increase in the concentration of zinc in the giant floater mussels. However, tissue concentrations on day 26 of the Control (first time point of the depuration phase; 193.73 ± 28.63 µg g^{-1}, dw; ± SD, n=3) exceeded tissue concentrations at any time point of the High treatment during the uptake phase (tissue concentrations at day 25; 184.43 ± 23.06 µg g^{-1}, dw; ± SD, n=3). Therefore, I did not attribute the rise in zinc concentrations in giant floater mussels to an increase in exposure to dilbit-contaminated waters. Furthermore, zinc concentrations in mussels collected from the High treatment on day 25 were only slightly higher to giant floater mussels collected from a reference lake and control group from a previous study conducted at the IISD-ELA (~150 µg g^{-1}, dw). The study conducted by Stewart et al. (1999) exposed giant floater mussels to a mixture of metals, including zinc (ranging from 23.4 ± 1.1 to 141 ± 4 µg L^{-1}, ± SD, n=2), and reported much higher zinc concentrations (~400 µg g^{-1}, dw) in mussels from their treatment groups after being exposed for 40 days. Zinc concentrations in

mussels from this study were also similar or lower than reported concentrations of freshwater mussels collected from the Control and/or reference lakes in other studies (Cooper et al., 2013; Gagnon et al., 2006; Oliveira et al., 2018; Pilote et al., 2018; Ravera et al., 2003). This further suggests that the zinc accumulation observed in this study was not a result of exposure to dilbit-contaminated water, but possibly from the significantly different zinc concentrations in the water collected from the High treatment and Control relative to Lake 260.

4.3. Metal Toxicokinetics

Uptake (k_1) and depuration (k_2) kinetic rate constants were determined for zinc using first-order toxicokinetics. I used total zinc concentrations of 37.6 µg L^{-1} for the High treatment and 6.75 µg L^{-1} for the Control to calculate the toxicokinetic parameter using equation 3, as mussels are filter feeders that incorporate both the dissolved and particulate fractions. Nonlinear curve fitting of the accumulation phase provided the most accurate models for both treatments (Figure 4.8) but there was large uncertainty associated with k_1 from the Control (30.4 ± 374.7 L g^{-1} day^{-1}, ± SE). Uptake rate constants of zinc from the High treatment was 0.584 ± 0.211 g^{-1} day^{-1}, ± SE. The large standard error can be attributed to the rapid increase in zinc and subsequent steady state conditions, which occurred at day 2 of the uptake phase. In order to model the rapid increase in zinc in giant floater mussels from the Control, earlier time points (< 1 day) would have been required.

Since zinc reached equilibrium in mussels on day 2 for the Control and on day 5 for the High treatment, I used equation 3 to calculate k_1 using k_2 (0.086 ± 0.019 day^{-1} for the High treatment and 0.036 ± 0.030 day^{-1}, ± SD for the Control), as previously determined from the slope of the natural log-transformed depuration phase. The resulting uptake rate constants (0.36 L g^{-1} day^{-1} for the High treatment and 4.01 L g^{-1} day^{-1} for the Control) generated bioaccumulation models that

overpredicts the accumulation of zinc in giant floater mussels (Figure 4.9). This result, in addition to relatively low tissue zinc concentrations in mussels from the High treatment, suggests that the slight initial increase in zinc tissue concentrations was due to variability between tissue samples and not from exposures to dilbit-contaminated water.

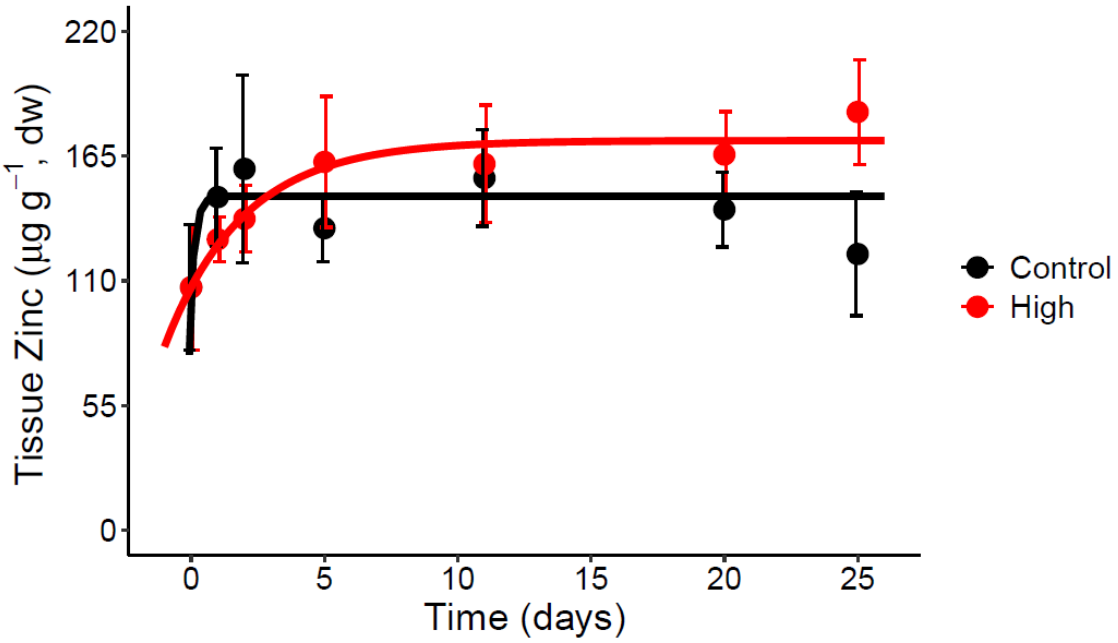

Figure 4.8: Mean (±SD) concentration (µg g^{-1}, dw) of zinc in giant floater mussels during the uptake phase. Samples in triplicate. Toxicokinetic parameters were calculated by nonlinear curve fitting of the accumulation phase using equation 3 and then used to model the accumulation of zinc.

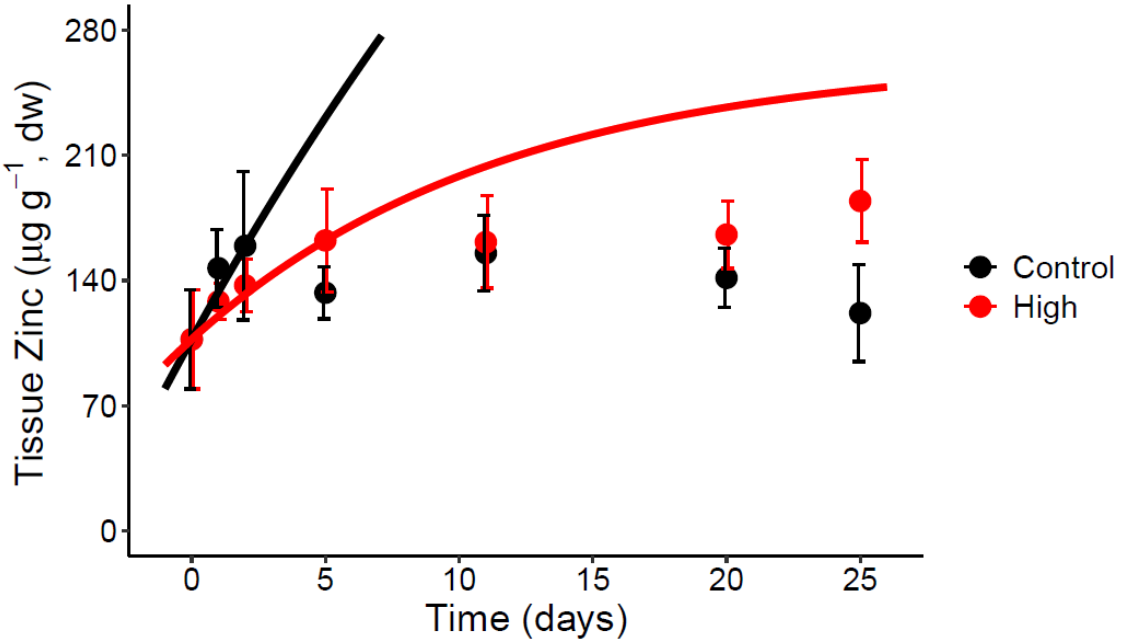

Figure 4.9: Mean (±SD) concentration (µg g^{-1}, dw) of zinc in giant floater mussels during the uptake phase. Samples in triplicate. The depuration rate constants were determined from the slope of the natural log-transformed depuration and then used to calculate the uptake kinetic constant using equation 4. The resulting toxicokinetic parameters were used to model the accumulation of zinc.

Even if there was no accumulation of zinc in mussel tissue, zinc concentrations did however decrease over time during the depuration phase. The resulting depuration rate constants for the High treatment and the Control (0.086 ± 0.019 day^{-1} and 0.036 ± 0.030 day^{-1}, ± SD, respectively) were determined from the slope of the natural log-transformed depuration phase and were not significantly different (Figure 4.10). Since, background zinc concentrations were attained at day 8 of the depuration phase, only the first four time points were used to determine k_2 values. Depuration rates generated from this study were slightly higher but relatively similar to k_2 values reported by other studies involving freshwater and marine bivalves (Chong & Wang, 2001; N. S. Fisher et al., 1996; Kalman et al., 2014; Thomann et al., 1995; L. Wang & Wang, 2014). For example, k_2 values reported in this study were higher than those reported by Wang & Wang (2014;

k_2 of 0.01 d^{-1}) but similar to those reported by Kalman et al. (2014; k_2 values ranging from 0.032 d^{-1} to 0.072 d^{-1}).

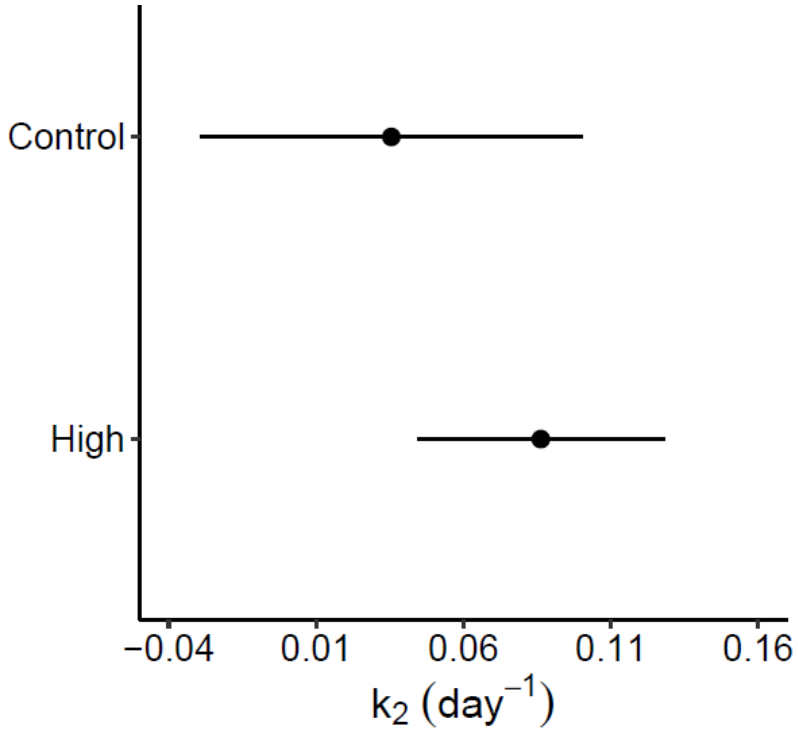

Figure 4.10: The 95% confidence intervals of each linear regression slopes (k_2) derived from the depuration phase of zinc in mussel. Confidence intervals were determined using R Studio. Since there is no overlap between treatments, there is no significant differences between depuration rate constants from the Control and High treatment.

4.4. Metals and Sulfur Chapter Conclusion

This study was the first to examine metal contamination following a controlled dilbit spill in a freshwater ecosystem and investigate the bioaccumulating potential of these metals in giant floater mussels (*Pyganodon grandis*). I found significantly greater concentrations of molybdenum, scandium, vanadium, strontium, zinc, magnesium, sulfur, and calcium (ordered by increasing concentration) in the water of the dilbit-contaminated aquaria compared to the Control limnocorral. Importantly, dissolved zinc concentrations surpassed the CCME water quality guidelines for a significant portion of the uptake phase, suggesting that biota may be exposed to harmful levels of zinc. Fortunately, zinc was the only metal to exceed the CCME water quality guidelines and it is still unclear if elevated zinc concentrations were a result of dilbit contamination. Further investigation by Rodriguez-Gil et al. (in preparation) should determine if dilbit-contamination caused elevated zinc concentrations in the water. Nevertheless, the concentration of metals, excluding zinc, were low in water samples from all dilbit-contaminated treatments, suggesting that dilbit did not contribute to greater metal concentrations in water. Accordingly, metals did not bioaccumulate in giant floater mussel tissues owing to their limited exposure. It is important to note that the metal concentrations recorded in this study may be detrimental to more sensitive species, or species at sensitive life stages. As such, it is critical that we continue to study and monitor metal partitioning and accumulation following a dilbit spill to anticipate metal contamination and exposure to biota, thus informing stakeholders on best practices when approaching future dilbit spills.

5. General Conclusion

Although several studies have examined the toxicokinetics and bioaccumulation of PACs in aquatic organisms, this thesis is the first to evaluate the accumulation and elimination of both parent and alkylated PACs in a freshwater mussel (*Pyganodon grandis*) exposed to naturally weathered dilbit. The results of this study are the largest, most comprehensive set of toxicokinetic and bioaccumulation information of PACs (44 analytes) in a freshwater bivalve obtained to date. As predicted, giant floater mussels exposed to naturally weathered dilbit experienced significantly greater concentrations of PACs compared to mussels in the Control. However, sediments in this study were not a source of PACs to giant floater mussels and more research is required to determine if sunken weathered dilbit could result in the uptake of PACs. Dilbit-contaminated water had clear petrogenic PAC profiles where alkylated PACs, especially C1-, C2-, and C3- alkyl PACs, were more prevalent than their parent counterpart, following the general chemical profiles of CLB bitumen used for the BOREAL project. None of the PACs surpassed Canadian water quality guidelines for the protection of aquatic life but these guidelines do not include alkyl PACs; potentially underestimating the impact of these compounds.

As predicted, giant floater mussels exposed to dilbit-contaminated water for 25 days accumulated PACs in their tissue while PACs in mussels from the Control were similar to background concentrations. ΣAlkyl PACs in mussel tissue were on average an order of magnitude higher than Σparent PACs throughout the experiment. We observed very similar PACs concentrations in mussel tissues across the three dilbit treatments even when the water from the High treatment had significantly greater PAC concentrations compared to the Low and Medium treatments. We believe that elevated PAC concentrations in the water from the High treatment caused differences in filtration and metabolism rates between the treatments, limiting the amount

of accumulation of PACs in mussels from the High treatment. This is also reflective when comparing uptake rate constants between treatments as generally, k_1 values from the High treatment were significantly lower than the Medium and Low treatments. Nonetheless, as soon as the mussels were placed in uncontaminated water for the depuration phase, PAC concentrations in all three treatments decreased similarly, demonstrating first-order elimination for all PACs except for the fluorene compounds (parent and alkylated compounds) which demonstrated apparent second-order elimination. Most PACs were still present in mussel tissue following the 16 day depuration phase. This combined with apparent accumulation of PACs in mussel tissue exposed to dilbit-contaminated water suggests that giant floater mussels could be used to biomonitor PAC contamination following an oil spill.

The accumulation of individual PACs (both parent and alkylated) demonstrated two general trends. Some of the PACs increased rapidly during the first few time points of the uptake phase and then slowed down as their concentrations approached steady state while most PACs increased in mussel tissue steadily through time, never approaching steady state. In fact, an uptake phase longer than 25 days would be required to attain steady state conditions for the large majority of PACs. Nonetheless, we were able to determine toxicokinetic parameters for all 29 PACs that accumulated in giant floater mussels by nonlinear curve fitting of the accumulation phase or by sequential estimation using the natural log-transformed depuration phase. In general, sequential estimation was the best method for defining uptake and elimination rate coefficients for individual PACs because it generated lower standard error associated with toxicokinetic parameters. This result stresses the importance of adding a depuration phase to bioaccumulation experiments and not solely rely on the accumulation phase to generate bioaccumulation models.

Based on BCF values calculated from uptake and depuration rate constants, all 29 PACs that accumulated in mussel tissue were considered to be bioaccumulative. As predicted, alkylated PACs had higher BCF values compared to their parent counterpart, suggesting that alkyl PACs have a greater bioaccumulation potential. This result demonstrates the importance of conducting a more inclusive assessment of petrochemical mixtures as several toxicokinetic studies only focus on the 16 parent PAHs selected by the U.S. EPA, a knowledge gap highlighted by the RSC report on the transportation of dilbit in Canada. We observed no significant relationship between PAC's log BCF values and log K_{OW} values while a number of studies involving fish have reported a parabolic relationship between log BCF and log K_{OW}. It is therefore evident that caution must be taken when comparing toxicokinetic parameters (k_1, k_2, BCF) between different types of aquatic species as differences in metabolism may lead to significant differences in toxicokinetic parameters values and trends.

As predicted, giant floater mussels exposed to dilbit-contaminated water experienced elevated vanadium concentrations but generally, differences between dilbit-contaminated treatments and the Control were minimal. Vanadium concentrations in contaminated water were also low enough to be regulated by mussels where we observed no accumulation of vanadium. Furthermore, nickel concentrations in dilbit-contaminated water were below detection limits, suggesting that both nickel and vanadium are not readily soluble in the water and are instead strongly associated with the dilbit. However, dilbit contamination could have caused elevated zinc concentrations in the water column, surpassing Canadian water quality guidelines for the protection of aquatic life. Even if we did not see any zinc accumulation in mussel tissue, elevated zinc concentrations in the water could be detrimental to more sensitive life stages and/or more sensitive aquatic organisms, demonstrating the importance of monitoring metal contamination following a dilbit spill.

References

Abdel-Shafy, H. I., & Mansour, M. S. M. (2016). A review on polycyclic aromatic hydrocarbons: Source, environmental impact, effect on human health and remediation. *Egyptian Journal of Petroleum*, *25*(1), 107–123. https://doi.org/10.1016/j.ejpe.2015.03.011

Alderman, S. L., Lin, F., Farrell, A. P., Kennedy, C. J., & Gillis, T. E. (2017). Effects of diluted bitumen exposure on juvenile sockeye salmon: From cells to performance: Effects of diluted bitumen on juvenile salmon hearts. *Environmental Toxicology and Chemistry*, *36*(2), 354–360. https://doi.org/10.1002/etc.3533

Alegbeleye, O. O., Opeolu, B. O., & Jackson, V. A. (2017). Polycyclic Aromatic Hydrocarbons: A Critical Review of Environmental Occurrence and Bioremediation. *Environmental Management*, *60*(4), 758–783. https://doi.org/10.1007/s00267-017-0896-2

Allen, E. W. (2008). Process water treatment in Canada's oil sands industry: I. Target pollutants and treatment objectives. *Journal of Environmental Engineering and Science*, *7*(2), 123–138. https://doi.org/10.1139/S07-038

Alsaadi, F., Hodson, P. V., & Langlois, V. S. (2018). An Embryonic Field of Study: The Aquatic Fate and Toxicity of Diluted Bitumen. *Bulletin of Environmental Contamination and Toxicology*, *100*(1), 8–13. https://doi.org/10.1007/s00128-017-2239-7

Andersson, J. T., & Achten, C. (2015). Time to Say Goodbye to the 16 EPA PAHs? Toward an Up-to-Date Use of PACs for Environmental Purposes. *Polycyclic Aromatic Compounds*, *35*(2–4), 330–354. https://doi.org/10.1080/10406638.2014.991042

Andrade, H., Massabuau, J.-C., Cochrane, S., Ciret, P., Tran, D., Sow, M., & Camus, L. (2016). High Frequency Non-invasive (HFNI) Bio-Sensors As a Potential Tool for Marine Monitoring and Assessments. *Frontiers in Marine Science*, *3*(187). https://doi.org/10.3389/fmars.2016.00187

André Lourenço, R., Francisco de Oliveira, F., Haddad Nudi, A., Rebello Wagener, Â. de L., Guadalupe Meniconi, M. de F., & Francioni, E. (2015). PAH assessment in the main Brazilian offshore oil and gas production area using semi-permeable membrane devices (SPMD) and transplanted bivalves. *Continental Shelf Research*, *101*, 109–116. https://doi.org/10.1016/j.csr.2015.04.010

Anyakora, C., Coker, H. A. B., & Arbabi, M. (2011). Application of polynuclear aromatic hydrocarbons 2390 in chemical fingerprinting: The Niger delta case study. Iranian Journal of Environmental Health 2391 Science & Engineering, 8(1), 75-84.

Arnot, J. A., & Gobas, F. A. (2006). A review of bioconcentration factor (BCF) and bioaccumulation factor (BAF) assessments for organic chemicals in aquatic organisms. *Environmental Reviews*, *14*(4), 257–297. https://doi.org/10.1139/a06-005

Azizi, G., Akodad, M., Baghour, M., Layachi, M., & Moumen, A. (2018). The use of Mytilus spp. Mussels as bioindicators of heavy metal pollution in the coastal environment. A review. *Environmental Science and Pollution Research International*, *9*(4), 1170–1181.

Barron, M. G., Conmy, R. N., Holder, E. L., Meyer, P., Wilson, G. J., Principe, V. E., & Willming, M. M. (2018). Toxicity of Cold Lake Blend and Western Canadian Select dilbits to standard aquatic test species. *Chemosphere*, *191*, 1–6. https://doi.org/10.1016/j.chemosphere.2017.10.014

Baumard, P., Budzinski, H., Garrigues, P., Narbonne, J. F., Michel, X., & Bellocq, J. (1999). Polycyclic Aromatic Hydrocarbon (PAH) Burden of Mussels (Mytilus Sp.) in Different Marine Environments in Relation with Sediment PAH Contamination, and Bioavailability. *Marine Environmental Research*, *47*(5), 415–439.

Baussant, T., Sanni, S., Skadsheim, A., Jonsson, G., Børseth, J. F., & Gaudebert, B. (2001). Bioaccumulation of polycyclic aromatic compounds: 2. Modeling bioaccumulation in marine organisms chronically exposed to dispersed oil. *Environmental Toxicology and Chemistry*, *20*(6), 1185–1195. https://doi.org/10.1002/etc.5620200607

Bebianno, M. J., Lopes, B., Guerra, L., Hoarau, P., & Ferreira, A. M. (2007). Glutathione S-tranferases and cytochrome P450 activities in Mytilus galloprovincialis from the South coast of Portugal: Effect of abiotic factors. *Environment International*, *33*(4), 550–558. https://doi.org/10.1016/j.envint.2006.11.002

Bender, M. E., Hargis, W. J., Huggett, R. J., & Roberts, M. H. (1988). Effects of polynuclear aromatic hydrocarbons on fishes and shellfish: An overview of research in virginia. *Marine Environmental Research*, *24*(1–4), 237–241. https://doi.org/10.1016/0141-1136(88)90307-8

Berntssen, M. H. G., Lundebye, A.-K., & Hamre, K. (2000). Tissue lipid peroxidative responses in Atlantic salmon (Salmo salar L.) parr fed high levels of dietary copper and cadmium. *Fish Physiology and Biochemistry*, *23*(1), 14.

Bilodeau, J. C., Gutierrez Villagomez, J. M., Kimpe, L. E., Thomas, P. J., Pauli, B. D., Trudeau, V. L., & Blais, J. M. (2019). Toxicokinetics and bioaccumulation of polycyclic aromatic compounds in wood frog tadpoles (Lithobates sylvaticus) exposed to Athabasca oil sands sediment. *Aquatic Toxicology*, *207*, 217–225. https://doi.org/10.1016/j.aquatox.2018.11.006

Boehm, P. D., Page, D. S., Brown, J. S., Neff, J. M., & Edward Bence, A. (2005). Comparison of mussels and semi-permeable membrane devices as intertidal monitors of polycyclic aromatic hydrocarbons at oil spill sites. *Marine Pollution Bulletin*, *50*(7), 740–750. https://doi.org/10.1016/j.marpolbul.2005.02.002

Bonneris, E., Giguère, A., Perceval, O., Buronfosse, T., Masson, S., Hare, L., & Campbell, P. G. C. (2005). Sub-cellular partitioning of metals (Cd, Cu, Zn) in the gills of a freshwater bivalve, Pyganodon grandis: Role of calcium concretions in metal sequestration. *Aquatic Toxicology*, *71*(4), 319–334. https://doi.org/10.1016/j.aquatox.2004.11.025

Bowen, L., Miles, A. K., Ballachey, B., Waters, S., Bodkin, J., Lindeberg, M., & Esler, D. (2018). Gene transcription patterns in response to low level petroleum contaminants in Mytilus trossulus from field sites and harbors in southcentral Alaska. *Deep Sea Research Part II: Topical Studies in Oceanography*, *147*, 27–35. https://doi.org/10.1016/j.dsr2.2017.08.007

Breitwieser, M., Thomas-Guyon, H., Huet, V., Sagerup, K., & Geraudie, P. (2018). Spatial and temporal impacts of the Skjervøy harbour diesel spill on native population of blue mussels: A sub-Arctic case study. *Ecotoxicology and Environmental Safety*, *153*, 168–174. https://doi.org/10.1016/j.ecoenv.2018.01.033

Brooks, S. J., Harman, C., Grung, M., Farmen, E., Ruus, A., Vingen, S., Godal, B. F., Baršienė, J., Andreikėnaitė, L., Skarphéðinsdóttir, H., Liewenborg, B., & Sundt, R. C. (2011). Water Column Monitoring of the Biological Effects of Produced Water from the Ekofisk Offshore Oil Installation from 2006 to 2009. *Journal of Toxicology and Environmental Health, Part A*, *74*(7–9), 582–604. https://doi.org/10.1080/15287394.2011.550566

Brown, D. J., Clark, G. C., & Van Beneden, R. J. (1998). A new cytochrome P450 (CYP30) family identified in the clam, Mercenaria mercenaria. *Comparative Biochemistry and Physiology Part C: Pharmacology, Toxicology and Endocrinology*, *121*(1–3), 351–360. https://doi.org/10.1016/S0742-8413(98)10056-7

Bruner, K. A., Fisher, S. W., & Landrum, P. F. (1994). The Role of the Zebra Mussel, Dreissena polymorpha, in Contaminant Cycling: I. The Effect of Body Size and Lipid Content on the Bioconcentration of PCBs and PAHs. *Journal of Great Lakes Research*, *20*(4), 725–734. https://doi.org/10.1016/S0380-1330(94)71190-4

Campbell, P. G. C., Giguère, A., Bonneris, E., & Hare, L. (2005). Cadmium-handling strategies in two chronically exposed indigenous freshwater organisms—The yellow perch (Perca flavescens) and the floater mollusc (Pyganodon grandis). *Aquatic Toxicology*, *72*(1–2), 83–97. https://doi.org/10.1016/j.aquatox.2004.11.023

Canada Energy Regulator. (2017). *Incident Data* [Data]. Canada Energy Regulator. https://www.cer-rec.gc.ca/sftnvrnmnt/sft/dshbrd/mp/dt-eng.html

Canadian Council of Ministers of the Environment. (1999). Canadian sediment quality guidelines for the protection of aquatic life: Polycyclic aromatic hydrocarbons (PAHs). *Canadian Environmental Quality Guidelines*, 16.

CAPP. (2019). *Canada's Energy Mix*. Canadian Association of Petroleum Producers. https://www.capp.ca/energy/canadas-energy-mix/

Carmichael, R. H., Jones, A. L., Patterson, H. K., Walton, W. C., Pérez-Huerta, A., Overton, E. B., Dailey, M., & Willett, K. L. (2012). Assimilation of Oil-Derived Elements by Oysters Due to the Deepwater Horizon Oil Spill. *Environmental Science & Technology*, *46*(23), 12787–12795. https://doi.org/10.1021/es302369h

Charbonneau, K. (2016). *Lethal and sub-lethal defects demonstrate the chronic toxicity of chemically-dispersed diluted bitumen to rainbow trout embryos (Oncorhynchus mykiss)* [Honours]. Queenès University.

Cheung, C. C. C., Zheng, G. J., Li, A. M. Y., Richardson, B. J., & Lam, P. K. S. (2001). Relationships between tissue concentrations of polycyclic aromatic hydrocarbons and antioxidative responses of marine mussels, Perna 6iridis. *Aquatic Toxicology*, *52*(3–4), 189–203. https://doi.org/10.1016/s0166-445x(00)00145-4

Chon, H.-S., Ohandja, D.-G., & Voulvoulis, N. (2012). The role of sediments as a source of metals in river catchments. *Chemosphere*, *88*(10), 1250–1256. https://doi.org/10.1016/j.chemosphere.2012.03.104

Chong, K., & Wang, W.-X. (2001). Comparative studies on the biokinetics of Cd, Cr, and Zn in the green mussel Perna viridis and the Manila clam Ruditapes philippinarum. *Environmental Pollution*, *115*(1), 107–121. https://doi.org/10.1016/S0269-7491(01)00087-2

Chow, S. S. T. (2016). *Effects of Bituminous Contaminants on Fathead Minnows (pimephales promelas) of the Lower Athabasca River Basin* [Masters of Science]. University of British Columbia.

Cohen, A. N. (2005). *A Review of Zebra Mussels' Environmental Requirements* (p. 33). California Department of Water Resources.

Cooper, S., Bonneris, E., Michaud, A., Pinel-Alloul, B., & Campbell, P. G. C. (2013). Influence of a step-change in metal exposure (Cd, Cu, Zn) on metal accumulation and subcellular partitioning in a freshwater bivalve, Pyganodon grandis: A long-term transplantation experiment between lakes with contrasting ambient metal levels. *Aquatic Toxicology*, *132–133*, 73–83. https://doi.org/10.1016/j.aquatox.2013.01.021

Cooper, S., Hare, L., & Campbell, P. G. C. (2010). Modeling cadmium uptake from water and food by the freshwater bivalve *Pyganodon grandis*. *Canadian Journal of Fisheries and Aquatic Sciences*, *67*(11), 1874–1888. https://doi.org/10.1139/F10-103

Couillard, Y., Campbell, P. G. C., Pellerin-Massicofte, J., & Auclair, J. C. (1995). Field transplantation of a freshwater bivalve, Pyganodon grandis, across a metal contamination gradient. 11. Metallothionein response to Cd and Zn exposure, evidence for cytotoxicity, and links to effects at higher levels of biological organization. *Canadian Journal of Fisheries and Aquatic Sciences*, *52*(4), 690–702.

Crawford, M. (2014). *Thermodynamic activity and fugacity applied to risk assessment and criteria development of petroleum hydrocarbons* [Master of Resource Management]. Simon Frazer University.

Deb, S. C., & Fukushima, T. (1999). Metals in aquatic ecosystems: Mechanisms of uptake, accumulation and release-Ecotoxicological perspectives. *International Journal of Environmental Studies*, *56*(3), 385–417. https://doi.org/10.1080/00207239908711212

Dew, W. A., Hontela, A., Rood, S. B., & Pyle, G. G. (2015). Biological effects and toxicity of diluted bitumen and its constituents in freshwater systems: Biological effects and toxicity of dilbit. *Journal of Applied Toxicology*, *35*(11), 1219–1227. https://doi.org/10.1002/jat.3196

DiMauro, M. (2012). *Development and Application of an In Vivo Test for Estimating Biotransformation Rate Constants and Bioconcentration Factors of Hydrophobic Organic Chemicals in Fish* [Master of Resource and Environmental Management]. Simon Frazer University.

Dong, J., Xia, X., Wang, M., Xie, H., Wen, J., & Bao, Y. (2016). Effect of recurrent sediment resuspension-deposition events on bioavailability of polycyclic aromatic hydrocarbons in aquatic environments. *Journal of Hydrology*, *540*, 934–946. https://doi.org/10.1016/j.jhydrol.2016.07.009

Emergencies Science and Technology Division. (2006). *Cold Lake Bitumen*. Environment and Climate Change Canada. http://www.etc-cte.ec.gc.ca/databases/oilproperties/pdf/WEB_Cold_Lake_Bitumen.pdf

Environment Canada, Fisheries and Oceans Canada, & Natural Resources Canada. (2013). *Federal government technical report—Properties, composition and marine spill behaviour, fate and transport of two diluted bitumen products from the Canadian oil sands.* (p. 87) [Technical Report]. http://www.deslibris.ca/ID/241728

Enwere, R., Pollard, P., Webster, L., Davies, I., & Moffat, C. (2009). Oil spill management: Elimination kinetics of PAHs in mussels (Mytilus edulis). *Journal of Environmental Monitoring*, *11*(6), 1284. https://doi.org/10.1039/b821346a

European Chemicals Agency. (2017). *Guidance on Information Requirements and Chemical Safety Assessment—Chapter R.11: PBT/vPvB Assessment* (ED-01-17-294-EN-N; ECHA-17-G-12-EN; Guidance on Information Requirements and Chemical Safety Assessment, p. 158). European Chemicals Agency. https://echa.europa.eu/documents/10162/13632/information_requirements_r11_en.pdf

Everitt, S. (2020). *Toxicity of Weathered Sediment-bound Dilbit to Freshwater Fish and Invertebrates* [Master of Science]. University of Lethbridge.

Farris, J. L., & Van Hassel, J. H. (2007). *Freshwater Bivalve Exotoxicology*. Society of Environmental Toxicology and Chemistry (SETAC).

Fernández, B., Campillo, J. A., Martínez-Gómez, C., & Benedicto, J. (2012). Assessment of the mechanisms of detoxification of chemical compounds and antioxidant enzymes in the digestive gland of mussels, Mytilus galloprovincialis, from Mediterranean coastal sites. *Chemosphere*, *87*(11), 1235–1245. https://doi.org/10.1016/j.chemosphere.2012.01.024

Filby, R. H. (1994). Origin and nature of trace element species in crude oils, bitumens and kerogens: Implications for correlation and other geochemical studies. *Geological Society, London, Special Publications*, *78*(1), 203–219. https://doi.org/10.1144/GSL.SP.1994.078.01.15

Fisher, N. S., Teyssié, J.-L., Fowler, S. W., & Wang, W.-X. (1996). Accumulation and Retention of Metals in Mussels from Food and Water: A Comparison under Field and Laboratory Conditions. *Environmental Science & Technology*, *30*(11), 3232–3242. https://doi.org/10.1021/es960009u

Fisher, S. W., Gossiaux, D. C., Bruner, K. A., & Landrum, P. F. (1993). Chapter 28: Investigations of the Toxicokinetics of Hydrophobic Contaminants in the Zebra Mussel (Dreissena polymorpha). In T. F. Nalepa & D. W. Schloesser (Eds.), *Zebra Mussels: Biology, Impacts, and Control* (pp. 465–490). Lewis Publishers.

Gagnon, C., Gagné, F., Turcotte, P., Saulnier, I., Blaise, C., Salazar, M. H., & Salazar, S. M. (2006). Exposure of caged mussels to metals in a primary-treated municipal wastewater plume. *Chemosphere*, *62*(6), 998–1010. https://doi.org/10.1016/j.chemosphere.2005.06.055

Gauthier, P. T., Norwood, W. P., Prepas, E. E., & Pyle, G. G. (2014). Metal–PAH mixtures in the aquatic environment: A review of co-toxic mechanisms leading to more-than-additive outcomes. *Aquatic Toxicology*, *154*, 253–269. https://doi.org/10.1016/j.aquatox.2014.05.026

Gewurtz, S. B., Drouillard, K. G., Lazar, R., & Haffner, G. D. (2002). Quantitative Biomonitoring of PAHs Using the Barnes Mussel (Elliptio complanata). *Archives of Environmental Contamination and Toxicology*, *43*(4), 497–504. https://doi.org/10.1007/s00244-002-1153-z

Gillis, P. L., Mitchell, R. J., Schwalb, A. N., McNichols, K. A., Mackie, G. L., Wood, C. M., & Ackerman, J. D. (2008). Sensitivity of the glochidia (larvae) of freshwater mussels to copper: Assessing the effect of water hardness and dissolved organic carbon on the sensitivity of endangered species. *Aquatic Toxicology*, *88*(2), 137–145. https://doi.org/10.1016/j.aquatox.2008.04.003

Gobas, F. A. P. C., & Morrison, H. A. (2000). Chapter 9: Bioconcentration and Biomagnification in the Aquatic Environment. In *Handbook of Property Estimation Methods for Chemicals* (pp. 189–231). CRC Press.

González-Macías, C., Schifter, I., Lluch-Cota, D. B., Méndez-Rodríguez, L., & Hernández-Vázquez, S. (2006). Distribution, Enrichment and Accumulation of Heavy Metals in Coastal Sediments of Salina Cruz Bay, México. *Environmental Monitoring and Assessment*, *118*(1–3), 211–230. https://doi.org/10.1007/s10661-006-1492-8

Gossiaux, D. C., Landrum, P. F., & Fisher, S. W. (1996). Effect of Temperature on the Accumulation Kinetics of PAHs and PCBs in the Zebra Mussel, Dreissena polymorpha. *Journal of Great Lakes Research*, *22*(2), 379–388. https://doi.org/10.1016/S0380-1330(96)70963-2

Government of Canada. (2000). *Persistence and Bioaccumulation Regulation.pdf*. Minister of Justice.

Grabarkiewicz, J., & Davis, W. (2008). *An introduction to freshwater mussels as biological indicators* (EPA-260-R08-015; p. 122). U.S. Environmental Protection Agency.

Guo, R., Pan, L., Lin, P., & Zheng, L. (2017). The detoxification responses, damage effects and bioaccumulation in the scallop Chlamys farreri exposed to single and mixtures of benzo[a]pyrene and chrysene. *Comparative Biochemistry and Physiology Part C: Toxicology & Pharmacology*, *191*, 36–51. https://doi.org/10.1016/j.cbpc.2016.09.004

Hodson, P. V. (2017). The Toxicity to Fish Embryos of PAH in Crude and Refined Oils. *Archives of Environmental Contamination and Toxicology*, *73*(1), 12–18. https://doi.org/10.1007/s00244-016-0357-6

Hodson, P. V., Adams, J., & Brown, R. S. (2019). Oil toxicity test methods must be improved. *Environmental Toxicology and Chemistry*, *38*(2), 302–311. https://doi.org/10.1002/etc.4303

Hogstrand, C., & Haux, C. (1991). Binding and detoxification of heavy metals in lower vertebrates with reference to metallothionein. *Comparative Biochemistry and Physiology Part C: Comparative Pharmacology*, *100*(1–2), 137–141. https://doi.org/10.1016/0742-8413(91)90140-O

Hwang, H.-M., Stanton, B., McBride, T., & Anderson, M. J. (2014). Polycyclic aromatic hydrocarbon body residues and lysosomal membrane destabilization in mussels exposed to the *Dubai Star* bunker fuel oil (intermediate fuel oil 380) spill in San Francisco Bay: PAHs and lysosomal destabilization in mussels exposed to oil. *Environmental Toxicology and Chemistry*, *33*(5), 1117–1121. https://doi.org/10.1002/etc.2518

Hwang, H.-M., Wade, T. L., & Sericano, J. L. (2008). Residue-response relationship between PAH body burdens and lysosomal membrane destabilization in eastern oysters (*Crassostrea virginica*) and toxicokinetics of PAHs. *Journal of Environmental Science and Health, Part A*, *43*(12), 1373–1380. https://doi.org/10.1080/10934520802232006

Iannuzzi, J., Butcher, M., & Iannuzzi, T. (2011). Evaluation of potential relationships between chemical contaminants in sediments and aquatic organisms from the lower Passaic River, New Jersey, USA. *Environmental Toxicology and Chemistry*, *30*(7), 1721–1728. https://doi.org/10.1002/etc.550

John, D. A., & Leventhal, J. S. (1995). *Bioavailability of Metals* (No. 95–831; Preliminary Compilation of Descriptive Geoenvironmental Mineral Deposit Models, pp. 10–18). Open-File Report. https://pubs.usgs.gov/of/1995/ofr-95-0831/CHAP2.pdf

Joung, D., & Shiller, A. M. (2013). Trace Element Distributions in the Water Column near the Deepwater Horizon Well Blowout. *Environmental Science & Technology*, *47*(5), 2161–2168. https://doi.org/10.1021/es303167p

Kalman, J., Smith, B. D., Bury, N. R., & Rainbow, P. S. (2014). Biodynamic modelling of the bioaccumulation of trace metals (Ag, As and Zn) by an infaunal estuarine invertebrate, the clam Scrobicularia plana. *Aquatic Toxicology*, *154*, 121–130. https://doi.org/10.1016/j.aquatox.2014.05.011

Kang, H.-J., Lee, S.-Y., & Kwon, J.-H. (2016). Physico-chemical properties and toxicity of alkylated polycyclic aromatic hydrocarbons. *Journal of Hazardous Materials*, *312*, 200–207. https://doi.org/10.1016/j.jhazmat.2016.03.051

Keesom, B., & Gieseman, J. (2018). *Bitumen Partial Upgrading 2018 Whitepaper* (Consulting No. AM0401A; p. 159). Jacobs Consultancy.

Kelly, E. N., Schindler, D. W., Hodson, P. V., Short, J. W., Radmanovich, R., & Nielsen, C. C. (2010). Oil sands development contributes elements toxic at low concentrations to the Athabasca River and its tributaries. *Proceedings of the National Academy of Sciences of the United States of America*, *107*(37), 16178–16183.

King, T., Mason, J., Thamer, P., Wohlgeschaffen, G., Lee, K., & Clyburne, J. A. C. (2017). Composition of bitumen blends relevant to ecological impacts and spill response. *Proceedings of the Fortieth AMOP Technical Seminar. Environment and Climate Change Canada, Ottawa, ON, Calgary AB*, 463–475.

Ko, F.-C., Pan, W.-L., Cheng, J.-O., Chen, T.-H., Kuo, F.-W., Kao, S.-J., Chang, C.-W., Ho, H.-C., Wang, W.-H., & Fang, L.-S. (2018). Persistent organic pollutants in Antarctic notothenioid fish and invertebrates associated with trophic levels. *PLOS ONE*, *13*(4), e0194147. https://doi.org/10.1371/journal.pone.0194147

Krohn, R. M., Palace, V., & Smits, J. E. G. (2020). Metal Changes in Pre- and Post-metamorphic Wood Frog (Lithobates sylvaticus) Tadpoles: Implications for Ecotoxicological Studies. *Archives of Environmental Contamination and Toxicology*. https://doi.org/10.1007/s00244-020-00735-w

Laity, J. H., & Andrews, G. K. (2007). Understanding the mechanisms of zinc-sensing by metal-response element binding transcription factor-1 (MTF-1). *Archives of Biochemistry and Biophysics*, *463*(2), 201–210. https://doi.org/10.1016/j.abb.2007.03.019

Landrum, P. F., Lydy, M. J., & Lee, H. (1992). Toxicokinetics in aquatic systems: Model comparisons and use in hazard assessment. *Environmental Toxicology and Chemistry*, *11*(12), 1709–1725. https://doi.org/10.1002/etc.5620111205

Lee, C.-H., Lee, J.-H., Sung, C.-G., Moon, S.-D., Kang, S.-K., Lee, J.-H., Yim, U. H., Shim, W. J., & Ha, S. Y. (2014). Bioaccumulation of polycyclic aromatic hydrocarbons in Manila clam (Ruditapes philippinarum) exposed to crude oil-contaminated sediments. *The Korean Journal of Malacology*, *30*(4), 371–381. https://doi.org/10.9710/kjm.2014.30.4.371

Lee, K. (1983). Vanadium in the aquatic ecosystem. In *Advances in Environmental Science and Technology* (Vol. 13, pp. 155–187). John Wiley and Sons.

Lee, K., Boufadel, M., & Chen, B. (2015). *The Royal Society of Canada Expert Panel Report.* Royal Society of Canada. http://public.eblib.com/choice/publicfullrecord.aspx?p=4429484

Lin, H., Morandi, G. D., Brown, R. S., Snieckus, V., Rantanen, T., Jørgensen, K. B., & Hodson, P. V. (2015). Quantitative structure–activity relationships for chronic toxicity of alkyl-chrysenes and alkyl-benz[a]anthracenes to Japanese medaka embryos (Oryzias latipes). *Aquatic Toxicology*, *159*, 109–118. https://doi.org/10.1016/j.aquatox.2014.11.027

Liu, H., Chen, X., Su, Y., Kang, I. J., Qiu, X., Shimasaki, Y., Oshima, Y., & Yang, J. (2016). Effects of Calcium and Magnesium Ions on Acute Copper Toxicity to Glochidia and Early Juveniles of the Chinese Pond Mussel Anodonta woodiana. *Bulletin of Environmental Contamination and Toxicology*, *97*(4), 504–509. https://doi.org/10.1007/s00128-016-1890-8

Livingstone, D. R. (1998). The fate of organic xenobiotics in aquatic ecosystems: Quantitative and qualitative differences in biotransformation by invertebrates and fish. *Comparative Biochemistry and Physiology Part A: Molecular & Integrative Physiology*, *120*(1), 43–49.

Livingstone, D. R. (2003). Oxidative Stress in Aquatic Organisms in Relation to Pollution and Aquaculture. *Revue de Medecine Veterinaire*, *154*(6), 427–430.

Livingstone, D. R., Moore, M. N., Lowe, D. M., Nasci, C., & Farrar, S. V. (1985). Responses of the cytochrome P-450 monooxygenase system to diesel oil in the common mussel, Mytilus edulis L., and the periwinkle, Littorina littorea L. *Aquatic Toxicology*, *7*(1–2), 79–91. https://doi.org/10.1016/0166-445X(85)90037-2

Loconto, P. R. (2006). Chapter 2: Calibration, Verification, Statistical Treatment of Analytical Data, Detection Limits, and Quality Assurance/Quality ContolTrace. In *Trace environmental quantitative analysis: Principles, techniques and applications* (Second Edition). CRC Press.

Lopes, B., Ferreira, A. M., & Bebianno, M. J. (2012). Responses of CYP450 dependent system to aliphatic and aromatic hydrocarbons body burden in transplanted mussels from South coast of Portugal. *Ecotoxicology*, *21*(3), 730–749. https://doi.org/10.1007/s10646-011-0834-7

Mackay, D., Shiu, W.-Y., Ma, K.-C., & Lee, S. C. (2006). *Handbook of Physical-Chemical Properties and Environmental Fate for Organic Chemicals: Vol. Volume 1* (2nd Edition). CRC Press.

Madison, B. N., Hodson, P. V., & Langlois, V. S. (2015). Diluted bitumen causes deformities and molecular responses indicative of oxidative stress in Japanese medaka embryos. *Aquatic Toxicology*, *165*, 222–230. https://doi.org/10.1016/j.aquatox.2015.06.006

Madison, B. N., Hodson, P. V., & Langlois, V. S. (2017). Cold Lake Blend diluted bitumen toxicity to the early development of Japanese medaka. *Environmental Pollution*, *225*, 579–586. https://doi.org/10.1016/j.envpol.2017.03.025

Madison, B. N., Wallace, S. J., Zhang, J., Hodson, P. V., & Langlois, V. S. (2020). Transcriptional responses in newly-hatched Japanese medaka (Oryzias latipes) associated with developmental malformations following diluted bitumen exposure. *Comparative Biochemistry and Physiology Part D: Genomics and Proteomics*, *35*, 100685. https://doi.org/10.1016/j.cbd.2020.100685

Manzetti, S. (2013). Polycyclic Aromatic Hydrocarbons in the Environment: Environmental Fate and Transformation. *Polycyclic Aromatic Compounds*, *33*(4), 311–330. https://doi.org/10.1080/10406638.2013.781042

Martínez-Álvarez, R. M., Morales, A. E., & Sanz, A. (2005). Antioxidant Defenses in Fish: Biotic and Abiotic Factors. *Reviews in Fish Biology and Fisheries*, *15*(1–2), 75–88. https://doi.org/10.1007/s11160-005-7846-4

Mathew, R., McGrath, J. A., & Di Toro, D. M. (2008). Modeling polycyclic aromatic hydrocarbon bioaccumulation and metabolism in time-variable early life-stage exposures.pdf. *Environmental Toxicology and Chemistry*, *27*(7), 1515–1525.

McDonnell, D., Madison, B. N., Baillon, L., Wallace, S. J., Brown, S. R., Hodson, P. V., & Langlois, V. S. (2019). Comparative toxicity of two diluted bitumens to developing yellow perch (Perca flavescens). *Science of The Total Environment*, *655*, 977–985. https://doi.org/10.1016/j.scitotenv.2018.11.199

Meador, J. P. (2003). Chapter 9: Bioaccumulation of PAHs in Marine Invertebrates. In P. E. T. Douben (Ed.), *Ecological and Environmental Toxicology Series* (pp. 147–171). John Wiley & Sons, Ltd. https://doi.org/10.1002/0470867132.ch9

Michel, X. R., & Beasse, C. (1995). In Vivo Metabolism of Benzo(a)pyrene in the Mussel Mytilus galloprovincialis. *Archives of Environmental Contamination and Toxicology*, *28*(2), 215–222.

Miller, A.-F. (2004). Superoxide dismutases: Active sites that save, but a protein that kills. *Current Opinion in Chemical Biology*, *8*(2), 162–168. https://doi.org/10.1016/j.cbpa.2004.02.011

Mirnaghi, F. S., Czachor, K., Aljawahari, M., Lambert, P., Kuang, W., Hollebone, B. P., & Brown, C. E. (2019). Metal Analysis in Eight Categories of Petroleum Products at Different Weathering States Using Microwave-assisted Acid Digestion ICP–MS. *Environment and Climate Change Canada*. AMOP, Halifax. N.S.

Mouabad, A., Fdil, M. A., Maarouf, A., & Pihan, J. C. (2001). Pumping behaviour and filtration rate of the freshwater mussel Potomida littoralis as a tool for rapid detection of water contamination. *Aquatic Ecology*, *35*(1), 51–60.

National Academies of Sciences, Engineering, and Medicine. (2016). *Spills of Diluted Bitumen from Pipelines: A Comparative Study of Environmental Fate, Effects, and Response*. National Academies Press. https://doi.org/10.17226/21834

Neff, J. M. (2002a). Chapter 2: Bioaccumulation Mechanisms. In *Bioaccumulation in Marine Organisms* (pp. 37–56). Elsevier Science.

Neff, J. M. (2002b). Chapter 15: Polycyclic Aromatic Hydrocarbons in the Ocean. In *Bioaccumulation in Marine Organisms* (pp. 241–318). Elsevier. https://doi.org/10.1016/B978-008043716-3/50016-6

Newman, M. C., & Unger, M. A. (2003). *Fundamentals of Ecotoxicology* (2nd ed.). Lewis Publishers.

Newton, T., & Gregory Cope, W. (2006). Chapter 10: Biomarker Responses of Unionid Mussels to Environmental Contaminants. In J. H. Van Hassel & J. Farris (Eds.), *Freshwater Bivalve Ecotoxicology* (pp. 257–284). CRC Press. https://doi.org/10.1201/9781420042856.ch10

Noh, J., Kim, H., Lee, C., Yoon, S. J., Chu, S., Kwon, B.-O., Ryu, J., Kim, J.-J., Lee, H., Yim, U. H., Giesy, J. P., & Khim, J. S. (2018). Bioaccumulation of Polycyclic Aromatic Hydrocarbons (PAHs) by the Marine Clam, *Mactra veneriformis* , Chronically Exposed to Oil-Suspended Particulate Matter Aggregates. *Environmental Science & Technology*, *52*(14), 7910–7920. https://doi.org/10.1021/acs.est.7b06692

OECD. (2012). *Test No. 305: Bioaccumulation in Fish: Aqueous and Dietary Exposure*. OECD Guidelines for the Testing of Chemicals, Section 3, OECD Publishing, Paris. https://doi.org/10.1787/9789264185296-en.

Oil Sands Magazine. (2018). *From Diluted Bitumen to Synthetic Crude: Upgrading Explained*. Oil Sands Magazine. https://www.oilsandsmagazine.com/technical/bitumen-upgrading

Oil Sands Magazine. (2020). *Oil Sands 101: Process Overview*. Oil Sands Magazine. https://www.oilsandsmagazine.com/technical/oilsands-101

Oliveira, L. F. de, Cabral, M. T., Risso, W. E., & Martinez, C. B. dos R. (2018). Single and combined effects of Zn, Mn and Fe on the Neotropical freshwater bivalve Anodontites trapesialis: Bioaccumulation and biochemical biomarkers. *Ecotoxicology and Environmental Safety*, *161*, 735–745. https://doi.org/10.1016/j.ecoenv.2018.06.029

Perceval, O., Couillard, Y., Pinel-Alloul, B., & Campbell, P. G. C. (2006). Linking changes in subcellular cadmium distribution to growth and mortality rates in transplanted freshwater bivalves (Pyganodon grandis). *Aquatic Toxicology*, *79*(1), 87–98. https://doi.org/10.1016/j.aquatox.2006.05.008

Perceval, O., Pinel-Alloul, B., Méthot, G., Couillard, Y., Giguère, A., Campbell, P. G. C., & Hare, L. (2002). Cadmium accumulation and metallothionein synthesis in freshwater bivalves (Pyganodon grandis): Relative influence of the metal exposure gradient versus limnological variability. *Environmental Pollution*, *118*(1), 5–17. https://doi.org/10.1016/S0269-7491(01)00282-2

Philibert, D. A., Philibert, C. P., Lewis, C., & Tierney, K. B. (2016). Comparison of Diluted Bitumen (Dilbit) and Conventional Crude Oil Toxicity to Developing Zebrafish. *Environmental Science & Technology*, *50*(11), 6091–6098. https://doi.org/10.1021/acs.est.6b00949

Pilote, M., André, C., Turcotte, P., Gagné, F., & Gagnon, C. (2018). Metal bioaccumulation and biomarkers of effects in caged mussels exposed in the Athabasca oil sands area. *Science of The Total Environment*, *610–611*, 377–390. https://doi.org/10.1016/j.scitotenv.2017.08.023

Prego, R. (2003). Zinc concentrations in the water column influenced by the oil spill in the vicinity of the Prestige shipwreck. *Ciencias Marinas*, *29*(1), 103–108. https://doi.org/10.7773/cm.v29i1.130

Rabodonirina, S., Net, S., Ouddane, B., Merhaby, D., Dumoulin, D., Popescu, T., & Ravelonandro, P. (2015). Distribution of persistent organic pollutants (PAHs, Me-PAHs, PCBs) in dissolved, particulate and sedimentary phases in freshwater systems. *Environmental Pollution*, *206*, 38–48. https://doi.org/10.1016/j.envpol.2015.06.023

Rantamäki, P. (1997). Release and retention of selected polycyclic aromatic hydrocarbons (PAH) 2767 and their methylated derivatives by the common mussel (Mytilus edulis) in the brackish 2768 water of the Baltic Sea. Chemosphere, 35(3), 487-502.

Rathore, R. S., & Khangarot, B. S. (2003). Effects of water hardness and metal concentration on a freshwater Tubifex tubifex Muller. *Water, Air, and Soil Pollution*, *142*(1–4), 341–356.

Ravera, O., Cenci, R., Beone, G. M., Dantas, M., & Lodigiani, P. (2003). Trace element concentrations in freshwater mussels and macrophytes as related to those in their environment. *Journal of Limnology*, *62*(1), 61. https://doi.org/10.4081/jlimnol.2003.61

Rebelo, M. de F., Moreira, J. C., Moraes, M. O., Coutinho, D., & Torres, J. P. M. (2003). Is There a CYP1A1 in Marine Bivalves? Expressed Sequences Related to Cytochrome P450 in Crassostrea Rhizophorae. *Comments on Toxicology*, *9*(5–6), 279–287. https://doi.org/10.1080/08865140390450377

Rewitz, K. F., Styrishave, B., Løbner-Olesen, A., & Andersen, O. (2006). Marine invertebrate cytochrome P450: Emerging insights from vertebrate and insect analogies. *Comparative Biochemistry and Physiology Part C: Toxicology & Pharmacology*, *143*(4), 363–381. https://doi.org/10.1016/j.cbpc.2006.04.001

Rhodes, S., Farwell, A., Mark Hewitt, L., MacKinnon, M., & George Dixon, D. (2005). The effects of dimethylated and alkylated polycyclic aromatic hydrocarbons on the embryonic development of the Japanese medaka. *Ecotoxicology and Environmental Safety*, *60*(3), 247–258. https://doi.org/10.1016/j.ecoenv.2004.08.002

Richardson, B. J., Tse, E. S.-C., De Luca-Abbott, S. B., Martin, M., & Lam, P. K. S. (2005). Uptake and depuration of PAHs and chlorinated pesticides by semi-permeable membrane devices (SPMDs) and green-lipped mussels (Perna viridis). *Marine Pollution Bulletin*, *51*(8–12), 975–993. https://doi.org/10.1016/j.marpolbul.2005.04.028

Robidoux, P. Y., Virginie, B., Judith, L., & Marc, D. (2018). Assessment of acute and chronic toxicity of unweathered and weathered diluted bitumen to freshwater fish and invertebrates. *Ecotoxicology and Environmental Safety*, *164*, 331–343. https://doi.org/10.1016/j.ecoenv.2018.08.010

Rowe, C. L., Heyes, A., & Hopkins, W. (2009). Effects of dietary vanadium on growth and lipid storage in a larval anuran: Results from studies employing ad libitum and rationed feeding. *Aquatic Toxicology*, *91*(2), 179–186. https://doi.org/10.1016/j.aquatox.2008.06.002

Rust, A. J., Burgess, R. M., Brownawell, B. J., & McElroy, A. E. (2004). Relationship between metabolism and bioaccumulation of benzo[a]pyrene in benthic invertebrates. *Environmental Toxicology and Chemistry*, *23*(11), 2587. https://doi.org/10.1897/03-354

Santos-Echeandía, J., Prego, R., & Cobelo-García, A. (2008). Influence of the heavy fuel spill from the Prestige tanker wreckage in the overlying seawater column levels of copper, nickel and vanadium (NE Atlantic ocean). *Journal of Marine Systems*, *72*(1–4), 350–357. https://doi.org/10.1016/j.jmarsys.2006.12.005

Schiffer, S. R. (2016). *Toxicity of Vanadium to Freshwater Organisms Representative of the Athabasca Oil Sands Region* [Masters of Science]. University of Saskatchewan.

Schmidt, S. N., Smith, K. E. C., Holmstrup, M., & Mayer, P. (2013). Uptake and toxicity of polycyclic aromatic hydrocarbons in terrestrial springtails-studying bioconcentration kinetics and linking toxicity to chemical activity. *Environmental Toxicology and Chemistry*, *32*(2), 361–369. https://doi.org/10.1002/etc.2051

Schøyen, M., Allan, I. J., Ruus, A., Håvardstun, J., Hjermann, D. Ø., & Beyer, J. (2017). Comparison of caged and native blue mussels (Mytilus edulis spp.) for environmental monitoring of PAH, PCB and trace metals. *Marine Environmental Research*, *130*, 221–232. https://doi.org/10.1016/j.marenvres.2017.07.025

Sereneo, M. (2016). *The sublethal effects of chemically-dispersed access western blend and cold lake blend diluted bitumen on rainbow trout embryos (Oncorhynchus mykiss).* [Honours]. Queen's University.

Shanese Crosby, Fay, R., Groark, C., Kani, A., Smith, J. R., Sullivan, T., Pavia, R., & Shigenaka, G. (2013). *Transporting Alberta Oil Sands Products: Defining the Issues and Assessing the Risks*. https://doi.org/10.13140/2.1.1893.0240

Smedes, F. (1999). Determination of total lipid using non-chlorinated solvents. *The Analyst*, *124*(11), 1711–1718. https://doi.org/10.1039/a905904k

Soares, S. S., Martins, H., Gutiérrez-Merino, C., & Aureliano, M. (2008). Vanadium and cadmium in vivo effects in teleost cardiac muscle: Metal accumulation and oxidative stress markers. *Comparative Biochemistry and Physiology Part C: Toxicology & Pharmacology*, *147*(2), 168–178. https://doi.org/10.1016/j.cbpc.2007.09.003

Sørensen, L., Hansen, B. H., Farkas, J., Donald, C. E., Robson, W. J., Tonkin, A., Meier, S., & Rowland, S. J. (2019). Accumulation and toxicity of monoaromatic petroleum hydrocarbons in early life stages of cod and haddock. *Environmental Pollution*, *251*, 212–220. https://doi.org/10.1016/j.envpol.2019.04.126

Soriano, J. A., Viñas, L., Franco, M. A., González, J. J., Ortiz, L., Bayona, J. M., & Albaigés, J. (2006). Spatial and temporal trends of petroleum hydrocarbons in wild mussels from the Galician coast (NW Spain) affected by the Prestige oil spill. *Science of The Total Environment*, *370*(1), 80–90. https://doi.org/10.1016/j.scitotenv.2006.06.012

Soto, M., Marigómez, I., & Cancio, I. (2003). *Biological aspects of metal accumulation and storage*. Zoology and Cell Biology Dept., Cell Biology and Histology Lab, Faculty of Science and Technology. University of the Basque Country.

Sreedevi, P., Suresh, A., Sivaramakrishna, B., Prabhavathl, B., & Radhakrishnalah, K. (1992). Bioaccumulation of nickel in the organs of the freshwater fish, Cyprinus carpio, and the freshwater mussel, Lamellidens marginalis, under lethal and sublethal nickel stress. *Chemosphere*, *24*(1), 29–36.

Stantec. (2012). *Summary of Clean up and Effects of the 2007 Spill of Oil from Trans Mountain Pipeline to Burrard Inlet* (Environmental Assessment No. 1231–10505; Part 1: Marine Environment, p. 13). Stantec.

Stegeman, J. J., & Lecht, J. J. (1991). Cytochrome P-450 Monooxygenase Systems in Aquatic Species: Carcinogen Metabolism and Biomarkers for Carcinogen and Pollutant Exposure. *Environmental Health Perspectives*, *90*, 101–109.

Stewart, A. R. (1999). Accumulation of Cd by a freshwater mussel (Pyganodon grandis) is reduced in the presence of Cu, Zn, Pb, and Ni. *Canadian Journal of Fisheries and Aquatic Sciences*, *56*(3), 467–478.

Stohs, S. J., & Bagchi, D. (1995). Oxidative mechanisms in the toxicity of metal ions. *Free Radical Biology and Medicine*, *18*(2), 321–336.

Stout, S. A., Emsbo-Mattingly, S. D., Douglas, G. S., Uhler, A. D., & McCarthy, K. J. (2015). Beyond 16 Priority Pollutant PAHs: A Review of PACs used in Environmental Forensic Chemistry. *Polycyclic Aromatic Compounds*, *35*(2–4), 285–315. https://doi.org/10.1080/10406638.2014.891144

Stowers, S. J., & Anderson, M. W. (1985). Formation and Persistence of Benzo(a)pyrene Metabolite-DNA Adducts. *Environmental Health Perspectives*, *62*(1), 31–39.

Stoyanovich, S. S., Yang, Z., Hanson, M., Hollebone, B. P., Orihel, D. M., Palace, V., Rodriguez-Gil, J. L., Faragher, R., Mirnaghi, F. S., Shah, K., & Blais, J. M. (2019). Simulating a Spill of Diluted Bitumen: Environmental Weathering and Submergence in a Model Freshwater System. *Environmental Toxicology and Chemistry*, *38*(12), 2621–2628. https://doi.org/10.1002/etc.4600

Sureda, A., Box, A., Tejada, S., Blanco, A., Caixach, J., & Deudero, S. (2011). Biochemical responses of Mytilus galloprovincialis as biomarkers of acute environmental pollution caused by the Don Pedro oil spill (Eivissa Island, Spain). *Aquatic Toxicology*, *101*(3–4), 540–549. https://doi.org/10.1016/j.aquatox.2010.12.011

Sureda, A., Tejada, S., Box, A., & Deudero, S. (2013). Polycyclic aromatic hydrocarbon levels and measures of oxidative stress in the Mediterranean endemic bivalve Pinna nobilis exposed to the Don Pedro oil spill. *Marine Pollution Bulletin*, *71*(1–2), 69–73. https://doi.org/10.1016/j.marpolbul.2013.03.033

Thirumoorthy, N., Manisenthil Kumar, K.-T., Shyam Sundar, A., Panayappan, L., & Chatterjee, M. (2007). Metallothionein: An Overview. *World Journal of Gastroenterology*, *13*(7), 993–1006.

Thomann, R. V., Mahony, J. D., & Mueller, R. (1995). Steady-state model of biota sediment accumulation factor for metals in two marine bivalves. *Environmental Toxicology and Chemistry: An International Journal*, *14*(11), 1989–1998.

Thomas, R. E., Lindeberg, M., Harris, P. M., & Rice, S. D. (2007). Induction of DNA strand breaks in the mussel (Mytilus trossulus) and clam (Protothaca staminea) following chronic field exposure to polycyclic aromatic hydrocarbons from the Exxon Valdez spill. *Marine Pollution Bulletin*, *54*(6), 726–732. https://doi.org/10.1016/j.marpolbul.2007.01.009

Thompson, K.-L., Picard, C. R., & Chan, H. M. (2017). Polycyclic aromatic hydrocarbons (PAHs) in traditionally harvested bivalves in northern British Columbia, Canada. *Marine Pollution Bulletin*, *121*(1–2), 390–399. https://doi.org/10.1016/j.marpolbul.2017.06.018

Thomsen, J., Ramesh, K., Sanders, T., Bleich, M., & Melzner, F. (2018). Calcification in a marginal sea – influence of seawater [Ca^{2+}] and carbonate chemistry on bivalve shell formation. *Biogeosciences*, *15*(5), 1469–1482. https://doi.org/10.5194/bg-15-1469-2018

Thorsen, W. A., Cope, W. G., & Shea, D. (2007). Chapter 8: Toxicokinetics of Environmental Contaminants in Freshwater Bivalves. In *Freshwater Bivalve Ecotoxicology* (pp. 169–214). Society of Environmental Toxicology and Chemistry (SETAC).

Thorsen, W. A., Forestier, D., Sandifer, T., Lazaro, P. R., Cope, W. G., & Shea, D. (2004). Elimination Rate Constants of 46 Polycyclic Aromatic Hydrocarbons in the Unionid Mussel, Elliptio complanata. *Archives of Environmental Contamination and Toxicology*, *47*(3). https://doi.org/10.1007/s00244-004-3186-y

Trisciani, A., Perra, G., Caruso, T., Focardi, S., & Corsi, I. (2012). Phase I and II biotransformation enzymes and polycyclic aromatic hydrocarbons in the Mediterranean mussel (Mytilus galloprovincialis, Lamarck, 1819) collected in front of an oil refinery. *Marine Environmental Research*, *79*(1), 29–36. https://doi.org/10.1016/j.marenvres.2012.04.006

Ujević, I., Vuletić, N., Lušić, J., Nazlić, N., & Kušpilić, G. (2015). Bioaccumulation of Trace Metals in Mussel (Mytilus galloprovincialis) from Mali Ston Bay during DSP Toxicity Episodes. *Molecules*, *20*(7), 13031–13040. https://doi.org/10.3390/molecules200713031

Uno, S., Koyama, J., Kokushi, E., Monteclaro, H., Santander, S., Cheikyula, J. O., Miki, S., Añasco, N., Pahila, I. G., Taberna, H. S., & Matsuoka, T. (2010). Monitoring of PAHs and alkylated PAHs in aquatic organisms after 1 month from the Solar I oil spill off the coast of Guimaras Island, Philippines. *Environmental Monitoring and Assessment*, *165*(1–4), 501–515. https://doi.org/10.1007/s10661-009-0962-1

U.S. EPA. (2012). *Estimation Programs Interface Suite for Microsoft Windows, Ver 4.11.* EPI Suite™-Estimation Program Interface. https://www.epa.gov/tsca-screening-tools/episuitetm-

U.S. Fish and Wildlife Service, Nottawaseppi Huron Band of the Potawatomi Tribe, & Match-E-Be-Nash-She-Wish Band of the Pottawatomi Indians. (2015). *Final Damage Assessment and Restoration Plan/Environmental Assessment for the July 25-26, 2010 Enbridge Line 6B Oil Discharges near Marshall, MI.pdf*. https://www.fws.gov/midwest/es/ec/nrda/MichiganEnbridge/pdf/FinalDARP_EA_EnbridgeOct2015.pdf

USDOT. (2017). *Hazardous Liquid Accident Data, 2010-2017*. Pipeline and Hazardous Materials Safety Administration, Ed. Pipeline Data and Statistics. https://www.phmsa.dot.gov/data-and-statistics/pipeline/data-and-statistics-overview

Vale, M. G. R., Silva, M. M., Damin, I. C. F., Sanches Filho, P. J., & Welz, B. (2008). Determination of volatile and non-volatile nickel and vanadium compounds in crude oil using electrothermal atomic absorption spectrometry after oil fractionation into saturates, aromatics, resins and asphaltenes. *Talanta*, *74*(5), 1385–1391. https://doi.org/10.1016/j.talanta.2007.09.009

van der Oost, R., Beyer, J., & Vermeulen, N. P. E. (2003). Fish bioaccumulation and biomarkers in environmental risk assessment: A review. *Environmental Toxicology and Pharmacology*, *13*(2), 57–149. https://doi.org/10.1016/S1382-6689(02)00126-6

van Haelst, A. G., Loonen, H., van der Wielen, F. W. M., & Govers, H. A. J. (1996). Comparison of bioconcentration factors of tetrachlorobenzyltoluenes in the guppy (Poecilia reticulata) and zebra mussel (Dreissena polymorpha). *Chemosphere*, *32*(6), 1117–1122.

Vlahogianni, T., Dassenakis, M., Scoullos, M. J., & Valavanidis, A. (2007). Integrated use of biomarkers (superoxide dismutase, catalase and lipid peroxidation) in mussels Mytilus galloprovincialis for assessing heavy metals' pollution in coastal areas from the Saronikos Gulf of Greece. *Marine Pollution Bulletin*, *54*(9), 1361–1371. https://doi.org/10.1016/j.marpolbul.2007.05.018

Wang, D., Couillard, Y., Campbell, P. G. C., & Jolicoeur, P. (1999). *Changes in subcellular metal partitioning in the gills of freshwater bivalves (Pyganodon grandis) living along an environmental cadmium gradient*. *56*, 11.

Wang, H., Cui, L., Cheng, H., Zhang, Y., Diao, X., & Wang, J. (2017). Comparative Studies on the Toxicokinetics of Benzo[a]pyrene in Pinctada martensii and Perna viridis. *Bulletin of Environmental Contamination and Toxicology*, *98*(5), 649–655. https://doi.org/10.1007/s00128-016-2015-0

Wang, L., & Wang, W.-X. (2014). Depuration of metals by the green-colored oyster *Crassostrea sikamea*: Toxic metal depuration by green-colored oysters. *Environmental Toxicology and Chemistry*, *33*(10), 2379–2385. https://doi.org/10.1002/etc.2695

Wang, Z., Fingas, M., Blenkinsopp, S., Sergy, G., Landriault, M., Sigouin, L., Foght, J., Semple, K., & Westlake, D. W. S. (1998). Comparison of oil composition changes due to biodegradation and physical weathering in different oils. *Journal of Chromatography A*, *809*(1–2), 89–107. https://doi.org/10.1016/S0021-9673(98)00166-6

Wang, Z., Hollebone, B. P., & Fieldhouse, B. (2003). Characteristics of spilled oils, fuels, and petroleum products: 1. Composition and properties of selected oils. *United States Enviromental Protection Agency*, 280.

Wayland, M., Headley, J. V., Peru, K. M., Crosley, R., & Brownlee, B. G. (2007). Levels of polycyclic aromatic hydrocarbons and dibenzothiophenes in wetland sediments and aquatic insects in the oil sands area of Northeastern Alberta, Canada. *Environmental Monitoring and Assessment*, *136*(1–3), 167–182. https://doi.org/10.1007/s10661-007-9673-7

Willis, A. M., & Oris, J. T. (2014). Acute photo-induced toxicity and toxicokinetics of single compounds and mixtures of polycyclic aromatic hydrocarbons in zebrafish. *Environmental Toxicology and Chemistry*, *33*(9), 2028–2037.

Wise, J. P., Wise, J. T. F., Wise, C. F., Wise, S. S., Gianios, C., Xie, H., Thompson, W. D., Perkins, C., Falank, C., & Wise, J. P. (2014). Concentrations of the Genotoxic Metals, Chromium and Nickel, in Whales, Tar Balls, Oil Slicks, and Released Oil from the Gulf of Mexico in the Immediate Aftermath of the Deepwater Horizon Oil Crisis: Is Genotoxic Metal Exposure Part of the Deepwater Horizon Legacy? *Environmental Science & Technology*, *48*(5), 2997–3006. https://doi.org/10.1021/es405079b

Xue, W., & Warshawsky, D. (2005). Metabolic activation of polycyclic and heterocyclic aromatic hydrocarbons and DNA damage: A review. *Toxicology and Applied Pharmacology*, *206*(1), 73–93. https://doi.org/10.1016/j.taap.2004.11.006

Yakan, S. D., Focks, A., Klasmeier, J., & Okay, O. S. (2017). Numerical evaluation of bioaccumulation and depuration kinetics of PAHs in Mytilus galloprovincialis. *Environmental Pollution*, *220*, 1244–1250. https://doi.org/10.1016/j.envpol.2016.11.009

Yakan, S. D., Henkelmann, B., Schramm, K.-W., & Okay, O. S. (2011). Bioaccumulation depuration kinetics and effects of benzo(a)anthracene on Mytilus galloprovincialis. *Marine Pollution Bulletin*, *63*(5–12), 471–476. https://doi.org/10.1016/j.marpolbul.2011.02.055

Yim, J. H., Kim, K. W., & Kim, S. D. (2006). Effect of hardness on acute toxicity of metal mixtures using Daphnia magna: Prediction of acid mine drainage toxicity. *Journal of Hazardous Materials*, *138*(1), 16–21. https://doi.org/10.1016/j.jhazmat.2005.11.107

Zanette, J., Goldstone, J. V., Bainy, A. C. D., & Stegeman, J. J. (2010). Identification of CYP genes in Mytilus (mussel) and Crassostrea (oyster) species: First approach to the full complement of cytochrome P450 genes in bivalves. *Marine Environmental Research*, *69*, S1–S3. https://doi.org/10.1016/j.marenvres.2009.10.013

Zhang, Y., Dong, S., Wang, H., Tao, S., & Kiyama, R. (2016). Biological impact of environmental polycyclic aromatic hydrocarbons (ePAHs) as endocrine disruptors. *Environmental Pollution*, *213*, 809–824. https://doi.org/10.1016/j.envpol.2016.03.050

Appendix A. List of All Analysed PACs and Metals

Table A.1: List of PACs analysed using GC-MS, their abbreviations, Canadian Council of Ministers of the Environment (CCME) water quality guidelines for the protection of aquatic life, molecular weight (MW), octanol/water coefficients (Kow), and number of rings.

Compound	Symbol	Type	CCME Guidelines	MW (g mol^{-1})	Log K_{ow}	Number of Rings
Naphthalene	C0-NAP	Parent	1.1 µg L^{-1}	128	3.37[1]	2
C1- Naphthalenes	C1-NAP	Alkyl	—	142	3.87[3]	2
C2- Naphthalenes	C2-NAP	Alkyl	—	156	4.37[3]	2
C3- Naphthalenes	C3-NAP	Alkyl	—	170	4.91[3]	2
C4- Naphthalenes	C4-NAP	Alkyl	—	184	5.36[1]	2
Acenaphthene	ACE	Parent	5.8 µg L^{-1}	154	3.92[1]	3
Acenaphthylene	ACY	Parent	—	152	4.07[1]	3
Fluorene	C0-FLU	Parent	3.0 µg L^{-1}	166	4.18[3]	3
C1-Fluorenes	C1-FLU	Alkyl	—	180	4.17[3]	3
C2-Fluorenes	C2-FLU	Alkyl	—	194	5.14[3]	3
C3-Fluorenes	C3-FLU	Alkyl	—	208	5.30[1]	3
Dibenzothiophene	C0-DBT	Parent	—	184	4.38[3]	3
C1-Dibenzothiophenes	C1-DBT	Alkyl	—	198	4.84[3]	3
C2-Dibenzothiophenes	C2-DBT	Alkyl	—	212	5.36[3]	3
C3-Dibenzothiophenes	C3-DBT	Alkyl	—	226	5.93[1]	3
Anthracene	ANT	Parent	0.012 µg L^{-1}	178	4.54[1]	3
Phenanthrene	C0-PHE	Parent	0.4 µg L^{-1}	178	4.57[2]	3
C1- Phenanthrenes	C1-PHE	Alkyl	—	192	5.13[1]	3
C2- Phenanthrenes	C2-PHE	Alkyl	—	206	5.44[3]	3
C3- Phenanthrenes	C3-PHE	Alkyl	—	220	5.90[3]	3
C4- Phenanthrenes	C4-PHE	Alkyl	—	234	6.43[1]	3
Retene	RET	Alkyl	—	234	6.50[4]	3
Pyrene	PYR	Parent	0.025 µg L^{-1}	202	5.18[1]	4
Fluoranthene	C0-FLA	Parent	0.04 µg L^{-1}	202	5.22[1]	4
C1- Fluoranthenes	C1-FLA	Alkyl	—	216	5.48[2]	4
C2- Fluoranthenes	C2-FLA	Alkyl	—	230	5.97[2]	4
C3- Fluoranthenes	C3-FLA	Alkyl	—	244	6.46[2]	4
C4- Fluoranthenes	C4-FLA	Alkyl	—	258	6.95[2]	4
Benzo[b]naphtho[2,3-/1,2-d]thiophene	BNT23	Parent	—	234	5.20[4]	4

Compound	Symbol	Type	CCME Guidelines	MW (g mol^{-1})	Log K_{ow}	Number of Rings
Benzo[b]naphtho[2,1-d]thiophene	BNT21	Parent	—	234	5.60[4]	4
C1-Benzonaphthothiophenes	C1-BNT	Alkyl	—	248	6.01[2]	4
C2-Benzonaphthothiophenes	C2-BNT	Alkyl	—	262	6.50[2]	4
C3-Benzonaphthothiophenes	C3-BNT	Alkyl	—	276	7.00[2]	4
C4-Benzonaphthothiophenes	C4-BNT	Alkyl	—	290	7.49[2]	4
Chrysene	C0-CHY	Parent	—	228	5.73[1]	4
C1-Chrysenes	C1-CHY	Alkyl	—	242	6.07[3]	4
C2-Chrysenes	C2-CHY	Alkyl	—	256	6.61[1]	4
C3-Chrysenes	C3-CHY	Alkyl	—	284	7.16[3]	4
Benz[a]anthracene	BaA	Parent	0.018 µg L^{-1}	228	5.91[1]	4
Benzo[b+k]fluoranthene	BbF+BkF	Parent	—	252	5.80 - 6.00[1]	5
Benzo[a]pyrene	BaP	Parent	0.015 µg L^{-1}	252	6.04[1]	5
Benzo[e]pyrene	BeP	Parent	—	252	6.44[1]	5
Benzo[g,h,i]perylene	BP	Parent	—	276	6.50[1]	6
Indeno[1,2,3-cd]pyrene	IP	Parent	—	276	6.72[1]	6
Dibenz[a,h]anthracene	DA	Parent	—	278	6.75[1]	5

[1] Mackay et al., 2006

[2] U.S. EPA, 2012

[3] Crawford, 2014

[4] pubchem.ncbi.nlm.nih.gov

Table A.2: List of metals analysed using ICP-ES/MS, their chemical symbols, and CCME water quality guidelines for the protection of aquatic life.

Metal	Symbol	CCME Guidelines	
		Short Term	Long Term
Aluminum	Al	—	—
Antimony	Sb	—	—
Arsenic	As	—	5.0 μg L^{-1}
Barium	Ba	—	—
Boron	B	29 mg L^{-1}	1.5 mg L^{-1}
Cadmium	Cd	0.09 μg L^{-1}	1.0 μg L^{-1}
Calcium	Ca	—	—
Chromium	Cr	—	1.0 μg L^{-1}
Cobalt	Co	—	—
Copper	Cu	—	—
Iron	Fe	—	—
Lead	Pb	—	—
Magnesium	Mg	—	—
Manganese	Mn	3.6 mg L^{-1}	0.4 mg L^{-1}
Molybdenum	Mo	—	73 μg L^{-1}
Nickel	Ni	—	—
Phosphorus	P	—	—
Potassium	K	—	—
Scandium	Sc	—	—
Sodium	Na	—	—
Strontium	Sr	—	—
Sulfur	S	—	—
Tin	Sn	—	—
Titanium	Ti	—	—
Vanadium	V	—	—
Zinc	Zn	37.0 μg L^{-1}	7.0 μg L^{-1}

Appendix B. Method Detection Limits of PACs and Metals

Table B.1: Method detection limits (MDL) of PACs for each matrix studied (mussel, water, and sediment).

Compound	Mussel MDL ($ng\ g^{-1}$)	Water MDL ($ng\ L^{-1}$)	Sediment MDL ($ng\ g^{-1}$)
Naphthalene	0.17	0.021	$7.98x10^{-4}$
Acenaphthylene	0.10	0.012	$4.70x10^{-4}$
Acenaphthene	0.52	0.067	$2.57x10^{-3}$
Fluorene	0.26	0.034	$1.28x10^{-3}$
Dibenzothiophene	0.10	0.010	$5.13x10^{-4}$
Phenanthrene	0.09	0.010	$4.88x10^{-4}$
Anthracene	0.21	0.023	$1.10x10^{-3}$
Fluoranthene	0.30	0.035	$1.47x10^{-3}$
Pyrene	0.87	0.10	$4.22x10^{-3}$
Benz[a]anthracene	0.18	0.021	$8.70x10^{-4}$
Chrysene	0.76	0.088	$3.68x10^{-3}$
Benzo[b]fluoranthene	0.61	0.13	$3.13x10^{-3}$
Benzo[k]fluoranthene	1.76	0.36	$8.99x10^{-3}$
Benzo[e]pyrene	1.34	0.27	$6.82x10^{-3}$
Benzo[a]pyrene	1.34	0.27	$6.82x10^{-3}$
Benzo[g,h,i]perylene	0.50	0.10	$2.54x10^{-3}$
Indeno[1,2,3-cd]pyrene	0.62	0.13	$3.17x10^{-3}$
Dibenz[a,h]anthracene	0.15	0.031	$7.85x10^{-4}$

Table B.2: Method detection limits (MDL) of metals for each matrix studied (mussel, water, and sediment).

Metal	Mussel and Sediment MDL (µg g^{-1})	Water MDL (µg L^{-1})
Aluminum	0.42	7.10×10^{-3}
Antimony	0.014	3.23×10^{-4}
Arsenic	0.046	4.64×10^{-3}
Barium	0.044	8.82×10^{-4}
Boron	0.15	0.079
Cadmium	8.89×10^{-3}	6.76×10^{-4}
Calcium	0.28	0.025
Chromium	0.049	4.50×10^{-3}
Cobalt	0.018	7.56×10^{-4}
Copper	0.10	1.63×10^{-3}
Iron	0.70	0.063
Lead	3.70×10^{-3}	1.13×10^{-3}
Magnesium	7.03	0.032
Manganese	9.43×10^{-3}	5.86×10^{-3}
Molybdenum	0.15	9.35×10^{-3}
Nickel	0.053	0.029
Phosphorus	0.043	8.05
Potassium	12.69	4.62
Scandium	14.17	5.90×10^{-3}
Silicon	0.066	1.50
Sodium	4.22	0.17
Strontium	0.015	3.76×10^{-3}
Sulfur	13.99	6.34
Tin	0.017	3.60×10^{-4}
Titanium	0.17	0.088
Vanadium	0.036	2.27×10^{-3}
Zinc	6.75	7.80×10^{-3}
Aluminum	0.42	7.10×10^{-3}

Appendix C. PAC Concentrations

Table C.1: PAC concentrations in the exposure water (ng L^{-1}) used for the mussel bioaccumulation experiment.

Sample	Day	Treatment	C0-NAP	C1-NAP	C2-NAP	C3-NAP	C4-NAP	ACE
DB-1333	0	Lake 260	0.45	0.015	0.24	0.21	0.015	0.094
DB-1383	0	High	1.02	6.00	20.59	64.71	314.74	0.33
DB-1334	1	Control	0.015	0.015	0.56	0.24	0.15	0.048
DB-1335	1	Low	3.53	3.14	13.99	28.60	39.80	0.82
DB-1336	1	Medium	0.65	1.90	8.78	17.59	42.89	0.49
DB-1390	1	High	1.13	4.30	16.24	66.46	236.82	1.47
DB-1338	2	Control	1.07	0.58	1.57	0.66	0.59	0.048
DB-1339	2	Low	1.22	3.01	11.56	70.93	105.77	0.54
DB-1340	2	Medium	2.41	2.15	10.03	31.28	114.70	0.69
DB-1384	2	High	1.79	4.92	16.82	65.45	275.34	0.68
DB-1380	5	Control	0.80	0.19	0.17	0.68	0.34	0.059
DB-1381	5	Low	0.92	3.18	11.56	50.68	79.11	0.67
DB-1382	5	Medium	1.67	2.85	8.00	28.71	124.94	0.46
DB-1528	5	High	0.80	4.61	16.61	64.38	266.74	0.49
DB-1525	11	Control	2.97	1.29	2.41	1.45	2.31	0.31
DB-1526	11	Low	0.75	9.57	47.05	103.22	106.17	1.76
DB-1527	11	Medium	0.020	5.12	25.53	77.63	147.08	1.74
DB-1563	11	High	0.83	4.96	15.72	52.75	216.24	0.72
DB-1560	20	Control	0.43	0.44	0.53	0.37	0.015	0.048
DB-1561	20	Low	7.16	10.37	53.29	107.69	96.86	2.55
DB-1562	20	Medium	2.00	11.31	45.82	82.66	88.09	2.96
DB-1760	20	High	2.45	13.36	65.53	205.32	340.13	5.45
DB-1761	25	Control	2.04	1.29	1.65	1.06	1.60	0.15
DB-1762	25	Low	2.47	7.98	34.93	72.43	61.14	1.73
DB-1763	25	Medium	0.40	3.60	15.42	41.01	67.11	1.23
DB-1829	25	High	2.34	15.66	78.84	199.11	258.29	6.60
DB-1794	27	Lake 260	1.79	0.98	0.99	0.93	1.50	0.12
DB-1795	27	Lake 260	2.48	0.85	0.43	0.015	0.015	0.10
DB-1793	27	Lake 260	1.15	0.56	0.015	0.48	0.12	0.11

Sample	Day	Treatment	ACY	C0-FLU	C1-FLU	C2-FLU	C3-FLU	C0-DBT
DB-1333	0	Lake 260	0.17	0.23	0.14	0.024	0.52	0.060
DB-1383	0	High	0.21	0.81	59.56	139.55	64.23	0.34
DB-1334	1	Control	0.0087	0.21	0.38	0.25	2.22	0.079
DB-1335	1	Low	0.29	2.83	23.26	34.58	18.47	0.47
DB-1336	1	Medium	0.0087	0.98	21.67	46.25	25.15	0.20
DB-1390	1	High	0.18	2.44	62.81	146.32	73.73	0.57
DB-1338	2	Control	0.0087	0.20	0.41	0.35	0.97	0.083
DB-1339	2	Low	0.0087	3.34	34.42	66.27	35.49	0.74
DB-1340	2	Medium	0.15	1.06	40.62	129.58	75.78	0.26
DB-1384	2	High	0.31	0.97	51.97	118.01	61.86	0.35
DB-1380	5	Control	0.0087	0.21	0.27	0.36	1.07	0.068
DB-1381	5	Low	0.0087	3.27	31.63	49.54	24.61	0.80
DB-1382	5	Medium	0.0087	1.00	33.44	96.48	162.15	0.38
DB-1528	5	High	0.15	1.23	63.12	151.59	74.54	0.36
DB-1525	11	Control	0.077	0.32	1.00	1.43	1.52	0.096
DB-1526	11	Low	0.0087	7.31	32.80	41.87	21.02	4.77
DB-1527	11	Medium	0.15	3.85	38.90	77.13	43.17	1.92
DB-1563	11	High	0.25	1.13	50.77	115.10	55.56	0.41
DB-1560	20	Control	0.0087	0.22	0.43	0.28	2.86	0.076
DB-1561	20	Low	0.60	9.40	32.28	54.30	28.59	7.79
DB-1562	20	Medium	0.13	7.75	30.70	66.96	33.94	5.56
DB-1760	20	High	0.25	11.52	82.25	178.54	92.64	4.53
DB-1761	25	Control	0.064	0.31	1.08	5.91	52.78	0.091
DB-1762	25	Low	0.13	6.63	22.60	36.77	19.09	3.02
DB-1763	25	Medium	0.079	2.33	20.28	55.80	55.86	0.95
DB-1829	25	High	0.24	15.17	80.77	153.73	75.13	6.58
DB-1794	27	Lake 260	0.40	0.35	0.63	2.02	17.51	0.056
DB-1795	27	Lake 260	0.39	0.28	0.23	0.024	0.62	0.052
DB-1793	27	Lake 260	0.40	0.40	0.30	0.33	0.83	0.050

Sample	Day	Treatment	C1-DBT	C2-DBT	C3-DBT	ANT	C0-PHE	C1-PHE
DB-1333	0	Lake 260	3.17	0.0074	0.0074	0.016	0.33	0.16
DB-1383	0	High	13.39	8.24	3.90	3.16	0.58	5.28
DB-1334	1	Control	3.30	0.0074	0.0074	0.016	0.41	0.14
DB-1335	1	Low	16.14	2.53	1.14	0.81	1.88	9.57
DB-1336	1	Medium	13.46	3.62	1.28	0.67	0.39	2.86
DB-1390	1	High	16.33	18.22	8.50	3.11	1.04	9.39
DB-1338	2	Control	2.25	0.0172	0.0074	0.016	0.66	0.46
DB-1339	2	Low	21.85	13.68	4.14	1.52	0.80	14.26
DB-1340	2	Medium	15.29	18.50	7.93	1.48	0.29	4.32
DB-1384	2	High	16.29	12.11	5.72	2.84	0.82	7.29
DB-1380	5	Control	2.77	0.0074	0.0074	0.016	0.30	0.25
DB-1381	5	Low	17.19	7.36	2.73	1.57	2.00	16.64
DB-1382	5	Medium	16.46	12.54	6.50	2.30	1.80	7.53
DB-1528	5	High	13.51	11.52	6.20	3.12	0.79	8.43
DB-1525	11	Control	2.47	0.034	0.0074	0.016	0.67	0.78
DB-1526	11	Low	23.38	8.16	2.59	1.22	11.25	24.84
DB-1527	11	Medium	22.50	15.08	6.57	1.57	4.43	15.37
DB-1563	11	High	15.44	12.91	6.22	2.08	0.81	6.28
DB-1560	20	Control	2.58	0.014	0.0074	0.016	0.55	0.14
DB-1561	20	Low	24.81	10.57	3.14	1.34	20.50	31.44
DB-1562	20	Medium	22.02	9.55	3.01	1.05	15.83	25.60
DB-1760	20	High	26.58	20.94	7.03	2.80	11.33	34.63
DB-1761	25	Control	2.04	0.040	0.018	0.016	0.92	0.77
DB-1762	25	Low	19.22	3.54	0.96	0.74	11.86	22.14
DB-1763	25	Medium	18.58	6.61	2.63	0.79	2.78	8.61
DB-1829	25	High	4.39	18.93	5.71	2.61	18.65	45.61
DB-1794	27	Lake 260	1.26	0.018	0.0074	0.016	0.62	0.37
DB-1795	27	Lake 260	2.07	0.0074	0.0074	0.016	0.35	0.14
DB-1793	27	Lake 260	1.75	0.012	0.0074	0.016	0.46	0.13

Sample	Day	Treatment	C2-PHE	C3-PHE	C4-PHE	RET	PYR	C0-FLA
DB-1333	0	Lake 260	0.0071	0.0071	0.16	0.70	0.19	0.070
DB-1383	0	High	30.18	19.40	3.98	3.25	2.71	1.73
DB-1334	1	Control	0.16	0.0071	0.11	0.55	0.071	0.039
DB-1335	1	Low	13.23	7.41	4.74	4.04	1.05	2.04
DB-1336	1	Medium	10.92	6.84	1.70	2.12	1.40	1.27
DB-1390	1	High	44.05	25.82	5.50	2.83	3.11	2.42
DB-1338	2	Control	0.12	0.0071	0.0071	0.0071	0.081	0.51
DB-1339	2	Low	29.22	13.84	2.33	1.68	0.86	2.42
DB-1340	2	Medium	31.98	24.63	7.30	7.75	1.85	1.38
DB-1384	2	High	48.01	29.82	5.68	3.18	3.33	2.57
DB-1380	5	Control	0.45	0.20	0.14	0.72	0.071	0.025
DB-1381	5	Low	29.40	12.17	1.81	0.96	0.64	1.78
DB-1382	5	Medium	48.00	32.09	5.51	3.57	2.21	1.99
DB-1528	5	High	49.39	32.69	7.06	3.69	3.48	2.71
DB-1525	11	Control	1.05	0.89	1.68	1.44	0.78	1.13
DB-1526	11	Low	25.35	10.95	2.36	0.89	0.70	1.44
DB-1527	11	Medium	40.50	22.29	4.60	2.11	3.01	1.98
DB-1563	11	High	36.23	20.94	4.00	3.15	3.20	2.55
DB-1560	20	Control	0.31	0.0071	0.0071	0.0071	0.75	0.43
DB-1561	20	Low	31.52	15.71	6.54	5.60	62.86	15.74
DB-1562	20	Medium	33.92	17.92	3.47	2.78	1.71	2.39
DB-1760	20	High	75.35	43.07	9.10	5.03	4.13	3.13
DB-1761	25	Control	1.08	3.81	0.80	0.52	0.25	0.69
DB-1762	25	Low	21.07	10.73	2.62	1.73	0.78	1.22
DB-1763	25	Medium	26.73	19.21	5.46	4.29	5.76	2.31
DB-1829	25	High	71.13	36.85	6.49	3.72	3.23	4.15
DB-1794	27	Lake 260	2.06	1.24	1.21	1.20	0.24	0.34
DB-1795	27	Lake 260	0.0071	0.0071	0.029	0.29	0.071	0.21
DB-1793	27	Lake 260	0.059	0.0071	0.0071	0.0071	0.071	0.22

Sample	Day	Treatment	C1-FLA	C2-FLA	C3-FLA	C4-FLA	BNT23	BNT21
DB-1333	0	Lake 260	0.24	0.025	0.025	0.025	0.062	0.062
DB-1383	0	High	7.12	5.22	2.21	0.025	0.88	0.22
DB-1334	1	Control	0.025	0.025	0.025	0.025	0.062	0.062
DB-1335	1	Low	5.59	6.83	6.40	0.025	2.23	0.30
DB-1336	1	Medium	5.39	4.02	1.44	0.025	1.30	0.33
DB-1390	1	High	8.26	7.41	3.64	0.025	1.71	0.38
DB-1338	2	Control	0.025	0.025	0.025	0.025	0.06	0.06
DB-1339	2	Low	4.72	5.08	2.52	0.025	2.60	0.87
DB-1340	2	Medium	9.95	10.96	8.62	0.025	3.10	0.59
DB-1384	2	High	8.16	6.28	2.18	0.025	1.34	0.33
DB-1380	5	Control	0.025	0.025	0.025	0.025	0.062	0.062
DB-1381	5	Low	2.33	3.82	1.67	0.025	1.00	0.35
DB-1382	5	Medium	6.53	7.49	4.15	0.025	1.41	0.20
DB-1528	5	High	9.09	7.77	3.53	0.025	1.64	0.40
DB-1525	11	Control	1.91	1.66	2.73	0.025	0.40	0.062
DB-1526	11	Low	2.41	3.97	1.69	0.025	1.06	0.34
DB-1527	11	Medium	4.65	4.86	2.06	0.025	1.67	0.41
DB-1563	11	High	8.29	6.15	2.34	0.025	1.59	0.34
DB-1560	20	Control	0.025	0.025	0.025	0.025	0.062	0.062
DB-1561	20	Low	6.00	9.71	9.51	0.025	2.25	0.59
DB-1562	20	Medium	5.09	6.82	3.62	0.025	2.10	0.59
DB-1760	20	High	12.58	12.39	6.12	0.025	2.90	0.93
DB-1761	25	Control	0.60	1.06	0.94	0.025	0.062	0.062
DB-1762	25	Low	3.07	5.04	3.11	0.025	1.01	0.32
DB-1763	25	Medium	3.89	7.48	5.22	0.025	1.55	0.42
DB-1829	25	High	10.92	9.27	4.38	0.025	2.69	0.91
DB-1794	27	Lake 260	0.50	1.20	1.12	0.025	0.062	0.062
DB-1795	27	Lake 260	0.025	0.025	0.025	0.025	0.062	0.062
DB-1793	27	Lake 260	0.025	0.025	0.025	0.025	0.062	0.062

Sample	Day	Treatment	C1-BNT	C2-BNT	C3-BNT	C4-BNT	C0-CHY	C1-CHY
DB-1333	0	Lake 260	0.062	0.062	0.062	0.062	0.070	0.062
DB-1383	0	High	2.06	1.28	0.40	0.062	2.90	2.03
DB-1334	1	Control	0.062	0.062	0.062	0.062	0.091	0.062
DB-1335	1	Low	4.42	1.95	0.062	0.062	2.14	1.84
DB-1336	1	Medium	3.14	2.65	1.08	0.062	2.16	2.06
DB-1390	1	High	3.80	2.11	1.05	0.062	3.40	2.77
DB-1338	2	Control	0.062	0.062	0.062	0.062	0.20	0.062
DB-1339	2	Low	4.06	2.68	1.11	0.062	3.57	2.54
DB-1340	2	Medium	7.22	6.21	3.19	0.062	3.48	4.37
DB-1384	2	High	2.89	1.62	0.63	0.062	3.60	2.22
DB-1380	5	Control	0.062	0.062	0.062	0.062	0.072	0.062
DB-1381	5	Low	1.49	0.87	0.41	0.062	2.37	1.28
DB-1382	5	Medium	3.92	2.28	1.00	0.31	2.95	1.92
DB-1528	5	High	3.82	2.82	1.13	0.062	3.92	3.03
DB-1525	11	Control	0.62	0.063	0.062	0.062	0.50	0.19
DB-1526	11	Low	1.68	1.14	0.31	0.062	2.10	1.25
DB-1527	11	Medium	3.26	2.13	0.94	0.062	2.94	1.80
DB-1563	11	High	3.11	2.07	0.68	0.062	4.06	2.51
DB-1560	20	Control	0.062	0.062	0.062	0.062	0.18	0.062
DB-1561	20	Low	3.73	2.68	0.86	0.062	2.93	2.83
DB-1562	20	Medium	3.20	1.93	0.88	0.062	3.18	2.28
DB-1760	20	High	5.73	3.38	1.19	0.062	4.17	4.25
DB-1761	25	Control	0.76	0.21	0.15	0.15	0.25	0.14
DB-1762	25	Low	1.89	1.19	0.34	0.062	2.04	1.68
DB-1763	25	Medium	3.98	3.28	1.56	0.37	2.37	2.53
DB-1829	25	High	4.27	2.31	0.87	0.062	4.01	3.18
DB-1794	27	Lake 260	0.062	0.062	0.062	0.062	0.16	0.062
DB-1795	27	Lake 260	0.062	0.062	0.062	0.062	0.14	0.062
DB-1793	27	Lake 260	0.062	0.062	0.062	0.062	0.11	0.062

Sample	Day	Treatment	C2-CHY	C3-CHY	BaA	BbF+BkF	BaP	BeP
DB-1333	0	Lake 260	0.062	0.062	0.015	0.089	0.19	0.19
DB-1383	0	High	1.85	0.062	0.21	0.39	0.19	0.36
DB-1334	1	Control	0.062	0.062	0.015	0.089	0.19	0.19
DB-1335	1	Low	1.84	0.062	0.27	3.71	0.19	1.91
DB-1336	1	Medium	0.29	0.42	0.17	0.089	0.19	0.19
DB-1390	1	High	3.46	0.45	0.26	0.81	0.19	0.43
DB-1338	2	Control	0.062	0.062	0.015	0.089	0.19	0.19
DB-1339	2	Low	2.27	0.24	0.11	1.86	0.19	0.74
DB-1340	2	Medium	5.13	0.062	0.30	2.25	0.19	1.24
DB-1384	2	High	1.93	0.17	0.24	0.92	0.19	0.57
DB-1380	5	Control	0.062	0.062	0.015	0.089	0.19	0.19
DB-1381	5	Low	1.06	0.062	0.078	0.34	0.19	0.19
DB-1382	5	Medium	2.83	5.87	0.18	7.83	0.19	0.37
DB-1528	5	High	2.89	0.062	0.32	0.80	0.19	0.47
DB-1525	11	Control	0.062	0.062	0.16	2.28	0.19	0.19
DB-1526	11	Low	0.83	0.062	0.086	0.39	0.19	0.19
DB-1527	11	Medium	1.50	0.062	0.18	0.60	0.19	0.48
DB-1563	11	High	2.04	0.062	0.22	0.84	0.19	0.55
DB-1560	20	Control	0.062	0.062	0.015	0.54	0.19	0.19
DB-1561	20	Low	4.90	0.062	0.59	2.94	1.43	3.62
DB-1562	20	Medium	2.58	0.062	0.15	0.86	0.19	0.51
DB-1760	20	High	4.01	0.94	0.30	0.82	0.19	0.58
DB-1761	25	Control	0.34	2.77	0.01	5.10	0.19	0.19
DB-1762	25	Low	1.50	0.37	0.14	0.99	0.19	0.28
DB-1763	25	Medium	4.11	1.09	0.21	3.49	0.19	1.11
DB-1829	25	High	2.86	0.53	0.25	1.15	0.19	0.62
DB-1794	27	Lake 260	0.062	0.15	0.015	1.97	0.19	0.19
DB-1795	27	Lake 260	0.062	0.062	0.015	0.089	0.19	0.19
DB-1793	27	Lake 260	0.062	0.062	0.015	0.089	0.19	0.19

Sample	Day	Treatment	BP	IP	DA	TPACs
DB-1333	0	Lake 260	0.072	0.090	0.022	8.59
DB-1383	0	High	0.072	0.090	0.022	795.57
DB-1334	1	Control	0.072	0.090	0.022	10.40
DB-1335	1	Low	0.072	0.090	0.022	274.41
DB-1336	1	Medium	0.072	0.090	0.022	238.29
DB-1390	1	High	0.072	0.090	0.022	793.21
DB-1338	2	Control	0.072	0.090	0.022	12.22
DB-1339	2	Low	0.072	0.090	0.022	475.34
DB-1340	2	Medium	0.35	0.090	0.022	598.87
DB-1384	2	High	0.072	0.090	0.022	769.69
DB-1380	5	Control	0.072	0.090	0.022	10.58
DB-1381	5	Low	0.072	0.090	0.022	368.03
DB-1382	5	Medium	0.072	0.090	0.022	650.21
DB-1528	5	High	0.072	0.090	0.022	829.38
DB-1525	11	Control	0.072	0.090	0.022	37.57
DB-1526	11	Low	0.072	0.090	0.022	507.43
DB-1527	11	Medium	0.072	0.090	0.022	590.23
DB-1563	11	High	0.072	0.090	0.022	663.58
DB-1560	20	Control	0.072	0.090	0.022	12.47
DB-1561	20	Low	4.02	1.04	0.29	700.70
DB-1562	20	Medium	0.072	0.090	0.022	551.46
DB-1760	20	High	0.21	0.090	0.022	1305.97
DB-1761	25	Control	0.11	0.090	0.022	92.21
DB-1762	25	Low	0.072	0.090	0.022	389.00
DB-1763	25	Medium	0.83	0.43	0.022	412.01
DB-1829	25	High	0.072	0.090	0.022	1162.64
DB-1794	27	Lake 260	0.072	0.090	0.022	42.05
DB-1795	27	Lake 260	0.072	0.090	0.022	10.16
DB-1793	27	Lake 260	0.072	0.090	0.022	8.95

Table C.2: TPACs concentration in the water (µg L^{-1}) collected from the limnocorrals for the 'fate and behaviour' subtheme (FaBS), another study within the BOREAL project.

Day	Treatment	FaBS TPACs (µg L^{-1})
28	High	2.10
28	High	2.33
28	High	2.01
28	Low	1.52
28	Medium	1.34
28	Control	0.047
42	High	1.75
42	High	1.67
42	High	1.39
42	Low	0.79
42	Medium	0.98
42	Control	0.036
56	High	1.38
56	High	1.41
56	High	1.34
56	Low	0.83
56	Medium	0.79
56	Control	0.029
70	High	2.14
70	High	2.25
70	High	2.48
70	Low	0.65
70	Medium	0.56
70	Control	0.023

Table C.3: TPACs, ΣParent and ΣAlkyl PAC concentrations in the exposure water (ng L^{-1}) used for the mussel bioaccumulation experiment.

Sample	Day	Treatment	TPACs	ΣParent	ΣAlkyl	%Parent	%Alkyl
DB-1333	0	Lake 260	8.59	2.35	6.24	27.33	72.67
DB-1383	0	High	795.57	15.13	780.44	1.90	98.10
DB-1334	1	Control	10.40	1.66	8.75	15.92	84.08
DB-1335	1	Low	274.41	22.14	252.27	8.07	91.93
DB-1336	1	Medium	238.29	9.06	229.24	3.80	96.20
DB-1390	1	High	793.21	20.75	772.46	2.62	97.38
DB-1338	2	Control	12.22	3.55	8.66	29.08	70.92
DB-1339	2	Low	475.34	18.12	457.22	3.81	96.19
DB-1340	2	Medium	598.87	17.53	581.34	2.93	97.07
DB-1384	2	High	769.69	19.38	750.31	2.52	97.48
DB-1380	5	Control	10.58	2.31	8.27	21.82	78.18
DB-1381	5	Low	368.03	15.02	353.01	4.08	95.92
DB-1382	5	Medium	650.21	23.53	626.68	3.62	96.38
DB-1528	5	High	829.38	19.04	810.34	2.30	97.70
DB-1525	11	Control	37.57	9.88	27.69	26.30	73.70
DB-1526	11	Low	507.43	32.36	475.07	6.38	93.62
DB-1527	11	Medium	590.23	23.24	567.00	3.94	96.06
DB-1563	11	High	663.58	18.04	645.55	2.72	97.28
DB-1560	20	Control	12.47	3.81	8.66	30.57	69.43
DB-1561	20	Low	700.70	144.80	555.90	20.66	79.34
DB-1562	20	Medium	551.46	44.46	507.00	8.06	91.94
DB-1760	20	High	1305.97	51.97	1254.00	3.98	96.02
DB-1761	25	Control	92.21	10.50	81.71	11.39	88.61
DB-1762	25	Low	389.00	32.43	356.57	8.34	91.66
DB-1763	25	Medium	412.01	25.29	386.72	6.14	93.86
DB-1829	25	High	1162.64	65.98	1096.65	5.68	94.32
DB-1794	27	Lake 260	42.05	6.63	35.42	15.76	84.24
DB-1795	27	Lake 260	10.16	4.76	5.40	46.86	53.14
DB-1793	27	Lake 260	8.95	3.67	5.28	41.03	58.97
Control (n=5)			16.65 ± 11.73	4.24 ± 3.27	12.41 ± 8.54	24.74 ± 5.95	75.26 ± 5.95
Low (n=5)			402.84 ± 92.32	24.01 ± 8.06	378.83 ± 90.26	6.13 ± 2.14	93.87 ± 2.14
Medium (n=6)			506.85 ± 154.33	23.85 ± 11.72	483.00 ± 149.41	4.75 ± 1.95	95.25 ± 1.95
High (n=7)			902.86 ± 235.90	30.04 ± 20.25	872.82 ± 217.78	3.10 ± 1.30	96.90 ± 1.30
L260 (n=3)			9.23 ± 0.82	3.59 ± 1.21	5.64 ± 0.53	32.74 ± 13.87	67.26 ± 10.03

Table C.4: PAC concentrations in the Cold Lake Blend diluted bitumen (μg g^{-1}) used in the BOREAL project.

Compound	Symbol	Concentration (μg g^{-1})
Naphthalene	C0-NAP	39.7
C1- Naphthalenes	C1-NAP	176.2
C2- Naphthalenes	C2-NAP	500.0
C3- Naphthalenes	C3-NAP	767.0
C4- Naphthalenes	C4-NAP	671.0
Fluorene	C0-FLU	21.7
C1-Fluorenes	C1-FLU	113.5
C2-Fluorenes	C2-FLU	265.0
C3-Fluorenes	C3-FLU	369.0
Dibenzothiophene	C0-DBT	35.4
C1-Dibenzothiophenes	C1-DBT	196.5
C2-Dibenzothiophenes	C2-DBT	526.0
C3-Dibenzothiophenes	C3-DBT	595.0
Phenanthrene	C0-PHE	67.8
C1- Phenanthrenes	C1-PHE	256.0
C2- Phenanthrenes	C2-PHE	409.0
C3- Phenanthrenes	C3-PHE	436.0
C4- Phenanthrenes	C4-PHE	223.0
Fluoranthene	C0-FLA	4.94
C1- Fluoranthenes	C1-FLA	29.9
C2- Fluoranthenes	C2-FLA	84.8
C3- Fluoranthenes	C3-FLA	107.4
C4- Fluoranthenes	C4-FLA	91.4
C0-Benzonaphthothiophenes	C0-BNT	38.8
C1-Benzonaphthothiophenes	C1-BNT	173.9
C2-Benzonaphthothiophenes	C2-BNT	289.0
C3-Benzonaphthothiophenes	C3-BNT	288.0
C4-Benzonaphthothiophenes	C4-BNT	203.0
Chrysene	C0-CHY	18.74
C1-Chrysenes	C1-CHY	46.0
C2-Chrysenes	C2-CHY	86.7
C3-Chrysenes	C3-CHY	90.0

Table C.5: PAC concentrations in the sand (ng g^{-1}) collected from the aquaria during the uptake phase of the mussel bioaccumulation study.

Sample	Day	Treatment	C0-NAP	C1-NAP	C2-NAP	C3-NAP	C4-NAP	ACE	ACY	C0-FLU	C1-FLU	C2-FLU	C3-FLU	C0-DBT	C1-DBT	C2-DBT
S-t0	0	Control	0.00056	0.00056	0.17	0.00056	0.043	0.0018	0.00033	0.00090	0.00090	0.036	0.00090	0.0014	0.00036	0.00051
S-t5-M3	2	Low	0.00056	0.00056	0.16	0.00056	0.13	0.0018	0.00033	0.00090	0.029	0.014	0.00090	0.0025	0.0093	0.016
S-t5-M8	2	Medium	0.076	0.00056	0.00056	0.00056	0.00056	0.0018	0.00033	0.00090	0.00090	0.00090	0.0081	0.0030	0.0079	0.016
S-t5-M1	2	High	0.065	0.048	0.00056	0.079	0.16	0.0018	0.00033	0.033	0.057	0.072	0.17	0.0049	0.010	0.019
S-t11-M4	11	Control	0.090	0.037	0.00056	0.051	0.00056	0.0018	0.00033	0.00090	0.021	0.042	0.10	0.0045	0.012	0.014
S-t11-M3	11	Low	0.065	0.031	0.00056	0.00056	0.00056	0.0018	0.00033	0.00090	0.0061	0.019	0.054	0.0039	0.011	0.018
S-t11-M8	11	Medium	0.00056	0.00056	0.051	0.00056	0.062	0.0018	0.00033	0.0066	0.045	0.084	0.11	0.0011	0.0095	0.0058
S-t11-M1	11	High	0.078	0.033	0.00056	0.00056	0.0094	0.0018	0.00033	0.00090	0.00090	0.00090	0.067	0.0016	0.0078	0.014
S-t20-M8	20	Medium	0.00056	0.00056	0.040	0.00056	0.00056	0.0018	0.00033	0.00090	0.026	0.037	0.040	0.00036	0.013	0.025
S-t25-M4	25	Control	0.099	0.058	0.045	0.10	0.080	0.0018	0.00033	0.041	0.024	0.041	0.12	0.0044	0.012	0.015
S-t25-M3	25	Low	0.00056	0.00056	0.039	0.00056	0.017	0.0018	0.00033	0.0019	0.013	0.043	0.00090	0.0013	0.0092	0.0095
S-t25-M8	25	Medium	0.00056	0.00056	0.00056	0.00056	0.00056	0.0018	0.00033	0.00090	0.00090	0.029	0.012	0.0033	0.011	0.020
S-t25-M1	25	High	0.00056	0.65	0.68	0.22	0.47	0.0018	0.00033	0.00090	0.12	0.12	2.17	0.00036	0.011	0.042

Sample	Day	Treatment	C3-DBT	ANT	C0-PHE	C1-PHE	C2-PHE	C3-PHE	C4-PHE	RET	PYR	C0-FLA	C1-FLA	C2-FLA	C3-FLA	C4-FLA
S-t0	0	Control	0.00051	0.0014	0.0056	0.019	0.00035	0.00035	0.0071	0.021	0.013	0.0064	0.012	0.0010	0.0010	0.0010
S-t5-M3	2	Low	0.0059	0.0012	0.019	0.067	0.0045	0.057	0.059	0.082	0.014	0.0086	0.011	0.012	0.0010	0.0065
S-t5-M8	2	Medium	0.029	0.00078	0.032	0.0061	0.012	0.042	0.051	0.068	0.021	0.0010	0.0010	0.0010	0.0010	0.0010
S-t5-M1	2	High	0.036	0.00078	0.043	0.039	0.043	0.085	0.069	0.086	0.029	0.0010	0.0010	0.0010	0.0010	0.0010
S-t11-M4	11	Control	0.021	0.00078	0.054	0.047	0.048	0.050	0.075	0.083	0.032	0.0010	0.0010	0.0010	0.0010	0.0010
S-t11-M3	11	Low	0.025	0.00078	0.051	0.058	0.049	0.081	0.083	0.14	0.034	0.0010	0.0010	0.0010	0.0010	0.0010
S-t11-M8	11	Medium	0.00051	0.00078	0.030	0.016	0.043	0.083	0.088	0.13	0.026	0.0067	0.023	0.020	0.0010	0.0010
S-t11-M1	11	High	0.021	0.00078	0.00035	0.00035	0.00035	0.050	0.043	0.030	0.013	0.0010	0.0010	0.0010	0.0010	0.0010
S-t20-M8	20	Medium	0.0014	0.0016	0.00035	0.020	0.0066	0.088	0.074	0.12	0.022	0.0066	0.036	0.029	0.0063	0.0068
S-t25-M4	25	Control	0.019	0.00078	0.049	0.031	0.0065	0.044	0.067	0.14	0.033	0.0010	0.0010	0.0010	0.0010	0.0010
S-t25-M3	25	Low	0.00051	0.0013	0.019	0.026	0.00035	0.062	0.050	0.11	0.022	0.015	0.011	0.012	0.0049	0.0010
S-t25-M8	25	Medium	0.041	0.00078	0.033	0.090	0.019	0.094	0.091	0.13	0.037	0.0010	0.0010	0.0010	0.0010	0.0010
S-t25-M1	25	High	0.0083	0.00078	0.00035	0.019	0.018	0.13	0.093	0.12	0.031	0.0010	0.0010	0.0010	0.0010	0.0010

Sample	Day	Treatment	BNT23	BNT21	C1-BNT	C2-BNT	C3-BNT	C4-BNT	C0-CHY	C1-CHY	C2-CHY	C3-CHY	BaA	BbF+BkF	BaP	BeP
S-t0	0	Control	0.0026	0.0026	0.0026	0.0026	0.0026	0.0026	0.0046	0.0026	0.0026	0.0026	0.00062	0.0022	0.0048	0.0048
S-t5-M3	2	Low	0.0026	0.0026	0.0099	0.011	0.0040	0.0026	0.012	0.020	0.020	0.0026	0.0067	0.0022	0.0048	0.0048
S-t5-M8	2	Medium	0.0026	0.0026	0.0051	0.023	0.0026	0.0026	0.0081	0.023	0.013	0.0026	0.00062	0.0022	0.0048	0.0048
S-t5-M1	2	High	0.0045	0.0026	0.025	0.033	0.0085	0.0026	0.013	0.036	0.024	0.0026	0.00062	0.0044	0.0048	0.0048
S-t11-M4	11	Control	0.0028	0.0026	0.010	0.017	0.0026	0.0026	0.0052	0.023	0.0067	0.0026	0.00062	0.0022	0.0048	0.0048
S-t11-M3	11	Low	0.0067	0.0026	0.022	0.061	0.0085	0.0026	0.027	0.042	0.013	0.0026	0.00062	0.0053	0.0048	0.0048
S-t11-M8	11	Medium	0.0026	0.0026	0.023	0.039	0.011	0.0026	0.015	0.035	0.015	0.031	0.00062	0.011	0.0048	0.012
S-t11-M1	11	High	0.0026	0.0026	0.0086	0.014	0.0026	0.0026	0.0029	0.017	0.0038	0.0026	0.00062	0.0022	0.0048	0.0048
S-t20-M8	20	Medium	0.0045	0.0026	0.014	0.024	0.013	0.0026	0.030	0.028	0.044	0.012	0.00062	0.019	0.0048	0.0048
S-t25-M4	25	Control	0.0026	0.0026	0.013	0.016	0.0030	0.0026	0.0067	0.025	0.0099	0.0026	0.00062	0.0022	0.0048	0.0048
S-t25-M3	25	Low	0.0026	0.0026	0.014	0.015	0.0076	0.0026	0.028	0.021	0.0026	0.015	0.012	0.030	0.0048	0.013
S-t25-M8	25	Medium	0.0058	0.0026	0.029	0.042	0.018	0.0026	0.028	0.044	0.0098	0.0026	0.0066	0.0022	0.0048	0.0048
S-t25-M1	25	High	0.0026	0.0026	0.059	0.068	0.025	0.0026	0.032	0.057	0.053	0.019	0.00062	0.018	0.0048	0.018

Sample	Day	Treatment	BP	IP	DA	TPACs
S-t0	0	Control	0.0018	0.0022	0.00055	0.39
S-t5-M3	2	Low	0.0018	0.0022	0.00055	0.83
S-t5-M8	2	Medium	0.0018	0.0022	0.00055	0.49
S-t5-M1	2	High	0.0018	0.0022	0.00055	1.32
S-t11-M4	11	Control	0.0018	0.0022	0.00055	0.89
S-t11-M3	11	Low	0.0018	0.0022	0.00055	0.95
S-t11-M8	11	Medium	0.0018	0.0022	0.00055	1.05
S-t11-M1	11	High	0.0018	0.0022	0.00055	0.46
S-t20-M8	20	Medium	0.0018	0.0022	0.00055	0.81
S-t25-M4	25	Control	0.0018	0.0022	0.00055	1.14
S-t25-M3	25	Low	0.0018	0.0022	0.00055	0.65
S-t25-M8	25	Medium	0.0018	0.0022	0.00055	0.83
S-t25-M1	25	High	0.0018	0.0022	0.00055	5.28

Table C.6: PAC concentrations (ng g^{-1}, ww Lipid) in mussel tissue collected from the Control, Low, Medium, and High treatments during the uptake phase of the bioaccumulation study.

Sample	Day	Treatment	C0-NAP	C1-NAP	C2-NAP	C3-NAP	C4-NAP	ACE	ACY
t0-A	0	—	32.99	40.38	57.77	51.16	218.65	0.72	0.31
t0-B	0	—	29.74	10.07	66.39	73.74	164.17	0.72	0.31
t0-C	0	—	29.37	34.93	14.75	48.32	143.77	0.72	0.31
t2-M4-2	2	Control	0.41	0.41	0.41	27.87	330.05	0.72	0.31
t2-M4-3	2	Control	0.41	0.41	71.92	62.96	101.07	0.72	0.31
t2-M3-1	2	Low	0.41	0.41	88.78	239.77	507.25	0.72	5.05
t2-M3-3	2	Low	0.41	0.41	94.20	306.82	874.92	0.72	9.37
t2-M8-1	2	Medium	82.67	20.85	97.00	143.90	284.99	0.72	0.31
t2-M8-2	2	Medium	57.28	62.08	233.69	473.32	1713.63	0.72	11.94
t2-M8-3	2	Medium	0.41	0.41	141.51	390.56	1489.89	0.72	8.09
t2-M1-1	2	High	110.61	39.56	176.41	493.42	2096.37	0.72	19.70
t2-M1-2	2	High	0.41	0.41	89.79	283.44	1382.51	0.72	11.14
t2-M1-3	2	High	0.41	6.69	125.68	469.02	2070.83	0.72	16.75
t5-M4-1	5	Control	20.87	6.41	0.41	13.13	34.91	0.72	0.31
t5-M4-2	5	Control	0.41	432.43	502.60	451.19	650.06	0.72	0.31
t5-M4-3	5	Control	0.41	0.41	8.57	29.73	36.99	0.72	0.31
t5-M3-1	5	Low	6.98	15.71	125.22	326.49	1059.59	0.72	8.38
t5-M3-2	5	Low	64.21	99.99	109.62	544.86	1131.80	0.72	0.31
t5-M3-3	5	Low	3.88	0.41	224.99	456.96	1572.40	0.72	7.50
t5-M8-1	5	Medium	161.38	131.40	163.09	642.59	2898.63	0.72	0.31
t5-M8-2	5	Medium	0.41	0.41	971.78	2173.83	12656.52	0.72	50.81
t5-M8-3	5	Medium	30.08	41.57	364.64	490.96	3020.16	0.72	15.56
t5-M1-1	5	High	72.11	58.49	257.63	637.70	3037.21	0.72	45.74
t5-M1-2	5	High	226.66	203.65	275.93	789.71	4028.83	0.72	0.31
t5-M1-3	5	High	230.53	129.62	303.73	798.87	3479.12	0.72	20.00
t11-M4-1	11	Control	41.90	2.73	75.14	105.96	163.90	0.72	0.31
t11-M4-2	11	Control	73.93	0.41	157.93	203.31	240.67	0.72	0.31
t11-M4-3	11	Control	0.41	0.41	27.21	66.19	0.41	0.72	0.31
t11-M3-1	11	Low	67.72	110.10	590.24	1095.93	3650.00	0.72	29.68
t11-M3-2	11	Low	0.41	53.29	257.65	576.46	1327.47	0.72	0.31
t11-M3-3	11	Low	8.61	43.04	254.98	345.21	1227.12	0.72	10.02
t11-M8-1	11	Medium	0.41	0.41	100.58	760.90	4233.84	0.72	28.96
t11-M8-2	11	Medium	0.41	0.41	73.50	245.70	1599.74	0.72	13.26
t11-M1-1	11	High	48.19	24.09	77.14	392.12	2407.91	0.72	51.99
t11-M1-2	11	High	28.06	68.97	251.26	646.92	4194.04	0.72	51.03
t11-M1-3	11	High	0.41	0.41	232.62	834.24	4098.91	0.72	35.80
t20-M4-1	20	Control	0.41	744.10	1064.43	738.39	826.55	0.72	0.31
t20-M4-2	20	Control	0.41	0.41	0.41	0.41	12.12	0.72	0.31
t20-M4-3	20	Control	0.41	0.41	13.24	28.91	25.39	0.72	0.31
t20-M3-1	20	Low	64.82	83.31	551.53	992.30	4137.95	0.72	16.63
t20-M3-2	20	Low	61.26	69.90	518.56	967.56	3610.57	0.72	15.75
t20-M8-1	20	Medium	109.92	436.12	414.12	749.54	3289.43	0.72	33.83
t20-M8-2	20	Medium	0.41	53.29	96.31	498.12	2482.59	0.72	26.59
t20-M8-3	20	Medium	85.27	105.52	275.84	868.96	2599.28	0.72	5.71
t20-M1-1	20	High	226.50	36.75	108.51	376.33	1676.92	4.05	100.14
t20-M1-2	20	High	0.41	194.27	450.17	1114.03	7237.33	0.72	68.61
t20-M1-3	20	High	70.73	72.11	238.89	630.17	2706.09	7.15	9.19
t25-M4-1	25	Control	46.10	54.59	26.08	70.79	154.10	0.72	0.31
t25-M4-2	25	Control	25.70	0.41	22.44	27.93	107.34	0.72	0.31
t25-M4-3	25	Control	58.16	43.29	56.09	45.37	139.86	0.72	0.31
t25-M3-1	25	Low	0.41	57.07	454.25	1047.22	3680.14	7.44	54.31
t25-M3-2	25	Low	0.41	21.24	415.84	1050.96	3475.22	0.72	16.13
t25-M3-3	25	Low	225.76	45.53	155.41	416.23	6227.76	10.62	34.35
t25-M8-1	25	Medium	0.41	26.49	579.88	1280.09	5668.03	0.72	26.15
t25-M8-2	25	Medium	85.76	137.13	353.96	893.94	2550.14	0.72	51.08
t25-M8-3	25	Medium	0.41	66.55	483.20	1195.98	4874.37	0.72	36.50
t25-M1-1	25	High	0.41	63.26	316.93	1016.97	4869.86	0.72	56.93
t25-M1-2	25	High	0.41	34.27	744.48	1833.77	7858.33	0.72	87.90
t25-M1-3	25	High	38.59	69.35	241.43	649.63	2858.37	0.72	30.07

Sample	Day	Treatment	C3-DBT	ANT	C0-PHE	C1-PHE	C2-PHE	C3-PHE	C4-PHE
t0-A	0	—	2.37	0.45	19.26	23.69	54.37	10.92	0.30
t0-B	0	—	5.26	0.45	16.31	35.02	113.06	99.51	32.08
t0-C	0	—	0.31	0.45	20.33	18.02	46.07	8.89	3.99
t2-M4-2	2	Control	20.60	0.45	7.99	55.23	155.44	73.12	31.92
t2-M4-3	2	Control	0.31	1.53	5.72	80.45	124.20	35.39	43.82
t2-M3-1	2	Low	37.82	0.45	32.41	201.61	364.20	188.56	60.35
t2-M3-3	2	Low	31.31	9.50	24.22	205.36	501.12	282.37	121.15
t2-M8-1	2	Medium	26.14	13.10	15.12	79.17	283.54	520.17	168.83
t2-M8-2	2	Medium	30.80	7.85	28.18	118.53	414.80	214.39	68.25
t2-M8-3	2	Medium	21.76	8.40	30.80	155.30	389.37	191.15	105.66
t2-M1-1	2	High	47.24	10.58	27.34	92.42	408.65	235.33	60.65
t2-M1-2	2	High	53.13	13.89	41.67	133.54	392.41	162.35	75.89
t2-M1-3	2	High	107.65	29.09	36.97	170.43	562.15	265.85	136.18
t5-M4-1	5	Control	7.40	2.82	13.08	25.15	37.31	26.73	17.12
t5-M4-2	5	Control	1.29	3.93	13.15	51.41	158.82	151.40	54.67
t5-M4-3	5	Control	0.31	1.49	9.23	50.10	105.07	58.69	51.04
t5-M3-1	5	Low	73.20	10.77	45.00	266.03	603.03	470.95	100.25
t5-M3-2	5	Low	63.01	9.71	46.00	252.92	588.80	193.60	90.13
t5-M3-3	5	Low	62.33	7.64	28.72	271.14	547.23	220.90	37.06
t5-M8-1	5	Medium	130.62	19.63	73.39	233.28	1148.60	629.65	146.77
t5-M8-2	5	Medium	535.40	51.33	133.13	1056.85	3712.31	6081.47	1153.95
t5-M8-3	5	Medium	91.17	15.44	38.94	186.00	825.18	450.46	93.18
t5-M1-1	5	High	83.61	16.38	33.65	145.79	653.23	341.08	74.66
t5-M1-2	5	High	111.22	16.88	57.66	125.98	791.90	413.47	10.33
t5-M1-3	5	High	96.83	0.45	37.37	189.39	939.33	529.17	214.52
t11-M4-1	11	Control	10.01	3.50	10.49	50.04	175.66	82.21	94.12
t11-M4-2	11	Control	12.57	6.13	28.07	97.33	268.04	105.92	62.07
t11-M4-3	11	Control	0.31	2.67	16.91	59.38	111.94	54.98	48.52
t11-M3-1	11	Low	69.74	13.79	66.01	477.90	962.98	261.84	88.28
t11-M3-2	11	Low	76.15	17.12	143.62	573.40	1178.87	343.87	76.57
t11-M3-3	11	Low	16.80	9.31	19.65	159.34	200.34	51.74	24.26
t11-M8-1	11	Medium	184.70	31.13	85.29	398.76	1068.46	530.38	166.00
t11-M8-2	11	Medium	106.38	13.60	51.11	297.49	734.14	362.36	110.01
t11-M1-1	11	High	251.24	10.81	33.60	152.19	953.20	517.19	137.93
t11-M1-2	11	High	226.17	17.91	28.99	208.77	803.86	518.98	95.91
t11-M1-3	11	High	211.80	24.49	40.81	229.52	1485.20	613.95	118.79
t20-M4-1	20	Control	1.86	1.32	7.90	51.07	85.58	54.14	33.22
t20-M4-2	20	Control	0.93	0.45	10.00	32.46	50.67	31.64	15.27
t20-M4-3	20	Control	0.31	0.45	5.27	51.05	83.79	48.93	23.63
t20-M3-1	20	Low	85.08	15.41	67.26	359.46	807.28	416.85	264.83
t20-M3-2	20	Low	96.95	17.35	87.30	416.33	935.65	513.09	247.58
t20-M8-1	20	Medium	125.09	33.92	125.06	457.58	1001.92	477.55	111.14
t20-M8-2	20	Medium	136.46	36.92	126.20	559.79	1205.92	591.89	187.02
t20-M8-3	20	Medium	251.06	17.92	129.70	482.11	1956.31	955.85	205.23
t20-M1-1	20	High	211.66	14.48	80.88	278.44	1294.54	871.85	213.93
t20-M1-2	20	High	229.25	29.41	71.22	259.55	1002.29	695.26	98.24
t20-M1-3	20	High	303.18	19.41	70.94	271.43	1459.44	906.21	176.98
t25-M4-1	25	Control	0.31	2.21	9.70	9.72	65.96	0.30	23.09
t25-M4-2	25	Control	0.31	3.27	6.54	15.04	53.57	18.70	8.62
t25-M4-3	25	Control	1.19	3.36	16.80	13.02	59.92	12.08	0.30
t25-M3-1	25	Low	177.06	28.30	166.07	778.71	1363.09	690.08	231.29
t25-M3-2	25	Low	136.26	31.01	123.78	728.94	1246.81	640.71	199.00
t25-M3-3	25	Low	140.95	14.85	165.28	922.30	1622.54	656.50	131.63
t25-M8-1	25	Medium	242.38	39.09	112.93	544.11	1520.57	943.65	263.67
t25-M8-2	25	Medium	179.79	39.29	145.39	331.22	1381.19	663.63	182.93
t25-M8-3	25	Medium	184.32	21.73	122.67	549.82	1502.08	868.36	209.59
t25-M1-1	25	High	329.32	39.66	129.17	617.20	1703.85	941.24	224.85
t25-M1-2	25	High	257.47	41.44	133.84	554.33	1746.47	1050.76	223.52
t25-M1-3	25	High	303.48	14.61	89.35	406.34	1471.16	856.63	254.05

Sample	Day	Treatment	RET	PYR	C0-FLA	C1-FLA	C2-FLA	C3-FLA	C4-FLA
t0-A	0	—	25.68	8.23	4.57	14.03	11.07	0.55	3.33
t0-B	0	—	74.36	8.55	15.50	59.42	23.98	0.55	154.52
t0-C	0	—	27.96	5.03	5.03	5.61	0.55	0.55	4.03
t2-M4-2	2	Control	43.15	6.23	32.58	41.84	26.80	13.37	86.73
t2-M4-3	2	Control	114.83	4.05	43.99	33.38	12.99	0.55	155.30
t2-M3-1	2	Low	59.03	8.65	34.09	86.65	66.71	34.07	228.54
t2-M3-3	2	Low	138.66	7.79	49.55	58.80	41.84	23.46	188.76
t2-M8-1	2	Medium	131.00	5.27	27.84	81.48	48.83	0.55	397.57
t2-M8-2	2	Medium	123.05	16.33	29.04	192.61	112.17	47.26	335.95
t2-M8-3	2	Medium	239.84	16.51	81.85	134.35	103.82	40.21	354.58
t2-M1-1	2	High	64.39	20.53	20.90	173.50	130.69	57.68	203.63
t2-M1-2	2	High	129.86	16.57	56.62	107.69	85.31	45.53	206.23
t2-M1-3	2	High	145.45	19.11	32.02	118.96	82.70	37.80	138.06
t5-M4-1	5	Control	14.28	5.42	21.68	30.54	11.34	0.55	82.96
t5-M4-2	5	Control	85.38	7.18	48.41	67.52	25.63	9.72	205.32
t5-M4-3	5	Control	30.06	4.51	19.80	32.57	8.34	0.55	79.91
t5-M3-1	5	Low	100.00	16.57	45.62	128.27	93.71	39.39	134.79
t5-M3-2	5	Low	70.53	24.69	33.89	64.12	73.90	32.41	22.66
t5-M3-3	5	Low	84.59	19.57	29.24	119.04	77.91	42.45	76.55
t5-M8-1	5	Medium	81.08	54.24	45.89	160.63	139.08	78.71	50.18
t5-M8-2	5	Medium	344.86	106.96	151.34	860.63	702.44	364.89	837.57
t5-M8-3	5	Medium	108.09	24.16	28.70	257.67	213.76	89.75	205.38
t5-M1-1	5	High	102.74	38.93	31.22	409.30	272.00	115.30	281.04
t5-M1-2	5	High	78.76	40.13	28.20	134.53	108.87	83.91	55.16
t5-M1-3	5	High	99.55	31.29	27.59	232.60	199.05	150.07	196.29
t11-M4-1	11	Control	61.97	8.15	15.74	90.91	16.02	0.55	234.08
t11-M4-2	11	Control	91.88	11.16	50.44	112.72	51.12	0.55	420.85
t11-M4-3	11	Control	21.81	8.48	37.64	32.69	14.77	0.55	194.07
t11-M3-1	11	Low	69.40	15.88	39.95	206.38	156.50	51.57	124.20
t11-M3-2	11	Low	104.93	46.72	61.88	179.09	115.08	57.19	51.68
t11-M3-3	11	Low	53.78	8.64	21.75	58.71	53.64	26.36	62.64
t11-M8-1	11	Medium	133.84	34.08	60.95	326.06	242.04	116.86	128.02
t11-M8-2	11	Medium	139.75	25.93	58.00	293.96	185.66	79.54	151.90
t11-M1-1	11	High	87.80	65.43	32.64	367.96	229.63	85.61	109.34
t11-M1-2	11	High	114.11	37.12	27.79	371.38	271.64	105.54	161.21
t11-M1-3	11	High	107.33	40.14	45.22	230.28	169.27	68.10	96.77
t20-M4-1	20	Control	39.52	5.06	21.45	21.56	12.87	0.55	69.29
t20-M4-2	20	Control	20.54	3.56	23.90	18.97	5.11	0.55	77.82
t20-M4-3	20	Control	25.44	3.15	18.52	16.75	5.77	0.55	94.96
t20-M3-1	20	Low	72.52	29.88	25.82	585.98	455.14	170.40	170.61
t20-M3-2	20	Low	70.51	26.70	27.52	595.67	477.68	173.38	185.97
t20-M8-1	20	Medium	129.23	54.28	56.29	299.44	240.79	93.55	105.11
t20-M8-2	20	Medium	145.67	48.59	69.54	416.37	333.22	129.46	145.45
t20-M8-3	20	Medium	110.93	81.45	57.50	301.77	208.67	124.61	54.37
t20-M1-1	20	High	69.58	110.14	44.95	733.99	540.98	207.06	139.40
t20-M1-2	20	High	74.67	33.82	27.26	432.76	311.78	123.11	67.76
t20-M1-3	20	High	78.97	69.78	37.53	280.09	201.28	109.34	51.77
t25-M4-1	25	Control	2.21	2.95	1.48	4.57	0.55	0.55	0.55
t25-M4-2	25	Control	25.89	3.46	7.16	22.74	8.05	0.55	74.76
t25-M4-3	25	Control	8.82	5.58	3.61	7.84	0.55	0.55	1.81
t25-M3-1	25	Low	77.93	36.38	53.87	605.00	504.83	234.93	223.98
t25-M3-2	25	Low	109.57	35.63	46.68	678.10	501.85	198.85	166.78
t25-M3-3	25	Low	73.73	57.06	52.97	502.94	372.05	146.77	145.68
t25-M8-1	25	Medium	136.28	60.61	69.57	773.42	643.46	281.18	207.49
t25-M8-2	25	Medium	144.64	60.27	49.17	162.88	113.78	67.95	29.65
t25-M8-3	25	Medium	142.59	54.92	47.17	1042.59	706.19	263.49	373.02
t25-M1-1	25	High	89.51	67.58	53.59	658.72	484.40	198.13	166.91
t25-M1-2	25	High	151.76	89.84	82.97	739.19	540.35	237.35	160.54
t25-M1-3	25	High	66.83	64.34	36.30	570.21	427.97	164.25	131.82

Sample	Day	Treatment	BNT23	BNT21	C1-BNT	C2-BNT	C3-BNT	C4-BNT	C0-CHY
t0-A	0	—	1.18	0.87	0.87	2.73	0.87	0.87	6.40
t0-B	0	—	0.87	0.87	8.80	3.66	21.91	30.67	0.80
t0-C	0	—	0.87	0.87	0.87	1.83	0.87	0.87	3.87
t2-M4-2	2	Control	2.90	0.87	11.17	0.87	33.67	48.92	8.38
t2-M4-3	2	Control	0.87	0.87	5.50	9.99	40.85	39.33	4.05
t2-M3-1	2	Low	5.65	2.28	42.99	39.29	72.09	111.33	18.77
t2-M3-3	2	Low	3.85	0.87	28.60	0.87	56.48	81.73	15.31
t2-M8-1	2	Medium	0.87	0.87	44.61	31.78	189.32	308.40	9.03
t2-M8-2	2	Medium	6.95	2.51	34.05	23.14	66.26	94.79	15.43
t2-M8-3	2	Medium	6.09	1.25	19.94	13.05	33.35	38.25	15.16
t2-M1-1	2	High	12.50	4.58	29.37	24.08	59.32	87.27	20.53
t2-M1-2	2	High	7.91	2.64	27.44	20.11	35.80	60.01	24.86
t2-M1-3	2	High	12.03	3.95	41.49	24.66	49.62	81.21	25.48
t5-M4-1	5	Control	0.87	0.87	5.70	227.08	40.25	95.82	1.31
t5-M4-2	5	Control	1.24	0.87	11.91	9.94	26.29	34.41	5.33
t5-M4-3	5	Control	0.87	0.87	1.76	0.87	27.46	43.18	2.74
t5-M3-1	5	Low	12.64	3.89	33.65	31.98	36.05	43.69	35.30
t5-M3-2	5	Low	20.55	6.20	30.42	7.30	0.87	0.87	52.72
t5-M3-3	5	Low	14.62	5.10	28.32	24.18	32.93	35.09	40.47
t5-M8-1	5	Medium	30.55	9.94	65.24	39.97	0.87	0.87	89.00
t5-M8-2	5	Medium	70.16	20.46	214.90	0.87	271.41	360.28	191.17
t5-M8-3	5	Medium	16.87	4.61	28.06	25.74	54.22	83.28	36.25
t5-M1-1	5	High	23.56	7.39	45.81	30.42	56.65	103.07	42.97
t5-M1-2	5	High	24.58	7.62	47.19	56.37	0.87	0.87	63.99
t5-M1-3	5	High	13.28	3.81	71.78	19.71	68.17	139.04	37.83
t11-M4-1	11	Control	0.87	0.87	12.65	24.98	126.96	198.68	1.41
t11-M4-2	11	Control	0.87	0.87	9.29	0.87	19.38	32.33	11.58
t11-M4-3	11	Control	0.87	0.87	0.87	0.87	15.13	25.01	11.19
t11-M3-1	11	Low	14.98	3.49	21.41	45.16	38.30	69.69	49.75
t11-M3-2	11	Low	40.26	10.27	44.54	20.81	41.62	46.81	144.39
t11-M3-3	11	Low	3.67	1.20	6.52	0.87	8.78	25.16	14.78
t11-M8-1	11	Medium	32.80	6.24	47.74	29.00	54.31	87.95	77.39
t11-M8-2	11	Medium	17.52	4.72	40.00	24.23	40.09	29.52	46.75
t11-M1-1	11	High	38.80	8.93	62.71	36.31	51.68	80.80	64.85
t11-M1-2	11	High	25.62	6.54	55.76	23.81	26.15	32.04	53.31
t11-M1-3	11	High	22.21	6.51	42.55	21.34	29.19	35.17	56.10
t20-M4-1	20	Control	0.87	0.87	4.47	3.24	30.45	42.32	4.05
t20-M4-2	20	Control	0.87	0.87	5.73	7.62	21.30	40.14	2.17
t20-M4-3	20	Control	0.87	0.87	2.90	0.87	31.27	43.50	2.36
t20-M3-1	20	Low	22.48	4.66	26.93	17.21	52.48	85.27	74.55
t20-M3-2	20	Low	21.22	4.31	35.00	19.31	47.31	77.01	79.27
t20-M8-1	20	Medium	27.40	4.55	28.52	18.72	18.10	33.47	134.32
t20-M8-2	20	Medium	37.92	6.29	39.00	28.73	23.44	46.32	101.19
t20-M8-3	20	Medium	97.73	20.89	128.98	71.46	0.87	0.87	277.89
t20-M1-1	20	High	60.06	13.19	82.26	39.21	37.22	48.66	129.58
t20-M1-2	20	High	28.54	6.59	52.48	24.14	16.75	23.17	69.15
t20-M1-3	20	High	71.89	18.23	138.70	66.45	40.17	0.87	168.10
t25-M4-1	25	Control	0.87	0.87	0.87	0.89	0.87	0.87	3.32
t25-M4-2	25	Control	0.87	0.87	0.87	4.62	19.64	22.69	0.78
t25-M4-3	25	Control	0.87	0.87	0.87	3.37	0.87	0.87	2.95
t25-M3-1	25	Low	43.02	9.70	67.60	27.68	50.94	92.34	147.63
t25-M3-2	25	Low	40.39	9.59	63.98	38.94	39.73	47.34	113.64
t25-M3-3	25	Low	42.61	9.69	45.87	21.89	28.29	31.41	125.54
t25-M8-1	25	Medium	61.41	10.46	85.56	43.71	64.74	77.40	160.05
t25-M8-2	25	Medium	53.29	11.39	69.18	36.59	0.87	0.87	175.03
t25-M8-3	25	Medium	43.21	9.52	76.45	38.10	56.03	51.57	124.97
t25-M1-1	25	High	56.67	15.22	93.50	46.97	40.23	56.26	129.00
t25-M1-2	25	High	68.74	16.85	125.99	56.03	28.73	32.06	164.10
t25-M1-3	25	High	71.70	17.90	126.13	62.18	33.10	45.27	125.45

Sample	Day	Treatment	C1-CHY	C2-CHY	C3-CHY	BaA	BbF+BkF	BaP	BeP
t0-A	0	—	5.65	7.97	0.87	0.87	1.33	1.16	1.16
t0-B	0	—	542.96	893.34	140.22	0.87	1.33	7.54	1.16
t0-C	0	—	7.50	8.41	2.44	0.87	5.45	1.16	2.72
t2-M4-2	2	Control	169.63	2000.36	182.80	0.87	5.37	18.91	5.37
t2-M4-3	2	Control	426.93	1644.64	277.58	0.87	5.61	16.83	4.49
t2-M3-1	2	Low	590.99	3910.41	403.99	3.71	2.49	72.86	17.66
t2-M3-3	2	Low	923.93	2962.38	317.22	1.39	13.67	32.55	10.09
t2-M8-1	2	Medium	1328.07	12785.42	1328.12	21.82	24.16	102.11	17.15
t2-M8-2	2	Medium	966.57	2072.12	389.67	1.81	1.33	71.54	13.27
t2-M8-3	2	Medium	691.31	1156.20	197.79	2.69	8.67	17.03	5.88
t2-M1-1	2	High	671.37	3157.88	278.42	2.20	5.00	41.93	9.62
t2-M1-2	2	High	689.12	766.43	286.12	4.14	1.33	35.05	10.42
t2-M1-3	2	High	380.60	3539.38	340.09	2.01	7.43	34.49	8.75
t5-M4-1	5	Control	145.95	3078.43	161.49	0.87	8.97	33.80	1.16
t5-M4-2	5	Control	653.33	1164.51	253.99	0.87	4.36	14.43	3.24
t5-M4-3	5	Control	208.88	1923.34	192.71	0.87	3.37	21.70	4.86
t5-M3-1	5	Low	368.02	1324.68	194.39	3.36	4.97	25.30	6.38
t5-M3-2	5	Low	35.70	40.42	0.87	1.26	1.33	5.14	6.68
t5-M3-3	5	Low	120.76	1148.17	185.46	1.57	6.51	15.41	7.77
t5-M8-1	5	Medium	69.59	94.80	0.87	3.48	1.33	11.07	14.48
t5-M8-2	5	Medium	2355.54	11374.63	1638.80	14.79	5.87	233.59	77.47
t5-M8-3	5	Medium	559.09	3465.26	447.34	5.03	19.58	40.67	13.06
t5-M1-1	5	High	775.03	2018.74	599.56	8.81	9.10	75.38	14.20
t5-M1-2	5	High	65.63	78.49	0.87	4.34	1.33	1.16	13.55
t5-M1-3	5	High	360.78	5003.77	580.83	4.84	16.96	46.45	15.97
t11-M4-1	11	Control	1096.42	6845.57	743.68	0.87	10.76	108.61	7.29
t11-M4-2	11	Control	281.26	1104.24	155.97	0.87	4.77	142.96	18.11
t11-M4-3	11	Control	159.78	917.01	91.48	0.87	3.16	47.42	10.19
t11-M3-1	11	Low	539.49	2774.11	262.92	2.96	5.95	22.82	9.80
t11-M3-2	11	Low	57.68	1277.86	253.89	2.43	18.02	27.72	21.48
t11-M3-3	11	Low	129.87	416.48	139.49	1.67	1.33	7.24	1.16
t11-M8-1	11	Medium	412.63	942.44	316.20	6.82	7.09	20.15	14.93
t11-M8-2	11	Medium	403.40	779.99	218.30	3.75	5.94	9.90	4.70
t11-M1-1	11	High	237.75	3731.65	301.88	5.22	12.86	56.43	14.97
t11-M1-2	11	High	370.28	969.20	243.54	3.44	8.31	29.25	7.84
t11-M1-3	11	High	304.78	1316.33	301.62	3.87	11.99	53.74	11.99
t20-M4-1	20	Control	210.00	1920.22	213.96	0.87	3.74	15.51	1.16
t20-M4-2	20	Control	222.15	1511.70	176.22	0.87	2.83	14.50	1.16
t20-M4-3	20	Control	288.50	2222.04	207.40	0.87	4.75	16.18	4.57
t20-M3-1	20	Low	520.14	2150.88	317.82	7.54	1.33	28.81	11.52
t20-M3-2	20	Low	379.80	2198.62	418.50	14.79	14.49	20.92	14.08
t20-M8-1	20	Medium	255.12	456.84	107.66	8.70	11.29	40.22	17.07
t20-M8-2	20	Medium	353.05	632.22	179.49	7.58	7.16	9.26	8.42
t20-M8-3	20	Medium	131.01	112.72	0.87	4.79	14.22	6.69	37.64
t20-M1-1	20	High	330.66	2090.95	217.63	7.29	17.26	22.23	17.74
t20-M1-2	20	High	152.03	962.49	108.67	4.56	6.55	12.96	17.73
t20-M1-3	20	High	99.37	91.72	0.87	5.29	7.69	4.73	23.08
t25-M4-1	25	Control	1.32	5.06	0.87	0.87	1.33	1.16	1.16
t25-M4-2	25	Control	278.12	603.01	102.18	0.87	1.33	5.83	1.16
t25-M4-3	25	Control	8.05	17.67	0.87	0.87	1.33	1.16	1.16
t25-M3-1	25	Low	769.11	1519.35	351.63	8.40	2.11	42.92	11.96
t25-M3-2	25	Low	420.09	1585.58	303.04	6.35	9.91	28.21	9.91
t25-M3-3	25	Low	365.78	892.81	254.36	6.73	23.75	20.56	14.53
t25-M8-1	25	Medium	617.16	3160.52	502.73	13.23	13.57	23.31	21.22
t25-M8-2	25	Medium	71.43	61.46	0.87	12.32	13.92	25.43	16.33
t25-M8-3	25	Medium	1036.29	1269.12	419.72	8.45	30.50	15.94	16.64
t25-M1-1	25	High	446.61	1835.79	219.78	8.77	7.05	15.85	15.85
t25-M1-2	25	High	474.75	625.81	189.25	11.92	10.05	10.05	15.64
t25-M1-3	25	High	351.17	1205.54	168.40	5.85	5.92	9.43	17.77

Sample	Day	Treatment	BP	IP	DA	TPACs
t0-A	0	—	0.71	0.79	0.39	896.62
t0-B	0	—	0.71	0.79	0.39	2621.13
t0-C	0	—	0.71	0.79	0.39	596.30
t2-M4-2	2	Control	0.71	0.79	0.39	2621.38
t2-M4-3	2	Control	0.71	0.79	0.39	2962.65
t2-M3-1	2	Low	0.71	0.79	0.39	7311.20
t2-M3-3	2	Low	0.71	0.79	0.39	8975.97
t2-M8-1	2	Medium	0.71	0.79	0.39	10426.38
t2-M8-2	2	Medium	0.71	0.79	0.39	10730.94
t2-M8-3	2	Medium	0.71	0.79	0.39	9048.18
t2-M1-1	2	High	0.71	0.79	0.39	11702.22
t2-M1-2	2	High	0.71	0.79	0.39	8703.11
t2-M1-3	2	High	0.71	0.79	0.39	10522.96
t5-M4-1	5	Control	0.71	0.79	0.39	1356.23
t5-M4-2	5	Control	0.71	0.79	0.39	5223.93
t5-M4-3	5	Control	0.71	0.79	0.39	2052.24
t5-M3-1	5	Low	0.71	0.79	0.39	9255.56
t5-M3-2	5	Low	0.71	0.79	0.39	6638.18
t5-M3-3	5	Low	0.71	0.79	0.39	11310.71
t5-M8-1	5	Medium	0.71	0.79	0.39	13781.66
t5-M8-2	5	Medium	0.41	0.79	0.39	76741.10
t5-M8-3	5	Medium	0.71	0.79	0.39	16383.21
t5-M1-1	5	High	0.71	0.79	0.39	18421.62
t5-M1-2	5	High	0.71	0.79	0.39	13016.16
t5-M1-3	5	High	0.71	0.79	0.39	17463.74
t11-M4-1	11	Control	0.71	0.79	0.39	5573.83
t11-M4-2	11	Control	0.71	0.79	0.39	6827.24
t11-M4-3	11	Control	0.71	0.79	0.39	2319.22
t11-M3-1	11	Low	0.71	0.79	0.39	20711.73
t11-M3-2	11	Low	0.71	0.79	0.39	10216.02
t11-M3-3	11	Low	0.41	0.79	0.39	6873.30
t11-M8-1	11	Medium	0.71	0.79	0.39	22462.94
t11-M8-2	11	Medium	0.71	0.79	0.39	11989.86
t11-M1-1	11	High	8.06	0.79	0.39	18975.53
t11-M1-2	11	High	0.71	0.79	0.39	24289.36
t11-M1-3	11	High	0.71	0.79	0.39	20315.32
t20-M4-1	20	Control	0.71	0.79	0.39	5343.92
t20-M4-2	20	Control	0.71	0.79	0.39	1514.40
t20-M4-3	20	Control	0.71	0.79	0.39	1876.16
t20-M3-1	20	Low	0.71	0.79	0.39	24482.01
t20-M3-2	20	Low	0.71	0.79	0.39	24862.58
t20-M8-1	20	Medium	0.71	0.79	0.39	20471.01
t20-M8-2	20	Medium	0.71	0.79	0.39	21010.69
t20-M8-3	20	Medium	0.71	0.79	0.39	15487.25
t20-M1-1	20	High	0.71	0.79	0.39	16092.31
t20-M1-2	20	High	0.71	0.79	0.39	33706.08
t20-M1-3	20	High	0.71	0.79	0.39	15501.60
t25-M4-1	25	Control	0.71	0.79	0.39	600.36
t25-M4-2	25	Control	0.71	0.79	0.39	1506.73
t25-M4-3	25	Control	0.71	0.79	0.39	704.85
t25-M3-1	25	Low	0.71	0.79	0.39	26491.11
t25-M3-2	25	Low	0.71	0.79	0.39	23898.85
t25-M3-3	25	Low	0.71	0.79	0.39	32060.63
t25-M8-1	25	Medium	0.71	0.79	0.39	31373.83
t25-M8-2	25	Medium	0.71	0.79	0.39	13170.89
t25-M8-3	25	Medium	0.71	0.79	0.39	33218.20
t25-M1-1	25	High	0.71	0.79	0.39	30902.19
t25-M1-2	25	High	0.71	0.79	0.39	32600.75
t25-M1-3	25	High	0.71	0.79	0.39	19871.94

Table C.7: PAC concentrations (ng g^{-1}, ww Lipid) in mussel tissue collected from the Control, Low, Medium, and High treatments during the depuration phase of the bioaccumulation study.

Sample	Day	Treatment	C0-NAP	C1-NAP	C2-NAP	C3-NAP	C4-NAP	ACE	ACY
t1-M3-1-D	26	Low	0.41	0.41	211.44	643.05	2216.82	0.72	10.38
t1-M3-3-D	26	Low	0.41	277.39	560.45	1198.43	4278.54	0.72	11.39
t1-M8-1-D	26	Medium	0.41	55.37	210.74	339.08	1339.90	0.72	10.62
t1-M8-2-D	26	Medium	0.41	121.47	461.33	628.36	2132.94	0.72	13.99
t1-M8-3-D	26	Medium	139.33	97.85	446.12	551.73	6940.73	0.72	11.49
t1-M1-1-D	26	High	0.41	16.37	221.64	677.33	3721.79	0.72	36.39
t1-M1-2-D	26	High	0.41	0.41	334.13	1091.47	4928.64	0.72	69.38
t1-M1-3-D	26	High	0.41	66.25	277.67	814.33	3889.82	0.72	47.57
t2-M3-1-D	27	Low	0.41	0.41	219.17	577.38	2144.03	0.72	9.88
t2-M3-2-D	27	Low	0.41	15.63	267.73	558.39	2450.21	0.72	17.69
t2-M3-3-D	27	Low	0.41	0.41	68.00	397.61	1365.05	0.72	6.36
t2-M8-1-D	27	Medium	0.41	0.41	157.09	550.98	2864.33	0.72	24.04
t2-M8-2-D	27	Medium	0.41	21.37	151.29	334.64	1658.74	0.72	11.21
t2-M8-3-D	27	Medium	0.41	0.41	158.35	339.73	1122.15	0.72	13.51
t2-M1-1-D	27	High	0.41	0.41	208.59	570.17	3041.43	0.72	32.78
t2-M1-2-D	27	High	0.41	9.59	253.90	699.27	3610.68	0.72	35.27
t2-M1-3-D	27	High	0.41	51.35	290.36	832.63	4114.72	0.72	53.89
t4-M4-1-D	29	Control	0.41	0.41	25.04	171.98	250.42	0.72	0.31
t4-M3-1-D	29	Low	19.16	13.88	149.81	246.21	941.98	0.72	9.06
t4-M3-2-D	29	Low	0.41	0.41	105.82	317.47	1637.98	0.72	13.63
t4-M3-3-D	29	Low	0.41	0.41	161.33	487.49	1838.30	0.72	9.16
t4-M8-1-D	29	Medium	81.57	81.87	127.12	420.55	2246.25	0.72	14.86
t4-M8-2-D	29	Medium	0.41	0.41	124.60	239.02	1181.94	0.72	10.42
t4-M8-3-D	29	Medium	105.93	80.26	90.42	337.83	1533.95	0.72	7.58
t4-M1-1-D	29	High	62.14	118.56	245.27	614.89	3244.07	0.72	54.69
t4-M1-2-D	29	High	0.41	29.85	132.52	490.44	2772.33	0.72	50.27
t4-M1-3-D	29	High	0.41	22.53	38.77	443.56	2219.73	0.72	42.82
t8-M3-1-D	33	Low	32.31	34.14	123.26	178.46	992.51	0.72	5.93
t8-M3-2-D	33	Low	0.41	0.41	231.07	320.32	1830.51	0.72	11.59
t8-M3-3-D	33	Low	227.53	103.98	384.07	528.34	2432.83	0.72	11.62
t8-M8-1-D	33	Medium	38.11	50.09	157.01	347.59	1529.17	0.72	6.43
t8-M8-1-D	33	Medium	181.80	138.92	498.41	981.45	3931.08	0.72	26.22
t8-M8-3-D	33	Medium	85.16	40.53	80.12	139.84	1178.96	0.72	15.19
t8-M1-1-D	33	High	8.93	53.64	106.11	227.68	1284.55	0.72	28.73
t8-M1-2-D	33	High	0.41	182.84	562.37	1045.94	6237.31	0.72	55.74
t8-M1-3-D	33	High	0.41	114.41	491.17	908.74	5471.46	0.72	53.74
t16-M3-1-D	41	Low	0.41	0.41	140.84	143.91	785.97	0.72	7.03
t16-M3-2-D	41	Low	9.49	100.73	442.39	779.04	4162.12	0.72	15.11
t16-M3-3-D	41	Low	43.31	59.18	415.30	834.11	3100.57	0.72	15.10
t16-M8-1-D	41	Medium	0.41	9.48	123.29	288.55	1107.59	0.72	8.08
t16-M8-2-D	41	Medium	0.41	0.41	137.63	247.41	1386.75	0.72	13.04
t16-M8-3-D	41	Medium	37.12	31.76	159.10	320.89	1450.69	0.72	11.29
t16-M1-1-D	41	High	0.41	7.39	177.07	323.02	1767.89	0.72	11.42
t16-M1-2-D	41	High	0.41	34.91	203.96	336.04	1805.51	0.72	20.55
t16-M1-3-D	41	High	12.18	88.03	421.49	890.04	4257.33	0.72	53.80

Sample	Day	Treatment	C0-FLU	C1-FLU	C2-FLU	C3-FLU	C0-DBT	C1-DBT
t1-M3-1-D	26	Low	161.63	1088.78	3772.62	3537.24	24.42	86.40
t1-M3-3-D	26	Low	257.64	1643.50	5495.62	4107.31	39.54	125.45
t1-M8-1-D	26	Medium	77.13	695.91	2570.04	2145.68	19.99	56.28
t1-M8-2-D	26	Medium	126.40	949.05	3226.15	2608.80	26.69	101.98
t1-M8-3-D	26	Medium	129.97	2338.23	7441.28	5776.51	34.18	140.14
t1-M1-1-D	26	High	158.55	1342.68	4146.94	3709.44	30.27	76.23
t1-M1-2-D	26	High	314.38	2079.85	6337.25	4886.22	41.81	117.57
t1-M1-3-D	26	High	250.42	1901.51	5546.10	3752.84	39.42	108.53
t2-M3-1-D	27	Low	180.81	1057.69	2805.55	1855.35	21.58	75.80
t2-M3-2-D	27	Low	139.34	1274.24	4684.94	4457.86	27.49	117.71
t2-M3-3-D	27	Low	81.54	338.58	1080.43	797.41	15.33	49.17
t2-M8-1-D	27	Medium	147.97	1319.33	4649.17	4734.07	33.63	97.76
t2-M8-2-D	27	Medium	122.65	983.08	3181.12	2681.77	18.23	72.61
t2-M8-3-D	27	Medium	83.33	658.42	2720.61	2356.31	24.68	79.03
t2-M1-1-D	27	High	158.77	1237.31	4163.33	3103.84	30.21	91.00
t2-M1-2-D	27	High	189.73	1478.02	4276.66	3211.75	42.60	35.89
t2-M1-3-D	27	High	186.60	1636.05	4880.52	3591.20	41.61	101.38
t4-M4-1-D	29	Control	13.48	56.77	553.35	429.75	1.41	8.81
t4-M3-1-D	29	Low	71.29	659.85	2686.96	2293.47	14.03	73.83
t4-M3-2-D	29	Low	101.71	660.78	2243.65	1306.58	17.32	49.06
t4-M3-3-D	29	Low	140.98	875.99	2832.37	2233.54	20.75	67.06
t4-M8-1-D	29	Medium	128.63	916.24	3968.62	2842.67	26.65	103.00
t4-M8-2-D	29	Medium	73.70	803.41	3077.43	2080.82	17.88	60.00
t4-M8-3-D	29	Medium	135.67	772.07	2922.57	2461.02	14.43	47.04
t4-M1-1-D	29	High	191.16	916.92	3619.13	2224.54	48.09	140.04
t4-M1-2-D	29	High	143.25	1182.74	3900.71	3078.41	34.10	83.57
t4-M1-3-D	29	High	169.99	1100.83	3501.02	2183.23	48.44	96.13
t8-M3-1-D	33	Low	73.02	383.79	1405.11	1367.74	9.69	39.49
t8-M3-2-D	33	Low	184.11	1529.95	4234.77	3179.97	23.43	56.50
t8-M3-3-D	33	Low	192.51	1238.27	5968.16	4326.10	18.71	87.00
t8-M8-1-D	33	Medium	69.68	758.77	3041.75	3907.31	17.16	45.77
t8-M8-1-D	33	Medium	277.37	2431.08	10801.91	8034.00	30.37	174.96
t8-M8-3-D	33	Medium	160.30	884.16	4016.48	3977.83	15.02	50.72
t8-M1-1-D	33	High	99.14	769.31	2873.31	2229.17	34.57	76.73
t8-M1-2-D	33	High	200.89	3181.34	7877.76	5236.57	33.59	109.56
t8-M1-3-D	33	High	239.20	2810.86	6961.52	4631.17	28.41	112.22
t16-M3-1-D	41	Low	65.13	538.33	2199.43	1424.00	14.49	32.43
t16-M3-2-D	41	Low	264.32	1641.64	5859.67	4908.75	25.86	80.32
t16-M3-3-D	41	Low	252.52	1432.73	4712.87	3780.25	16.29	79.65
t16-M8-1-D	41	Medium	77.99	589.05	2018.71	1366.85	13.30	32.30
t16-M8-2-D	41	Medium	89.67	715.24	2618.75	2149.10	15.96	38.17
t16-M8-3-D	41	Medium	108.56	650.82	2358.70	1913.41	8.76	38.91
t16-M1-1-D	41	High	69.26	722.12	2650.29	2225.44	12.99	37.06
t16-M1-2-D	41	High	85.90	633.26	2051.01	1390.84	16.29	27.63
t16-M1-3-D	41	High	222.39	1642.33	4896.59	3758.99	17.20	60.16

Sample	Day	Treatment	C2-DBT	C3-DBT	ANT	C0-PHE	C1-PHE	C2-PHE
t1-M3-1-D	26	Low	148.72	73.50	23.03	83.07	430.94	790.65
t1-M3-3-D	26	Low	207.23	85.37	35.14	107.82	539.79	1021.42
t1-M8-1-D	26	Medium	134.20	70.88	22.49	63.09	295.91	639.25
t1-M8-2-D	26	Medium	187.46	143.26	28.84	99.86	425.08	967.34
t1-M8-3-D	26	Medium	409.00	181.45	21.32	95.43	382.02	1046.95
t1-M1-1-D	26	High	170.84	99.50	23.49	66.75	293.02	739.25
t1-M1-2-D	26	High	247.02	175.11	34.30	94.08	414.15	1235.32
t1-M1-3-D	26	High	237.36	142.56	29.35	69.61	309.55	865.61
t2-M3-1-D	27	Low	125.02	53.55	20.68	73.98	364.28	630.52
t2-M3-2-D	27	Low	195.12	111.17	16.97	91.98	526.05	958.15
t2-M3-3-D	27	Low	66.81	31.19	14.31	42.92	202.03	371.53
t2-M8-1-D	27	Medium	201.27	138.91	30.33	65.70	331.43	863.39
t2-M8-2-D	27	Medium	197.61	114.27	13.59	52.45	268.65	775.58
t2-M8-3-D	27	Medium	193.92	138.19	27.91	75.21	332.65	902.99
t2-M1-1-D	27	High	245.78	128.08	19.69	51.79	232.64	735.88
t2-M1-2-D	27	High	36.96	0.31	40.06	87.73	410.12	1184.54
t2-M1-3-D	27	High	259.80	166.05	35.90	91.08	389.19	1236.39
t4-M4-1-D	29	Control	19.90	0.30	2.82	14.47	59.78	71.86
t4-M3-1-D	29	Low	134.90	70.29	11.27	56.36	286.70	512.91
t4-M3-2-D	29	Low	79.45	36.48	16.70	52.64	255.42	427.94
t4-M3-3-D	29	Low	102.29	43.15	19.80	57.99	302.54	512.26
t4-M8-1-D	29	Medium	198.11	107.57	21.24	57.17	378.35	831.04
t4-M8-2-D	29	Medium	127.57	75.18	14.12	53.65	254.79	612.30
t4-M8-3-D	29	Medium	108.79	30.25	14.75	33.89	188.51	337.98
t4-M1-1-D	29	High	291.51	143.71	37.13	79.21	408.19	986.45
t4-M1-2-D	29	High	199.46	131.52	25.41	57.22	278.20	759.74
t4-M1-3-D	29	High	253.06	105.44	37.99	83.58	269.34	736.31
t8-M3-1-D	33	Low	49.80	28.04	12.04	31.12	201.15	258.92
t8-M3-2-D	33	Low	76.65	36.13	40.59	74.07	265.37	509.85
t8-M3-3-D	33	Low	79.95	45.96	17.05	39.08	219.29	284.79
t8-M8-1-D	33	Medium	113.09	37.09	16.66	37.31	159.99	388.28
t8-M8-1-D	33	Medium	213.09	167.78	39.15	91.84	575.21	1459.49
t8-M8-3-D	33	Medium	92.01	32.44	13.95	28.96	127.22	180.89
t8-M1-1-D	33	High	170.50	61.40	23.50	42.29	210.76	353.34
t8-M1-2-D	33	High	148.72	130.17	26.74	65.00	226.07	581.18
t8-M1-3-D	33	High	152.33	142.05	22.59	44.50	218.92	604.95
t16-M3-1-D	41	Low	35.78	13.59	13.79	31.09	132.61	187.91
t16-M3-2-D	41	Low	78.17	64.61	21.84	48.34	215.19	463.68
t16-M3-3-D	41	Low	94.89	54.88	14.91	53.56	308.94	656.46
t16-M8-1-D	41	Medium	50.33	30.36	16.00	38.10	138.46	266.88
t16-M8-2-D	41	Medium	39.45	29.29	16.35	29.23	117.64	258.33
t16-M8-3-D	41	Medium	79.89	35.28	7.73	24.99	142.55	395.36
t16-M1-1-D	41	High	53.65	33.70	13.08	32.38	122.67	272.69
t16-M1-2-D	41	High	35.10	14.04	14.35	33.55	92.91	207.59
t16-M1-3-D	41	High	105.94	58.00	10.51	44.91	195.31	566.84

Sample	Day	Treatment	C3-PHE	C4-PHE	RET	PYR	C0-FLA	C1-FLA
t1-M3-1-D	26	Low	494.62	140.42	75.70	42.11	48.21	384.41
t1-M3-3-D	26	Low	456.89	189.12	79.47	40.32	66.39	631.10
t1-M8-1-D	26	Medium	324.36	85.61	66.85	43.44	48.63	254.82
t1-M8-2-D	26	Medium	684.35	177.35	98.57	84.28	45.72	548.16
t1-M8-3-D	26	Medium	415.18	123.71	126.56	61.85	93.80	476.62
t1-M1-1-D	26	High	371.38	101.74	39.55	33.41	28.73	334.45
t1-M1-2-D	26	High	894.39	213.35	74.15	38.69	42.35	574.77
t1-M1-3-D	26	High	468.41	114.52	64.37	57.38	51.33	762.45
t2-M3-1-D	27	Low	269.56	102.43	51.18	29.00	42.13	284.69
t2-M3-2-D	27	Low	502.13	208.95	42.09	28.88	41.36	597.44
t2-M3-3-D	27	Low	181.11	64.44	42.92	22.08	36.80	265.46
t2-M8-1-D	27	Medium	498.08	158.50	59.71	30.68	43.75	508.21
t2-M8-2-D	27	Medium	334.66	110.08	56.06	27.19	37.51	404.55
t2-M8-3-D	27	Medium	536.32	160.72	105.76	19.62	28.06	283.04
t2-M1-1-D	27	High	366.06	83.03	55.03	44.46	38.04	421.67
t2-M1-2-D	27	High	629.83	214.19	124.96	55.89	43.41	469.98
t2-M1-3-D	27	High	595.68	125.01	88.23	58.49	45.16	399.31
t4-M4-1-D	29	Control	70.39	0.55	9.88	3.90	18.52	209.65
t4-M3-1-D	29	Low	213.37	100.86	37.32	14.89	22.25	225.79
t4-M3-2-D	29	Low	154.07	68.60	39.71	13.80	34.46	167.90
t4-M3-3-D	29	Low	285.77	96.95	62.71	19.53	30.32	260.43
t4-M8-1-D	29	Medium	555.26	196.82	104.29	41.95	53.98	738.11
t4-M8-2-D	29	Medium	255.96	118.49	52.24	20.32	31.98	300.32
t4-M8-3-D	29	Medium	184.21	58.83	73.11	21.53	28.63	232.73
t4-M1-1-D	29	High	568.45	154.70	84.16	48.66	58.62	709.03
t4-M1-2-D	29	High	367.05	96.73	42.80	26.80	25.25	301.79
t4-M1-3-D	29	High	281.15	69.51	88.80	51.44	64.30	505.91
t8-M3-1-D	33	Low	196.19	71.09	43.15	17.25	25.87	343.06
t8-M3-2-D	33	Low	299.26	139.61	78.25	15.14	31.74	328.10
t8-M3-3-D	33	Low	155.29	64.19	29.13	16.61	26.01	294.15
t8-M8-1-D	33	Medium	173.65	69.76	56.21	22.85	32.21	301.34
t8-M8-1-D	33	Medium	1084.48	357.36	57.81	33.21	23.46	946.90
t8-M8-3-D	33	Medium	112.61	36.76	48.00	19.97	32.96	268.70
t8-M1-1-D	33	High	185.91	62.60	60.42	32.90	32.90	327.10
t8-M1-2-D	33	High	277.76	80.70	73.19	27.57	31.44	506.55
t8-M1-3-D	33	High	292.14	84.60	34.40	32.82	17.23	653.79
t16-M3-1-D	41	Low	90.14	41.97	32.85	8.55	32.54	136.19
t16-M3-2-D	41	Low	311.12	121.01	79.71	33.38	38.66	469.97
t16-M3-3-D	41	Low	365.19	157.86	54.11	24.67	18.14	519.06
t16-M8-1-D	41	Medium	141.25	86.65	41.15	15.57	22.85	189.58
t16-M8-2-D	41	Medium	181.47	57.27	29.62	13.08	18.04	274.73
t16-M8-3-D	41	Medium	196.73	70.78	35.03	19.43	13.67	271.67
t16-M1-1-D	41	High	173.49	75.52	15.50	11.65	14.15	170.08
t16-M1-2-D	41	High	103.55	44.45	37.62	25.74	27.54	303.06
t16-M1-3-D	41	High	316.73	119.41	37.27	31.22	18.21	517.94

Sample	Day	Treatment	C2-FLA	C3-FLA	C4-FLA	BNT23	BNT21	C1-BNT
t1-M3-1-D	26	Low	233.11	85.94	403.44	16.99	3.25	50.40
t1-M3-3-D	26	Low	508.53	170.94	221.81	23.00	4.11	29.35
t1-M8-1-D	26	Medium	186.36	68.68	84.89	26.52	5.09	25.60
t1-M8-2-D	26	Medium	256.18	89.79	97.53	22.46	4.97	29.17
t1-M8-3-D	26	Medium	282.82	103.80	261.05	37.37	11.34	57.53
t1-M1-1-D	26	High	231.95	90.13	68.50	23.74	5.20	33.24
t1-M1-2-D	26	High	402.92	130.14	89.06	31.00	5.57	36.62
t1-M1-3-D	26	High	515.36	174.54	128.20	43.63	12.16	71.63
t2-M3-1-D	27	Low	186.51	73.35	169.89	12.04	3.15	28.55
t2-M3-2-D	27	Low	486.41	193.61	206.43	29.55	5.50	50.61
t2-M3-3-D	27	Low	188.53	72.06	123.20	12.16	2.52	23.70
t2-M8-1-D	27	Medium	360.00	152.35	265.78	34.46	6.48	45.89
t2-M8-2-D	27	Medium	306.22	117.36	110.05	30.38	5.42	34.43
t2-M8-3-D	27	Medium	216.35	80.17	83.40	19.36	3.55	26.55
t2-M1-1-D	27	High	278.54	107.50	100.73	33.57	8.36	43.25
t2-M1-2-D	27	High	346.53	129.13	78.79	27.06	5.72	39.47
t2-M1-3-D	27	High	274.98	106.85	74.96	40.24	9.53	55.66
t4-M4-1-D	29	Control	68.71	0.55	234.78	0.87	0.87	23.55
t4-M3-1-D	29	Low	179.79	74.61	68.20	16.74	3.49	21.70
t4-M3-2-D	29	Low	120.12	45.86	76.97	10.79	2.15	12.43
t4-M3-3-D	29	Low	194.89	72.21	55.63	13.60	2.50	14.29
t4-M8-1-D	29	Medium	444.39	171.38	160.10	44.73	7.64	63.76
t4-M8-2-D	29	Medium	230.69	88.51	103.08	18.90	3.77	25.93
t4-M8-3-D	29	Medium	182.28	75.20	50.39	19.51	3.93	24.78
t4-M1-1-D	29	High	417.99	144.88	135.30	34.99	8.75	40.43
t4-M1-2-D	29	High	213.17	74.11	58.39	22.12	5.51	28.53
t4-M1-3-D	29	High	331.74	150.80	186.81	24.82	5.14	34.90
t8-M3-1-D	33	Low	282.29	136.78	121.73	8.27	0.87	27.44
t8-M3-2-D	33	Low	287.83	95.39	85.63	14.40	1.89	14.66
t8-M3-3-D	33	Low	221.70	105.48	68.54	6.28	0.87	10.67
t8-M8-1-D	33	Medium	230.65	96.54	68.21	14.68	2.18	17.40
t8-M8-1-D	33	Medium	762.49	272.63	297.66	37.44	5.17	40.98
t8-M8-3-D	33	Medium	210.84	79.21	72.26	12.98	1.84	18.63
t8-M1-1-D	33	High	218.68	89.74	91.25	18.10	3.10	28.54
t8-M1-2-D	33	High	358.26	132.43	65.99	13.25	2.05	21.86
t8-M1-3-D	33	High	471.23	174.19	86.80	17.43	2.69	28.78
t16-M3-1-D	41	Low	99.33	42.96	61.03	5.16	0.87	9.47
t16-M3-2-D	41	Low	368.15	137.59	125.20	14.09	0.87	26.26
t16-M3-3-D	41	Low	394.67	135.57	140.32	17.18	3.56	21.65
t16-M8-1-D	41	Medium	134.24	50.03	96.54	6.40	0.87	6.27
t16-M8-2-D	41	Medium	219.20	81.20	67.79	6.32	0.87	9.11
t16-M8-3-D	41	Medium	174.98	65.92	116.53	7.86	1.72	13.83
t16-M1-1-D	41	High	131.40	44.99	42.05	5.60	0.99	7.97
t16-M1-2-D	41	High	220.86	76.06	61.74	6.05	1.14	10.92
t16-M1-3-D	41	High	351.74	116.18	73.43	18.11	4.18	24.36

Sample	Day	Treatment	C2-FLA	C3-FLA	C4-FLA	BNT23	BNT21	C1-BNT
t1-M3-1-D	26	Low	233.11	85.94	403.44	16.99	3.25	50.40
t1-M3-3-D	26	Low	508.53	170.94	221.81	23.00	4.11	29.35
t1-M8-1-D	26	Medium	186.36	68.68	84.89	26.52	5.09	25.60
t1-M8-2-D	26	Medium	256.18	89.79	97.53	22.46	4.97	29.17
t1-M8-3-D	26	Medium	282.82	103.80	261.05	37.37	11.34	57.53
t1-M1-1-D	26	High	231.95	90.13	68.50	23.74	5.20	33.24
t1-M1-2-D	26	High	402.92	130.14	89.06	31.00	5.57	36.62
t1-M1-3-D	26	High	515.36	174.54	128.20	43.63	12.16	71.63
t2-M3-1-D	27	Low	186.51	73.35	169.89	12.04	3.15	28.55
t2-M3-2-D	27	Low	486.41	193.61	206.43	29.55	5.50	50.61
t2-M3-3-D	27	Low	188.53	72.06	123.20	12.16	2.52	23.70
t2-M8-1-D	27	Medium	360.00	152.35	265.78	34.46	6.48	45.89
t2-M8-2-D	27	Medium	306.22	117.36	110.05	30.38	5.42	34.43
t2-M8-3-D	27	Medium	216.35	80.17	83.40	19.36	3.55	26.55
t2-M1-1-D	27	High	278.54	107.50	100.73	33.57	8.36	43.25
t2-M1-2-D	27	High	346.53	129.13	78.79	27.06	5.72	39.47
t2-M1-3-D	27	High	274.98	106.85	74.96	40.24	9.53	55.66
t4-M4-1-D	29	Control	68.71	0.55	234.78	0.87	0.87	23.55
t4-M3-1-D	29	Low	179.79	74.61	68.20	16.74	3.49	21.70
t4-M3-2-D	29	Low	120.12	45.86	76.97	10.79	2.15	12.43
t4-M3-3-D	29	Low	194.89	72.21	55.63	13.60	2.50	14.29
t4-M8-1-D	29	Medium	444.39	171.38	160.10	44.73	7.64	63.76
t4-M8-2-D	29	Medium	230.69	88.51	103.08	18.90	3.77	25.93
t4-M8-3-D	29	Medium	182.28	75.20	50.39	19.51	3.93	24.78
t4-M1-1-D	29	High	417.99	144.88	135.30	34.99	8.75	40.43
t4-M1-2-D	29	High	213.17	74.11	58.39	22.12	5.51	28.53
t4-M1-3-D	29	High	331.74	150.80	186.81	24.82	5.14	34.90
t8-M3-1-D	33	Low	282.29	136.78	121.73	8.27	0.87	27.44
t8-M3-2-D	33	Low	287.83	95.39	85.63	14.40	1.89	14.66
t8-M3-3-D	33	Low	221.70	105.48	68.54	6.28	0.87	10.67
t8-M8-1-D	33	Medium	230.65	96.54	68.21	14.68	2.18	17.40
t8-M8-1-D	33	Medium	762.49	272.63	297.66	37.44	5.17	40.98
t8-M8-3-D	33	Medium	210.84	79.21	72.26	12.98	1.84	18.63
t8-M1-1-D	33	High	218.68	89.74	91.25	18.10	3.10	28.54
t8-M1-2-D	33	High	358.26	132.43	65.99	13.25	2.05	21.86
t8-M1-3-D	33	High	471.23	174.19	86.80	17.43	2.69	28.78
t16-M3-1-D	41	Low	99.33	42.96	61.03	5.16	0.87	9.47
t16-M3-2-D	41	Low	368.15	137.59	125.20	14.09	0.87	26.26
t16-M3-3-D	41	Low	394.67	135.57	140.32	17.18	3.56	21.65
t16-M8-1-D	41	Medium	134.24	50.03	96.54	6.40	0.87	6.27
t16-M8-2-D	41	Medium	219.20	81.20	67.79	6.32	0.87	9.11
t16-M8-3-D	41	Medium	174.98	65.92	116.53	7.86	1.72	13.83
t16-M1-1-D	41	High	131.40	44.99	42.05	5.60	0.99	7.97
t16-M1-2-D	41	High	220.86	76.06	61.74	6.05	1.14	10.92
t16-M1-3-D	41	High	351.74	116.18	73.43	18.11	4.18	24.36

Sample	Day	Treatment	C2-BNT	C3-BNT	C4-BNT	C0-CHY	C1-CHY	C2-CHY
t1-M3-1-D	26	Low	701.59	107.34	307.90	64.05	493.28	7249.71
t1-M3-3-D	26	Low	12.64	38.52	65.34	81.68	302.04	2714.69
t1-M8-1-D	26	Medium	22.29	40.25	30.20	73.89	158.27	946.30
t1-M8-2-D	26	Medium	19.53	24.16	20.91	69.98	192.65	606.08
t1-M8-3-D	26	Medium	0.87	45.92	73.88	91.74	755.80	2712.84
t1-M1-1-D	26	High	15.25	22.70	21.99	61.03	186.65	825.07
t1-M1-2-D	26	High	16.98	10.82	14.31	63.20	195.04	286.36
t1-M1-3-D	26	High	32.34	24.07	30.70	96.34	367.49	936.29
t2-M3-1-D	27	Low	381.24	74.97	200.53	53.87	293.75	4818.10
t2-M3-2-D	27	Low	57.25	60.22	99.01	105.09	549.94	3269.11
t2-M3-3-D	27	Low	15.46	21.38	29.60	55.89	331.27	881.96
t2-M8-1-D	27	Medium	1067.72	103.33	404.56	95.41	664.67	8123.69
t2-M8-2-D	27	Medium	24.14	41.51	62.28	90.86	279.75	2416.63
t2-M8-3-D	27	Medium	20.10	21.67	24.10	55.26	207.16	1235.30
t2-M1-1-D	27	High	18.06	28.65	46.94	77.86	263.75	1841.25
t2-M1-2-D	27	High	20.04	13.45	16.41	79.04	218.38	390.86
t2-M1-3-D	27	High	22.85	18.52	17.81	106.22	223.44	468.94
t4-M4-1-D	29	Control	494.07	36.24	164.62	8.53	203.54	3623.01
t4-M3-1-D	29	Low	13.96	24.26	57.17	59.74	154.63	724.89
t4-M3-2-D	29	Low	14.11	28.34	22.57	45.31	172.82	1012.80
t4-M3-3-D	29	Low	0.87	8.25	15.00	57.43	135.81	308.24
t4-M8-1-D	29	Medium	31.93	67.87	93.88	133.06	377.10	3599.26
t4-M8-2-D	29	Medium	18.89	50.97	37.48	69.63	249.25	1611.54
t4-M8-3-D	29	Medium	12.92	17.30	13.82	59.09	101.84	568.31
t4-M1-1-D	29	High	20.31	37.19	27.01	92.35	293.05	1283.86
t4-M1-2-D	29	High	14.62	18.47	14.58	58.78	173.94	611.85
t4-M1-3-D	29	High	0.87	28.87	45.41	91.85	345.03	1605.29
t8-M3-1-D	33	Low	0.87	13.44	17.95	43.39	199.75	479.15
t8-M3-2-D	33	Low	0.87	19.86	30.12	49.32	202.11	922.02
t8-M3-3-D	33	Low	0.87	15.51	18.29	29.83	106.09	831.82
t8-M8-1-D	33	Medium	18.78	20.22	16.40	53.53	164.59	513.60
t8-M8-1-D	33	Medium	39.68	77.22	160.29	99.02	624.64	4356.81
t8-M8-3-D	33	Medium	11.27	23.37	28.85	55.93	168.65	947.30
t8-M1-1-D	33	High	14.57	21.65	20.66	53.81	226.40	618.28
t8-M1-2-D	33	High	8.71	16.42	31.91	55.40	145.43	1017.14
t8-M1-3-D	33	High	12.25	20.83	41.97	73.36	191.29	1337.87
t16-M3-1-D	41	Low	5.66	26.02	38.19	29.38	154.80	1153.55
t16-M3-2-D	41	Low	16.23	35.40	53.07	60.35	351.87	2035.30
t16-M3-3-D	41	Low	15.69	42.78	77.96	66.02	414.95	2669.58
t16-M8-1-D	41	Medium	171.72	30.48	87.64	30.09	226.52	2423.83
t16-M8-2-D	41	Medium	0.87	16.15	17.42	25.34	153.96	701.36
t16-M8-3-D	41	Medium	7.79	29.58	43.99	25.84	380.63	1264.45
t16-M1-1-D	41	High	0.87	11.28	23.06	28.01	109.09	821.96
t16-M1-2-D	41	High	1.99	12.26	14.75	26.10	146.82	502.69
t16-M1-3-D	41	High	12.30	9.62	24.94	46.40	237.86	421.12

Sample	Day	Treatment	C3-CHY	BaA	BbF+BkF	BaP	BeP	BP
t1-M3-1-D	26	Low	531.43	5.26	47.80	38.95	11.30	0.71
t1-M3-3-D	26	Low	234.61	7.30	8.81	23.59	15.73	0.71
t1-M8-1-D	26	Medium	158.53	6.59	5.73	5.16	7.75	0.71
t1-M8-2-D	26	Medium	195.28	4.60	4.91	10.50	5.81	0.71
t1-M8-3-D	26	Medium	370.30	7.22	16.36	24.55	11.13	0.71
t1-M1-1-D	26	High	114.05	5.13	2.65	6.65	4.75	0.71
t1-M1-2-D	26	High	89.93	4.73	4.99	4.99	6.79	0.71
t1-M1-3-D	26	High	184.54	7.37	3.81	6.58	7.10	0.71
t2-M3-1-D	27	Low	309.02	3.72	12.80	36.95	7.80	0.71
t2-M3-2-D	27	Low	366.58	6.24	4.10	32.84	9.30	0.71
t2-M3-3-D	27	Low	126.57	5.29	7.31	9.24	6.45	0.71
t2-M8-1-D	27	Medium	457.50	6.74	28.33	75.85	12.26	0.71
t2-M8-2-D	27	Medium	305.07	4.94	2.84	12.92	11.89	0.71
t2-M8-3-D	27	Medium	117.06	3.62	3.89	4.83	4.24	0.71
t2-M1-1-D	27	High	191.86	4.20	5.44	11.64	7.89	0.71
t2-M1-2-D	27	High	115.09	10.31	5.94	7.06	8.18	0.71
t2-M1-3-D	27	High	113.15	7.86	2.57	6.04	8.86	0.71
t4-M4-1-D	29	Control	140.71	0.87	12.02	84.11	7.93	0.41
t4-M3-1-D	29	Low	196.20	3.25	1.86	26.61	5.42	0.71
t4-M3-2-D	29	Low	128.99	3.25	3.46	5.16	3.99	0.71
t4-M3-3-D	29	Low	109.84	4.37	13.50	6.49	5.45	0.71
t4-M8-1-D	29	Medium	469.86	12.72	12.06	20.47	13.46	0.71
t4-M8-2-D	29	Medium	258.02	5.66	1.33	18.09	6.74	0.71
t4-M8-3-D	29	Medium	112.55	3.89	1.79	8.35	8.35	0.71
t4-M1-1-D	29	High	174.82	6.08	2.78	6.32	8.85	0.71
t4-M1-2-D	29	High	124.07	4.07	2.04	7.66	6.64	0.71
t4-M1-3-D	29	High	177.06	6.25	4.55	11.70	10.07	0.71
t8-M3-1-D	33	Low	145.73	5.01	1.68	10.35	6.16	0.71
t8-M3-2-D	33	Low	216.90	4.39	3.47	9.31	4.98	0.71
t8-M3-3-D	33	Low	100.51	2.94	2.91	8.88	5.17	0.71
t8-M8-1-D	33	Medium	98.06	6.53	4.85	8.09	10.51	0.71
t8-M8-1-D	33	Medium	768.95	8.23	9.29	32.53	18.59	0.41
t8-M8-3-D	33	Medium	126.50	5.24	6.36	7.22	4.64	0.71
t8-M1-1-D	33	High	146.40	3.32	2.90	8.71	6.25	0.71
t8-M1-2-D	33	High	147.99	5.24	4.02	10.72	6.57	0.71
t8-M1-3-D	33	High	195.15	6.24	4.90	32.95	15.94	0.71
t16-M3-1-D	41	Low	158.35	3.56	1.33	9.41	4.28	0.71
t16-M3-2-D	41	Low	240.49	13.96	9.56	10.43	9.91	0.71
t16-M3-3-D	41	Low	361.39	4.59	1.33	27.33	8.23	0.71
t16-M8-1-D	41	Medium	178.70	3.23	2.07	16.54	6.16	0.71
t16-M8-2-D	41	Medium	145.75	3.44	3.31	5.94	2.97	0.71
t16-M8-3-D	41	Medium	195.93	3.20	1.33	11.36	3.41	0.71
t16-M1-1-D	41	High	96.46	2.45	1.43	5.74	3.55	0.71
t16-M1-2-D	41	High	96.32	2.88	3.36	4.67	3.18	0.71
t16-M1-3-D	41	High	63.52	8.24	1.33	6.18	6.41	0.71

Sample	Day	Treatment	IP	DA	TPACs
t1-M3-1-D	26	Low	18.14	0.39	17610.98
t1-M3-3-D	26	Low	0.79	0.39	23206.35
t1-M8-1-D	26	Medium	0.79	0.39	10479.09
t1-M8-2-D	26	Medium	0.79	0.39	14938.89
t1-M8-3-D	26	Medium	0.79	0.39	29635.74
t1-M1-1-D	26	High	0.79	0.39	17336.37
t1-M1-2-D	26	High	0.79	0.39	25348.92
t1-M1-3-D	26	High	0.79	0.39	21575.84
t2-M3-1-D	27	Low	0.79	0.39	12845.83
t2-M3-2-D	27	Low	0.79	0.39	19597.22
t2-M3-3-D	27	Low	0.79	0.39	6575.13
t2-M8-1-D	27	Medium	0.79	0.39	21293.10
t2-M8-2-D	27	Medium	0.79	0.39	13072.01
t2-M8-3-D	27	Medium	0.79	0.39	11255.22
t2-M1-1-D	27	High	0.79	0.39	16291.25
t2-M1-2-D	27	High	0.79	0.39	18264.93
t2-M1-3-D	27	High	0.79	0.39	20363.16
t4-M4-1-D	29	Control	0.79	0.39	3478.45
t4-M3-1-D	29	Low	0.79	0.39	9776.70
t4-M3-2-D	29	Low	0.79	0.39	8500.93
t4-M3-3-D	29	Low	0.79	0.39	11174.28
t4-M8-1-D	29	Medium	0.79	0.39	16368.97
t4-M8-2-D	29	Medium	0.79	0.39	10776.49
t4-M8-3-D	29	Medium	0.79	0.39	10520.58
t4-M1-1-D	29	High	0.79	0.39	16503.05
t4-M1-2-D	29	High	0.79	0.39	15039.87
t4-M1-3-D	29	High	0.79	0.39	13872.76
t8-M3-1-D	33	Low	0.79	0.39	6947.42
t8-M3-2-D	33	Low	0.79	0.39	14541.57
t8-M3-3-D	33	Low	0.79	0.39	17497.76
t8-M8-1-D	33	Medium	0.79	0.39	12211.11
t8-M8-1-D	33	Medium	0.79	0.39	35814.47
t8-M8-3-D	33	Medium	0.79	0.39	12475.21
t8-M1-1-D	33	High	0.79	0.39	10312.17
t8-M1-2-D	33	High	0.79	0.39	27928.27
t8-M1-3-D	33	High	0.79	0.39	25502.20
t16-M3-1-D	41	Low	0.79	0.39	6761.76
t16-M3-2-D	41	Low	0.79	0.39	21711.18
t16-M3-3-D	41	Low	0.79	0.39	18800.34
t16-M8-1-D	41	Medium	0.79	0.39	7722.91
t16-M8-2-D	41	Medium	0.79	0.39	9239.29
t16-M8-3-D	41	Medium	0.79	0.39	9469.63
t16-M1-1-D	41	High	0.79	0.39	9510.44
t16-M1-2-D	41	High	0.79	0.39	8237.52
t16-M1-3-D	41	High	0.79	0.39	19350.21

Table C.8: ΣParent and Σalkyl PACs (ng g^{-1}, ww lipid) in mussel tissue collected from the Control, Low, Medium, and High treatments during the uptake phase of the bioaccumulation study.

Sample	Day	Treatment	Parent (ng g^{-1}, ww lipid)	Alkyl (ng g^{-1}, ww lipid)	%Parent	%Alkyl
t0-A	0	—	86.36	810.26	9.63	90.37
t0-B	0	—	91.90	2529.23	3.51	96.49
t0-C	0	—	84.21	512.10	14.12	85.88
t2-M4-2	2	Control	95.74	2525.63	3.65	96.35
t2-M4-3	2	Control	94.78	2867.88	3.20	96.80
t2-M3-1	2	Low	275.16	7036.04	3.76	96.24
t2-M3-3	2	Low	266.15	8709.82	2.97	97.03
t2-M8-1	2	Medium	327.73	10098.65	3.14	96.86
t2-M8-2	2	Medium	354.35	10376.59	3.30	96.70
t2-M8-3	2	Medium	266.42	8781.76	2.94	97.06
t2-M1-1	2	High	425.33	11276.89	3.63	96.37
t2-M1-2	2	High	320.48	8382.63	3.68	96.32
t2-M1-3	2	High	335.06	10187.90	3.18	96.82
t5-M4-1	5	Control	115.21	1241.03	8.49	91.51
t5-M4-2	5	Control	122.91	5101.02	2.35	97.65
t5-M4-3	5	Control	80.64	1971.60	3.93	96.07
t5-M3-1	5	Low	342.14	8913.42	3.70	96.30
t5-M3-2	5	Low	288.11	6350.07	4.34	95.66
t5-M3-3	5	Low	378.52	10932.19	3.35	96.65
t5-M8-1	5	Medium	531.32	13250.33	3.86	96.14
t5-M8-3	5	Medium	388.29	15994.92	2.37	97.63
t5-M1-1	5	High	673.45	17748.17	3.66	96.34
t5-M1-2	5	High	486.64	12529.52	3.74	96.26
t5-M1-3	5	High	637.96	16825.78	3.65	96.35
t11-M4-1	11	Control	222.05	5351.79	3.98	96.02
t11-M4-2	11	Control	380.15	6447.09	5.57	94.43
t11-M4-3	11	Control	160.51	2158.72	6.92	93.08
t11-M3-1	11	Low	616.60	20095.13	2.98	97.02
t11-M3-2	11	Low	673.44	9542.58	6.59	93.41
t11-M8-1	11	Medium	613.10	21849.84	2.73	97.27
t11-M8-2	11	Medium	345.17	11644.69	2.88	97.12
t11-M1-1	11	High	535.13	18440.40	2.82	97.18
t11-M1-2	11	High	571.11	23718.25	2.35	97.65
t11-M1-3	11	High	521.47	19793.86	2.57	97.43
t20-M4-1	20	Control	73.28	5270.64	1.37	98.63
t20-M4-2	20	Control	65.98	1448.42	4.36	95.64
t20-M4-3	20	Control	64.97	1811.19	3.46	96.54
t20-M3-1	20	Low	693.64	23788.37	2.83	97.17
t20-M3-2	20	Low	645.10	24217.48	2.59	97.41
t20-M8-1	20	Medium	977.46	19493.55	4.77	95.23
t20-M8-2	20	Medium	715.41	20295.27	3.41	96.59
t20-M8-3	20	Medium	789.52	14697.74	5.10	94.90
t20-M1-1	20	High	1123.33	14968.98	6.98	93.02
t20-M1-2	20	High	654.60	33051.49	1.94	98.06
t20-M1-3	20	High	556.78	14944.83	3.59	96.41
t25-M4-1	25	Control	77.21	523.15	12.86	87.14
t25-M4-2	25	Control	61.75	1444.98	4.10	95.90
t25-M4-3	25	Control	101.25	603.60	14.36	85.64
t25-M3-1	25	Low	845.38	25645.73	3.19	96.81
t25-M3-2	25	Low	823.49	23075.36	3.45	96.55
t25-M3-3	25	Low	1056.24	31004.39	3.29	96.71
t25-M8-1	25	Medium	860.68	30513.15	2.74	97.26
t25-M8-2	25	Medium	1074.06	12096.82	8.15	91.85
t25-M8-3	25	Medium	743.24	32474.96	2.24	97.76
t25-M1-1	25	High	871.93	30030.26	2.82	97.18
t25-M1-2	25	High	1021.75	31579.00	3.13	96.87
t25-M1-3	25	High	594.06	19277.88	2.99	97.01

Table C.9: ΣParent and Σalkyl PACs (ng g^{-1}, ww lipid) in mussel tissue collected from the Control, Low, Medium, and High treatments during the depuration phase of the bioaccumulation study.

Sample	Day	Treatment	Parent (ng g^{-1}, ww lipid)	Alkyl (ng g^{-1}, ww lipid)	%Parent	%Alkyl
t1-M3-1-D	26	Low	580.59	17030.39	3.30	96.70
t1-M3-3-D	26	Low	698.36	22507.99	3.01	96.99
t1-M8-1-D	26	Medium	387.54	10091.56	3.70	96.30
t1-M8-2-D	26	Medium	524.59	14414.30	3.51	96.49
t1-M8-3-D	26	Medium	740.98	28894.76	2.50	97.50
t1-M1-1-D	26	High	460.82	16875.54	2.66	97.34
t1-M1-2-D	26	High	722.70	24626.21	2.85	97.15
t1-M1-3-D	26	High	669.30	20906.54	3.10	96.90
t2-M3-1-D	27	Low	496.23	12349.61	3.86	96.14
t2-M3-2-D	27	Low	524.30	19072.92	2.68	97.32
t2-M3-3-D	27	Low	306.53	6268.61	4.66	95.34
t2-M8-1-D	27	Medium	597.72	20695.38	2.81	97.19
t2-M8-2-D	27	Medium	409.30	12662.71	3.13	96.87
t2-M8-3-D	27	Medium	347.18	10908.04	3.08	96.92
t2-M1-1-D	27	High	485.78	15805.46	2.98	97.02
t2-M1-2-D	27	High	608.20	17656.73	3.33	96.67
t2-M1-3-D	27	High	647.30	19715.87	3.18	96.82
t4-M3-1-D	29	Low	317.80	9458.90	3.25	96.75
t4-M3-2-D	29	Low	314.44	8186.48	3.70	96.30
t4-M3-3-D	29	Low	388.81	10785.47	3.48	96.52
t4-M8-1-D	29	Medium	620.44	15748.53	3.79	96.21
t4-M8-2-D	29	Medium	326.53	10449.96	3.03	96.97
t4-M8-3-D	29	Medium	446.48	10074.10	4.24	95.76
t4-M1-1-D	29	High	698.71	15804.34	4.23	95.77
t4-M1-2-D	29	High	444.50	14595.37	2.96	97.04
t4-M1-3-D	29	High	625.99	13246.77	4.51	95.49
t8-M3-1-D	33	Low	276.41	6671.01	3.98	96.02
t8-M3-2-D	33	Low	455.17	14086.41	3.13	96.87
t8-M3-3-D	33	Low	601.46	16896.30	3.44	96.56
t8-M8-1-D	33	Medium	326.52	11884.59	2.67	97.33
t8-M8-1-D	33	Medium	453.50	12021.70	3.64	96.36
t8-M8-3-D	33	Medium	380.57	9931.60	3.69	96.31
t8-M1-1-D	33	High	525.94	27402.33	1.88	98.12
t8-M1-3-D	33	High	574.90	24927.30	2.25	97.75
t16-M3-1-D	41	Low	223.57	6538.19	3.31	96.69
t16-M3-2-D	41	Low	563.83	21147.35	2.60	97.40
t16-M3-3-D	41	Low	548.59	18251.76	2.92	97.08
t16-M8-1-D	41	Medium	253.01	7469.90	3.28	96.72
t16-M8-2-D	41	Medium	239.39	8999.90	2.59	97.41
t16-M8-3-D	41	Medium	279.29	9190.34	2.95	97.05
t16-M1-1-D	41	High	209.11	9301.33	2.20	97.80
t16-M1-2-D	41	High	267.13	7970.38	3.24	96.76
t16-M1-3-D	41	High	481.59	18868.62	2.49	97.51

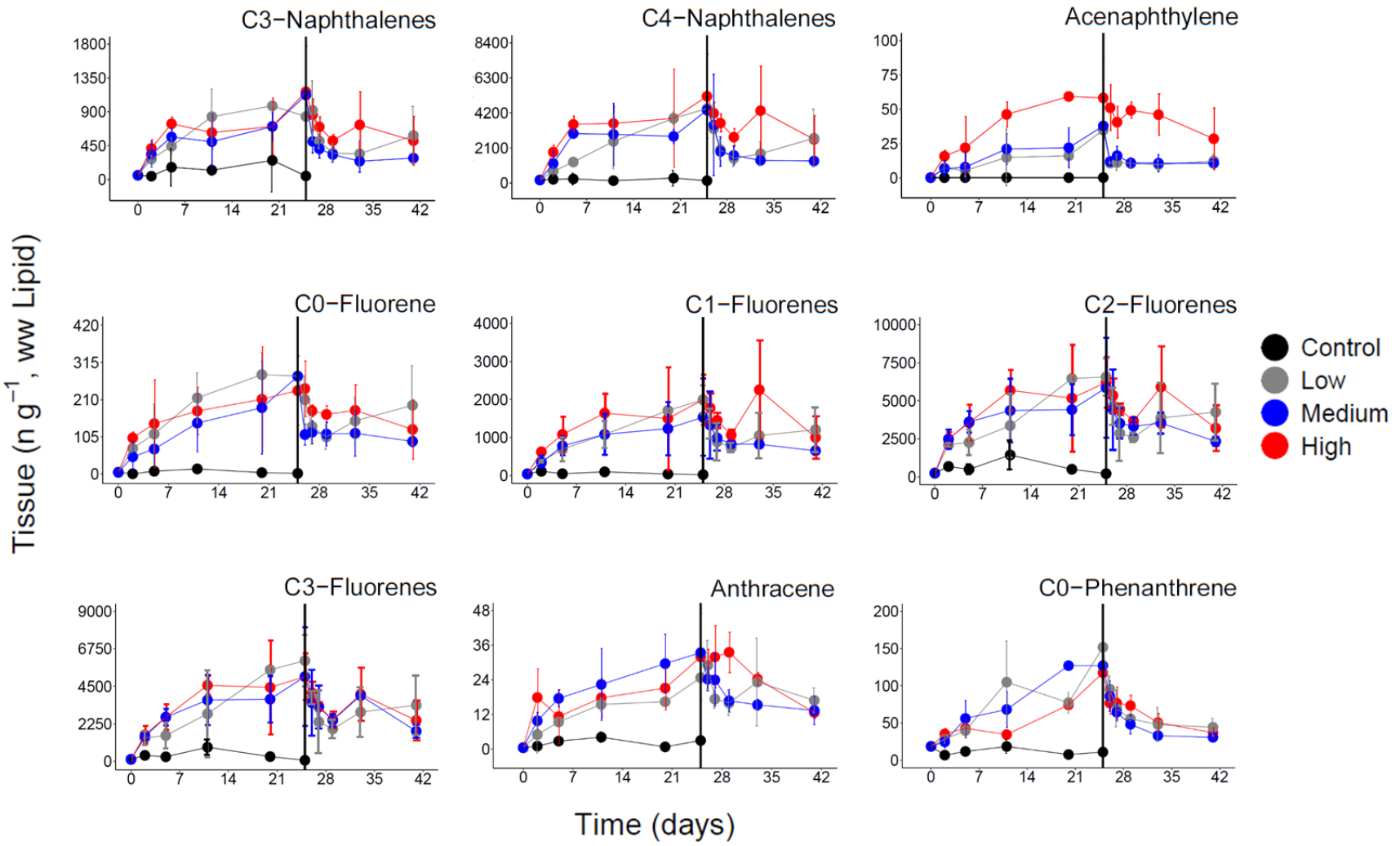

Figure C.1a: Mean (±SD) concentration (ng g^{-1}, ww Lipid) of the 29 PACs that accumulated in giant floater mussels throughout the 25 day uptake phase and the 16-day depuration phase. Samples in triplicate. Black line at day 25 denotes the end of the uptake phase and the start of the depuration phase.

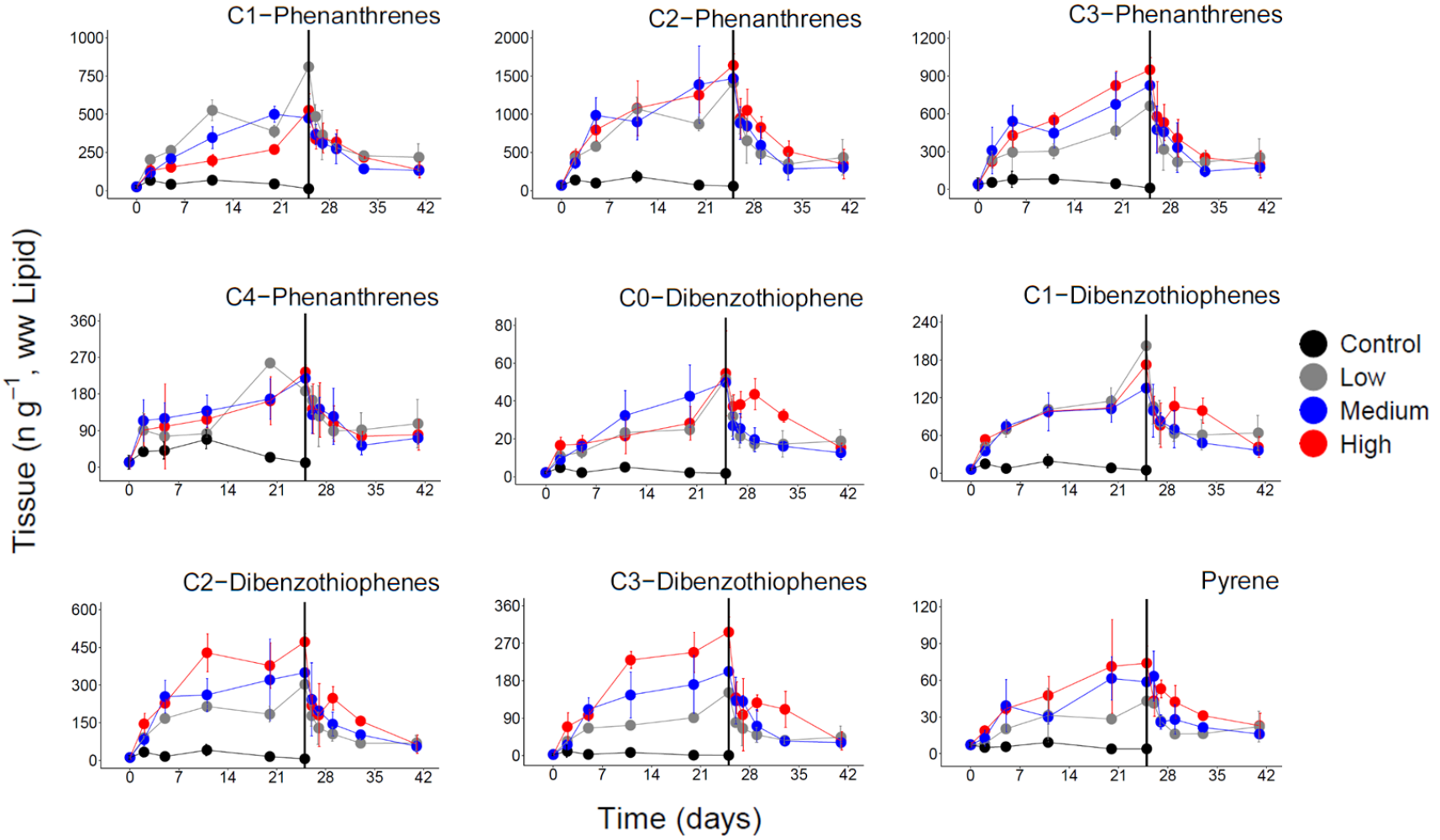

Figure C.1b: Mean (±SD) concentration (ng g^{-1}, ww Lipid) of the 29 PACs that accumulated in giant floater mussels throughout the 25 day uptake phase and the 16-day depuration phase. Samples in triplicate. Black line at day 25 denotes the end of the uptake phase and the start of the depuration phase.

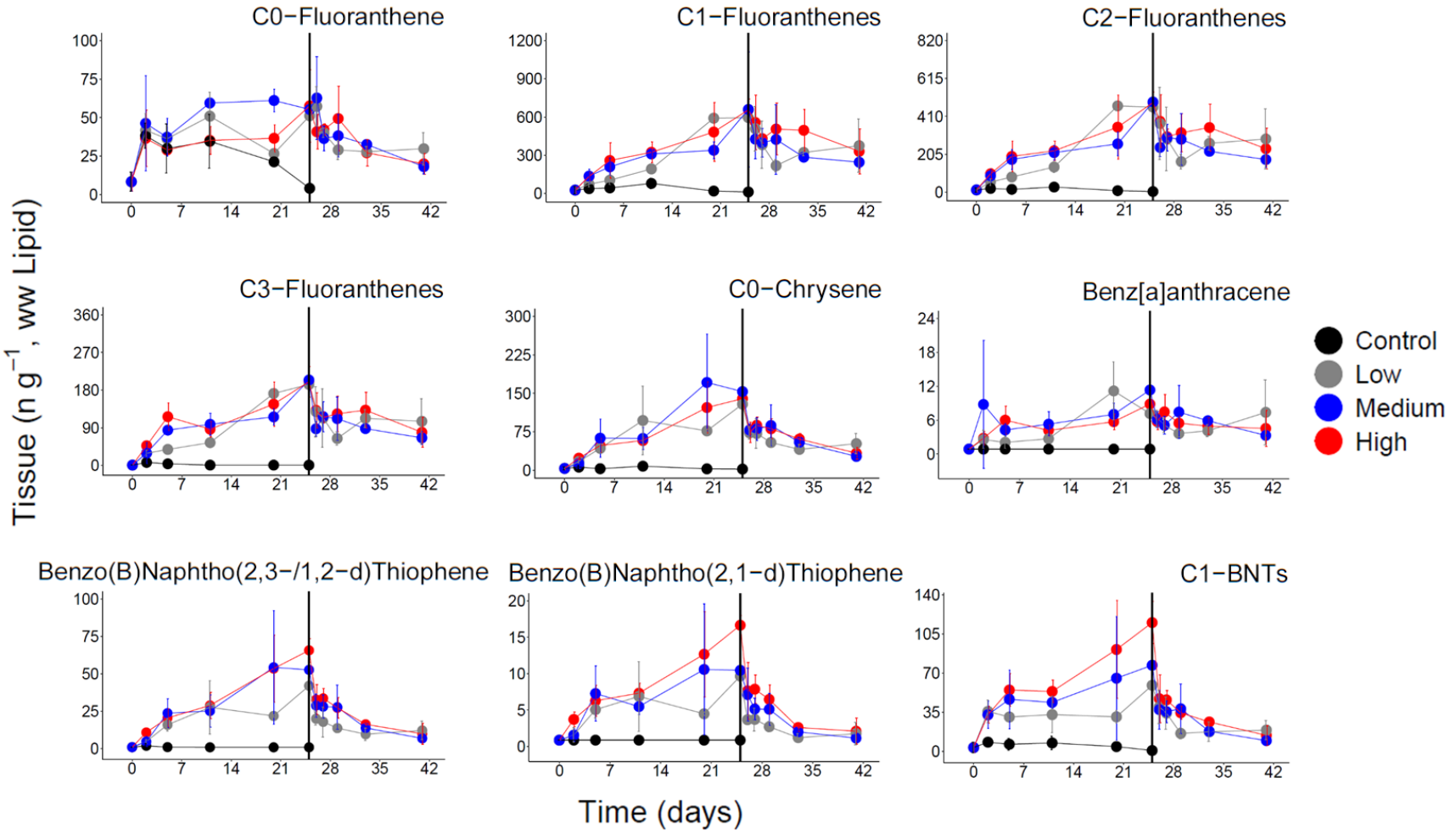

Figure C.1c: Mean (±SD) concentration (ng g^{-1}, ww Lipid) of the 29 PACs that accumulated in giant floater mussels throughout the 25 day uptake phase and the 16-day depuration phase. Samples in triplicate. Black line at day 25 denotes the end of the uptake phase and the start of the depuration phase.

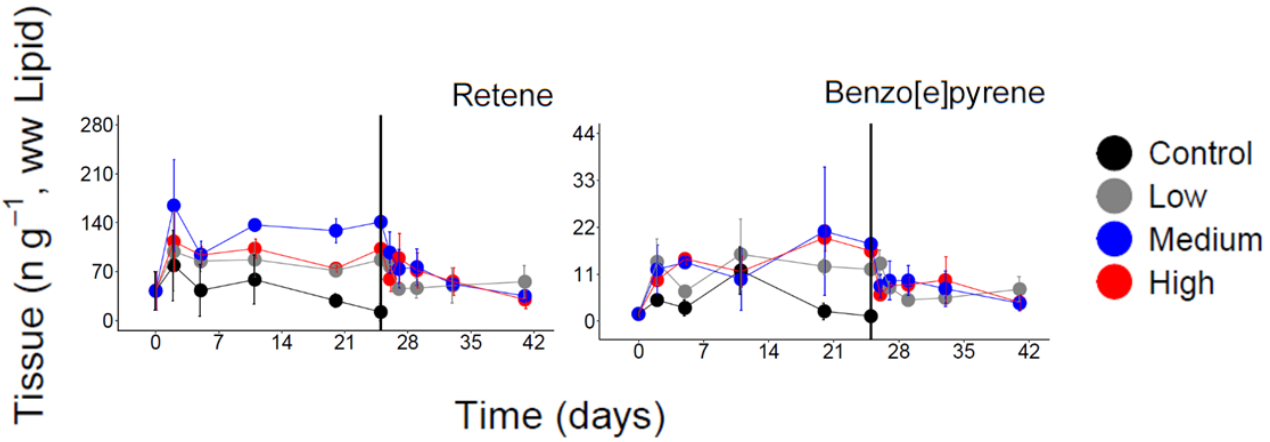

Figure C.1d: Mean (±SD) concentration (ng g^{-1}, ww Lipid) of the 29 PACs that accumulated in giant floater mussels throughout the 25 day uptake phase and the 16-day depuration phase. Samples in triplicate. Black line at day 25 denotes the end of the uptake phase and the start of the depuration phase.

Appendix D. PAC Toxicokinetic Parameters and Bioaccumulation Models

Table D.1: Uptake (k_1; L g^{-1} day^{-1}) and depuration (k_2; day^{-1}) rate constants of PACs that accumulated in giant floater mussels from the Low treatment. Bioaccumulation models and toxicokinetic parameters were determined by nonlinear curve fitting of the uptake phase using equation 3.Toxicokinetic parameters and their respective standard error (SE), as well as bioaccumulation models were determined using R studio. Abbreviations are found in Appendix A.

PAC	k_1	SE	k_2	SE	Bioaccumulation Model (Equation 3)
C3-NAP	2.23	0.65	0.16	0.06	y = 2.23 / 0.16 * 65.2 * (1 – e^(-0.16 * x))
C4-NAP	3.61	1.08	0.040	0.033	y = 3.61 / 0.040 * 78.4 * (1 - e^(-0.040 * x))
ACY	15.69	10.74	0.012	0.06	y = 15.69 / 0.012 * 0.891 * (1 - e^(-0.012 * x))
C0-FLU	6.85	1.74	0.10	0.04	y = 6.85 / 0.10 * 4.68 * (1 - e^(-0.10 * x))
C1-FLU	4.95	0.94	0.054	0.022	y = 4.95 / 0.054 * 28.9 * (1 - e^(-0.054 * x))
C2-FLU	11.22	2.74	0.060	0.030	y = 11.22 / 0.060 * 45.8 * (1 - e^(-0.060 * x))
C3-FLU	14.40	4.49	0.028	0.032	y = 14.40 / 0.028 * 23.7 * (1 - e^(-0.028 * x))
C0-DBT	0.98	0.33	0.0019	0.0302	y = 0.98 /0.0019 * 1.96 * (1 - e^(-0.0019 * x))
C1-DBT	0.62	0.15	0.046	0.027	y = 0.62 /0.046 * 19.6 * (1 - e^(-0.046 * x))
C2-DBT	7.07	1.50	0.19	0.05	y = 7.07 /0.19 * 7.05 * (1 - e^(-0.19 * x))
C3-DBT	5.13	1.25	0.076	0.032	y = 5.13 / 0.076* 2.31 * (1 - e^(-0.076 * x))
ANT	1.78	0.54	0.081	0.041	y = 1.78 / 0.081 * 1.17 * (1 - e^(-0.081 * x))
C0-PHE	1.85	0.66	0.059	0.043	y = 1.85 / 0.059 * 5.56 * (1 - e^(-0.059 * x))
C1-PHE	3.64	1.03	0.079	0.038	y = 3.64 / 0.079 * 17.5 * (1 - e^(-0.079 * x))
C2-PHE	7.25	1.56	0.13	0.04	y = 7.25 / 0.13 * 23.7 * (1 - e^(-0.13 * x))
C3-PHE	5.38	1.52	0.089	0.040	y = 5.38 / 0.089 * 11.0 * (1 - e^(-0.089 * x))
C4-PHE	6.49	2.42	0.072	0.048	y = 6.49 / 0.072 * 2.77 * (1 - e^(-0.072 * x))
RET	—	—	—	—	—
PYR	6.38	2.21	0.13	0.06	y = 6.38 / 0.13 * 0.806 * (1 - e^(-0.13 * x))
C0-FLA	104.55	$1.91x10^4$	4.46	813.77	y = 104.55 / 4.46 * 1.78 * (1 - e^(-4.46 * x))
C1-FLA	7.60	1.68	0.010	0.021	y = 7.60 / 0.010 * 3.63 * (1 - e^(-0.010 * x))
C2-FLA	4.31	1.04	0.010	0.022	y = 4.31 / 0.010 * 4.95 * (1 - e^(-0.010 * x))
C3-FLA	2.80	0.69	0.010	0.023	y = 2.80 / 0.010 * 3.08 * (1 - e^(-0.010 * x))
BNT23	2.14	0.68	0.080	0.043	y = 2.14 / 0.080 * 1.58 * (1 - e^(-0.080 * x))
BNT21	3.02	1.12	0.16	0.08	y = 3.02 / 0.16 * 0.435 * (1 - e^(-0.16 * x))
C1-BNT	12.93	10.34	0.87	0.73	y = 12.93 / 0.87 * 2.71 * (1 - e^(-0.87 * x))
C0-CHY	4.53	1.48	0.083	0.045	y = 4.53 / 0.083 * 2.44 * (1 - e^(-0.083 * x))
BaA	3.85	1.95	0.038	0.055	y = 3.85 / 0.038 * 0.138 * (1 - e^(-0.038 * x))
BeP	360.60	$1.65x10^{17}$	12.00	$5.51x10^{15}$	y = 360.60 / 12.00 * 0.667 * (1 - e^(-12.00 * x))

Table D.2: Uptake (k_1; L g^{-1} day^{-1}) and depuration (k_2; day^{-1}) rate constants of PACs that accumulated in giant floater mussels from the Medium treatment. Bioaccumulation models and toxicokinetic parameters were determined by nonlinear curve fitting of the uptake phase using equation 3.Toxicokinetic parameters and their respective standard error (SE), as well as bioaccumulation models, were determined using R studio. Abbreviations are found in Appendix A.

PAC	k_1	SE	k_2	SE	Bioaccumulation Model (Equation 3)
C3-NAP	2.31	0.87	0.11	0.07	y = 2.31 / 0.11 * 46.5 * (1 - e^(-0.11 * x))
C4-NAP	8.61	3.46	0.24	0.11	y = 8.61 / 0.24 * 97.5 * (1 - e^(-0.24 * x))
ACY	19.42	10.60	0.019	0.054	y = 19.42 / 0.019 * 0.0882 * (1 - e^(-0.019 * x))
C0-FLU	4.92	2.36	0.026	0.049	y = 4.92 / 0.026 * 2.83 * (1 - e^(-0.026 * x))
C1-FLU	6.12	3.20	0.13	0.09	y = 6.12 / 0.13 * 30.9 * (1 - e^(-0.13 * x))
C2-FLU	18.24	8.19	0.29	0.14	y = 18.24 / 0.29* 78.7 * (1 - e^(-0.29 * x))
C3-FLU	11.60	5.08	0.17	0.09	y = 11.60 / 0.17 * 66.0 * (1 - e^(-0.17 * x))
C0-DBT	2.60	0.76	0.067	0.037	y =2.60 / 0.067 * 1.55 * (1 - e^(-0.067 * x))
C1-DBT	1.11	0.30	0.16	0.05	y = 1.11 / 0.16 * 18.1 * (1 - e^(-0.16 * x))
C2-DBT	5.80	1.75	0.19	0.07	y = 5.80 / 0.19 * 11.0 * (1 - e^(-0.19 * x))
C3-DBT	5.08	1.44	0.12	0.04	y = 5.08 / 0.12* 4.65 * (1 - e^(-0.12 * x))
ANT	3.46	1.07	0.14	0.055	y = 3.46 / 0.14 * 1.37 * (1 - e^(-0.14 * x))
C0-PHE	2.59	0.55	0.070	0.027	y = 2.59 / 0.070 * 4.25 * (1 - e^(-0.070 * x))
C1-PHE	5.29	1.01	0.11	0.029	y = 5.29 / 0.11 * 10.7 * (1 - e^(-0.11 * x))
C2-PHE	6.82	1.77	0.15	0.049	y = 6.82 / 0.15 * 32.0 * (1 - e^(-0.15 * x))
C3-PHE	7.88	2.65	0.23	0.088	y = 7.88 / 0.23 * 20.5 * (1 - e^(-0.23 * x))
C4-PHE	13.96	4.99	0.37	0.14	y = 13.96 / 0.37 * 4.67 * (1 - e^(-0.37 * x))
RET	—	—	—	—	—
PYR	2.69	0.85	0.11	0.05	y = 2.69 / 0.11 * 2.66 * (1 - e^(-0.11 * x))
C0-FLA	22.72	11.82	0.78	0.43	y = 22.72 / 0.78 * 1.89 * (1 - e^(-0.78 * x))
C1-FLA	4.69	3.16	0.015	0.065	y = 4.69 / 0.015 * 5.92 * (1 - e^(-0.015 * x))
C2-FLA	2.93	1.93	0.014	0.063	y = 2.93 / 0.014 * 6.94 * (1 - e^(-0.014 * x))
C3-FLA	2.61	1.42	0.037	0.058	y = 2.61 / 0.037 * 4.18 * (1 - e^(-0.037 * x))
BNT23	2.07	1.05	0.049	0.058	y = 2.07 / 0.049 * 1.86 * (1 - e^(-0.049 * x))
BNT21	2.88	1.60	0.11	0.09	y = 2.88 / 0.11 * 0.425 * (1 - e^(-0.11 * x))
C1-BNT	3.81	1.93	0.23	0.13	y = 3.81 / 0.23 * 4.12 * (1 - e^(-0.23 * x))
C0-CHY	3.53	1.66	0.035	0.050	y = 3.53 / 0.035 * 2.85 * (1 - e^(-0.035 * x))
BaA	3.31	1.18	0.031	0.037	y = 3.31 / 0.031 * 0.177 * (1 - e^(-0.031* x))
BeP	14.23	9.58	0.55	0.40	y = 14.23 / 0.55 * 0.668 * (1 - e^(-0.55 * x))

Table D.3: Uptake (k_1; L g^{-1} day^{-1}) and depuration (k_2; day^{-1}) rate constants of PACs that accumulated in giant floater mussels from the High treatment. Bioaccumulation models and toxicokinetic parameters were determined by nonlinear curve fitting of the uptake phase using equation 3. Toxicokinetic parameters and their respective standard error (SE), as well as bioaccumulation models, were determined using R studio. Abbreviations are found in Appendix A.

PAC	k_1	SE	k_2	SE	Bioaccumulation Model (Equation 3)
C3-NAP	2.63	1.27	0.31	0.17	y = 2.63 / 0.31 * 103 * (1 - e^(-0.31 * x))
C4-NAP	4.40	1.95	0.27	0.14	y = 4.40 / 0.27 * 273 * (1 - e^(-0.27 * x))
ACY	29.83	13.91	0.10	0.07	y = 29.83 / 0.10 * 0.228 * (1 - e^(-0.10 * x))
C0-FLU	10.50	4.97	0.23	0.13	y = 10.50 / 0.23 * 4.75 * (1 - e^(-0.23 * x))
C1-FLU	5.43	2.30	0.20	0.10	y = 5.43 / 0.20 * 64.5 * (1 - e^(-0.20 * x))
C2-FLU	9.34	3.19	0.23	0.09	y = 9.34 / 0.23 * 143.3 * (1 - e^(-0.23 * x))
C3-FLU	12.34	3.80	0.18	0.07	y = 12.34 / 0.18 * 71.1* (1 - e^(-0.18 * x))
C0-DBT	1.26	0.56	0.019	0.045	y = 1.26 / 0.019 * 1.87 * (1 - e^(-0.019 * x))
C1-DBT	1.12	0.25	0.11	0.04	y = 1.12 / 0.11 * 15.1 * (1 - e^(-0.11 * x))
C2-DBT	5.33	0.90	0.18	0.04	y = 5.33 / 0.18 * 14.7 * (1 - e^(-0.18 * x))
C3-DBT	4.95	0.74	0.10	0.02	y = 4.95 / 0.10 * 6.19 * (1 - e^(-0.10 * x))
ANT	1.53	0.75	0.17	0.10	y = 1.53 / 0.17 * 2.82 * (1 - e^(-0.17 * x))
C0-PHE	0.91	0.33	0.0024	0.0334	y = 0.91 / 0.0024 * 4.86 * (1 - e^(-0.0024 * x))
C1-PHE	1.23	0.40	0.010	0.031	y = 1.23 / 0.010 * 16.7* (1 - e^(-0.010 * x))
C2-PHE	4.00	0.74	0.13	0.03	y = 4.00 / 0.13 * 50.6 * (1 - e^(-0.13 * x))
C3-PHE	3.01	0.41	0.088	0.019	y = 3.01 / 0.088 * 29.8 * (1 - e^(-0.088 * x))
C4-PHE	3.85	1.42	0.11	0.06	y = 3.85 / 0.11 * 5.97 * (1 - e^(-0.11 * x))
RET	—	—	—	—	—
PYR	2.56	0.75	0.11	0.05	y = 2.56 / 0.11 * 3.31 * (1 - e^(-0.11 * x))
C0-FLA	16.12	15.90	1.11	1.15	y = 16.12 / 1.11 * 2.75 * (1 - e^(-1.11 * x))
C1-FLA	4.87	1.39	0.056	0.035	y = 4.87 / 0.056 * 9.20 * (1 - e^(-0.056 * x))
C2-FLA	3.99	1.14	0.050	0.033	y = 3.99 / 0.050 * 7.78 * (1 - e^(-0.050 * x))
C3-FLA	5.65	1.69	0.11	0.05	y = 5.65 / 0.11 * 3.49 * (1 - e^(-0.11 * x))
BNT23	1.86	0.47	0.023	0.026	y = 1.86 / 0.023 * 1.82 * (1 - e^(-0.023 * x))
BNT21	2.00	0.53	0.041	0.030	y = 2.00 / 0.041 * 0.501 * (1 - e^(-0.041 * x))
C1-BNT	2.69	0.78	0.081	0.040	y = 2.69 / 0.081 * 3.67 * (1 - e^(-0.081 * x))
C0-CHY	2.04	0.52	0.026	0.027	y = 2.04 / 0.026 * 3.72 * (1 - e^(-0.026 * x))
BaA	7.35	3.05	0.29	0.14	y = 7.35 / 0.29 * 0.259 * (1 - e^(-0.29 * x))
BeP	13.58	3.68	0.44	0.13	y = 13.58 / 0.44 * 0.518 * (1 - e^(-0.44 * x))

Table D.4: Uptake (k_1; L g^{-1} day^{-1}) and depuration (k_2; day^{-1}) rate constants of PACs that accumulated in giant floater mussels from the Low treatment. Bioaccumulation models and toxicokinetic parameters were determined by sequential estimation using equation 3. Toxicokinetic parameters and their respective standard error (SE), as well as bioaccumulation models, were determined using R studio. Abbreviations are found in Appendix A.

PAC	k_1	SE	k_2	SE	Bioaccumulation Model (Equation 3)
C3-NAP	1.89	0.15	0.12	0.04	y = 1.89 / 0.12 * 65.2 * (1 - e^(-0.12 * x))
C4-NAP	3.15	0.23	0.026	0.025	y = 3.15 / 0.026 * 78.4 * (1 - e^(-0.026 * x))
ACY	—	—	—	—	—
C0-FLU	5.59	0.38	0.075	0.043	y = 5.59 / 0.075 * 4.68 * (1 - e^(-0.075 * x))
C1-FLU	5.96	0.29	0.079	0.052	y= 5.96 / 0.079 * 28.9 * (1 - e^(-0.079 * x))
C2-FLU	11.57	0.71	0.064	0.053	y = 11.57 /0.064 * 45.8 * (1 - e^(-0.064 * x))
C3-FLU	21.27	1.67	0.076	0.058	y = 21.27 / 0.076 * 23.7 * (1 - e^(-0.076 * x))
C0-DBT	1.48	0.11	0.045	0.019	y = 1.48 / 0.045 * 1.96 * (1 - e^(-0.045 * x))
C1-DBT	0.66	0.04	0.053	0.021	y = 0.66 / 0.053 * 19.6 * (1 - e^(-0.053 * x))
C2-DBT	6.24	0.34	0.16	0.03	y = 6.24 / 0.16 * 7.05 * (1 - e^(-0.16 * x))
C3-DBT	4.85	0.30	0.068	0.024	y = 4.85 / 0.068 * 2.31 * (1 - e^(-0.068 * x))
ANT	2.36	0.19	0.13	0.06	y = 2.36 / 0.13 * 1.17 * (1 - e^(-0.13 * x))
C0-PHE	1.89	0.17	0.062	0.017	y = 1.89 / 0.062 * 5.56 * (1 - e^(-0.062 * x))
C1-PHE	3.33	0.24	0.067	0.017	y = 3.33 / 0.067 * 17.5 * (1 - e^(-0.067 * x))
C2-PHE	8.41	0.49	0.16	0.03	y = 8.41 / 0.16 * 23.7 * (1 - e^(-0.16 * x))
C3-PHE	4.11	0.31	0.054	0.023	y = 4.11 / 0.054 * 11.0 * (1 - e^(-0.054 * x))
C4-PHE	7.50	0.72	0.092	0.035	y = 7.50 / 0.092 * 2.77 * (1 - e^(-0.092 * x))
RET	9.26	1.44	0.17	0.05	y = 9.26 / 0.17 * 1.86 * (1 - e^(-0.17 * x))
PYR	6.31	0.58	0.13	0.03	y = 6.31 / 0.13 * 0.806 * (1 - e^(-0.13 * x))
C0-FLA	4.64	0.55	0.16	0.03	y = 4.64 / 0.16 * 1.78 * (1 - e^(-0.16 * x))
C1-FLA	8.80	0.46	0.025	0.020	y = 8.80 / 0.025 * 3.63 * (1 - e^(-0.025 * x))
C2-FLA	4.85	0.27	0.022	0.022	y = 4.85 / 0.022 * 4.95 * (1 - e^(-0.022 * x))
C3-FLA	3.17	0.18	0.022	0.022	y = 3.17 / 0.022 * 3.08 * (1 - e^(-0.022 * x))
BNT23	1.91	0.16	0.065	0.023	y = 1.91 / 0.065 * 1.58 * (1 - e^(-0.065 * x))
BNT21	3.99	0.39	0.23	0.03	y = 3.99 / 0.23 * 0.435 * (1 - e^(-0.23 * x))
C1-BNT	5.27	0.52	0.32	0.06	y = 5.27 / 0.32 * 2.71 * (1 - e^(-0.32 * x))
C0-CHY	5.92	0.51	0.13	0.03	y = 5.92 / 0.13 * 2.44 * (1 - e^(-0.13 * x))
BaA	5.04	0.62	0.071	0.024	y = 5.04 / 0.071 * 0.138 * (1 - e^(-0.07 * x))
BeP	6.13	0.71	0.31	0.06	y = 6.13 / 0.31 * 0.668 * (1 - e^(-0.31 * x))

Table D.5: Uptake (k_1; L g^{-1} day^{-1}) and depuration (k_2; day^{-1}) rate constants of PACs that accumulated in giant floater mussels from the Medium treatment. Bioaccumulation models and toxicokinetic parameters were determined by sequential estimation using equation 3. Toxicokinetic parameters and their respective standard error (SE), as well as bioaccumulation models, were determined using R studio. Abbreviations are found in Appendix A.

PAC	k_1	SE	k_2	SE	Bioaccumulation Model (Equation 3)
C3-NAP	3.33	0.30	0.18	0.04	y = 3.33 / 0.18 * 46.5 * (1 - e^(-0.18 * x))
C4-NAP	8.84	0.82	0.23	0.10	y = 8.84 / 0.23 * 94.0 * (1 - e^(-0.23 * x))
ACY	—	—	—	—	—
C0-FLU	7.84	0.82	0.082	0.046	y= 7.84 / 0.082 * 2.83 * (1 - e^(-0.082 * x))
C1-FLU	4.99	0.62	0.10	0.11	y = 4.99 / 0.10 * 30.9 * (1 - e^(-0.10 * x))
C2-FLU	7.75	0.88	0.10	0.09	y = 7.75 / 0.10 * 78.7 * (1 - e^(-0.10 * x))
C3-FLU	9.41	0.99	0.13	0.09	y = 9.41 / 0.13 * 66.0 * (1 - e^(-0.13 * x))
C0-DBT	2.60	0.17	0.067	0.015	y = 2.60 / 0.067 * 1.55 * (1 - e^(-0.067 * x))
C1-DBT	0.86	0.056	0.12	0.03	y = 0.86 / 0.12 * 18.1 * (1 - e^(-0.12 * x))
C2-DBT	4.69	0.34	0.14	0.03	y = 4.69 / 0.14 * 11.0 * (1 - e^(-0.14 * x))
C3-DBT	4.86	0.33	0.11	0.02	y = 5.86 / 0.11 * 4.65 * (1 - e^(-0.11 * x))
ANT	3.82	0.28	0.16	0.06	y = 3.82 / 0.16 * 1.31 * (1 - e^(-0.16 * x))
C0-PHE	2.74	0.13	0.077	0.014	y = 2.74 / 0.077 * 4.25 * (1 - e^(-0.077 * x))
C1-PHE	6.39	0.30	0.14	0.02	y =6.39 / 0.14 * 10.7 * (1 - e^(-0.14 * x))
C2-PHE	8.51	0.54	0.20	0.03	y = 8.51 / 0.20 * 32.0 * (1 - e^(-0.20 * x))
C3-PHE	3.83	0.33	0.087	0.019	y = 3.83 / 0.087 * 20.3 * (1 - e^(-0.087 * x))
C4-PHE	6.81	0.57	0.16	0.04	y = 6.81 / 0.16 * 4.67 * (1 - e^(-0.16 * x))
RET	6.02	0.66	0.11	0.03	y = 6.02 / 0.11 * 2.97 * (1 - e^(-0.11 * x))
PYR	3.06	0.23	0.14	0.04	y = 3.06 / 0.14 * 2.66 * (1 - e^(-0.14 * x))
C0-FLA	4.45	0.50	0.12	0.06	y = 4.45 / 0.12 * 1.89 * (1 - e^(-0.12 * x))
C1-FLA	5.97	0.83	0.041	0.021	y = 5.97 / 0.041 * 5.92 * (1 - e^(-0.041 * x))
C2-FLA	3.66	0.50	0.037	0.020	y = 3.66 / 0.037 * 6.94 * (1 - e^(-0.037 * x))
C3-FLA	2.75	0.32	0.043	0.018	y = 2.75 / 0.043 * 4.18 * (1 - e^(-0.043 * x))
BNT23	3.25	0.38	0.11	0.01	y = 3.25 / 0.11 * 1.86 * (1 - e^(-0.11 * x))
BNT21	3.28	0.43	0.13	0.02	y = 3.28 / 0.13 * 0.425 * (1 - e^(-0.13 * x))
C1-BNT	2.14	0.26	0.11	0.02	y = 2.14 / 0.11 * 4.12 * (1 - e^(-0.11 * x))
C0-CHY	5.40	0.57	0.089	0.013	y = 5.40 / 0.089 * 2.85 * (1 - e^(-0.089 * x))
BaA	3.99	0.30	0.052	0.016	y = 3.99 / 0.052 * 0.177 * (1 - e^(-0.052 * x))
BeP	9.98	1.28	0.37	0.18	y = 9.98 / 0.37 * 0.668 * (1 - e^(-0.37 * x))

Table D.6: Uptake (k_1; L g^{-1} day^{-1}) and depuration (k_2; day^{-1}) rate constants of PACs that accumulated in giant floater mussels from the High treatment. Bioaccumulation models and toxicokinetic parameters were determined by sequential estimation using equation 3. Toxicokinetic parameters and their respective standard error (SE), as well as bioaccumulation models, were determined using R studio. Abbreviations are found in Appendix A.

PAC	k_1	SE	k_2	SE	Bioaccumulation Model (Equation 3)
C3-NAP	1.67	0.18	0.18	0.06	y = 1.67 / 0.18 * 103 * (1 - e^(-0.18 * x))
C4-NAP	2.58	0.28	0.14	0.05	y = 2.58 / 0.14 * 273 * (1 - e^(-0.14 * x))
ACY	19.22	2.42	0.045	0.018	y = 19.22 / 0.045 * 0.228 * (1 - e^(-0.045 * x))
C0-FLU	4.90	0.61	0.081	0.057	y = 4.90 / 0.081 * 4.75 * (1 - e^(-0.081 * x))
C1-FLU	4.45	0.47	0.15	0.04	y = 4.45 / 0.15 * 64.5 * (1 - e^(-0.15 * x))
C2-FLU	5.81	0.51	0.13	0.03	y = 5.81 / 0.13 * 143.3 * (1 - e^(-0.13 * x))
C3-FLU	12.17	0.95	0.17	0.03	y = 12.17 / 0.17 * 71.1 * (1 - e^(-0.17 * x))
C0-DBT	1.87	0.20	0.065	0.011	y = 1.87 / 0.065 * 1.87 * (1 - e^(-0.065 * x))
C1-DBT	0.82	0.05	0.065	0.017	y = 0.82 / 0.065 * 15.1 * (1 - e^(-0.065 * x))
C2-DBT	3.51	0.18	0.10	0.02	y = 3.51 / 0.10 * 14.7 * (1 - e^(-0.10 * x))
C3-DBT	4.43	0.17	0.081	0.067	y = 4.43 / 0.081 * 6.19 * (1 - e^(-0.081 * x))
ANT	0.94	0.12	0.081	0.010	y = 0.94 / 0.081 * 2.82 * (1 - e^(-0.081 * x))
C0-PHE	1.56	0.13	0.062	0.010	y = 1.56 / 0.062 * 4.86 * (1 - e^(-0.062 * x))
C1-PHE	2.13	0.18	0.075	0.011	y = 2.13 / 0.075 * 16.7 * (1 - e^(-0.075 * x))
C2-PHE	3.83	0.18	0.13	0.02	y = 3.8 / 0.13 * 50.6 * (1 - e^(-0.13 * x))
C3-PHE	3.09	0.11	0.092	0.017	y = 3.09 / 0.092 * 29.8 * (1 - e^(-0.092 * x))
C4-PHE	4.18	0.40	0.12	0.03	y = 4.18 / 0.12 * 5.97 * (1 - e^(-0.12 * x))
RET	2.80	0.52	0.067	0.017	y = 2.80 / 0.067 * 3.55 * (1 - e^(-0.067 * x))
PYR	2.22	0.17	0.086	0.024	y = 2.22 / 0.086 * 3.31 * (1 - e^(-0.086 * x))
C0-FLA	1.71	0.21	0.074	0.032	y = 1.71 / 0.074 * 2.75 * (1 - e^(-0.074 * x))
C1-FLA	4.17	0.30	0.037	0.015	y = 4.17 / 0.037 * 9.20 * (1 - e^(-0.037 * x))
C2-FLA	3.55	0.26	0.036	0.014	y = 3.55 / 0.036 * 7.78 * (1 - e^(-0.036 * x))
C3-FLA	3.56	0.29	0.043	0.014	y = 3.56 / 0.043 * 3.49 * (1 - e^(-0.043 * x))
BNT23	3.55	0.26	0.11	0.02	y = 3.55 / 0.11 * 1.82 * (1 - e^(-0.11 * x))
BNT21	3.60	0.27	0.13	0.02	y = 3.60 / 0.13 * 0.501 * (1 - e^(-0.13 * x))
C1-BNT	3.20	0.24	0.11	0.02	y = 3.20 / 0.11 * 3.67 * (1 - e^(-0.11 * x))
C0-CHY	3.00	0.20	0.073	0.011	y = 3.00 / 0.073 * 3.72 * (1 - e^(-0.073 * x))
BaA	3.00	0.31	0.088	0.065	y = 3.01 / 0.088 * 0.259 * (1 - e^(-0.088 * x))
BeP	10.88	0.59	0.34	0.15	y = 10.88 / 0.34 * 0.518 * (1 - e^(-0.34 * x))

Table D.7: Model accuracy metrics, including residual standard error (Sigma), Bayesian Information Criteria (BIC), and Akaike's Information Criteria (AIC) for PAC bioaccumulation models from the Low treatments. Bioaccumulation models were determined by nonlinear curve fitting of the accumulation phase (Model 1) using equation 3 and by sequential estimation (Model 2) using equation 3. Model accuracy metrics were determined using R studio. The PAC bioaccumulation models that best fit the accumulation phase were determined by ANOVA analyses in R studio and by comparing model accuracy metrics. Abbreviations are found in Appendix A.

PAC	Model	Sigma	AIC	BIC	ANOVA Analysis					Winner
					Res. DF	Res. Sum. Sq.	Sum. Sq.	F-value	Pr(>F)	
C3-NAP	2	191	203	204	14	509838				✓
	1	195	205	207	13	494654	15184	0.40	0.54	
C4-NAP	2	757	244	246	14	8029636				✓
	1	780	246	248	13	7903245	126391	0.21	0.66	
ACY	2	—	—	—	—	—				
	1	10.6	117	119	—	—	—	—	—	✓
C0-FLU	2	49.6	163	164	14	34510				✓
	1	50.2	164	166	13	32756	0.70	0.70	0.42	
C1-FLU	2	229	209	210	14	732076				✓
	1	229	209	212	13	679836	52240	1.00	0.34	
C2-FLU	2	978	252	254	14	13394419				✓
	1	1014	254	256	13	13378618	15800	0.02	0.90	
C3-FLU	2	1089	255	257	14	16608918				
	1	1058	255	257	13	14548247	2060672	1.84	0.20	✓
C0-DBT	2	7.6	107	108	14	843.3				✓
	1	7.7	108	110	13	770.0	73.29	1.24	0.29	
C1-DBT	2	24.7	142	143	14	8509.5				✓
	1	25.5	144	146	13	8473.7	35.79	35.79	0.82	
C2-DBT	2	39.5	156	157	14	21796				✓
	1	40.5	157	160	13	21320	476.40	0.29	0.60	
C3-DBT	2	20.4	136	137	14	5839.1				✓
	1	21.2	138	140	13	5822.5	16.61	0.04	0.85	
ANT	2	4.5	90.4	91.8	14	277.9				✓
	1	4.5	91.5	93.6	13	261.7	16.23	0.81	0.39	
C0-PHE	2	28	146	148	14	11487				✓
	1	29	148	150	13	1148	2.00	0	0.96	
C1-PHE	2	125	190	192	14	218606				✓
	1	129	192	194	13	217294	1311.40	0.08	0.78	
C2-PHE	2	190	203	204	14	503859				✓
	1	194	204	207	13	487681	16179	0.43	0.52	
C3-PHE	2	112	187	188	14	174899				✓
	1	113	188	190	13	167365	7534.10	0.59	0.46	
C4-PHE	2	48.8	162	164	14	33383				✓

PAC	Model	Sigma	AIC	BIC	ANOVA Analysis					Winner
					Res. DF	Res. Sum. Sq.	Sum. Sq.	F-value	Pr(>F)	
RET	1	50.4	164	166	13	32973	409.39	0.16	0.69	
	2	42.9	158	160	—	—				✓
PYR	1	—	—	—	—	—	—	—	—	
	2	9.26	112	114	14	1199.6				✓
C0-FLA	1	9.61	114	116	13	1199.5	0.08	0.00	0.98	
	2	16.3	129	131	—	—				✓
C1-FLA	1	—	—	—	—	—	—	—	—	
	2	71.0	173	175	14	70659				✓
C2-FLA	1	68.5	173	175	13	60986	9672.30	2.06	0.17	
	2	58.9	168	169	14	48613				✓
C3-FLA	1	58.0	168	170	13	43705	4907.90	1.46	0.25	
	2	24.4	141	143	14	8325.6				✓
BNT23	1	23.9	142	144	13	7401.2	924.40	1.62	0.22	
	2	7.4	106	107	14	774.37				✓
BNT21	1	7.7	108	110	13	767.87	6.49	0.11	0.75	
	2	2.1	68.2	69.6	14	63.511				✓
C1-BNT	1	2.2	69.7	71.8	13	61.185	2.33	0.49	0.49	
	2	13.3	123	125	14	2485.2				✓
C0-CHY	1	13.5	125	127	13	2370.5	114.64	0.63	0.44	
	2	25.0	142	144	14	8780.1				✓
BaA	1	25.3	143	145	13	8331.0	449.11	0.70	0.42	
	2	2.5	72.5	73.9	14	84.5				✓
BeP	1	2.5	74	76.2	13	82.0	2.50	0.40	0.54	
	2	4.6	91.5	92.9	14	299.28				✓
	1	4.2	89.7	91.8	13	233.15	66.13	3.69	0.08	

Table D.8: Model accuracy metrics, including residual standard error (Sigma), Bayesian Information Criteria (BIC), and Akaike's Information Criteria (AIC) for PAC bioaccumulation models from the Medium treatments. Bioaccumulation models were determined by nonlinear curve fitting of the accumulation phase (Model 1) using equation 3 and by sequential estimation (Model 2) using equation 3. Model accuracy metrics were determined using R studio. The PAC bioaccumulation models that best fit the accumulation phase were determined by ANOVA analyses in R studio and by comparing model accuracy metrics. Abbreviations are found in Appendix A.

PAC	ANOVA Analysis						Sigma	AIC	BIC	Winner
	Model	Res. DF	Res. Sum. Sq.	Sum. Sq.	F-value	Pr(>F)				
C3-NAP	2	17	1720458				318	262	263	✓
	1	16	1661199	59260	0.57	0.46	322	263	266	
C4-NAP	2	17	39933108				1533	318	320	✓
	1	16	37087273	2845836	1.23	0.28	1522	319	321	
ACY	2	17	7745.4				21.3	164	166	✓
	1	16	7317.7	427.75	0.94	0.35	21.4	165	168	
C0-FLU	2	17	121851				84.7	214	216	✓
	1	16	107128	14723	2.20	0.16	81.8	214	216	
C1-FLU	2	17	5922267				590	284	286	✓
	1	16	5841028	81238	0.22	0.64	604	286	288	
C2-FLU	2	17	45254562				1632	320	322	✓
	1	16	40045776	5208786	2.08	0.17	1582	320	323	
C3-FLU	2	17	23302993				1171	308	310	✓
	1	16	23299547	3446.20	0.00	0.96	1207	310	313	
C0-DBT	2	17	2610.9				12.4	145	146	✓
	1	16	2530.8	80.02	0.51	0.49	12.6	146	149	
C1-DBT	2	17	10544.1				24.9	170	172	✓
	1	16	9774.3	769.75	1.26	0.28	24.7	170	173	
C2-DBT	2	17	81475				69.2	207	208	
	1	16	57329	24146	6.74	0.02	59.9	202	205	✓
C3-DBT	2	17	16948				31.6	178	180	✓
	1	16	16361	587.44	0.57	0.46	32.0	180	182	
ANT	2	17	1657.5				9.9	136	138	✓
	1	16	1612.3	45.15	0.45	0.51	10.0	138	141	
C0-PHE	2	17	8305.8				22.1	165	167	✓
	1	16	7532.6	773.23	1.64	0.22	21.7	166	168	
C1-PHE	2	17	137471				89.9	216	218	✓
	1	16	114760	22711	3.17	0.09	84.7	215	217	
C2-PHE	2	17	718468				206	246	248	✓
	1	16	716441	2027.20	0.05	0.83	212	248	250	
C3-PHE	2	17	134016				88.8	216	217	✓
	1	16	133723	293.64	0.04	0.85	91.4	218	220	
C4-PHE	2	17	50788				54.7	198	200	✓

PAC	ANOVA Analysis						Sigma	AIC	BIC	Winner
	Model	Res. DF	Res. Sum. Sq.	Sum. Sq.	F-value	Pr(>F)				
	1	16	50698	90.27	0.03	0.87	56.3	200	203	
RET	2	—	—				57.8	200	202	✓
	1	—	—	—	—	—	—	—	—	
PYR	2	17	4308.5				15.9	154	155	✓
	1	16	4248.8	59.76	0.23	0.64	16.3	155	158	
C0-FLA	2	17	5680.2				18.0	158	160	✓
	1	16	3784.7	1895.50	8.01	0.01	15.4	153	156	
C1-FLA	2	17	225548				115	225	227	✓
	1	16	222276	3271.20	0.24	0.63	118	227	229	
C2-FLA	2	17	117201				83	213	215	✓
	1	16	116231	970.45	0.13	0.72	85.2	215	218	
C3-FLA	2	17	26988				39.8	187	188	✓
	1	16	24816	2171.80	1.40	0.25	39.4	187	190	
BNT23	2	17	2243.6				11.5	142	144	
	1	16	1547.3	696.26	7.20	0.02	9.83	137	140	✓
BNT21	2	17	152.9				3	93.6	95.4	
	1	16	121.0	31.83	4.21	0.06	2.75	91.4	94.1	✓
C1-BNT	2	17	8143.6				21.9	165	167	✓
	1	16	8014.4	129.14	0.26	0.62	22.4	167	170	
C0-CHY	2	17	8986.4				23	167	169	
	1	16	7810.5	1175.90	2.41	0.14	2.1	166	169	✓
BaA	2	17	91.5				2.26	83.4	85.2	✓
	1	16	73.5	17.98	3.91	0.07	2.17	82.8	85.5	
BeP	2	17	160.4				3.07	94.5	96.2	✓
	1	16	155.0	5.47	0.56	0.46	3.11	95.8	98.5	

Table D.9: Model accuracy metrics, including residual standard error (Sigma), Bayesian Information Criteria (BIC), and Akaike's Information Criteria (AIC) for PAC bioaccumulation models from the High treatments. Bioaccumulation models were determined by nonlinear curve fitting of the accumulation phase (Model 1) using equation 3 and by sequential estimation (Model 2) using equation 3. Model accuracy metrics were determined using R studio. The PAC bioaccumulation models that best fit the accumulation phase were determined by ANOVA analyses in R studio and by comparing model accuracy metrics. Abbreviations are found in Appendix A.

PAC	ANOVA Analysis						Sigma	AIC	BIC	Winner
	Model	Res. DF	Res. Sum. Sq.	Sum. Sq.	F-value	Pr(>F)				
C3-NAP	2	17	1720458				318	262	263	✓
	1	16	1661199	59260	0.57	0.46	322	263	266	
C4-NAP	2	17	39933108				1533	318	320	✓
	1	16	37087273	2845836	1.23	0.28	1522	319	321	
ACY	2	17	7745.4				21.3	164	166	✓
	1	16	7317.7	427.75	0.94	0.35	21.4	165	168	
C0-FLU	2	17	121851				84.7	214	216	✓
	1	16	107128	14723	2.20	0.16	81.8	214	216	
C1-FLU	2	17	5922267				590	284	286	✓
	1	16	5841028	81238	0.22	0.64	604	286	288	
C2-FLU	2	17	45254562				1632	320	322	✓
	1	16	40045776	5208786	2.08	0.17	1582	320	323	
C3-FLU	2	17	23302993				1171	308	310	✓
	1	16	23299547	3446.20	0.00	0.96	1207	310	313	
C0-DBT	2	17	2610.9				12.4	145	146	✓
	1	16	2530.8	80.02	0.51	0.49	12.6	146	149	
C1-DBT	2	17	10544.1				24.9	170	172	✓
	1	16	9774.3	769.75	1.26	0.28	24.7	170	173	
C2-DBT	2	17	81475				69.2	207	208	
	1	16	57329	24146	6.74	0.02	59.9	202	205	✓
C3-DBT	2	17	16948				31.6	178	180	✓
	1	16	16361	587.44	0.57	0.46	32	180	182	
ANT	2	17	1657.5				9.87	136	138	✓
	1	16	1612.3	45.15	0.45	0.51	10	138	141	
C0-PHE	2	17	8305.8				22.1	165	167	✓
	1	16	7532.6	773.23	1.64	0.22	21.7	166	168	
C1-PHE	2	17	137471				89.9	216	218	✓
	1	16	114760	22711.0	3.17	0.09	84.7	215	217	
C2-PHE	2	17	718468				206	246	248	✓
	1	16	716441	2027.20	0.05	0.83	212	248	250	
C3-PHE	2	17	134016				88.8	216	217	✓
	1	16	133723	293.64	0.04	0.85	91.4	218	220	
C4-PHE	2	17	50788				54.7	198	200	✓

PAC	ANOVA Analysis						Sigma	AIC	BIC	Winner
	Model	Res. DF	Res. Sum. Sq.	Sum. Sq.	F-value	Pr(>F)				
RET	1	16	50698	90.27	0.03	0.87	56.3	200	203	
	2	—	—				57.8	200	202	✓
	1	—	—	—	—	—	—	—	—	
PYR	2	17	4308.5				15.9	154	155	✓
	1	16	4248.8	59.76	0.23	0.64	16.3	155	158	
C0-FLA	2	17	5680.2				18	158	160	✓
	1	16	3784.7	1895.50	8.01	0.01	15.4	153	156	
C1-FLA	2	17	225548				115	225	227	✓
	1	16	222276	3271.20	0.24	0.63	118	227	229	
C2-FLA	2	17	117201				83	213	215	✓
	1	16	116231	970.45	0.13	0.72	85.2	215	218	
C3-FLA	2	17	26988				39.8	187	188	✓
	1	16	24816	2171.80	1.40	0.25	39.4	187	190	
BNT23	2	17	2243.6				11.5	142	144	
	1	16	1547.3	696.26	7.20	0.02	9.83	137	140	✓
BNT21	2	17	152.9				3	93.6	95.4	
	1	16	121.0	31.83	4.21	0.06	2.75	91.4	94.1	✓
C1-BNT	2	17	8143.6				21.9	165	167	✓
	1	16	8014.4	129.14	0.26	0.62	22.4	167	170	
C0-CHY	2	17	8986.4				23	167	169	
	1	16	7810.5	1175.90	2.41	0.14	2.1	166	169	✓
BaA	2	17	91.5				2.26	83.4	85.2	✓
	1	16	73.5	17.98	3.91	0.07	2.17	82.8	85.5	
BeP	2	17	160.4				3.07	94.5	96.2	✓
	1	16	155.0	5.47	0.56	0.46	3.11	95.8	98.5	

Table D.10: Depuration rate constants (k_2; day^{-1}) and their 95% confidence intervals. Abbreviations are found in Appendix A. Confidence intervals and k_2 values were determined in R Studio.

	Low			Medium			High		
PAC	**k_2**	**2.50%**	**97.50%**	**k_2**	**0.025**	**97.50%**	**k_2**	**2.50%**	**97.50%**
C3-NAP	0.12	0.04	0.21	0.18	0.08	0.27	0.18	0.06	0.30
C4-NAP	0.026	-0.028	0.079	0.23	0	0.46	0.14	0.03	0.26
ACY	0.012	-0.164	0.187	0.019	-0.116	0.213	0.045	0.007	0.083
C0-FLU	0.075	-0.018	0.168	0.082	-0.017	0.181	0.081	-0.046	0.207
C1-FLU	0.079	-0.034	0.191	0.095	-0.148	0.339	0.15	0.06	0.24
C2-FLU	0.064	0	0.140	0.098	-0.099	0.295	0.13	0.05	0.20
C3-FLU	0.028	-0.038	0.109	0.13	-0.07	0.33	0.17	0.10	0.25
ANT	0.13	-0.01	0.26	0.16	0.03	0.28	0.081	0.056	0.105
C0-PHE	0.062	0.025	0.099	0.077	0.047	0.108	0.062	0.040	0.084
C1-PHE	0.067	0.030	0.104	0.14	0.09	0.19	0.075	0.053	0.098
C2-PHE	0.16	0.10	0.23	0.20	0.13	0.27	0.13	0.07	0.18
C3-PHE	0.054	0.006	0.102	0.087	0.046	0.129	0.092	0.056	0.127
C4-PHE	0.092	0.015	0.169	0.16	0.07	0.24	0.12	0.05	0.19
C0-DBT	0.045	0.004	0.086	0.067	0.036	0.099	0.065	0.042	0.089
C1-DBT	0.053	0.009	0.097	0.12	0.05	0.19	0.065	0.028	0.102
C2-DBT	0.16	0.09	0.24	0.14	0.07	0.21	0.18	0.11	0.27
C3-DBT	0.068	0.017	0.120	0.11	0.07	0.15	0.081	-0.061	0.224
PYR	0.13	0.07	0.18	0.14	0.05	0.22	0.086	0.034	0.138
C0-FLA	0.16	0.08	0.24	0.12	-0.01	0.26	0.074	0.006	0.142
C1-FLA	0.025	-0.019	0.068	0.041	-0.003	0.085	0.037	0.006	0.069
C2-FLA	0.022	-0.025	0.069	0.037	-0.005	0.079	0.036	0.006	0.066
C3-FLA	0.022	-0.024	0.069	0.043	0.003	0.082	0.043	0.012	0.073
C0-CHY	0.13	0.07	0.18	0.089	0.062	0.115	0.026	-0.030	0.094
BaA	0.071	0.019	0.124	0.052	0.018	0.087	0.088	0.056	0.233
BNT23	0.065	0.016	0.113	0.11	0.08	0.14	0.023	-0.031	0.088
BNT21	0.23	0.16	0.31	0.13	0.10	0.16	0.041	-0.025	0.131
C1-BNT	0.32	0.19	0.45	0.11	0.08	0.15	0.11	0.07	0.15
RET	0.17	0.06	0.28	0.11	0.04	0.18	0.067	0.031	0.103
BeP	0.31	0.16	0.45	0.37	-0.06	0.80	0.34	-0.01	0.70

Appendix E. PACs Statistics

Table E.1: Statistical analysis to compare water PAC concentrations between Lake 260 water (n=3), the Control (n=5), Low (n=5), Medium (n=6), and High (n=7) treatments. One-way ANOVA tests were conducted when the normality (Shapiro-Wilk test) and homogeneity of variances (Levene's test) assumptions were met. Welch one-way tests were conducted when only the normality assumption was met. When no assumptions were met, Kruskal-Wallis rank sum test were conducted. All statistical analyses were conducted in R Studio.

PAC	Transformation	Statistical Test	p-value	Shapiro-Wilk Test	Levene's Test
C0-NAP	—	Kruskal-Wallis	0.63	—	—
C1-NAP	—	Kruskal-Wallis	0.0014	—	—
C2-NAP	—	Kruskal-Wallis	0.0013	—	—
C3-NAP	Log transformation	ANOVA	1.87×10^{-11}	0.36	0.35
C4-NAP	—	Welch	5.01×10^{-7}	0.28	0.022
ACE	—	Kruskal-Wallis	0.0028	—	—
ACY	—	ANOVA	0.00017	0.29	0.59
C0-FLU	—	Kruskal-Wallis	0.0017	—	—
C1-FLU	Log transformation	ANOVA	1.46×10^{-18}	0.51	0.77
C2-FLU	—	Kruskal-Wallis	0.00015	—	—
C3-FLU	Log transformation	ANOVA	3.67×10^{-14}	0.34	0.099
C0-DBT	—	Kruskal-Wallis	0.0018	—	—
C1-DBT	—	Kruskal-Wallis	0.0014	—	—
C2-DBT	Log transformation	ANOVA	8.11×10^{-17}	0.76	0.47
C3-DBT	—	Kruskal-Wallis	0.0051	—	—
ANT	—	Kruskal-Wallis	0.00018	—	—
C0-PHE	—	Kruskal-Wallis	0.025	—	—
C1-PHE	Log transformation	ANOVA	5.79×10^{-10}	0.23	0.41
C2-PHE	Log transformation	ANOVA	1.95×10^{-14}	0.22	0.46
C3-PHE	—	Kruskal-Wallis	0.00029	—	—
C4-PHE	—	ANOVA	4.03×10^{-6}	0.24	0.19
RET	—	Kruskal-Wallis	0.0013	—	—
PYR	—	Kruskal-Wallis	0.00027	—	—
C0-FLA	—	ANOVA	7.14×10^{-7}	0.54	0.64
C1-FLA	—	Kruskal-Wallis	0.00025	—	—
C2-FLA	—	Kruskal-Wallis	0.00079	—	—
C3-FLA	—	Kruskal-Wallis	0.0091	—	—
C4-FLA	—	BDL	—	—	—
BNT23	—	Kruskal-Wallis	0.0021	—	—
BNT21	—	Kruskal-Wallis	0.0021	—	—
C1-BNT	—	Kruskal-Wallis	0.0019	—	—
C2-BNT	Log transformation	ANOVA	3.00×10^{-15}	0.073	0.14
C3-BNT	—	Kruskal-Wallis	0.00091	—	—
C4-BNT	—	Kruskal-Wallis	0.14	—	—
C0-CHY	—	ANOVA	1.72×10^{-11}	0.69	0.54
C1-CHY	—	Kruskal-Wallis	0.00062	—	—
C2-CHY	—	Kruskal-Wallis	0.00086	—	—
C3-CHY	—	Kruskal-Wallis	0.17	—	—
BaA	—	Kruskal-Wallis	0.00092	—	—
BbF+BkF	—	Kruskal-Wallis	0.058	—	—
BaP	—	BDL	—	—	—

PAC	Transformation	Statistical Test	p-value	Shapiro-Wilk Test	Levene's Test
BeP	—	Kruskal-Wallis	0.0082	—	—
BP	—	Kruskal-Wallis	0.33	—	—
IP	—	BDL	—	—	—
DA	—	BDL	—	—	—
TPACs	—	ANOVA	1.12×10^{-8}	0.11	0.28

Table E.2: Pairwise comparisons using Tukey's HSD tests, Welch t-test, and Wilcoxon rank sum tests to compare water PAC concentrations between the Control (n=5), Low (n=5), Medium (n=6), and High (n=7) treatments and Lake 260 water (n=3). Tukey's HSD tests were conducted when normality and homogeneity of variances assumptions were met while Wilcoxon rank sum tests were conducted when no assumptions were met (see Table E.1). Welch t-tests were used when the normality assumption was met but the homogeneity of variances assumption was not. All statistical analyses were conducted in R Studio.

PAC	Transformation	Statistical Test	Group 1	Group 2	p-value
C1-NAP	—	Wilcoxon	Low	Control	0.026
C1-NAP			Medium	Control	0.022
C1-NAP			High	Control	0.022
C1-NAP			Lake 260	Control	1.00
C1-NAP			Medium	Low	0.60
C1-NAP			High	Low	0.33
C1-NAP			Lake 260	Low	0.060
C1-NAP			High	Medium	0.14
C1-NAP			Lake 260	Medium	0.048
C1-NAP			Lake 260	High	0.042
C2-NAP	—	Wilcoxon	Low	Control	0.026
C2-NAP			Medium	Control	0.022
C2-NAP			High	Control	0.022
C2-NAP			Lake 260	Control	0.18
C2-NAP			Medium	Low	0.43
C2-NAP			High	Low	0.30
C2-NAP			Lake 260	Low	0.060
C2-NAP			High	Medium	0.18
C2-NAP			Lake 260	Medium	0.048
C2-NAP			Lake 260	High	0.042
C3-NAP	Log transformation	Tukey HSD	Low	Control	6.59×10^{-8}
C3-NAP			Medium	Control	1.44×10^{-7}
C3-NAP			High	Control	4.37×10^{-9}
C3-NAP			Lake 260	Control	0.075
C3-NAP			Medium	Low	0.92
C3-NAP			High	Low	0.92
C3-NAP			Lake 260	Low	4.56×10^{-9}
C3-NAP			High	Medium	0.42
C3-NAP			Lake 260	Medium	8.32×10^{-9}
C3-NAP			Lake 260	High	5.58×10^{-10}
C4-NAP	—	Welch t-test	Low	Control	0.0047
C4-NAP			Medium	Control	0.0028
C4-NAP			High	Control	9.51×10^{-6}
C4-NAP			Lake 260	Control	0.23
C4-NAP			Medium	Low	0.37
C4-NAP			High	Low	9.51×10^{-6}
C4-NAP			Lake 260	Low	0.0047
C4-NAP			High	Medium	2.31×10^{-5}
C4-NAP			Lake 260	Medium	0.0028
C4-NAP			Lake 260	High	9.51×10^{-6}
ACE	—	Wilcoxon	Low	Control	0.037
ACE			Medium	Control	0.037
ACE			High	Control	0.037
ACE			Lake 260	Control	0.32
ACE			Medium	Low	1.00
ACE			High	Low	1.00

PAC	Transformation	Statistical Test	Group 1	Group 2	p-value
ACE			Lake 260	Low	0.060
ACE			High	Medium	1.00
ACE			Lake 260	Medium	0.048
ACE			Lake 260	High	0.042
ACY			Low	Control	0.70
ACY			Medium	Control	0.68
ACY			High	Control	0.0026
ACY			Lake 260	Control	5.76×10^{-4}
ACY	—	Tukey HSD	Medium	Low	1.00
ACY			High	Low	0.057
ACY			Lake 260	Low	0.0076
ACY			High	Medium	0.040
ACY			Lake 260	Medium	0.0055
ACY			Lake 260	High	0.52
C0-FLU			Low	Control	0.026
C0-FLU			Medium	Control	0.022
C0-FLU			High	Control	0.022
C0-FLU			Lake 260	Control	0.20
C0-FLU	—	Wilcoxon	Medium	Low	0.30
C0-FLU			High	Low	0.30
C0-FLU			Lake 260	Low	0.060
C0-FLU			High	Medium	0.95
C0-FLU			Lake 260	Medium	0.048
C0-FLU			Lake 260	High	0.042
C1-FLU			Low	Control	4.13×10^{-4}
C1-FLU			Medium	Control	4.13×10^{-4}
C1-FLU			High	Control	5.25×10^{-5}
C1-FLU			Lake 260	Control	0.12
C1-FLU	Log transformation	Tukey HSD	Medium	Low	0.65
C1-FLU			High	Low	3.75×10^{-4}
C1-FLU			Lake 260	Low	4.13×10^{-4}
C1-FLU			High	Medium	4.13×10^{-4}
C1-FLU			Lake 260	Medium	4.13×10^{-4}
C1-FLU			Lake 260	High	5.25×10^{-5}
C2-FLU			Low	Control	0.016
C2-FLU			Medium	Control	0.012
C2-FLU			High	Control	0.012
C2-FLU			Lake 260	Control	0.13
C2-FLU	—	Wilcoxon	Medium	Low	0.038
C2-FLU			High	Low	0.012
C2-FLU			Lake 260	Low	0.040
C2-FLU			High	Medium	0.012
C2-FLU			Lake 260	Medium	0.038
C2-FLU			Lake 260	High	0.037
C3-FLU			Low	Control	1.24×10^{-8}
C3-FLU			Medium	Control	3.41×10^{-11}
C3-FLU			High	Control	4.75×10^{-12}
C3-FLU			Lake 260	Control	0.050
C3-FLU	Log transformation	Tukey HSD	Medium	Low	0.020
C3-FLU			High	Low	0.0013
C3-FLU			Lake 260	Low	8.89×10^{-10}
C3-FLU			High	Medium	0.79
C3-FLU			Lake 260	Medium	8.72×10^{-12}
C3-FLU			Lake 260	High	1.86×10^{-12}

PAC	Transformation	Statistical Test	Group 1	Group 2	p-value
C0-DBT	—	Wilcoxon	Low	Control	0.026
C0-DBT			Medium	Control	0.022
C0-DBT			High	Control	0.022
C0-DBT			Lake 260	Control	0.051
C0-DBT			Medium	Low	0.60
C0-DBT			High	Low	0.33
C0-DBT			Lake 260	Low	0.051
C0-DBT			High	Medium	0.84
C0-DBT			Lake 260	Medium	0.048
C0-DBT			Lake 260	High	0.042
C1-DBT	—	Wilcoxon	Low	Control	0.026
C1-DBT			Medium	Control	0.022
C1-DBT			High	Control	0.022
C1-DBT			Lake 260	Control	0.44
C1-DBT			Medium	Low	0.54
C1-DBT			High	Low	0.15
C1-DBT			Lake 260	Low	0.060
C1-DBT			High	Medium	0.37
C1-DBT			Lake 260	Medium	0.048
C1-DBT			Lake 260	High	0.042
C2-DBT	Log transformation	Tukey HSD	Low	Control	$3.71x10^{-13}$
C2-DBT			Medium	Control	$6.96x10^{-14}$
C2-DBT			High	Control	$4.83x10^{-14}$
C2-DBT			Lake 260	Control	0.78
C2-DBT			Medium	Low	0.58
C2-DBT			High	Low	0.083
C2-DBT			Lake 260	Low	$1.48X10^{-12}$
C2-DBT			High	Medium	0.72
C2-DBT			Lake 260	Medium	$2.14X10^{-13}$
C2-DBT			Lake 260	High	$7.72x10^{-14}$
C3-DBT	—	Wilcoxon	Low	Control	0.017
C3-DBT			Medium	Control	0.016
C3-DBT			High	Control	0.016
C3-DBT			Lake 260	Control	1.00
C3-DBT			Medium	Low	0.14
C3-DBT			High	Low	0.016
C3-DBT			Lake 260	Low	0.042
C3-DBT			High	Medium	0.53
C3-DBT			Lake 260	Medium	0.038
C3-DBT			Lake 260	High	0.038
ANT	—	Wilcoxon	Low	Control	0.013
ANT			Medium	Control	0.012
ANT			High	Control	0.012
ANT			Lake 260	Control	1.00
ANT			Medium	Low	1.00
ANT			High	Low	0.011
ANT			Lake 260	Low	0.037
ANT			High	Medium	0.011
ANT			Lake 260	Medium	0.033
ANT			Lake 260	High	0.032
C0-PHE	—	Wilcoxon	Low	Control	0.051
C0-PHE			Medium	Control	0.54
C0-PHE			High	Control	0.051
C0-PHE			Lake 260	Control	0.54

PAC	Transformation	Statistical Test	Group 1	Group 2	p-value
C0-PHE			Medium	Low	0.74
C0-PHE			High	Low	0.54
C0-PHE			Lake 260	Low	0.089
C0-PHE			High	Medium	1.00
C0-PHE			Lake 260	Medium	0.52
C0-PHE			Lake 260	High	0.056
C1-PHE			Low	Control	9.13×10^{-8}
C1-PHE			Medium	Control	9.69×10^{-7}
C1-PHE			High	Control	1.12×10^{-7}
C1-PHE			Lake 260	Control	0.69
C1-PHE	Log transformation	Tukey HSD	Medium	Low	0.50
C1-PHE			High	Low	0.92
C1-PHE			Lake 260	Low	7.72×10^{-8}
C1-PHE			High	Medium	0.90
C1-PHE			Lake 260	Medium	6.23×10^{-7}
C1-PHE			Lake 260	High	1.07×10^{-7}
C2-PHE			Low	Control	5.5×10^{-9}
C2-PHE			Medium	Control	9.0×10^{-10}
C2-PHE			High	Control	6.84×10^{-11}
C2-PHE			Lake 260	Control	1.44×10^{-5}
C2-PHE	Log transformation	Tukey HSD	Medium	Low	0.97
C2-PHE			High	Low	0.29
C2-PHE			Lake 260	Low	3.67×10^{-12}
C2-PHE			High	Medium	0.62
C2-PHE			Lake 260	Medium	1.05×10^{-12}
C2-PHE			Lake 260	High	2.03×10^{-13}
C3-PHE			Low	Control	0.028
C3-PHE			Medium	Control	0.025
C3-PHE			High	Control	0.025
C3-PHE			Lake 260	Control	0.33
C3-PHE	—	Wilcoxon	Medium	Low	0.091
C3-PHE			High	Low	0.025
C3-PHE			Lake 260	Low	0.046
C3-PHE			High	Medium	0.091
C3-PHE			Lake 260	Medium	0.043
C3-PHE			Lake 260	High	0.042
C4-PHE			Low	Control	0.11
C4-PHE			Medium	Control	7.85×10^{-4}
C4-PHE			High	Control	1.76×10^{-5}
C4-PHE			Lake 260	Control	1.00
C4-PHE	—	Tukey HSD	Medium	Low	0.24
C4-PHE			High	Low	0.010
C4-PHE			Lake 260	Low	0.12
C4-PHE			High	Medium	0.52
C4-PHE			Lake 260	Medium	0.0019
C4-PHE			Lake 260	High	7.66×10^{-5}
RET			Low	Control	0.060
RET			Medium	Control	0.040
RET			High	Control	0.040
RET	—	Wilcoxon	Lake 260	Control	0.76
RET			Medium	Low	0.074
RET			High	Low	0.092
RET			Lake 260	Low	0.060
RET			High	Medium	0.70

PAC	Transformation	Statistical Test	Group 1	Group 2	p-value
RET			Lake 260	Medium	0.060
RET			Lake 260	High	0.056
PYR			Low	Control	0.10
PYR			Medium	Control	0.020
PYR			High	Control	0.019
PYR			Lake 260	Control	0.53
PYR			Medium	Low	0.019
PYR	—	Wilcoxon	High	Low	0.019
PYR			Lake 260	Low	0.051
PYR			High	Medium	0.092
PYR			Lake 260	Medium	0.046
PYR			Lake 260	High	0.044
C0-FLA			Low	Control	0.0056
C0-FLA			Medium	Control	0.0017
C0-FLA			High	Control	2.79×10^{-6}
C0-FLA			Lake 260	Control	0.96
C0-FLA			Medium	Low	1.00
C0-FLA	—	Tukey HSD	High	Low	0.04
C0-FLA			Lake 260	Low	0.0043
C0-FLA			High	Medium	0.061
C0-FLA			Lake 260	Medium	0.0016
C0-FLA			Lake 260	High	6.81×10^{-6}
C1-FLA			Low	Control	0.024
C1-FLA			Medium	Control	0.022
C1-FLA			High	Control	0.022
C1-FLA			Lake 260	Control	1.00
C1-FLA			Medium	Low	0.14
C1-FLA	—	Wilcoxon	High	Low	0.022
C1-FLA			Lake 260	Low	0.045
C1-FLA			High	Medium	0.037
C1-FLA			Lake 260	Medium	0.039
C1-FLA			Lake 260	High	0.037
C2-FLA			Low	Control	0.032
C2-FLA			Medium	Control	0.032
C2-FLA			High	Control	0.032
C2-FLA			Lake 260	Control	0.63
C2-FLA			Medium	Low	0.22
C2-FLA	—	Wilcoxon	High	Low	0.042
C2-FLA			Lake 260	Low	0.046
C2-FLA			High	Medium	0.63
C2-FLA			Lake 260	Medium	0.043
C2-FLA			Lake 260	High	0.042
C3-FLA			Low	Control	0.087
C3-FLA			Medium	Control	0.064
C3-FLA			High	Control	0.064
C3-FLA			Lake 260	Control	0.67
C3-FLA			Medium	Low	0.67
C3-FLA	—	Wilcoxon	High	Low	0.67
C3-FLA			Lake 260	Low	0.065
C3-FLA			High	Medium	0.95
C3-FLA			Lake 260	Medium	0.064
C3-FLA			Lake 260	High	0.064
BNT23			Low	Control	0.032
BNT23	—	Wilcoxon	Medium	Control	0.032

PAC	Transformation	Statistical Test	Group 1	Group 2	p-value
BNT23			High	Control	0.032
BNT23			Lake 260	Control	0.67
BNT23			Medium	Low	0.61
BNT23			High	Low	0.66
BNT23			Lake 260	Low	0.054
BNT23			High	Medium	1.00
BNT23			Lake 260	Medium	0.051
BNT23			Lake 260	High	0.051
BNT21			Low	Control	0.022
BNT21			Medium	Control	0.022
BNT21			High	Control	0.022
BNT21			Lake 260	Control	1.00
BNT21	—	Wilcoxon	Medium	Low	0.75
BNT21			High	Low	0.56
BNT21			Lake 260	Low	0.049
BNT21			High	Medium	0.95
BNT21			Lake 260	Medium	0.046
BNT21			Lake 260	High	0.046
C1-BNT			Low	Control	0.032
C1-BNT			Medium	Control	0.032
C1-BNT			High	Control	0.032
C1-BNT			Lake 260	Control	0.61
C1-BNT	—	Wilcoxon	Medium	Low	0.54
C1-BNT			High	Low	0.49
C1-BNT			Lake 260	Low	0.054
C1-BNT			High	Medium	0.59
C1-BNT			Lake 260	Medium	0.051
C1-BNT			Lake 260	High	0.051
C2-BNT			Low	Control	1.42×10^{-11}
C2-BNT			Medium	Control	1.66×10^{-13}
C2-BNT			High	Control	3.48×10^{-13}
C2-BNT			Lake 260	Control	1.00
C2-BNT	Log transformation	Tukey HSD	Medium	Low	0.024
C2-BNT			High	Low	0.30
C2-BNT			Lake 260	Low	2.08×10^{-10}
C2-BNT			High	Medium	0.57
C2-BNT			Lake 260	Medium	2.89×10^{-12}
C2-BNT			Lake 260	High	7.75×10^{-12}
C3-BNT			Low	Control	0.046
C3-BNT			Medium	Control	0.025
C3-BNT			High	Control	0.025
C3-BNT			Lake 260	Control	1.00
C3-BNT	—	Wilcoxon	Medium	Low	0.078
C3-BNT			High	Low	0.091
C3-BNT			Lake 260	Low	0.091
C3-BNT			High	Medium	0.18
C3-BNT			Lake 260	Medium	0.046
C3-BNT			Lake 260	High	0.046
C0-CHY			Low	Control	1.00×10^{-6}
C0-CHY			Medium	Control	3.08×10^{-8}
C0-CHY	—	Tukey HSD	High	Control	9.30×10^{-11}
C0-CHY			Lake 260	Control	1.00
C0-CHY			Medium	Low	0.58
C0-CHY			High	Low	7.11×10^{-4}

PAC	Transformation	Statistical Test	Group 1	Group 2	p-value
C0-CHY			Lake 260	Low	4.57×10^{-6}
C0-CHY			High	Medium	0.016
C0-CHY			Lake 260	Medium	2.21×10^{-7}
C0-CHY			Lake 260	High	1.15×10^{-9}
C1-CHY			Low	Control	0.032
C1-CHY			Medium	Control	0.032
C1-CHY			High	Control	0.032
C1-CHY			Lake 260	Control	0.61
C1-CHY	—	Wilcoxon	Medium	Low	0.16
C1-CHY			High	Low	0.042
C1-CHY			Lake 260	Low	0.046
C1-CHY			High	Medium	0.33
C1-CHY			Lake 260	Medium	0.043
C1-CHY			Lake 260	High	0.042
C2-CHY			Low	Control	0.022
C2-CHY			Medium	Control	0.022
C2-CHY			High	Control	0.022
C2-CHY			Lake 260	Control	—
C2-CHY	—	Wilcoxon	Medium	Low	0.28
C2-CHY			High	Low	0.038
C2-CHY			Lake 260	Low	0.042
C2-CHY			High	Medium	0.95
C2-CHY			Lake 260	Medium	0.038
C2-CHY			Lake 260	High	0.038
BaA			Low	Control	0.094
BaA			Medium	Control	0.058
BaA			High	Control	0.049
BaA			Lake 260	Control	0.61
BaA	—	Wilcoxon	Medium	Low	0.094
BaA			High	Low	0.069
BaA			Lake 260	Low	0.058
BaA			High	Medium	0.058
BaA			Lake 260	Medium	0.058
BaA			Lake 260	High	0.058
BeP			Low	Control	0.057
BeP			Medium	Control	0.057
BeP			High	Control	0.038
BeP			Lake 260	Control	1.00
BeP	—	Wilcoxon	Medium	Low	0.80
BeP			High	Low	0.80
BeP			Lake 260	Low	0.12
BeP			High	Medium	1.00
BeP			Lake 260	Medium	0.11
BeP			Lake 260	High	0.057
TPACs			Low	Control	0.0052
TPACs			Medium	Control	2.52×10^{-4}
TPACs			High	Control	2.06×10^{-8}
TPACs			Lake 260	Control	1.00
TPACs	—	Tukey HSD	Medium	Low	0.79
TPACs			High	Low	1.30×10^{-4}
TPACs			Lake 260	Low	0.015
TPACs			High	Medium	0.0011
TPACs			Lake 260	Medium	0.0013
TPACs			Lake 260	High	2.88×10^{-7}

Table E.3: Unpaired two samples t-tests, Welch t-test, and Wilcoxon rank sum test to compare water TPAC concentrations between this bioaccumulation study and the 'fate and behaviour' subtheme (FaBS) of the BOREAL project. T-tests were conducted when normality (Shapiro-Wilk test) and homogeneity of variances (Levene's test) assumptions were met. A Welch t-test was conducted when the normality assumption is met but the homogeneity of variances assumption is not. When assumptions were not met, unpaired two-samples Wilcoxon tests were conducted. All statistical analyses were conducted in R Studio.

Statistical Test	TPACs Aquaria	TPACs Limnocorral	p-value	Shapiro-Wilk Test		Levene's Test
				Aquaria	Limnocorral	
Wilcoxon	Control – n=5 0.017 ± 0.012 μg L^{-1}	Control – n=4 0.034 ± 0.010 μg L^{-1}	0.11	—	—	—
T-test	Low – n=5 0.40 ± 0.09 μg L^{-1}	Low – n=4 0.95 ± 0. μg L^{-1}	0.018	0.78	0.11	0.31
T-test	Medium – n=6 0.51 ± 0.15 μg L^{-1}	Medium – n=4 0.92 ± 0.33 μg L^{-1}	0.027	0.20	0.94	0.19
Welch t-test	High – n=7 0.90 ± 0.24 μg L^{-1}	High – n=4 1.85 ± 0.41 μg L^{-1}	6.89×10^{-6}	0.070	0.17	0.025

Table E.4: Unpaired two samples t-test, Welch t-test, and Wilcoxon rank sum tests to compare parent and alkylated PAC concentrations in the water. A t-test was conducted when normality (Shapiro-Wilk test) and homogeneity of variances (Levene's test) assumptions were met. A Welch t-test was conducted when the normality assumption is met but the homogeneity of variances assumption is not. When assumptions were not met, unpaired two-samples Wilcoxon tests were conducted. All statistical analyses were conducted in R Studio.

Statistical Test	Parent PACs	Alkyl PACs	p-value	Shapiro-Wilk Test		Levene's Test
				Aquaria	Limnocorral	
Wilcoxon	Control – n=5 0.0042 ± 0.0033 μg L^{-1}	Control – n=5 0.012 ± 0.009 μg L^{-1}	0.095	—	—	—
T-test	Low – n=5 0.024 ± 0.008 μg L^{-1}	Low – n=5 0.38 ± 0.09 μg L^{-1}	2.27×10^{-5}	0.26	0.54	0.054
Welch t-test	Medium – n=6 0.024 ± 0.012 μg L^{-1}	Medium – n=6 0.48 ± 0.15 μg L^{-1}	6.30×10^{-4}	0.43	0.33	6.30×10^{-4}
Wilcoxon	High – n=7 0.030 ± 0.020 μg L^{-1}	High – n=7 0.87 ± 0.22 μg L^{-1}	0.0022	—	—	—

Table E.5: Linear regressions between log PAC concentrations in the water (ng L^{-1}) and their associated log K_{OW} values for all three dilbit-contaminated treatments. Water concentrations are the averages of all uptake time points (n=5, 6, and 7 for the Low, Medium, and High treatment, respectively). All regression analyses were conducted in R studio.

Treatment	Sample Size	Equation	R^2	p-value
Low	36 PACs	y = -0.19x + 1.58	0.054	0.17
Medium	36 PACs	y = -0.059 + 0.98	0.0053	0.67
High	36 PACs	y = -0.18x + 1.77	0.044	0.22

Table E.6: Linear regressions between log PAC concentrations in the water (ng L^{-1}) and log PAC in CLB dilbit. Water concentrations are the averages of all uptake time points (n=5, 6, and 7 for the Low, Medium, and High treatment, respectively). PACs were only included if they were significantly higher in dilbit treatments compared to the Control and if they are listed in Table C.4. All regression analyses were conducted in R studio.

Treatment	Sample Size	Equation	R^2	p-value
Low	28 PACs	y = 0.54x – 0.38	0.27	0.0049
Medium	28 PACs	y = 0.63x – 0.46	0.40	0.00029
High	28 PACs	y = 0.67x – 0.43	0.32	0.0017

Table E.7: Linear regressions between log PAC concentrations in the water (ng L^{-1}) and their associated molecular weight (g mol^{-1}). Water concentrations are the averages of all uptake time points (n=5, 6, and 7 for the Low, Medium, and High treatment, respectively). All regression analyses were conducted in R studio.

Treatment	Sample Size	Equation	R^2	p-value
Low	36 PACs	y = -0.0068x + 1.97	0.11	0.049
Medium	36 PACs	y = -0.0036x + 1.41	0.032	0.30
High	36 PACs	y = -0.0072x + 2.28	0.11	0.048

Table E.8: Statistical analysis to compare sediment PAC concentrations between the Control (n=3), Low (n=3), Medium (n=4), and High (n=3) treatments. One-way ANOVA tests were conducted when normality (Shapiro-Wilk test) and homogeneity of variances (Levene's test) assumptions were met. Kruskal-Wallis rank sum tests were conducted when no assumptions were met. All statistical analyses were conducted in R Studio.

PAC	Transformation	Statistical Test	p-value	Shapiro-Wilk Test	Levene's Test
C0-NAP	—	ANOVA	0.53	0.35	0.97
C1-NAP	Log transformation	ANOVA	0.024	0.79	0.63
C2-NAP	Log transformation	ANOVA	0.94	0.71	0.99
C3-NAP	—	Kruskal-Wallis	0.11	—	—
C4-NAP	—	ANOVA	0.22	0.054	0.20
ACE	—	—	—	—	—
ACY	—	—	—	—	—
C0-FLU	—	Kruskal-Wallis	0.96	—	—
C1-FLU	—	ANOVA	0.31	0.41	0.18
C2-FLU	—	ANOVA	0.60	0.35	0.24
C3-FLU	Log transformation	ANOVA	0.14	0.42	0.97
C0-DBT	—	ANOVA	0.73	0.33	0.92
C1-DBT	—	ANOVA	0.87	0.21	0.61
C2-DBT	—	ANOVA	0.32	0.44	0.78
C3-DBT	—	ANOVA	0.81	0.34	0.41
ANT	—	ANOVA	0.68	0.052	0.83
C0-PHE	—	ANOVA	0.66	0.60	0.96
C1-PHE	—	ANOVA	0.60	0.14	0.88
C2-PHE	Log transformation	ANOVA	0.83	0.30	0.68
C3-PHE	—	ANOVA	0.12	0.34	0.74
C4-PHE	—	ANOVA	0.59	0.30	0.89
RET	—	ANOVA	0.62	0.64	0.70
PYR	—	ANOVA	0.97	0.35	0.99
C0-FLA	—	ANOVA	0.24	0.82	0.18
C1-FLA	Log transformation	ANOVA	0.47	0.28	0.21
C2-FLA	—	Kruskal-Wallis	0.22	—	—
C3-FLA	—	Kruskal-Wallis	0.60	—	—
C4-FLA	—	Kruskal-Wallis	0.60	—	—
BNT23	—	ANOVA	0.68	0.13	0.56
BNT21	—	—	—	—	—
C1-BNT	—	ANOVA	0.32	0.69	0.29
C2-BNT	—	ANOVA	0.44	0.34	0.66
C3-BNT	—	ANOVA	0.34	0.25	0.30
C4-BNT	—	—	—	—	—
C0-CHY	—	ANOVA	0.24	0.85	0.33
C1-CHY	—	ANOVA	0.37	0.99	0.84
C2-CHY	—	ANOVA	0.43	0.31	0.50
C3-CHY	—	ANOVA	0.64	0.088	0.50

PAC	Transformation	Statistical Test	p-value	Shapiro-Wilk Test	Levene's Test
BaA	Log transformation	ANOVA	0.17	0.19	0.49
BbF+BkF	—	ANOVA	0.62	0.17	0.53
BaP	—	—	—	—	—
BeP	—	Kruskal-Wallis	0.72	—	—
BP	—	—	—	—	—
IP	—	—	—	—	—
DA	—	—	—	—	—
TPACs	Log transformation	ANOVA	0.55	0.56	0.24

Table E.9: Pairwise comparisons using a Tukey's HSD test to compare sediment C1-naphthalenes concentrations between the Control (n=3), Low (n=3), Medium (n=4), and High (n=3) treatments. Normality assumptions and homogeneity of variances assumptions were met (See Table E.8). The statistical analysis was conducted in R Studio.

PAC	Transformation	Statistical Test	Group 1	Group 2	p-value
C1-NAP	Log transformation	Tukey HSD	Low	Control	0.71
			Medium	Control	0.21
			High	Control	0.46
			Medium	Low	0.77
			High	Low	0.11
			High	Medium	0.019

Table E.10: Unpaired two samples Wilcoxon rank sum test to compare parent and alkylated PAC uptake rate constants (k_1; L g^{-1} day^{-1}). Dilbit-contaminated treatments were pooled together. Only parent PACs with alkylated homologues analysed were included. The statistical analysis was conducted in R Studio.

Statistical Test	Parent PACs log k_1	Alkyl PACs log k_1	p-value	Shapiro-Wilk Test		Levene's Test
				Parent	Alkyl	
Wilcoxon	0.48 ± 0.23 L g^{-1} day^{-1} n=21	0.64 ± 0.29 L g^{-1} day^{-1} n=48	0.0089	0.069	0.021	0.23

Table E.11: Unpaired two samples t-test to compare parent and alkylated PAC depuration rate constants (k_2; day^{-1}). Normality (Shapiro-Wilk test) and homogeneity of variances (Levene's test) assumptions were met. Dilbit-contaminated treatments were pooled together. Only parent PACs with alkylated homologues analysed were included. The statistical analysis was conducted in R Studio.

Statistical Test	Parent PACs log k_2	Alkyl PACs log k_2	p-value	Shapiro-Wilk Test		Levene's Test
				Parent	Alkyl	
T-test	-1.12 ± 0.24 day^{-1} n=21	-1.06 ± 0.29 day^{-1} n=48	0.37	0.63	0.057	0.40

Table E.12: Unpaired two samples Welch t-test to compare 2-3 ring and 3-4 ring PACs uptake rate constants (k_1; L g^{-1} day^{-1}). Normality (Shapiro-Wilk test) assumption was met but homogeneity of variances (Levene's test) assumption was not. Dilbit-contaminated treatments were pooled together. The statistical analysis was conducted in R Studio.

Statistical Test	2-3 rings PACs log k_1	4-5 rings PACs log k_1	p-value	Shapiro-Wilk Test		Levene's Test
				2-3 rings	4-5 rings	
Welch t-test	0.63 ± 0.34 L g^{-1} day^{-1} n=54	0.59 ± 0.22 L g^{-1} day^{-1} n=30	0.59	0.63	0.38	0.011

Table E.13: Unpaired two samples Wilcoxon rank sum test to compare 2-3 ring and 3-4 ring PACs depuration rate constants (k_2; day^{-1}). Normality (Shapiro-Wilk test) and homogeneity of variances (Levene's test) assumption were not met to conduct a parametric statistical test. The statistical analysis was conducted in R Studio.

Statistical Test	2-3 rings PACs k_2	4-5 rings PACs log k_2	p-value	Shapiro-Wilk Test		Levene's Test
				2-3 rings	4-5 rings	
Wilcoxon	0.10 ± 0.05 L g^{-1} day^{-1} n=54	0.11 ± 0.10 L g^{-1} day^{-1} n=30	0.27	0.18	$1.96x10^{-5}$	$1.62x10^{-5}$

Table E.14: Linear regressions between the uptake rate constants (k_1; L g^{-1} day^{-1}) of PACs and their associated log K_{OW} values for all three dilbit-contaminated treatments. All regression analyses were conducted in R studio.

Treatment	Sample Size	Equation	R^2	p-value
Low	29 PACs	y = 0.14x + 4.94	0.00077	0.89
Medium	29 PACs	y = -0.89x + 10.23	0.032	0.35
High	29 PACs	y = -0.60x + 7.35	0.012	0.57

Table E.15: Linear regressions between the depuration rate constants (k_2; day^{-1}) of PACs and their associated log K_{OW} values for all three dilbit-contaminated treatments. All regression analyses were conducted in R studio.

Treatment	Sample Size	Equation	R^2	p-value
Low	29 PACs	y = 0.038x – 0.10	0.12	0.071
Medium	29 PACs	y = 0.022x – 0.0018	0.054	0.23
High	29 PACs	y = 0.013x + 0.026	0.021	0.45

Table E.16: Linear regressions between the uptake rate constants (k_1; L g^{-1} day^{-1}) of PACs and their associated molecular weights (g mol^{-1}) for all three dilbit-contaminated treatments. All regression analyses were conducted in R studio.

Treatment	Sample Size	Equation	R^2	p-value
Low	29 PACs	y = -0.0083x + 7.42	0.0037	0.75
Medium	29 PACs	y = -0.043x + 14.44	0.10	0.087
High	29 PACs	y = -0.022x + 8.78	0.024	0.42

Table E.17: Linear regressions between the depuration rate constants (k_2; day^{-1}) of PACs and their associated molecular weights (g mol^{-1}) for all three dilbit-contaminated treatments. All regression analyses were conducted in R studio.

Treatment	Sample Size	Equation	R^2	p-value
Low	29 PACs	y = 0.0013x – 0.17	0.19	0.019
Medium	29 PACs	y = 0.00040x + 0.035	0.024	0.42
High	29 PACs	y = 0.00014x + 0.068	0.0032	0.77

Table E.18: Kruskal-Wallis rank sum test to compare PAC BCF values (L day^{-1}) between the Low (n=29), Medium (n=29), and High treatments (n=29). Normality (Shapiro-Wilk test) assumption was not met to conduct a parametric statistical test. The statistical analysis was conducted in R Studio.

Statistical Test	Transformation	p-value	Shapiro-Wilk Test	Levene's Test
Kruskal-Wallis	Log-transformation	0.24	1.98×10^{-4}	0.24

Table E.19: Unpaired two samples Welch t-test to compare parent and alkylated PAC BCF values (L day^{-1}). Normality (Shapiro-Wilk test) assumption was met but homogeneity of variances (Levene's test) assumption was not. Dilbit-contaminated treatments were pooled together. Only parent PACs with alkylated homologues analysed were included. The statistical analysis was conducted in R Studio.

Statistical Test	Parent PACs log BCFs	Alkyl PACs log BCFs	p-value	Shapiro-Wilk Test		Levene's Test
				Parent	Parent	
Welch t-test	4.60 ± 0.20 L day^{-1} n=54	4.69 ± 0.38 L day^{-1} n=30	0.18	0.95	0.74	0.0043

Table E.20: Linear regressions between log-transformed bioconcentration factors of the 29 PACs that accumulated in mussel tissue and their associated log K_{OW} values. Linear regressions were conducted in R Studio.

Treatment	Sample Size	Equation	R^2	p-value
Low	29	y = -0.033x + 4.96	0.0024	0.80
Medium	29	y = -0.080x + 5.09	0.024	0.43
High	29	y = 0.032x + 4.42	0.0046	0.73

Appendix F: Metal and Sulfur Concentrations

Table F.1: Total metal and sulfur concentrations in exposure water (μg L^{-1}) used for the mussel bioaccumulation experiment. Samples from Lake 260 (L260) were also collected.

Sample	Day	Treatment	Aluminum	Antimony	Arsenic	Barium	Boron	Cadmium	Calcium
DB-1389	1	High	68.03	0.044	0.13	3.28	4.15	0.00048	3032.78
DB-1343	2	Control	31.50	0.042	0.15	5.55	3.79	0.00048	2491.48
DB-1345	2	Medium	11.27	0.039	0.10	3.48	4.21	0.00048	2559.48
DB-1463	2	High	16.39	0.046	0.10	2.61	3.55	0.00048	2894.98
DB-1385	5	Control	25.53	0.061	0.16	5.89	3.77	0.00048	2509.68
DB-1386	5	Low	10.30	0.042	0.11	3.10	3.33	0.00048	2529.48
DB-1387	5	Medium	14.63	0.040	0.12	3.45	3.57	0.00048	2423.48
DB-1532	5	High	22.60	0.043	0.10	2.58	3.48	0.00048	3081.78
DB-1529	11	Control	22.53	0.049	0.15	6.69	3.83	0.00048	2487.58
DB-1530	11	Low	14.40	0.049	0.099	2.79	3.48	0.00048	2561.18
DB-1531	11	Medium	105.51	0.047	0.11	7.60	3.66	0.00048	2445.28
DB-1575	11	High	19.95	0.042	0.089	3.00	3.37	0.00048	2932.08
DB-1572	20	Control	21.59	0.050	0.15	4.59	3.62	0.00048	2610.68
DB-1573	20	Low	14.95	0.043	0.091	2.19	3.45	0.00048	2564.28
DB-1574	20	Medium	21.90	0.039	0.090	3.24	3.85	0.00048	2467.08
DB-1769	20	High	11.09	0.048	0.098	1.73	3.49	0.00048	2972.68
DB-1770	25	Control	106.50	0.062	0.17	5.23	4.04	0.00048	2747.88
DB-1771	25	Low	32.88	0.064	0.10	2.65	3.78	0.00048	2610.28
DB-1772	25	Medium	86.74	0.044	0.12	3.59	4.12	0.00048	2507.88
DB-1830	25	High	10.90	0.054	0.11	1.62	3.69	0.00048	3007.48
DB-1798	27	L260	2.83	0.031	0.072	4.12	3.63	0.00048	2044.68
DB-1837	29	L260	2.50	0.032	0.077	5.18	3.57	0.00048	2041.18
DB-1867	33	L260	4.77	0.028	0.068	4.01	3.64	0.00048	2107.88
DB-2014	41	L260	4.28	0.029	0.083	4.11	3.57	0.00048	2152.18

Sample	Day	Treatment	Chromium	Cobalt	Copper	Iron	Lead	Magnesium
DB-1389	1	High	0.0032	0.00053	0.55	58.82	0.00080	686.96
DB-1343	2	Control	0.0032	0.00053	0.0012	68.75	0.00080	596.39
DB-1345	2	Medium	0.0032	0.00053	0.064	32.62	0.00080	588.17
DB-1463	2	High	0.0032	0.00053	0.0012	29.68	0.00080	665.41
DB-1385	5	Control	0.0032	0.00053	0.0012	78.11	0.00080	589.50
DB-1386	5	Low	0.0032	0.00053	0.0012	45.13	0.00080	587.78
DB-1387	5	Medium	0.0032	0.00053	0.18	33.04	0.00080	572.77
DB-1532	5	High	0.0032	0.00053	0.0012	38.63	0.00080	673.46
DB-1529	11	Control	0.0032	0.00053	0.0012	73.85	0.00080	593.62
DB-1530	11	Low	0.0032	0.00053	0.0012	43.70	0.00080	595.41
DB-1531	11	Medium	0.0032	0.00053	0.0012	41.53	0.00080	582.75
DB-1575	11	High	0.0032	0.00053	0.0012	27.10	0.00080	669.15
DB-1572	20	Control	0.0032	0.00053	0.0012	35.42	0.00080	617.13
DB-1573	20	Low	0.0032	0.00053	0.0012	38.04	0.00080	595.72
DB-1574	20	Medium	0.0032	0.00053	0.0012	32.30	0.00080	587.95
DB-1769	20	High	0.0032	0.00053	0.0012	29.33	0.00080	679.97
DB-1770	25	Control	0.0032	0.00053	0.26	85.10	0.00080	657.88
DB-1771	25	Low	0.0032	0.00053	0.0012	49.20	0.00080	606.26
DB-1772	25	Medium	0.0032	0.00053	0.18	76.28	0.00080	605.61
DB-1830	25	High	0.0032	0.00053	0.0012	34.29	0.00080	688.45
DB-1798	27	L260	0.0032	0.00053	0.44	22.36	0.00080	532.32
DB-1837	29	L260	0.0032	0.00053	0.0012	16.35	0.00080	530.25
DB-1867	33	L260	0.0032	0.00053	0.0012	18.17	0.00080	533.32
DB-2014	41	L260	0.0032	0.00053	0.0012	20.32	0.00080	539.97

Sample	Day	Treatment	Manganese	Molybdenum	Nickel	Phosphorus	Potassium	Scandium
DB-1389	1	High	19.76	0.067	0.020	5.69	483.10	0.061
DB-1343	2	Control	49.72	0.038	0.020	5.69	452.19	0.014
DB-1345	2	Medium	10.07	0.070	0.020	5.69	402.11	0.040
DB-1463	2	High	19.28	0.046	0.020	5.69	445.75	0.033
DB-1385	5	Control	55.58	0.048	0.020	5.69	451.98	0.015
DB-1386	5	Low	18.78	0.034	0.020	5.69	424.29	0.033
DB-1387	5	Medium	10.33	0.031	0.020	5.69	404.18	0.038
DB-1532	5	High	19.03	0.065	0.020	5.69	480.86	0.044
DB-1529	11	Control	48.60	0.039	0.020	5.69	455.38	0.011
DB-1530	11	Low	13.52	0.031	0.020	5.69	426.55	0.042
DB-1531	11	Medium	11.50	0.032	0.020	5.69	394.61	0.049
DB-1575	11	High	20.07	0.052	0.020	5.69	440.82	0.050
DB-1572	20	Control	16.73	0.053	0.020	5.69	476.44	0.018
DB-1573	20	Low	11.28	0.029	0.020	5.69	423.53	0.045
DB-1574	20	Medium	9.90	0.035	0.020	5.69	391.93	0.054
DB-1769	20	High	22.65	0.049	0.020	5.69	452.64	0.058
DB-1770	25	Control	16.24	0.043	0.020	13.10	517.95	0.023
DB-1771	25	Low	10.25	0.030	0.020	11.03	445.76	0.034
DB-1772	25	Medium	11.76	0.031	0.020	5.69	412.14	0.075
DB-1830	25	High	25.58	0.051	0.020	13.45	459.21	0.064
DB-1798	27	L260	7.42	0.013	0.020	5.69	334.70	0.053
DB-1837	29	L260	7.22	0.010	0.020	5.69	324.21	0.072
DB-1867	33	L260	7.39	0.0084	0.020	5.69	321.63	0.061
DB-2014	41	L260	7.26	0.0075	0.020	5.69	328.59	0.066

Sample	Day	Treatment	Sodium	Strontium	Sulfur	Tin	Titanium	Vanadium	Zinc
DB-1389	1	High	768.84	14.06	907.98	0.00025	2.69	0.21	39.48
DB-1343	2	Control	748.77	11.61	445.51	0.00025	0.98	0.096	10.26
DB-1345	2	Medium	717.58	11.85	639.99	0.00025	0.55	0.14	30.26
DB-1463	2	High	720.69	13.64	915.40	0.00025	0.96	0.16	31.22
DB-1385	5	Control	748.90	11.46	433.08	0.00025	0.84	0.096	8.12
DB-1386	5	Low	705.99	11.99	567.80	0.00025	0.64	0.15	49.80
DB-1387	5	Medium	722.41	11.55	623.33	0.00025	0.78	0.14	26.60
DB-1532	5	High	792.09	13.74	932.58	0.00025	1.77	0.17	43.90
DB-1529	11	Control	757.74	11.51	447.83	0.00025	0.61	0.081	6.14
DB-1530	11	Low	710.99	12.10	554.99	0.00025	0.89	0.14	44.35
DB-1531	11	Medium	708.67	11.77	628.01	0.00025	1.41	0.17	23.14
DB-1575	11	High	716.95	13.70	944.47	0.00025	0.51	0.16	24.41
DB-1572	20	Control	777.01	12.06	447.45	0.00025	0.66	0.062	2.48
DB-1573	20	Low	721.43	12.07	574.83	0.00025	0.67	0.16	37.05
DB-1574	20	Medium	711.20	11.75	627.86	0.00025	1.40	0.16	16.54
DB-1769	20	High	737.41	13.86	978.42	0.00025	0.72	0.18	49.16
DB-1770	25	Control	869.51	12.74	495.13	0.00025	4.06	0.16	46.77
DB-1771	25	Low	815.18	12.19	605.12	0.00025	1.61	0.19	63.22
DB-1772	25	Medium	802.47	11.94	638.12	0.00025	4.36	0.25	42.45
DB-1830	25	High	747.02	13.95	1001.52	0.00025	0.97	0.20	87.09
DB-1798	27	L260	662.58	9.66	439.45	0.00025	0.47	0.020	0.28
DB-1837	29	L260	657.19	9.63	433.12	0.00025	0.43	0.018	0.068
DB-1867	33	L260	657.24	9.69	452.29	0.00025	0.70	0.020	0.0055
DB-2014	41	L260	665.93	9.79	460.70	0.00025	0.51	0.022	0.0055

Table F.2: Dissolved metal and sulfur concentrations in exposure water (µg L^{-1}) used for the mussel bioaccumulation experiment. Samples from Lake 260 (L260) were also collected.

Sample	Day	Treatment	Aluminum	Antimony	Arsenic	Barium	Boron	Cadmium
DB-1389 (D)	1	High	3.61	0.0047	0.084	2.14	3.76	0.00048
DB-1343 (D)	2	Control	1.90	0.012	0.11	7.06	4.00	0.00048
DB-1342 (D)	2	Low	0.80	0.0079	0.083	2.79	3.33	0.012
DB-1345 (D)	2	Medium	1.34	0.00023	0.070	2.92	3.86	0.00048
DB-1463 (D)	2	High	4.30	0.020	0.097	2.30	3.90	0.00048
DB-1385 (D)	5	Control	0.0050	0.0084	0.12	4.82	3.86	0.00048
DB-1386 (D)	5	Low	1.25	0.0048	0.090	2.54	3.38	0.0069
DB-1387 (D)	5	Medium	4.22	0.0055	0.084	3.18	3.69	0.00048
DB-1532 (D)	5	High	30.23	0.027	0.12	3.02	11.70	0.0021
DB-1529 (D)	10	Control	1.06	0.015	0.13	5.05	4.04	0.00048
DB-1530 (D)	10	Low	1.33	0.011	0.082	2.45	3.67	0.00048
DB-1531 (D)	10	Medium	10.55	0.022	0.16	5.62	4.20	0.00048
DB-1575 (D)	10	High	0.69	0.0017	0.079	1.85	3.67	0.00048
DB-1572 (D)	20	Control	6.91	0.035	0.12	4.15	4.24	0.0025
DB-1573 (D)	20	Low	3.22	0.010	0.100	1.95	3.99	0.00051
DB-1574 (D)	20	Medium	8.25	0.0017	0.081	2.73	4.15	0.00048
DB-1769 (D)	20	High	2.06	0.013	0.10	2.06	3.97	0.00048
DB-1770 (D)	25	Control	1.66	0.021	0.13	4.19	4.00	0.00048
DB-1771 (D)	25	Low	11.96	0.23	0.14	5.77	10.64	0.050
DB-1772 (D)	25	Medium	2.03	0.0057	0.078	2.69	4.31	0.00048
DB-1830 (D)	25	High	0.32	0.024	0.076	1.83	3.76	0.00048
DB-1798(D)	27	L260	0.0050	0.00023	0.058	3.84	3.82	0.00048
DB-1837(D)	29	L260	0.48	0.00023	0.060	4.51	3.70	0.00048
DB-1867(D)	33	L260	0.0050	0.00023	0.048	4.00	3.82	0.00048
DB-2014(D)	42	L260	0.0050	0.0021	0.055	3.97	3.78	0.00048

Sample	Day	Treatment	Calcium	Chromium	Cobalt	Copper	Iron	Lead
DB-1389 (D)	1	High	3183.28	0.0032	0.0058	0.34	24.30	0.00080
DB-1343 (D)	2	Control	2482.68	0.0032	0.0036	0.32	11.45	0.00080
DB-1342 (D)	2	Low	2531.58	0.0032	0.00053	0.11	8.15	0.00080
DB-1345 (D)	2	Medium	2421.38	0.0032	0.00053	0.26	9.33	0.00080
DB-1463 (D)	2	High	2944.88	0.0032	0.0021	0.38	14.60	0.00080
DB-1385 (D)	5	Control	2438.88	0.0032	0.0033	0.15	10.16	0.00080
DB-1386 (D)	5	Low	2536.78	0.0032	0.0092	0.21	35.01	0.00080
DB-1387 (D)	5	Medium	2466.78	0.0032	0.0037	0.43	14.89	0.00080
DB-1532 (D)	5	High	3802.08	0.0032	0.023	4.51	22.25	0.00080
DB-1529 (D)	10	Control	2497.28	0.0032	0.0020	0.20	8.06	0.00080
DB-1530 (D)	10	Low	2563.38	0.0032	0.00053	0.14	7.49	0.00080
DB-1531 (D)	10	Medium	2483.08	0.0032	0.060	0.70	353.95	0.00080
DB-1575 (D)	10	High	2903.78	0.0032	0.00053	0.12	4.28	0.00080
DB-1572 (D)	20	Control	2666.08	0.23	0.014	0.27	253.37	5.43
DB-1573 (D)	20	Low	2578.38	0.0032	0.0051	0.29	11.33	0.00080
DB-1574 (D)	20	Medium	2487.78	0.0032	0.0086	0.17	14.29	0.00080
DB-1769 (D)	20	High	2954.88	0.0032	0.0033	0.15	7.73	0.00080
DB-1770 (D)	25	Control	2710.38	0.0032	0.0034	0.28	4.68	0.00080
DB-1771 (D)	25	Low	2878.48	0.054	0.054	4.56	14.43	0.00080
DB-1772 (D)	25	Medium	2471.28	0.0032	0.00053	0.34	8.02	0.00080
DB-1830 (D)	25	High	2976.08	0.0032	0.00053	0.073	15.43	0.00080
DB-1798(D)	27	L260	2050.08	0.0032	0.0047	0.38	3.92	0.00080
DB-1837(D)	29	L260	2047.38	0.0032	0.0012	0.056	10.66	0.00080
DB-1867(D)	33	L260	2041.38	0.0032	0.0023	0.046	6.05	0.00080
DB-2014(D)	42	L260	1987.68	0.0032	0.00053	0.25	10.33	0.00080

Sample	Day	Treatment	Magnesium	Manganese	Molybdenum	Nickel	Phosphorus
DB-1389 (D)	1	High	708.26	0.25	0.0066	0.27	5.69
DB-1343 (D)	2	Control	596.10	9.69	0.0066	0.38	5.69
DB-1342 (D)	2	Low	594.56	0.13	0.0066	0.15	5.69
DB-1345 (D)	2	Medium	581.67	0.13	0.0066	0.073	5.69
DB-1463 (D)	2	High	679.82	0.22	0.033	0.22	5.69
DB-1385 (D)	5	Control	587.23	16.89	0.0066	0.11	5.69
DB-1386 (D)	5	Low	592.26	0.31	0.0093	1.15	5.69
DB-1387 (D)	5	Medium	579.26	0.14	0.0066	0.29	5.69
DB-1532 (D)	5	High	747.15	1.51	0.38	0.74	5.69
DB-1529 (D)	10	Control	591.64	0.28	0.0066	0.54	5.69
DB-1530 (D)	10	Low	599.28	0.11	0.0066	0.40	5.69
DB-1531 (D)	10	Medium	590.67	3.75	0.012	0.69	5.69
DB-1575 (D)	10	High	667.56	0.014	0.0066	0.33	5.69
DB-1572 (D)	20	Control	624.75	1.17	0.027	0.27	5.69
DB-1573 (D)	20	Low	602.33	0.14	0.0066	0.34	5.69
DB-1574 (D)	20	Medium	587.39	5.32	0.0066	0.22	5.69
DB-1769 (D)	20	High	683.44	0.090	0.0076	0.083	5.69
DB-1770 (D)	25	Control	634.94	6.40	0.0066	0.088	5.69
DB-1771 (D)	25	Low	627.48	6.07	0.16	3.84	15.19
DB-1772 (D)	25	Medium	588.75	0.12	0.0066	0.13	5.69
DB-1830 (D)	25	High	687.20	0.11	0.016	0.020	5.69
DB-1798(D)	27	L260	539.09	0.026	0.0066	0.041	5.69
DB-1837(D)	29	L260	539.83	0.099	0.0066	0.020	5.69
DB-1867(D)	33	L260	538.43	0.083	0.0066	0.13	5.69
DB-2014(D)	42	L260	527.31	0.14	0.0066	2.12	5.69

Sample	Day	Treatment	Potassium	Scandium	Sodium	Strontium	Sulfur
DB-1389 (D)	1	High	517.12	0.055	876.93	14.27	925.54
DB-1343 (D)	2	Control	456.49	0.022	796.72	11.46	439.63
DB-1342 (D)	2	Low	419.79	0.048	733.38	11.95	550.59
DB-1345 (D)	2	Medium	389.25	0.048	730.70	11.53	626.39
DB-1463 (D)	2	High	458.57	0.064	781.57	13.75	898.60
DB-1385 (D)	5	Control	439.67	0.021	780.51	11.23	439.58
DB-1386 (D)	5	Low	423.28	0.060	743.19	11.93	559.48
DB-1387 (D)	5	Medium	395.10	0.056	756.07	11.54	613.32
DB-1532 (D)	5	High	577.48	0.059	956.01	15.27	1002.77
DB-1529 (D)	10	Control	451.35	0.021	793.82	11.31	503.36
DB-1530 (D)	10	Low	421.17	0.050	743.19	12.05	552.96
DB-1531 (D)	10	Medium	395.12	0.059	759.23	11.75	619.56
DB-1575 (D)	10	High	431.52	0.053	742.44	13.53	913.00
DB-1572 (D)	20	Control	477.06	0.026	812.25	12.08	437.61
DB-1573 (D)	20	Low	421.36	0.059	757.66	12.02	564.55
DB-1574 (D)	20	Medium	394.02	0.079	748.09	11.71	629.17
DB-1769 (D)	20	High	450.36	0.059	792.07	13.75	964.04
DB-1770 (D)	25	Control	488.97	0.023	880.96	12.39	453.51
DB-1771 (D)	25	Low	977.15	0.035	1705.79	12.68	708.17
DB-1772 (D)	25	Medium	390.41	0.078	885.79	11.71	628.60
DB-1830 (D)	25	High	445.05	0.068	771.34	13.77	1018.37
DB-1798(D)	27	L260	333.26	0.088	695.04	9.63	443.88
DB-1837(D)	29	L260	324.54	0.084	692.09	9.66	448.51
DB-1867(D)	33	L260	321.27	0.085	694.30	9.62	440.87
DB-2014(D)	42	L260	317.77	0.068	682.88	9.41	438.55

Sample	Day	Treatment	Tin	Titanium	Vanadium	Zinc
DB-1389 (D)	1	High	0.00025	0.22	0.083	34.62
DB-1343 (D)	2	Control	0.00025	1.07	0.031	7.08
DB-1342 (D)	2	Low	0.00025	0.14	0.072	46.32
DB-1345 (D)	2	Medium	0.00025	0.12	0.082	25.05
DB-1463 (D)	2	High	0.00025	0.39	0.095	26.35
DB-1385 (D)	5	Control	0.00025	0.062	0.028	4.00
DB-1386 (D)	5	Low	0.00025	0.20	0.081	39.68
DB-1387 (D)	5	Medium	0.00025	0.32	0.10	21.73
DB-1532 (D)	5	High	0.00025	0.88	0.12	33.83
DB-1529 (D)	10	Control	0.00025	0.062	0.023	2.86
DB-1530 (D)	10	Low	0.00025	0.20	0.082	37.85
DB-1531 (D)	10	Medium	0.00025	0.41	0.12	30.56
DB-1575 (D)	10	High	0.00025	0.18	0.084	17.38
DB-1572 (D)	20	Control	0.00025	1.53	0.024	1.67
DB-1573 (D)	20	Low	0.00025	0.22	0.095	29.20
DB-1574 (D)	20	Medium	0.00025	0.33	0.11	14.47
DB-1769 (D)	20	High	0.00025	0.33	0.11	40.25
DB-1770 (D)	25	Control	0.00025	0.062	0.035	40.52
DB-1771 (D)	25	Low	0.25	0.69	0.13	87.92
DB-1772 (D)	25	Medium	0.00025	0.21	0.11	36.15
DB-1830 (D)	25	High	0.00025	0.20	0.11	70.24
DB-1798(D)	27	L260	0.00025	0.25	0.0096	0.0055
DB-1837(D)	29	L260	0.00025	0.25	0.009	0.0055
DB-1867(D)	33	L260	0.00025	0.23	0.007	0.0055
DB-2014(D)	42	L260	0.00025	0.24	0.006	0.060

Table F.3: Metal and sulfur concentrations in the sand ($\mu g\ g^{-1}$, dw) collected from the mussel bioaccumulation study.

Sample	Day	Treatment	Aluminum	Antimony	Arsenic	Barium	Boron	Cadmium	Calcium	Chromium	Cobalt	Copper	Iron
A	0	Control	2847.78	0.010	0.12	14.06	1.11	0.050	737.77	3.00	1.20	3.65	2876.60
B	0	High	2328.95	0.010	0.12	9.26	1.16	0.018	439.55	2.86	1.15	3.94	2663.68
O	11	Control	3120.13	0.010	0.16	20.08	1.27	0.031	1535.24	3.11	1.34	4.95	3373.21
R	11	High	3111.90	0.010	0.20	19.05	1.22	0.087	673.96	3.07	1.15	4.75	2987.78
W	25	Control	2922.60	0.010	0.17	11.46	1.17	0.032	496.43	2.73	1.45	4.76	3086.06
Z	25	High	2740.86	0.010	0.16	12.36	0.87	0.054	554.87	2.92	1.11	4.70	2521.66

Sample	Day	Treatment	Lead	Magnesium	Manganese	Molybdenum	Nickel	Phosphorus	Potassium	Scandium	Sodium
A	0	Control	3.84	794.29	60.08	0.037	1.84	360.02	986.47	0.24	331.46
B	0	High	2.98	687.29	49.39	0.037	1.95	282.39	705.48	0.14	197.86
O	11	Control	4.58	796.04	85.29	0.037	2.27	456.23	940.51	0.26	309.16
R	11	High	6.26	790.44	58.02	0.037	2.13	339.70	908.88	0.31	318.52
W	25	Control	4.40	769.49	58.43	0.037	2.23	365.92	760.12	0.21	251.19
Z	25	High	4.31	639.41	52.81	0.037	2.23	337.48	619.61	0.22	223.60

Sample	Day	Treatment	Strontium	Sulfur	Tin	Titanium	Vanadium	Zinc
A	0	Control	12.46	79.92	10.92	171.8	4.83	4.77
B	0	High	2.48	56.37	6.12	250.82	4.83	7.14
O	11	Control	38.52	61.51	13.24	175.43	5.63	6.02
R	11	High	6.97	64.6	12.19	199.81	4.79	5.28
W	25	Control	2.53	61.71	10.75	178.01	4.94	4.77
Z	25	High	2.99	63.32	8.49	121.43	4.35	5.5

Table F.4: Metal and sulfur concentrations (µg g^{-1}, dw) in mussel tissue collected from the Control and High treatment during the uptake phase of the bioaccumulation study.

Sample	Day	Treatment	Aluminum	Antimony	Arsenic	Barium	Boron	Cadmium	Calcium
1	0	—	725.7	0.010	1.90	578.1	1.00	0.62	21978
2	0	—	1037.4	0.010	2.15	394.1	1.13	0.65	28969
3	0	—	1430.2	0.010	3.02	968.1	1.21	0.95	38975
5	1	Control	1928.3	0.010	2.26	1021.4	1.38	0.52	52197
6	1	Control	1343.3	0.010	3.20	847.3	1.37	0.56	24627
7	1	Control	1904.9	0.010	2.97	1209.2	1.19	0.77	45027
14	1	High	447.3	0.010	2.39	554.2	1.19	0.80	21872
15	1	High	675.4	0.010	2.23	487.4	1.48	0.67	16355
16	1	High	562.8	0.010	3.05	840.3	1.41	0.90	21304
17	2	Control	1026.3	0.010	2.19	1005.6	1.65	0.69	83055
24	2	Control	943.4	0.020	2.35	709.3	1.17	0.86	50893
19	2	Control	801.7	0.010	2.21	598.1	1.06	0.63	17822
26	2	High	551.4	0.010	1.98	642.4	1.15	0.72	50694
27	2	High	520.2	0.010	2.51	947.1	1.21	0.88	24752
28	2	High	1205.2	0.010	1.80	302.9	1.09	0.67	43150
29	5	Control	600.0	0.010	2.47	759.1	1.37	0.97	41090
30	5	Control	566.4	0.010	4.21	661.8	1.18	1.30	20009
31	5	Control	443.2	0.010	2.06	564.4	1.22	0.83	36298
38	5	High	390.8	0.010	1.92	378.3	1.02	0.60	14941
39	5	High	374.1	0.010	2.66	555.8	1.32	0.81	23546
40	5	High	696.5	0.010	2.62	798.3	1.80	0.77	48203
41	11	Control	1033.7	0.010	2.15	594.0	1.04	0.81	64126
42	11	Control	808.9	0.010	3.07	857.9	1.42	1.02	26672
43	11	Control	1370.0	0.010	2.44	744.5	1.22	0.72	59591
50	11	High	941.1	0.010	1.91	542.7	1.04	0.64	37911
51	11	High	726.8	0.010	2.32	476.1	1.09	0.74	12198
52	11	High	864.8	0.050	3.29	1033.0	4.00	0.87	27523
53	20	Control	992.0	0.010	2.30	601.3	0.96	0.87	48917
54	20	Control	895.8	0.010	2.21	923.6	1.51	1.00	64942
55	20	Control	652.8	0.010	2.13	559.6	0.82	1.02	52705
62	20	High	727.5	0.010	1.86	470.2	0.96	0.66	56185
63	20	High	657.1	0.010	1.80	566.0	0.86	0.62	60095
64	20	High	352.3	0.010	1.89	451.8	0.94	0.65	56285
65	25	Control	254.2	0.010	1.43	409.5	0.10	0.54	16499
67	25	Control	847.8	0.010	2.03	453.9	0.10	0.85	21520
74	25	High	353.8	0.020	1.88	731.2	0.92	0.66	50134
75	25	High	289.3	0.050	2.95	1032.4	0.10	0.58	22867
76	25	High	239.2	0.010	1.27	714.1	0.10	0.44	41348

Sample	Day	Treatment	Chromium	Cobalt	Copper	Iron	Lead	Magnesium	Manganese
1	0	—	3.40	0.91	7.9	6698	4.86	618	4751
2	0	—	4.87	1.02	8.6	5239	2.65	706	3219
3	0	—	7.45	1.67	9.4	9861	3.08	1004	10100
5	1	Control	34.90	1.89	8.9	8340	3.39	1088	12407
6	1	Control	6.71	1.50	10.4	17176	2.71	716	4975
7	1	Control	9.90	1.87	10.0	17492	3.27	1003	12095
14	1	High	4.19	1.11	7.6	6159	2.24	739	5348
15	1	High	8.20	0.86	7.7	8093	1.53	695	3179
16	1	High	7.15	1.13	9.4	14774	3.20	855	3934
17	2	Control	9.64	1.65	10.5	10457	3.27	1085	12307
24	2	Control	6.86	1.57	9.8	9370	2.76	792	12494
19	2	Control	4.63	1.06	8.7	8170	3.58	646	3484
26	2	High	7.31	1.01	11.0	5311	4.27	825	6985
27	2	High	6.93	1.18	14.7	15485	7.23	783	5037
28	2	High	3.77	1.02	10.4	4611	3.69	743	5961
29	5	Control	6.00	1.30	37.1	4236	6.56	917	9830
30	5	Control	5.97	1.34	11.3	8282	22.20	738	3527
31	5	Control	6.45	1.41	11.1	7760	5.32	785	8230
38	5	High	5.01	0.77	10.0	4629	3.43	697	2106
39	5	High	4.20	1.07	10.2	7576	3.11	951	4824
40	5	High	10.22	1.37	12.6	9371	3.72	1165	11230
41	11	Control	6.25	1.38	38.9	5324	7.11	832	7797
42	11	Control	9.62	1.33	13.0	9726	3.98	991	5735
43	11	Control	5.80	1.67	17.9	7702	6.42	1240	12985
50	11	High	4.47	1.25	17.9	6346	2.75	908	6548
51	11	High	5.14	1.00	9.6	8164	3.38	744	1804
52	11	High	7.85	1.24	33.8	16285	3.41	1029	4013
53	20	Control	8.48	1.57	35.8	6905	5.07	897	6197
54	20	Control	16.05	1.49	42.0	7860	4.04	1067	9823
55	20	Control	4.10	1.16	11.5	4462	3.99	1003	7107
62	20	High	18.28	1.19	11.1	4603	3.24	1064	5959
63	20	High	5.63	1.01	11.0	5233	5.23	1006	6458
64	20	High	10.10	1.11	31.0	3910	5.88	771	5522
65	25	Control	4.92	0.75	24.7	3735	16.76	722	2929
67	25	Control	11.18	1.27	10.2	8901	15.58	1000	4145
74	25	High	7.17	1.16	44.2	10919	5.46	750	10330
75	25	High	7.18	1.23	448.1	14699	5.62	850	4867
76	25	High	3.86	1.15	20.0	6361	4.07	779	9267

Sample	Day	Treatment	Molybdenum	Nickel	Phosphorus	Potassium	Scandium	Sodium
1	0	—	0.33	1.34	17747	1652	0.047	1480
2	0	—	0.37	2.33	15945	1766	0.047	1223
3	0	—	0.64	2.93	31537	1686	0.047	1591
5	1	Control	0.40	15.76	39462	807	0.047	1298
6	1	Control	0.46	1.81	24957	951	0.047	1641
7	1	Control	0.53	3.55	37666	780	0.047	1595
14	1	High	0.43	1.56	19746	1318	0.047	3677
15	1	High	0.33	3.43	15925	1076	0.047	2640
16	1	High	0.52	2.21	21459	1367	0.047	3833
17	2	Control	0.43	4.65	36541	902	0.047	2283
24	2	Control	0.39	2.55	37208	1050	0.047	2555
19	2	Control	0.36	1.59	16844	984	0.047	2160
26	2	High	0.33	4.04	24978	1354	0.047	3319
27	2	High	0.44	2.97	22267	1345	0.047	3986
28	2	High	0.31	2.43	20199	1300	0.047	2794
29	5	Control	0.46	3.01	30641	1347	0.047	2694
30	5	Control	0.64	1.66	18025	955	0.047	2544
31	5	Control	0.51	2.62	27173	1380	0.047	3018
38	5	High	0.37	2.19	12960	1269	0.047	3417
39	5	High	0.41	1.92	20261	1692	0.047	6553
40	5	High	0.54	4.54	34057	1706	0.047	5278
41	11	Control	0.37	4.86	26953	1367	0.047	3891
42	11	Control	0.51	3.69	22984	1324	0.047	4199
43	11	Control	0.45	3.03	36183	1462	0.047	4695
50	11	High	0.32	2.82	23164	1395	0.047	3596
51	11	High	0.37	1.75	13829	1459	0.047	4276
52	11	High	0.51	7.84	21223	1505	0.047	3893
53	20	Control	0.42	4.30	22256	2033	0.047	5979
54	20	Control	0.48	9.16	31020	1646	0.047	4801
55	20	Control	0.40	2.40	24682	2189	0.047	7609
62	20	High	0.40	9.11	22259	1943	0.047	6148
63	20	High	0.34	3.48	23504	1258	0.047	3741
64	20	High	0.39	5.93	20861	1474	0.047	5729
65	25	Control	0.37	2.26	12568	1248	0.047	5062
67	25	Control	0.61	4.63	17869	1434	0.047	6161
74	25	High	0.37	2.28	31327	871	0.047	3540
75	25	High	0.56	3.56	20990	1314	0.047	4840
76	25	High	0.35	2.39	25095	928	0.047	3852

Sample	Day	Treatment	Strontium	Sulfur	Tin	Titanium	Vanadium	Zinc
1	0	—	120.0	5071	96.75	63.2	0.79	85.1
2	0	—	100.9	5452	66.48	70.8	1.26	98.0
3	0	—	242.0	6293	62.73	122.5	1.53	138.3
5	1	Control	307.1	5290	67.34	146.5	1.91	138.7
6	1	Control	169.5	7164	72.74	107.0	1.58	130.5
7	1	Control	315.3	6243	37.37	152.9	2.05	171.5
14	1	High	135.0	7128	68.51	62.8	0.48	123.4
15	1	High	113.1	6475	54.01	66.1	0.71	121.7
16	1	High	159.2	8963	77.09	70.4	0.75	139.8
17	2	Control	351.5	6429	85.38	136.7	1.28	175.1
24	2	Control	267.3	6601	62.22	130.6	1.13	190.5
19	2	Control	114.4	6630	56.98	70.4	0.89	112.4
26	2	High	214.0	6673	52.70	89.0	0.76	130.9
27	2	High	187.0	7480	30.14	75.2	0.78	154.1
28	2	High	167.4	6007	51.50	91.5	1.41	127.0
29	5	Control	236.0	6824	36.51	94.1	1.04	146.2
30	5	Control	130.7	7836	46.37	64.7	4.47	117.3
31	5	Control	198.9	6791	43.13	78.2	0.47	136.1
38	5	High	81.8	6815	72.40	41.4	0.50	141.3
39	5	High	144.1	7759	26.69	61.9	0.39	150.6
40	5	High	336.2	7121	63.58	131.1	0.88	195.3
41	11	Control	240.7	6507	50.87	111.3	1.48	144.2
42	11	Control	180.5	7932	33.62	84.4	1.12	141.9
43	11	Control	306.7	7531	63.13	149.4	1.84	179.8
50	11	High	188.8	6130	57.48	114.4	1.31	152.9
51	11	High	87.8	6777	77.30	59.4	0.88	141.1
52	11	High	432.9	7188	20.14	78.1	8.05	190.6
53	20	Control	195.8	6949	56.04	89.7	1.09	126.4
54	20	Control	288.7	6810	60.08	116.3	1.18	159.2
55	20	Control	220.8	7152	42.26	84.2	0.80	138.8
62	20	High	208.4	7118	58.85	86.9	1.10	145.1
63	20	High	222.9	6272	64.36	82.2	0.92	182.4
64	20	High	191.0	6234	46.92	59.3	0.48	169.5
65	25	Control	94.4	5361	15.14	25.6	0.39	102.6
67	25	Control	150.3	6233	32.96	52.2	1.13	141.0
74	25	High	280.3	4650	141.26	96.6	0.43	161.1
75	25	High	182.7	6062	61.41	42.4	0.52	207.2
76	25	High	227.6	4026	63.07	48.5	0.34	185.0

Table F.5: Metal and sulfur concentrations (µg g^{-1}, dw) in mussel tissue collected from the Control and High treatment during the depuration phase of the bioaccumulation study.

Sample	Day	Treatment	Aluminum	Antimony	Arsenic	Barium	Boron	Cadmium	Calcium
77	26	Control	1642.1	0.010	2.20	525.0	0.86	0.90	25071
78	26	Control	2158.2	0.010	2.83	823.3	0.88	1.08	51519
79	26	Control	734.8	0.010	2.37	513.2	0.83	1.27	36069
86	26	High	1449.4	0.010	2.09	613.6	0.98	0.76	59025
87	26	High	1298.7	0.020	2.65	342.2	1.00	0.93	12906
88	26	High	591.9	0.010	2.50	413.3	1.01	1.02	17954
89	27	Control	343.8	0.010	1.32	285.9	0.10	0.71	12646
90	27	Control	1171.2	0.010	2.22	713.4	0.10	1.07	43608
91	27	Control	457.9	0.010	1.35	516.6	0.10	0.59	10113
98	27	High	602.1	0.090	1.78	709.5	0.10	0.67	46875
99	27	High	1045.5	0.050	2.69	165.7	0.10	0.90	19278
100	27	High	654.5	0.020	1.58	309.3	0.10	0.62	11214
101	29	Control	444.2	0.010	1.82	788.7	0.10	1.11	46543
102	29	Control	98.4	0.020	2.16	309.1	0.10	1.12	15192
103	29	Control	124.9	0.010	1.69	374.1	0.10	0.85	12664
110	29	High	511.5	0.010	1.60	511.9	0.10	0.80	18985
111	29	High	789.2	0.010	1.37	332.1	0.10	0.52	11804
112	29	High	686.4	0.010	2.13	1231.1	0.10	1.21	35694
113	33	Control	355.8	0.010	1.72	489.2	0.10	1.12	31563
114	33	Control	956.1	0.010	1.60	660.4	0.29	0.72	38820
115	33	Control	481.8	0.010	1.67	285.9	0.76	0.91	16305
122	33	High	728.3	0.010	1.98	351.9	0.41	0.65	15424
123	33	High	853.2	0.040	1.96	723.5	0.98	0.74	13557
124	33	High	433.7	0.010	1.21	531.7	0.63	0.47	61954
125	41	Control	945.4	0.030	1.62	449.3	0.73	0.70	14152
126	41	Control	386.8	0.010	1.92	879.3	0.78	0.79	45107
127	41	Control	463.4	0.010	1.52	792.5	0.65	0.92	41708
134	41	High	515.3	0.020	1.31	594.0	0.78	0.81	49403
135	41	High	656.5	0.010	1.50	174.4	0.61	0.83	17025
136	41	High	874.5	0.070	1.76	348.8	0.91	0.98	17243

Sample	Day	Treatment	Chromium	Cobalt	Copper	Iron	Lead	Magnesium	Manganese
77	26	Control	6.81	1.23	55.6	7712	4.41	1018	4178
78	26	Control	10.59	2.11	111.7	7248	9.30	1532	10533
79	26	Control	13.47	1.32	88.3	8901	7.32	937	7334
86	26	High	13.42	1.46	133.3	4894	12.48	984	6682
87	26	High	11.67	1.33	106.2	6075	8.15	1049	1698
88	26	High	18.64	1.34	90.2	5574	7.80	1006	2513
89	27	Control	14.06	0.87	100.6	4580	5.54	672	1910
90	27	Control	13.65	1.98	103.3	7301	8.90	1106	10528
91	27	Control	5.70	0.75	41.3	5444	6.58	486	1640
98	27	High	42.51	1.76	372.0	7785	10.25	688	6849
99	27	High	27.35	1.42	485.0	5555	11.11	963	3388
100	27	High	18.41	0.99	150.1	4753	21.24	664	1780
101	29	Control	5.05	1.53	6.8	7945	22.02	1106	12253
102	29	Control	5.83	1.39	28.6	6840	10.19	773	2837
103	29	Control	2.45	0.77	9.2	6908	13.12	663	2089
110	29	High	3.14	0.85	20.0	9131	11.06	755	3383
111	29	High	7.39	1.03	62.8	5260	15.51	640	1717
112	29	High	5.15	1.73	21.9	18938	23.40	1270	8612
113	33	Control	8.00	1.47	75.6	9610	7.62	801	7682
114	33	Control	4.06	1.47	11.4	6284	9.58	813	5458
115	33	Control	4.52	0.69	13.6	4025	17.45	765	2392
122	33	High	6.18	1.04	33.9	7035	6.44	943	2537
123	33	High	11.86	1.08	88.1	11543	22.98	675	2280
124	33	High	2.28	0.83	9.8	4008	65.27	650	5732
125	41	Control	21.26	1.15	195.4	5418	18.33	800	2179
126	41	Control	4.45	1.96	16.6	9068	20.50	932	11415
127	41	Control	9.13	1.07	52.7	6100	5.19	581	5641
134	41	High	21.48	1.42	122.1	5565	8.49	773	4399
135	41	High	2.50	0.74	31.2	4025	3.56	906	2586
136	41	High	31.99	1.66	336.4	5244	14.13	992	3106

Sample	Day	Treatment	Molybdenum	Nickel	Phosphorus	Potassium	Scandium	Sodium
77	26	Control	0.36	3.15	21661	1481	0.047	4047
78	26	Control	0.58	6.56	33011	2397	0.047	10086
79	26	Control	0.48	6.50	27105	1623	0.047	5400
86	26	High	0.42	9.06	23892	1672	0.047	6246
87	26	High	0.50	6.59	12425	1754	0.047	6008
88	26	High	0.65	12.29	15720	2418	0.047	9147
89	27	Control	0.42	9.53	11484	1576	0.047	4707
90	27	Control	0.67	8.51	31832	1408	0.047	4990
91	27	Control	0.32	2.78	9724	1086	0.047	2898
98	27	High	0.86	27.63	21810	1173	0.047	4509
99	27	High	0.74	17.65	16221	1840	0.047	6183
100	27	High	0.47	10.41	11086	1491	0.047	4070
101	29	Control	0.47	2.09	34211	1214	0.047	5866
102	29	Control	0.55	1.56	12840	1590	0.047	6680
103	29	Control	0.34	1.18	12274	1357	0.047	3844
110	29	High	0.39	1.41	15582	1421	0.047	5035
111	29	High	0.36	4.26	10112	1108	0.047	3569
112	29	High	0.66	2.27	29174	1454	0.047	8298
113	33	Control	0.44	4.85	23757	1194	0.047	4672
114	33	Control	0.33	2.65	18338	1364	0.047	4993
115	33	Control	0.35	2.16	13674	1639	0.047	5002
122	33	High	0.47	3.89	13425	1367	0.047	4942
123	33	High	0.42	5.57	15044	1469	0.047	4518
124	33	High	0.26	2.06	18407	737	0.047	2646
125	41	Control	0.53	14.84	11854	1561	0.047	5282
126	41	Control	0.43	1.78	31925	639	0.047	5223
127	41	Control	0.35	4.40	17134	1184	0.047	4044
134	41	High	0.56	18.83	15539	1324	0.047	5799
135	41	High	0.28	1.49	13116	1556	0.047	6420
136	41	High	0.72	25.76	14045	2048	0.047	7912

Sample	Day	Treatment	Strontium	Sulfur	Tin	Titanium	Vanadium	Zinc
77	26	Control	139.0	7380	37.52	106.0	16.79	166.4
78	26	Control	267.4	8620	14.61	124.5	2.77	223.5
79	26	Control	200.0	7478	62.48	78.6	0.90	191.3
86	26	High	212.7	6932	32.78	98.0	1.90	249.2
87	26	High	75.0	7923	22.70	64.5	1.72	225.4
88	26	High	96.4	8576	67.27	50.7	0.93	258.8
89	27	Control	77.1	5288	16.24	25.4	0.49	127.4
90	27	Control	261.2	6247	62.41	79.0	1.49	197.7
91	27	Control	70.5	4390	28.50	32.8	0.60	76.9
98	27	High	205.0	4963	78.86	59.8	0.98	241.8
99	27	High	104.1	6786	41.37	47.6	1.62	257.4
100	27	High	66.5	4726	27.49	41.3	0.94	166.1
101	29	Control	290.0	5697	60.99	77.3	0.49	177.0
102	29	Control	102.7	6907	13.80	23.6	0.19	103.6
103	29	Control	96.2	5145	30.96	25.0	0.21	99.8
110	29	High	132.7	5385	16.98	39.5	0.67	116.3
111	29	High	69.7	4646	7.19	36.7	1.10	145.4
112	29	High	286.2	7036	56.36	77.1	0.83	193.8
113	33	Control	202.0	4922	54.44	55.0	0.41	130.3
114	33	Control	175.6	5234	34.95	68.2	1.22	100.1
115	33	Control	92.5	6475	27.14	35.2	0.54	114.9
122	33	High	111.8	5750	8.98	40.4	0.93	121.2
123	33	High	105.9	4855	156.91	55.2	0.88	114.0
124	33	High	213.6	4216	41.30	52.4	0.46	99.9
125	41	Control	81.8	5434	18.27	53.8	1.18	153.3
126	41	Control	298.1	4192	66.54	86.3	0.37	129.2
127	41	Control	173.0	4381	44.58	55.4	0.53	90.8
134	41	High	182.8	4921	15.98	52.2	0.64	155.8
135	41	High	99.9	5961	4.81	42.8	0.83	104.2
136	41	High	104.8	6443	9.12	50.6	1.29	270.2

Appendix G. Metals and Sulfur Statistics

Table G.1: Statistical analysis to compare water total metal and sulfur concentrations between Lake 260 water (n=4), the Control (n=4), Low (n=3), Medium (n=4), and High (n=5) treatments. One-way ANOVA tests were conducted when the normality (Shapiro-Wilk test) and homogeneity of variances (Levene's test) assumptions were met. When no assumptions were met, Kruskal-Wallis rank sum test were conducted.

Metal	Transformation	Statistical Test	p-value	Shapiro-Wilk Test	Levene's Test
Aluminum	—	Kruskal-Wallis	0.015	—	—
Antimony	Log-transformed	ANOVA	1.22×10^{-5}	0.13	0.76
Arsenic	—	ANOVA	5.07×10^{-7}	0.70	0.92
Barium	Log-transformed	ANOVA	0.0016	0.32	0.87
Boron	—	Kruskal-Wallis	0.030	—	—
Cadmium	—	—	—	—	—
Calcium	—	ANOVA	1.97×10^{-11}	0.16	0.60
Chromium	—	—	—	—	—
Cobalt	—	—	—	—	—
Copper	—	Kruskal-Wallis	0.52	—	—
Iron	—	ANOVA	0.0011	0.11	0.53
Lead	—	—	—	—	—
Magnesium	—	ANOVA	2.10×10^{-12}	0.35	0.71
Manganese	—	Kruskal-Wallis	0.0022	—	—
Molybdenum	Log-transformed	ANOVA	1.30×10^{-7}	0.053	0.70
Nickel	—	—	—	—	—
Phosphorus	—	—	—	—	—
Potassium	—	ANOVA	3.92×10^{-10}	0.24	0.19
Scandium	—	ANOVA	8.27×10^{-6}	0.85	0.31
Sodium	—	ANOVA	1.46×10^{-5}	0.10	0.074
Strontium	—	ANOVA	1.35×10^{-14}	0.089	0.58
Sulfur	—	ANOVA	7.89×10^{-17}	0.15	0.15
Tin	—	—	—	—	—
Titanium	—	ANOVA	0.22	0.089	0.14
Vanadium	—	ANOVA	7.15×10^{-10}	0.77	0.18
Zinc	—	ANOVA	2.37×10^{-7}	0.61	0.086

Table G.2: Pairwise comparisons using Tukey's HSD tests and Wilcoxon rank sum tests to compare water total and sulfur metal concentrations between the Control (n=4), Low (n=3), Medium (n=4), and High (n=5) treatments and Lake 260 water (n=4). Tukey's HSD tests were conducted when normality and homogeneity of variances assumptions were met while Wilcoxon rank sum tests were conducted when assumptions were not met (see Table G.1.).

Metal	Transformation	Statistical Test	Group 1	Group 2	p-value
Aluminum	—	Wilcoxon	High	Control	0.52
			L260	Control	0.095
			Low	Control	0.11
			Medium	Control	0.54
			L260	High	0.095
			Low	High	0.24
			Medium	High	1.00
			Low	L260	0.11
			Medium	L260	0.095
			Medium	Low	0.52
Antimony	Log-transformed	Tukey HSD	High	Control	0.37
			L260	Control	7.98×10^{-6}
			Low	Control	0.53
			Medium	Control	0.046
			L260	High	8.47×10^{-5}
			Low	High	1.00
			Medium	High	0.63
			Low	L260	2.96×10^{-4}
			Medium	L260	0.0018
			Medium	Low	0.68
Arsenic	—	Tukey HSD	High	Control	3.01×10^{-5}
			L260	Control	1.71×10^{-7}
			Low	Control	5.99×10^{-5}
			Medium	Control	6.29×10^{-5}
			L260	High	0.0058
			Low	High	0.99
			Medium	High	1.00
			Low	L260	0.037
			Medium	L260	0.0076
			Medium	Low	0.98
Barium	Log-transformed	Tukey HSD	High	Control	0.0022
			L260	Control	0.58
			Low	Control	0.0093
			Medium	Control	0.43
			L260	High	0.047
			Low	High	1.00
			Medium	High	0.076
			Low	L260	0.13
			Medium	L260	1.00
			Medium	Low	0.19
Boron	—	Wilcoxon	High	Control	0.24
			L260	Control	0.23
			Low	Control	0.19
			Medium	Control	0.89
			L260	High	0.24
			Low	High	0.24
			Medium	High	0.23

Metal	Transformation	Statistical Test	Group 1	Group 2	p-value
			Low	L260	0.19
			Medium	L260	0.38
			Medium	Low	0.19
Calcium	—	Tukey HSD	High	Control	6.82×10^{-8}
			L260	Control	2.48×10^{-7}
			Low	Control	0.97
			Medium	Control	0.74
			L260	High	5.71×10^{-12}
			Low	High	4.71×10^{-7}
			Medium	High	1.62×10^{-8}
			Low	L260	3.13×10^{-7}
			Medium	L260	1.24×10^{-6}
			Medium	Low	0.45
Copper	—	Wilcoxon	High	Control	0.85
			L260	Control	0.85
			Low	Control	—
			Medium	Control	0.85
			L260	High	1.00
			Low	High	0.85
			Medium	High	0.85
			Low	L260	0.85
			Medium	L260	0.98
			Medium	Low	0.85
Iron	—	Tukey HSD	High	Control	0.02
			L260	Control	4.38×10^{-4}
			Low	Control	0.14
			Medium	Control	0.018
			L260	High	0.20
			Low	High	0.96
			Medium	High	1.00
			Low	L260	0.11
			Medium	L260	0.34
			Medium	Low	0.91
Magnesium	—	Tukey HSD	High	Control	5.38×10^{-9}
			L260	Control	8.78×10^{-8}
			Low	Control	0.85
			Medium	Control	0.083
			L260	High	7.94×10^{-14}
			Low	High	5.90×10^{-9}
			Medium	High	3.27×10^{-10}
			Low	L260	9.06×10^{-7}
			Medium	L260	3.65×10^{-6}
			Medium	Low	0.51
Manganese	—	Wilcoxon	High	Control	0.29
			L260	Control	0.057
			Low	Control	0.13
			Medium	Control	0.057
			L260	High	0.057
			Low	High	0.060
			Medium	High	0.057
			Low	L260	0.082
			Medium	L260	0.057
			Medium	Low	0.13
Molybdenum	Log-transformed	Tukey HSD	High	Control	0.60

Metal	Transformation	Statistical Test	Group 1	Group 2	p-value
			L260	Control	1.05×10^{-6}
			Low	Control	0.37
			Medium	Control	0.96
			L260	High	8.39×10^{-8}
			Low	High	0.033
			Medium	High	0.24
			Low	L260	5.17×10^{-5}
			Medium	L260	2.74×10^{-6}
			Medium	Low	0.73
Potassium	—	Tukey HSD	High	Control	1.00
			L260	Control	1.23×10^{-9}
			Low	Control	0.016
			Medium	Control	3.20×10^{-5}
			L260	High	4.78×10^{-10}
			Low	High	0.0080
			Medium	High	1.25×10^{-5}
			Low	L260	2.27×10^{-7}
			Medium	L260	5.02×10^{-6}
			Medium	Low	0.075
Scandium	—	Tukey HSD	High	Control	1.02×10^{-4}
			L260	Control	3.55×10^{-6}
			Low	Control	0.0068
			Medium	Control	5.85×10^{-4}
			L260	High	0.13
			Low	High	0.55
			Medium	High	0.96
			Low	L260	0.015
			Medium	L260	0.051
			Medium	Low	0.90
Sodium	—	Tukey HSD	High	Control	0.90
			L260	Control	1.56×10^{-5}
			Low	Control	0.037
			Medium	Control	0.031
			L260	High	3.40×10^{-5}
			Low	High	0.13
			Medium	High	0.12
			Low	L260	0.015
			Medium	L260	0.0060
			Medium	Low	1.00
Strontium	—	Tukey HSD	High	Control	4.98×10^{-11}
			L260	Control	3.03×10^{-10}
			Low	Control	0.048
			Medium	Control	0.98
			L260	High	0
			Low	High	2.85×10^{-9}
			Medium	High	7.54×10^{-11}
			Low	L260	7.25×10^{-11}
			Medium	L260	1.90×10^{-10}
			Medium	Low	0.12
Sulfur	—	Tukey HSD	High	Control	0
			L260	Control	1.00
			Low	Control	6.18×10^{-7}
			Medium	Control	6.56×10^{-10}
			L260	High	0

Metal	Transformation	Statistical Test	Group 1	Group 2	p-value
			Low	High	0
			Medium	High	0
			Low	L260	$8.45x10^{-7}$
			Medium	L260	$8.26x10^{-10}$
			Medium	Low	0.0011
Titanium	—	Tukey HSD	High	Control	0.50
			L260	Control	0.96
			Low	Control	1.00
			Medium	Control	0.95
			L260	High	0.19
			Low	High	0.52
			Medium	High	0.91
			Low	L260	0.98
			Medium	L260	0.64
			Medium	Low	0.94
Vanadium	—	Tukey HSD	High	Control	$1.25x10^{-6}$
			L260	Control	$1.34x10^{-4}$
			Low	Control	$2.58x10^{-4}$
			Medium	Control	$6.84x10^{-5}$
			L260	High	$8.03Ex10^{-10}$
			Low	High	0.19
			Medium	High	0.22
			Low	L260	$5.83x10^{-8}$
			Medium	L260	$1.49x10^{-8}$
			Medium	Low	1.00
Zinc	—	Tukey HSD	High	Control	$2.52x10^{-5}$
			L260	Control	0.59
			Low	Control	$1.39x10^{-5}$
			Medium	Control	0.011
			L260	High	$2.33x10^{-6}$
			Low	High	0.69
			Medium	High	0.044
			Low	L260	$1.79x10^{-6}$
			Medium	L260	$6.75x10^{-4}$
			Medium	Low	0.0083

Table G.3: Statistical analysis to compare water dissolved metal and sulfur concentrations between Lake 260 water (n=4), the Control (n=4), Low (n=4), Medium (n=4), and High (n=5) treatments. One-way ANOVA tests were conducted when the normality (Shapiro-Wilk test) and homogeneity of variances (Levene's test) assumptions were met. When no assumptions were met, Kruskal-Wallis rank sum test were conducted.

Metal	Transformation	Statistical Test	p-value	Shapiro-Wilk Test	Levene's Test
Aluminum	Log transformation	ANOVA	0.0034	0.27	0.68
Antimony	—	ANOVA	0.12	0.063	0.31
Arsenic	—	Kruskal-Wallis	0.012	—	—
Barium	—	Kruskal-Wallis	0.0044	—	—
Boron	—	Kruskal-Wallis	0.10	—	—
Cadmium	—	Kruskal-Wallis	0.081	—	—
Calcium	—	Kruskal-Wallis	0.0015	—	—
Chromium	—	Kruskal-Wallis	0.37	—	—
Cobalt	—	Kruskal-Wallis	0.75	—	—
Copper	Log transformation	ANOVA	0.38	0.14	0.28
Iron	—	Kruskal-Wallis	0.41	—	—
Lead	—	Kruskal-Wallis	0.37	—	—
Magnesium	—	Kruskal-Wallis	0.0013	—	—
Manganese	—	Kruskal-Wallis	0.047	—	—
Molybdenum	—	Kruskal-Wallis	0.37	—	—
Nickel	—	Kruskal-Wallis	0.65	—	—
Phosphorus	—	Kruskal-Wallis	—	—	—
Potassium	—	Kruskal-Wallis	0.0012	—	—
Scandium	—	ANOVA	2.85×10^{-7}	0.31	0.45
Sodium	—	Kruskal-Wallis	0.0048	—	—
Strontium	—	Kruskal-Wallis	0.0016	—	—
Sulfur	—	Kruskal-Wallis	0.0010	—	—
Tin	—	Kruskal-Wallis	—	—	—
Titanium	Log transformation	ANOVA	0.89	0.092	1.65×10^{-5}
Vanadium	—	ANOVA	4.15×10^{-5}	0.66	0.061
Zinc	—	ANOVA	3.20×10^{-7}	0.26	0.22

Table G.4: Pairwise comparisons using Tukey's HSD tests and Wilcoxon rank sum tests to compare water dissolved metal and sulfur concentrations between the Control (n=4), Low (n=4), Medium (n=4), and High (n=5) treatments and Lake 260 water (n=4). Tukey's HSD tests were conducted when normality and homogeneity of variances assumptions were met while Wilcoxon rank sum tests were conducted when assumptions were not met (see Table G.3.).

Metal	Transformation	Statistical Test	Group 1	Group 2	p-value
Aluminum	—	Wilcoxon	High	Control	1.00
			L260	Control	0.33
			Low	Control	0.52
			Medium	Control	0.25
			L260	High	0.14
			Low	High	0.41
			Medium	High	0.088
			Low	L260	0.81
			Medium	L260	0.088
			Medium	Low	0.088
Arsenic	—	Wilcoxon	High	Control	0.057
			L260	Control	0.49
			Low	Control	0.11
			Medium	Control	0.057
			L260	High	0.73
			Low	High	0.69
			Medium	High	0.057
			Low	L260	0.73
			Medium	L260	0.057
			Medium	Low	0.057
Barium	—	Wilcoxon	High	Control	0.071
			L260	Control	0.25
			Low	Control	0.071
			Medium	Control	0.091
			L260	High	0.091
			Low	High	0.56
			Medium	High	0.071
			Low	L260	0.091
			Medium	L260	0.38
			Medium	Low	0.071
Calcium	—	Wilcoxon	High	Control	0.38
			L260	Control	0.49
			Low	Control	0.036
			Medium	Control	0.036
			L260	High	0.036
			Low	High	0.036
			Medium	High	0.036
			Low	L260	0.036
			Medium	L260	0.036
			Medium	Low	0.036
Magnesium	—	Wilcoxon	High	Control	0.69
			L260	Control	0.13
			Low	Control	0.036
			Medium	Control	0.036
			L260	High	0.036
			Low	High	0.036
			Medium	High	0.036

Metal	Transformation	Statistical Test	Group 1	Group 2	p-value
			Low	L260	0.036
			Medium	L260	0.036
			Medium	Low	0.036
Manganese	—	Wilcoxon	High	Control	0.21
			L260	Control	0.46
			Low	Control	0.21
			Medium	Control	0.21
			L260	High	0.46
			Low	High	1.00
			Medium	High	0.23
			Low	L260	0.46
			Medium	L260	0.23
			Medium	Low	0.46
Potassium	—	Wilcoxon	High	Control	0.032
			L260	Control	0.032
			Low	Control	0.73
			Medium	Control	0.032
			L260	High	0.032
			Low	High	0.032
			Medium	High	0.032
			Low	L260	0.032
			Medium	L260	0.032
			Medium	Low	0.032
Scandium	—	Tukey HSD	High	Control	2.29×10^{-4}
			L260	Control	2.59×10^{-5}
			Low	Control	3.38×10^{-5}
			Medium	Control	8.46×10^{-8}
			L260	High	0.75
			Low	High	0.94
			Medium	High	0.0011
			Low	L260	0.98
			Medium	L260	0.012
			Medium	Low	0.0027
Sodium	—	Wilcoxon	High	Control	0.049
			L260	Control	0.049
			Low	Control	1.00
			Medium	Control	0.049
			L260	High	0.74
			Low	High	0.14
			Medium	High	0.049
			Low	L260	0.14
			Medium	L260	0.049
			Medium	Low	0.049
Strontium	—	Wilcoxon	High	Control	0.34
			L260	Control	0.34
			Low	Control	0.036
			Medium	Control	0.036
			L260	High	0.036
			Low	High	0.036
			Medium	High	0.036
			Low	L260	0.036
			Medium	L260	0.036
			Medium	Low	0.036
Sulfur		Wilcoxon	High	Control	0.032

Metal	Transformation	Statistical Test	Group 1	Group 2	p-value
			L260	Control	0.032
			Low	Control	0.032
			Medium	Control	0.69
			L260	High	0.032
	—		Low	High	0.032
			Medium	High	0.032
			Low	L260	0.032
			Medium	L260	0.032
			Medium	Low	0.032
			High	Control	6.22×10^{-5}
			L260	Control	8.61×10^{-7}
			Low	Control	1.35×10^{-6}
			Medium	Control	0.25
Vanadium	—	Tukey HSD	L260	High	0.11
			Low	High	0.33
			Medium	High	1.74×10^{-6}
			Low	L260	0.93
			Medium	L260	4.54×10^{-8}
			Medium	Low	5.76×10^{-8}
			High	Control	6.26×10^{-6}
			L260	Control	0.0039
			Low	Control	7.56×10^{-5}
			Medium	Control	0.90
Zinc	—	Tukey HSD	L260	High	0.022
			Low	High	0.37
			Medium	High	1.55×10^{-6}
			Low	L260	0.40
			Medium	L260	6.72×10^{-4}
			Medium	Low	1.47×10^{-5}

Table G.5: Welch one-way test to compare total suspended solids (TSS) between the Control (n=20), Low (n=20), Medium (n=20), and High (n=20) treatments. Normality (Shapiro-Wilk test) assumption was met but the homogeneity of variances (Levene's test) was not. Water samples were collected directly from the limnocorrals.

Statistical Test	p-value	Shapiro-Wilk Test	Levene's Test
Welch	0.17	0.33	0.045

Table G.6: Unpaired two samples t-tests, Welch t-tests, and Wilcoxon rank sum tests to compare sediment metal and sulfur concentrations between the Control (n=3) and High (n=3) treatment. T-tests were conducted when normality (Shapiro-Wilk test) and homogeneity of variances (Levene's test) assumptions were met. Welch t-tests were conducted when the normality assumption is met but the homogeneity of variances assumption is not. When assumptions were not met, unpaired two-samples Wilcoxon tests were conducted.

Metal	Statistical Test	p-value	Shapiro-Wilk Test		Levene's Test
			Control	High	
Aluminum	T-test	0.38	0.51	0.94	0.23
Antimony	BDL	—	—	—	—
Arsenic	T-test	0.76	0.45	0.92	0.68
Barium	T-test	0.69	0.57	0.60	0.88
Boron	T-test	0.45	0.73	0.32	0.31
Cadmium	T-test	0.50	0.12	0.95	0.18
Calcium	T-test	0.32	0.43	0.98	0.089
Chromium	T-test	0.99	0.60	0.57	0.48
Cobalt	T-test	0.054	0.85	0.27	0.088
Copper	T-test	0.98	0.25	0.11	0.59
Iron	T-test	0.12	0.83	0.58	0.96
Lead	T-test	0.81	0.46	0.79	0.10
Magnesium	T-test	0.15	0.11	0.60	0.071

Metal	Statistical Test	p-value	Shapiro-Wilk Test		Levene's Test
			Control	High	
Manganese	T-test	0.18	0.10	0.77	0.15
Molybdenum	BDL	—	—	—	—
Nickel	T-test	0.94	0.14	0.72	0.50
Phosphorus	T-test	0.11	0.10	0.065	0.53
Potassium	T-test	0.24	0.37	0.56	0.79
Scandium	T-test	0.78	0.91	0.94	0.21
Sodium	T-test	0.31	0.52	0.39	0.60
Strontium	Welch t-test	0.27	0.52	0.20	0.034
Sulfur	Wilcoxon	1.00	—	—	—
Tin	T-test	0.24	0.12	0.76	0.34
Titanium	Welch t-test	0.72	0.81	0.77	0.0046
Vanadium	T-test	0.20	0.24	0.14	0.56
Zinc	Wilcoxon	0.38	—	—	—